Strategies for enhancing lipid production from native microalgae isolates for biofuel production: Process optimization and Intensification

Thesis submitted in partial fulfillment of the requirements for the degree of
Doctor of Philosophy

by

Garima Srivastava
(126151003)

Centre for Energy

Indian Institute of Technology Guwahati

Guwahati-781039

March 2018

STATEMENT

I, hereby declare that the content embodied in this thesis entitled "**Strategies for enhancing lipid production from native microalgae isolates for biofuel production: Process optimization and Intensification**" is a result of investigations carried out by me at Centre for Energy, Indian Institute of Technology Guwahati, Guwahati, India under the guidance of Dr. Vaibhav V. Goud.

In keeping with the general practice of reporting scientific observations, due acknowledgements have been made wherever the work described is based on the findings of other investigators.

March, 2018

Garima Srivastava
(126151003)

Centre for Energy
Indian Institute of Technology Guwahati

CERTIFICATE

This is to certify that the work contained in the thesis entitled "**Strategies for enhancing lipid production from native microalgae isolates for biofuel production: Process optimization and Intensification"** by Ms. Garima Srivastava (Roll No. 126151003), for the award of degree of Doctor of Philosophy, has been carried out under our guidance of Dr. Vaibhav V. Goud and that the work has not been submitted elsewhere for a degree.

March, 2018

Dr. Vaibhav V. Goud
Associate Professor
Department of Chemical Engineering
Indian Institute of Technology Guwahati
Guwahati-781039

ACKNOWLEDGMENT

I take utmost pleasure to express my gratitude to all who made this thesis possible. I am especially grateful to my supervisor Dr. Vaibhav V. Goud for giving me an opportunity to be a part of his research group. I always owe you for your patience, support and constant motivation throughout my PhD journey. I would also like to acknowledge my previous supervisors Dr. K.N Guruprasad and Dr. S. M Bhatt for believing in me. Your belief in me made me believe in myself and helped me to grow better and imbibed scientific temperament. I am also thankful to Prof. M.C Kalita for providing us the microalgae consortia.

I am thankful to my doctoral committee members Prof. Pranab Goswami, Prof. A Ramesh and Dr. Chandan Das for their valuable suggestions and guidance during my progress seminar reviews that has led to the successful completion of my PhD thesis.

I am pleased to provide my gratitude to Prof. V. S Moholkar, Professor Pranab Goswami and Professor Alok Ghoshal, the current and former Heads of Centre for Energy, IIT Guwahati, with the necessary facilities and support.

I would like to thank the present and previous staffs of Centre for Energy Dr. L Borbora, Dr. Pankaj Kalita, Mr. Dhiren Huzuri, Mrs. Gitanjali Hazarika, Mr. Deborshi Barua and Mr. Paragjyoti Sharma for their cooperation.

I am thankful to Centre for energy, Department of Biosciences and Bioengineering, Department of Chemical Engineering, Central Instruments Facility, Department of

Physics, Department of Civil Engineering and Biotech Park for providing me with the state of art infrastructure for advanced level research.

I also would like to thank my seniors, colleagues and juniors for their continuous support. I will miss all my lab members, you guys made my journey remarkable. I would like to especially thank my superman Atanu Dada and Pushpita, I am thankful to my trainee Anisha for her love and support. Swaroopa for believing in me and our heart to heart sharing. The list is not over yet Vikas, Nishchal, Pravin, Chittaranjan, Sukumar, Rahul, Debeni, Sutapa, Mohan, Robinson, Roopjyoti, Ravi, Abebe. I am grateful to everyone belong to VVG research group for always being there for me. Please forgive me if I missed anyone's name mentioning here.

I am also thankful to my seniors Adreeja di, Amrita di, Souvika di, Suchi di, Deepti di, Devendra Sir, Ayan bhaiya and Sonika mam for their constant support and motivation.

Some people arrive and make such a beautiful impact on your life, you can't barely remember what life was like without them. The most precious time of my life spent in IITG with my loved ones will always be cherished deep in my heart. Thank you so much Arti, Sharbani, Babul, Sumitha, Papori, Arup, Navodit, Balwant, Meenakshi, without you I could not think my IITG life so beautiful. Saikat, Trapti, Nalini and Vinita for you "true friend never apart may be in distance but never in heart". I am also thankful to my critics for helping me to grow better and able to survive. Last but not the least, my best friend for life Ajeet without him I can't think my life so beautiful. Your constant encouragement and support help me to stand independently.

No words would suffice to express my gratitude to my mummy for her constant love, support, understanding and sacrifice who has been a constant inspiration for me. My

PhD endeavor would not have been successful without the trust, support and blessings of my parents-in-law. I am also grateful to my paternal and maternal aunts for their support and timely help during my studies and all the tough times.

Last but not the least my late father who made this possible. Papa wherever you are thanking you for all your efforts. You fought for me struggled and a lot, compromised all your happiness. I regret that I could not be able to take you up to here but believe that you will be always with me. Thank you so much.

I owe my achievements to my family. Thank you, everyone.

Garima Srivastava

DEDICATED TO MY FAMILY

Table of Contents

Abstract

Biomass can play the pivotal role in the production of high-quality carbon-neutral fuels as well as providing feedstocks for various other processes. Among all the available biomass, microalgae biomass is one of the most vital raw material for biodiesel production. Apart from biodiesel, microalgae biomass can be used to synthesize other forms of biofuel such as bioethanol, biogas, bio-crude etc. Therefore, instead of producing single product *viz.* biodiesel, in recent years, microalgal research continued with the prospect of a microalgae biorefinery, where microalgal byproducts and coproducts are extracted to valorize the entire microalgae biomass.

The present study is intended to select potent microalgae strains native to Northeast India for biodiesel production and use the defatted microalgae residues remained after oil extraction for anaerobic digestion (AD) which essentially recovers more energy than energy derived only from microalgae oil exclusively. The freshwater microalgae samples were collected from water bodies near Gauhati University. The mixed consortia of algae and bacteria present in water samples were serially diluted and plated on BG-11 agar plates for single microalgae colony isolation. The primary identification of isolated microalgae strains was performed on its morphology and pigmentation system. The pure cultures were sent for 18S rDNA sequencing. The obtained genome sequence was BLAST using multiple sequence alignment tool and the corresponding phylogenetic tree was constructed by neighbor end joining method. The sequences were submitted to NCBI and annotated as *Chlorella* CG12 (KR905186) and *Desmodesmus* GS12 (KR905187).

A set of preliminary experiments were conducted (light intensity 1000-4000 lux, temperature 19-31°C and pH 5-9) to fix the range of selected variables and find their effects on the growth study, biomass productivity, lipid content and lipid productivity

of both the microalgae under laboratory conditions. Based on the results of preliminary experiments the statistical and mathematical model of RSM and ANN design technique was employed to optimize the effect of these variables on the lipid yield. The optimized culture conditions obtained for CG12 (light intensity-3.46 Klux; temperature-21.07 °C; and pH-8.74) and GS12 (light intensity-3.19 Klux; temperature-23.12 °C; and pH-7.53) were evaluated and compared with ANN model. The highest lipid yield obtained at the final optimized conditions for CG12 and GS12 were 13.36 % and 25.85 %, respectively. Furthermore, the sensitivity analysis revealed that light intensity plays a decisive role in lipid accumulation with a relative importance of 87.78 % and 49.09 % in CG12 and GS12, respectively. The high palmitic and oleic acid content in microalgae oil compositions indicates potentiality of these species to be used as a promising bioenergy feedstock.

Furthermore, to increase the lipid content salinity induced lipid enrichment was employed with major macronutrients such as NaCl, KCl, $MgCl_2$, and $CaCl_2$ with varying concentrations from 5 mM to 25 mM. It was observed that this induced salt concentration decreases the chlorophyll and biomass concentration in microalgae whereas increases the lipid content. Additionally, $CaCl_2$ showed a remarkable response in lipid accumulation in both the microalgae and attains a maximum lipid enhancement up to 40 % and 45 % in CG12 and GS12, respectively.

After attaining the high lipid content in microalgae the small batch cultures were extended to mass cultivation of up to 100 L. Subsequently, lipid extraction was performed from the harvested biomass. However, supercritical methanol (SCM) transesterification method was used to convert microalgae oil to FAME. A stepwise hybrid optimization of RSM-ANN-GA was performed for operating parameters (temperature, time and MeOH: oil) to obtain the high conversion efficiency of

microalgae oil to biodiesel. The globally optimized reaction conditions for SCM were temperature 285.21 °C, time 25.57 min, and MeOH: oil molar ratio-23.47 resulted in 98.12 % conversion of microalgae oil to biodiesel. The biodiesel properties such as acid value, iodine number, cetane number, calorific value etc. were analyzed and exhibit analogous trend with the standard ASTM D6571 standards.

Further, high production costs are the major limitation for commercialization of algal biofuels. Hence, to reduce the nutrient requirement microalgae were grown in different waste media formulations such as cow-dung (CD), biogas plant digest sludge (BPW) and vermicompost (VM). Initial growth response and lipid content were recorded in all the media and the best growth supporting media i.e. BPW was used for further optimization study. Optimization was performed considering three important parameters light intensity (2-4 Klux), leachate concentration (10-30 %) and $NaHCO_3$ supplementation (0.5 -1.5 %). An optimized culture condition resulted in lipid accumulation of 44.56 % and 41.89 % in CG12 and GS12, respectively.

The defatted microalgae biomass remained after oil/lipid extraction was co-digested with rice straw (RS) for biogas production. The co-digestion of defatted microalgae biomass with RS yielded 382 mL/g VS of biomethane in CG12 whereas 311 mL/g VS in GS12. The high carbon to nitrogen ratio (C/N) in RS and low C/N ratio in microalgae balances the typical C/N ratio of the anaerobic digester and provides high bio-methane potential (BMP). As established earlier that BPW is a good source of nutrient for microalgae cultivation hence, combining the production of biodiesel with biogas would definitely be a potent solution to suffice the energy demand, reduce the production cost, without environmental pollution. This combined approach of microalgae biodiesel and biogas production together presents not only a way to sustainable fuel production indeed also help in waste stabilization and additional revenue generation.

Abbreviations

2FI	Two factor interaction
AAD	Absolute average deviation
ABA	Abscisic acid
A–CoD	Anaerobic co–digestion
AD	Anaerobic digestion
AM	Allen medium
ANN	Artificial neural network
ANOVA	Analysis of variance
ASP	Aquatic species program
ASTM	American society for testing and material
ATP	Adenosine triphosphate
BBM	Bold's basal medium
BD	Biodegradability
BG–11	Blue green medium
BLAST	Basic local alignment search tool
BMP	Bio–methane potential
BP	British petroleum
BPA	Back propagation algorithm
BPW	Biogas plant digested sludge
C	Carbon
C/N	Carbon to nitrogen
$CaCl_2$	Calcium chloride
CaO	Calcium oxide
CCAP	Culture Collection of Algae and Protozoa
CCD	Central composite design
CCM	Carbon concentration mechanism
CD	Cow–dung
$CDCl_3$	Deuterated chloroform
CH_2	methylene
$CHCl_3$	Chloroform
CLSM	Confocal laser scanning microscope
CO	Carbon mono–oxide
CO_2	Carbon dioxide
CV	Coefficient of variation
DMSO	Dimethyl sulfoxide
DTG	Differential of thermogravimetric
EDX	Electron dispersive x ray spectroscopy
EMY	Experimental methane yield
EU	European union
FAME	Fatty acid methyl ester
FESEM	Field emission scanning electron microscope
FID	Flame ionization detector
FTIR	Fourier transformation infrared spectroscopy
GA	Genetic algorithm
GC	Gas chromatography
GCMS	Gas chromatography mass spectroscopy

GHG's	Greenhouse gases
H_2O	Water
H_2SO_4	Sulphuric acid
HCA	Hierarchical cluster analysis
HHV	High heating value (calorific value)
HPLC	High performance liquid chromatography
HRAP	High rate algal pond
HRT	Hydraulic retention time
KBr	Potassium bromide
KCl	Potassium chloride
KOH	Potassium hydroxide
L	Linoleic acid
LM	Levenberg–Marquardt
Ln	Linolenic acid
logsig	log sigmoid
MATLAB	Matrix laboratory
Me	Methyl ester
MEGA	Molecular Evolutionary Genetics Analysis
MeOH	Methanol
MgO	Magnesium oxide
$MgCl_2$	Magnesium chloride
MgO	Magnesium oxide
$MgSO_4.7H_2O$	Magnesium sulphate heptahydrate
MUFA	Monounsaturated fatty acid
MUSCLE	Multiple Sequence Comparison by Log–Expectation
N_2	Nitrogen
Na_2SO_3	Sodium sulfite
NaAc	Sodium acetate
NaCl	Sodium Chloride
NADPH	Nicotinamide adenine dinucleotide phosphate
NDA	National Democratic Alliance
$NaHCO_3$	Sodium bicarbonate
$NaNO_3$	Sodium nitrate
NaOH	Sodium hydroxide
NCBI	National Center for Biotechnology Information
NMR	Nuclear magnetic resonance
NPQ	Non photochemical quenching
NREL	National Renewable Energy Laboratory
O	Oleic acid
P	Phosphorous
PCE	Photo conversion efficiency
PRESS	Predicted residual sum of squares
PS II	Photosystem II
PUFA	Polyunsaturated fatty acid
purelin	linear transfer function
r–DNA	Ribosomal genes
RH	Rice husk
RMSE	Root mean square error
ROS	Reactive oxygen species

ROS	Reactive oxygen species
RS	Rice straw
RSM	Response surface methodology
S-ZrO_2	Sulphated zirconia oxide
SCM	Supercritical methanol
sCOD	Soluble chemical oxygen demand
S	Saturated fatty acid
SMA	Specific methanogenic activity
SO_2	Sulphur di-oxide
SOS	salt overlay sensitive protein
T1	Relaxation time
TAG	Triacylglycerol
TE	Echo time
TGA	Thermo gravimetric analysis
TMY	Theoretical methane yield
TS	Total solids
UV	Ultraviolet
VFA	Volatile fatty acid
VM	Vermicompost
VS	Volatile solid
WAS	Waste activated sludge
WH	Wheat husk
WS	Wheat straw
APHA	American Public Health Association
EPS	Extra polymeric substance

Symbols and units

α	Alpha
Wt.%	Weight percent
v/v	Volume/volume
V	Volts
tg	Division time
R^2	Coefficient of determination
ppm	Part per million
^oC	Degree centigrade
nm	Nanometer
N	Normality
MR	Molar ratio
MPa	Mega Pascal
mM	Mill molar
mg	Milligram
L	Liter
Klux	Kilo lux
kHz	Kilohertz
ha.	Hectare
h	Hour
g/L	Gram/liter
Eq.	Equation
^1H	Proton
µg	microgram
% dcw	Percent dry cell weight

List of tables

List of figures

CHAPTER 1

INTRODUCTION

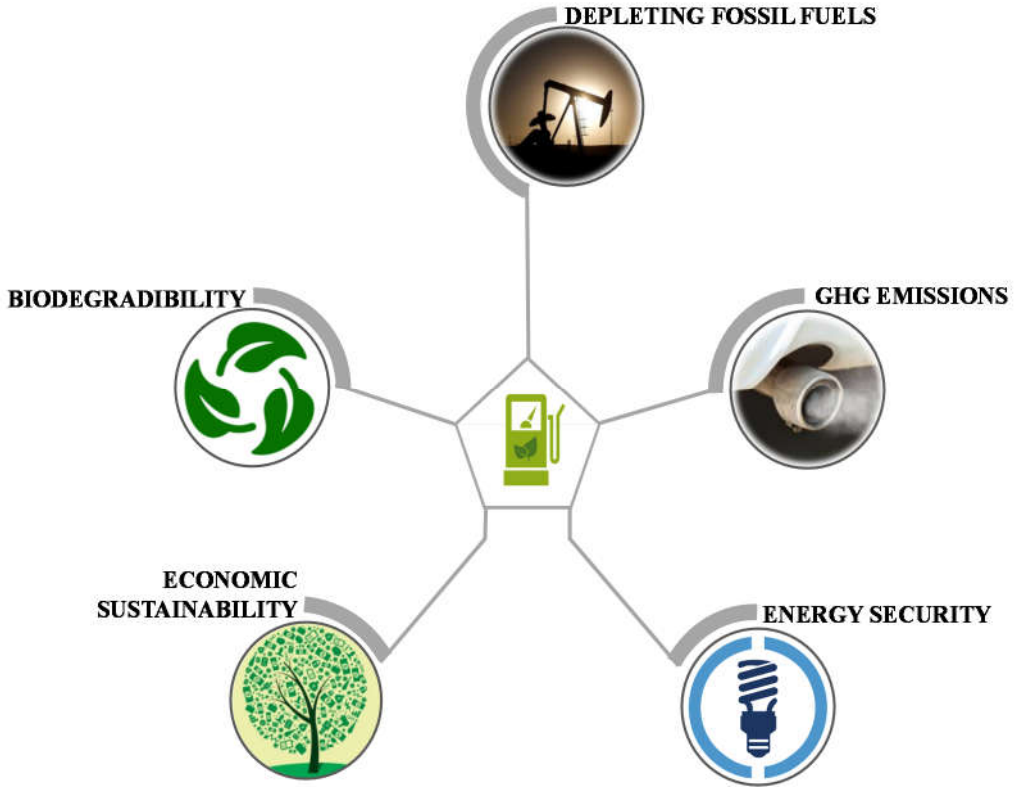

General introduction and motivation for the thesis

1.1 Foreword

India has emerged as third largest energy consumer after US and China. Till 2015–16 India has imported 80 % crude oil and 18 % natural gas. According to the British Petroleum (BP) energy outlook 2017, the estimated crude oil import in India would be possibly upsurge by 165 %. India has imported 202 million tons of oil in the year 2015–2016 costing around $150 billion. According to the National Democratic Alliance (NDA) the import of renewable energy in India will expect to reach $300 billion by the year 2030. Hence, the government intended to cut 10 % in energy imports by 2022 and a 50 % cut by 2030 and planned to produce renewable energy by its own in order to boost the economy (Snow, 2017).

The rapid industrialization, as well as high population growth, is progressively raising the energy demand that largely depends on fossil fuels. Disproportionate demand and limited availability of fossil fuels have shifted the energy research paradigm towards other alternative energy resources that can supplement conventional energy assets. In the mid–1970's, fuel shortages spurred interest in diversifying fuel resources, and thus biodiesel as fatty esters were developed as an alternative to petroleum diesel. The concept of using vegetable oil as an engine fuel likely dates to when Rudolf Diesel developed the first engine to run on peanut oil (Ma and Hanna, 1999). With this advent concern for the supply of fossil fuel, the recent emergence of biodiesel has been a forefront topic of consideration.

Biodiesel is one of the most important liquid biofuel, derived from a variety of feedstock's comprising vegetable oils, animal fats and microorganisms. Biodiesel is often regarded as "biofuel" due to its origin from biomass. Moreover, the "biofuel"

term was coined for any solid, liquid, or gaseous fuel that is principally synthesized from biomass (Clark et al., 2012).

Technically biodiesel is a mono–alkyl ester synthesized by the reaction of fatty acids with alcohol. Biodiesel has similar energy efficiency and immense potential to be utilized in compression–ignition engines (Knothe et al., 2015). The renewability, inherent lubricity, biodegradability, the absence of sulfur content, reduction in obnoxious gas emission, safer handling and compatibility with existing engine make biodiesel to stand alone as prominent alternative energy. Therefore, till today the biodiesel is still being produced from rapeseed in Europe, soybean oil in the United States and palm oil in Malaysia (Demirbas, 2008).

Conventionally, based on the production technologies biodiesel is categorized as the first generation, second generation and third generation. The first generation of biodiesel involved edible oil seed crops such as soybean, sunflower, mustard etc. However, due to skepticism for the sustainability issues and food *vs* fuel crisis, the existence of first generation biodiesel became questionable. Further, to solve the issues related with first generation biodiesel the second generation of biodiesel was evolved using non–edible oil seeds crops such as Jatropha, Pongamia and Castor etc. as presented in Figure 1.1 (Naik et al., 2010).

Recently, the third generation of biodiesel i.e., microalgae biodiesel production has been reported as a promising way to overlook the problems associated with first and second generations (Chuah et al., 2017; Piemonte et al., 2016). Microalgae belong to a diverse class of photosynthetic organisms, capable of converting radiation energy into chemical energy in the form of biomolecules, specifically carbohydrates, proteins,and lipids. More than 40,000 microalgae species are known for their high biomass productivity, lipid content and secondary metabolite synthesis. Subsequently, these

metabolic end products can be used to produce biofuel in the form of bioethanol, biogas and biodiesel (Chisti, 2007; Chng et al., 2016; Rawat et al., 2013).

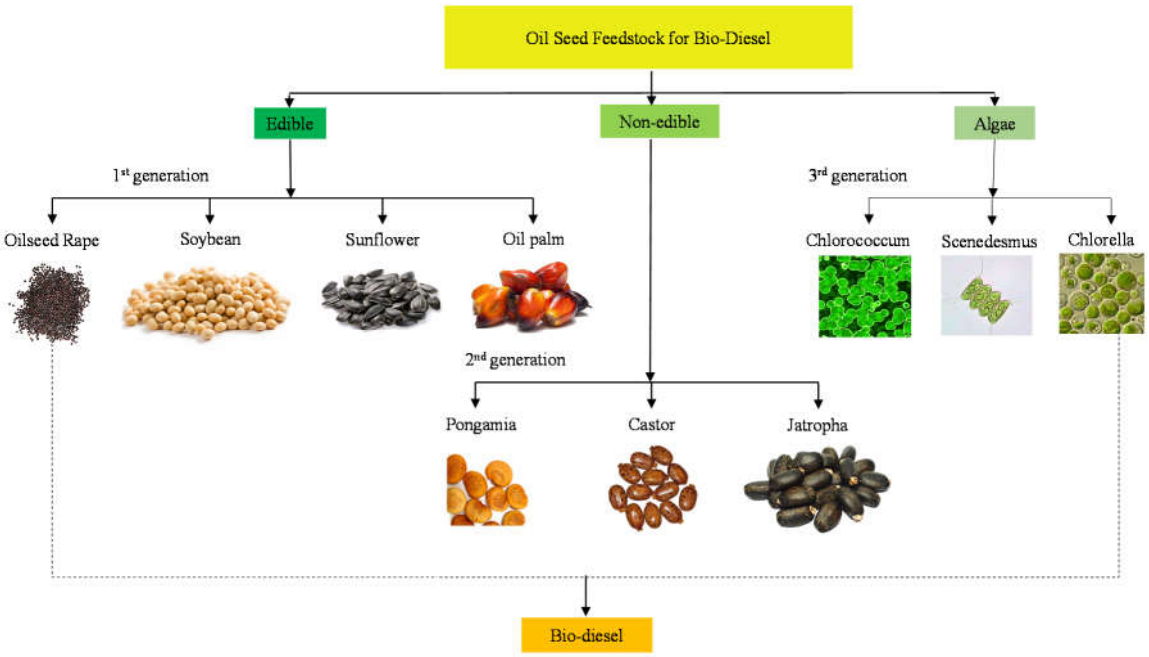

Figure 1.1: Edible and non–edible feedstocks used for biodiesel production.

Indeed, the composition of microalgae cellular constituents varies greatly according to microalgae strain and culture conditions. Therefore, it is quite easy to exploit such metabolic flexibility of microalgae. The National Renewable Energy Laboratory (NREL) is actively engaged in algae biodiesel production since 1980. A pioneer report was submitted by a research group covering all the aspects of algae biodiesel. The technical aspects of aquatic species program (ASP) were highlighted by the report starting from isolation and collection of high lipid–containing microalgae to shedding light on the physiology and biochemistry of this tiny organism. Further, it was also advocated that genetic engineering and mass cultivation will be the major breakthrough for the development of microalgae biodiesel (Sheehan et al., 1998).

Microalgae are able to produce 15–300 times more oil than traditional crops on land area basis illustrated in table 1.1 (Rajvanshi and Sharma, 2012). Furthermore, compared

with conventional crop plants which are usually harvested once or twice a year, microalgae have a very short harvesting cycle (≈1– 20 days depending on the process), allowing multiple or continuous harvests with significantly increased oil yields. Moreover, the annual productivity and oil content of algae is far greater than seed crops. Additionally, microalgae have several other advantages over oil seed feedstock such as it is incompetent with land and food market, have high oil yield, minimizes exhaust gas emission, helpful in CO_2 mitigation and wastewater remediation (Chisti, 2007; Mata et al., 2010; Rodolfi et al., 2009).

Table 1.1: Comparison of various feedstock for their land use and corresponding biodiesel yield.

Feedstock		Oil content (% dcw)	Oil yield (L/ha/annum)	Land use (m^2/annum/L biodiesel)	Biodiesel yield (L/ha/annum)
Corn/Maize		44	172	56	179
Hemp		33	363	26	378
Soybean		18	636	15	661
Jatropha		28	741	13	772
Camelina		42	915	10	952
Canola/Rapeseed		41	974	10	1014
Sunflower		40	1070	9	1113
Castor		48	1307	8	1360
Palm		36	5366	2	5585
Microalgae	**Low oil**	**30**	**58,700**	**0.2**	**61,091**
	Medium oil	**50**	**97,800**	**0.1**	**101,782**
	High oil	**70**	**1,36,900**	**0.1**	**142,475**

The benefits associated with microalgae have shifted the paradigm of biofuel research more towards microalgae–based biofuel production (Cuellar–Bermudez et al., 2015). All the above mentioned unique qualities of microalgae made it invincible raw material for biofuel production. Therefore, bio–prospectors are looking not only to find strains with high lipid content rather microalgae strains with superior growth, adaptability, bioremediation and additional metabolite synthesis along with superior harvesting characteristics. Hence, to overlook the issues, microalgae bio–refinery approach has been suggested where from a single feedstock multiple products can be synthesized. The bio–refinery concept of microalgae biomass presents a self–subsidizing model for high–value co–product synthesis in addition to biodiesel as depicted in Figure 1.2 (Srirangan et al., 2012). Therefore, it is encouraged that the integration of microalgae biodiesel with co–product synthesis such as bioethanol or biogas and/or integration with wastewater treatment not only reduces the production cost of microalgae biodiesel but will also generate additional revenue.

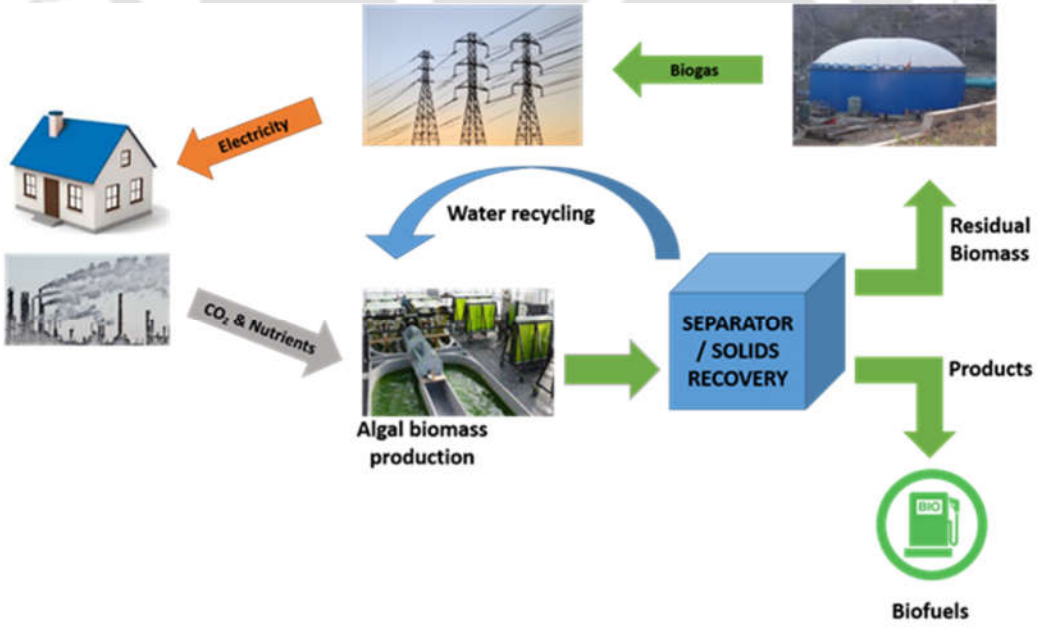

Figure 1.2: The integrated biorefinery of microalgae en–route to produce various chemicals, biofuels, fertilizers, and nutraceuticals.

It is quite evident from the aforementioned discussion that the microalgae biodiesel has a huge potential with respect to its non–toxicity, biodegradability and as a renewable source of energy. Indeed, not only biodiesel, in fact, whole algae biomass can be used to produce multiple forms of biofuels (Mussgnug et al., 2010; Yen et al., 2013). However, till today the most of the studies were carried out on microalgae biodiesel downstream processing, lacking the technical and economic aspect. Hence, more in–depth investigation needed using various advanced methodologies for the process improvement. Further, very few studies have been conducted so far where utilization of the residual microalgae biomass after lipid extraction has been used to produce other chemicals or fuels. Possibly, the microalgae biodiesel economic deployment can be sustained by enhancing productivities, improving downstream process technologies, minimizing intermediate steps and shifting it to one pot biodiesel synthesis. Furthermore, integration of microalgae biodiesel system with wastewater treatment and co–product synthesis will be advantageous for microalgae biofuel commercialization. Based on this the detailed state–of–the–art has been presented in the review of the literature.

CHAPTER 2

REVIEW OF LITERATURE

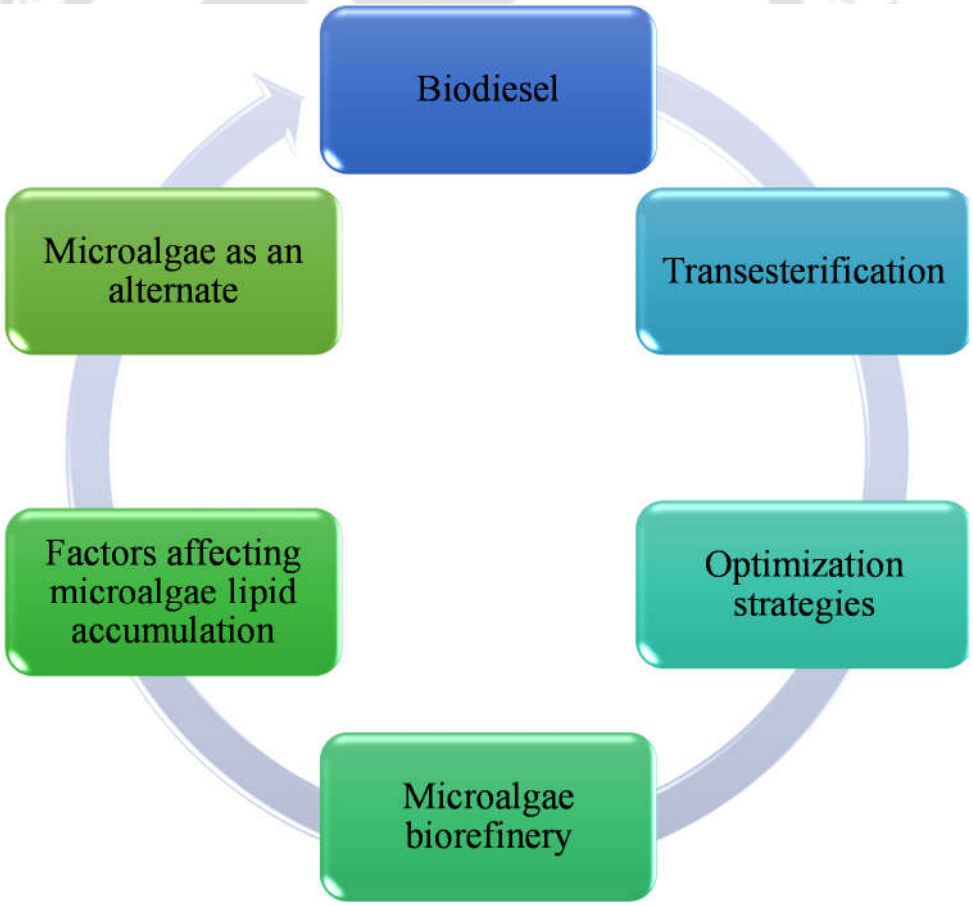

Review of literature

The present chapter discusses the role of microalgae as a potential source of biofuel. With the advent of microalgae contribution towards biofuel synthesis, the present chapter dealt with the opportunities and challenges of microalgae biofuel commercialization and the possible solutions. Majorly, the review has been focused considering the importance of microalgae species involved in biofuel synthesis, factors governing their metabolism, optimization strategies involved to enhance oil production yield, conversion of microalgae oil to biodiesel using advanced techniques and finally utilization of microalgae defatted residue for co–product synthesis in order to establish the sustainable microalgae biorefinery.

2.1 Biodiesel

Petroleum is one of the largest resources of energy, consumed by world's population. Due to increased global demand petroleum is rapidly exhausting creating serious environmental issues. The continuous depletion of the fossil fuel lead emergence of an alternative fuel source. Biodiesel is an alternative fuel similar to conventional or "fossil/petroleum" diesel. Biodiesel is simply a liquid fuel derived from vegetable oils and fats, which has similar combustion properties as regular petroleum diesel fuel.

The advantages of biodiesel include renewability, easy to manufacture, have positive fossil energy imprint, superior emission characteristics, compatible with existing engines and supports domestic agriculture (Nautiyal et al., 2014; Pradhan et al., 2008). On the other hand, biodiesel being non–toxic, biodegradable and essentially free from sulfur, can reduce carcinogenicity by 95 % and air pollution by 90 % (Forero, 2004). The commercial fuel quality of biodiesel is measured by the American Society for Testing and Materials

(ASTM) standard designated D6751 and European Union (EU) 14214. The standards ensure that biodiesel must reach to complete reaction, it must not have any traces of glycerin, catalyst, and alcohol. Moreover, it also certifies that it must be free from free fatty acids (FFA) and have low sulfur content.

Biodiesel can be used in its pure form as well as blended with petroleum diesel. The commonly used biodiesel blend is B20 which is a mixture of 1:4 biodiesel: petroleum diesel. The above–mentioned advantages of biodiesel have made it a potential replacement of conventional diesel with a significant reduction in greenhouse gas (GHG) emission (Chuah et al., 2017; Piemonte et al., 2016).

2.2 Microalgae as an alternate

Microalgae biodiesel production has emerged as a potential alternative energy source with considerable obnoxious gas emission that shows its enormous application over conventional energy resources (Medeiros et al., 2015). The fast and independent seasonal growth, high productivity compared to other oilseed crops, the minimum requirement of cultivation land, utilization of wastewater and no competition with the food market has made microalgae as one of the most demanding raw material for the biodiesel production (Rajvanshi and Sharma, 2012). Hence, due to various advantages over conventional oilseed feedstocks presently the production of algae–based biodiesel is being intensively investigated by nearly every major oil company as a promising alternative for petroleum (Mascarelli, 2009).

Northeast region of India is rich in microalgae biodiversity and provide a hotspot for microalgae–based biofuel research. Microalgae species such as *Chlorella*, *Scenedesmus*, *Desmodesmus*, *Chlorococcum, Botryococcus, Euglena, Navicula, Nitzchia*, etc. are dominantly present in this region (Difusa et al., 2015; Goswami and Kalita, 2011; Kaur et

al., 2012; Talukdar et al., 2011). Several species of Northeast India have been known for their fast growth, high biomass, and oil content. The biochemical and thermal characterization of *Chlorella* species existing in this region represent 9.46 % carbohydrates, 43.22 % protein and 28.82 % of lipid suggesting its applicability as a bioenergy feedstock (Phukan et al., 2011).

Botryococcus braunii strain GUBIOTJTBB1 was reported as the first superior strain from Northeast India for biofuel application. It has high specific growth rate, huge biomass quantity and biochemical composition presenting total lipid of 57.14 % and hydrocarbon content of 52.6 % that suggested its perspective towards biofuel production (Talukdar et al., 2013).

Another high oil–producing microalgae *Chlorella ellipsoidea* in this region was cultivated in various nutrient media for biomass and lipid production. The highest biomass accumulation of 3.2 g/L was reported in BG–11 medium whereas maximum lipid accumulation was found in Wright Culture (WC) medium up to 37 % when re–inoculated from BG–11 medium to WC medium after late exponential growth phase. Additionally, *C. ellipsoidea* was also reported as a good source of carbohydrate and protein (Purkayastha et al., 2017).

Chlorella sp. FC2IITG, another microalgae isolate of Northeast, India was grown under controlled optimization condition. Maximum biomass and lipid productivity obtained was 92.7 g/L/day and 9.76 g/L/day. It has been reported that acetate enrichment to the culture medium enhances the lipid accumulation of *Chlorella* sp. (Palabhanvi et al., 2017).

A huge number of reports available in the literature where microalgae species are reported for their high biomass and lipid content. A critical review on the microalgae species and its perspective towards biofuel application was highlighted by Mata et al., (2010) suggesting the importance of biofuel production potential of various microalgae species as presented

in following Table 2.1 (a and b). The huge disparity between microalgae strain can be easily observed in their biomass and lipid content. The changes in growth profile, biomass concentration and lipid content in microalgae is a product of their genetic and environmental counter parts. Hence, there is a great scope to modulate the microalgae biochemical profile by altering the environmental and genetic factors.

Table 2.1 (a): Biomass productivity, lipid content and lipid productivity of freshwater microalgae species.

Freshwater species	**Biomass productivity (gm/L/day)**	**Lipid content (% dcw)**	**Lipid productivity (mg/L/day)**
Botryococcus braunii	0.02	25–75	–
Chlorococcum sp.	0.28	193	53.7
Chlorella emersonii	0.03–0.04	25–63	10.3–50
Chlorella protothecoides	2–7.70	14.6–57.80	12–14
Chlorella sorokiniana	0.23–1.47	19–22	44.70
Chlorella vulgaris	0.02–0.20	5–58	11.2–40
Chlorella sp.	0.02–0.25	10–48	42.1
Chlorella pyrenoidosa	2.90–3.64	2	–
Chlorella	–	18–57	18.7
Heamatococcus pluvialis	0.05–0.06	25	–
Euglena gracialis	7.70	14–20	–
Scenedesmus obliquos	0.04–0.74	11–55	–
Scenedesmus quadricauda	0.19	1.9–18.4	35.1
Scenedesmus sp.	0.03–0.26	19.6–21.1	40.8–53.90

Table 2.1 (b): Biomass productivity, lipid content and lipid productivity of marine microalgae species.

Marine species	Biomass productivity (gm/L/day)	Lipid content (% dcw)	Lipid productivity (mg/L/day)
Chaetoceros muelleri	0.07	33.6	21.8
Chaetoceros calcitrans	0.04	14.6–16.4	17.6
Dunaliella salina	0.22–0.34	6–25	116.0
Dunaliella salina	0.09	23.1	–
Dunaliella tertiolecta	0.12	16.7–71	–
Dunaliella sp	–	17.5–67	33.5
Monallanthus salina	0.08	20–22	–
Nannochloris sp.	0.17–0.51	20–56	60.9–76.5
Nannochloropsis oculata	0.37–0.48	22.7–29.7	84–142
Nannochloropsis	0.17–1.43	12–53	37.6–90
Pavlova salina	30.9	30.9	49.4
Thalassiosira pseudonana	0.08	20.6	17.4
Tetraselmis suecica	0.12–0.32	8.5–23	27–36.4
Tetraselmis sp.	0.30	12.6–14.7	43.4

2.3 Factors affecting microalgae growth and lipid accumulation

Mechanistic insight into the metabolic process in microalgae has revealed several pathways which are associated with various physicochemical factors (Singh et al., 2016). The physicochemical changes in the culture environment of microalgae tend to change its biochemical composition. Various available reports suggested that the changes in the culture medium, light intensity, pH, temperature, nutrient level and salt concentration can significantly affect the lipid quantity and quality of microalgae (Difusa et al., 2015; Rai et al., 2015; Van Wagenen et al., 2012).

2.3.1 Light

Light is an essential energy source for the autotrophic growth and photosynthetic activity of microalgae (Blair et al., 2014; Richardson et al., 1983). The flexibility of microalgae to synthesize raw material for biofuel production system is basically light driven process called photosynthesis. Microalgae utilizes atmospheric CO_2 as an inorganic carbon source and sunlight as an energy source to synthesize organic products of photosynthesis and liberate O_2 as a byproduct.

$$CO_2 + H_2O \rightarrow (CH_2O)_n + O_2 \quad 2.1$$

This is the first step of conversion of light energy into chemical energy which is eventually responsible for the production of feedstocks. The incident light energy conversion into biomass is called photochemical conversion and the conversion efficiency of light energy to biomass is regarded as photo conversion–efficiency (PCE). The light energy was absorbed by chlorophyll molecules and converted into adenosine tri phosphate (ATP) and nicotinamide adenine dinucleotide phosphate (NADPH) which were subsequently used in Calvin cycle for production of sugars, starch, oils, and other biomolecules (which collectively known as biomass), required to synthesize bioethanol, biodiesel, bio–methane and other biofuels (Schenk et al., 2008).

Moreover, microalgae have been reported to grow at various light intensities exhibiting remarkable changes in their gross chemical composition, pigment content and photosynthetic activity (Bhandari and Sharma, 2006). Light availability and distribution determines the biomass productivity of microalgae in photobioreactors. Therefore, various modelling strategies have been developed to design the photobioreactors for the maximum utilization of incident light (Naderi et al., 2017).

Synergistic effect of light intensity and nitrate concentration on growth and lipid accumulation of microalgae *Chlorella vulgaris* was investigated in a waveguide flat–plate

photobioreactor. It was found that higher light intensities favors more lipid accumulation and reached maximum up to 41.66 % dcw. Moreover, it was also concluded that composition of monounsaturated fatty acid (MUFA) content increased under high light intensity (Liao et al., 2017). The variation in light intensities and wavelengths changes the lipid metabolism in microalgae by altering the lipid profile. Cells grown under saturated light conditions accumulate carbohydrate and triacylglycerol as storage materials resulting in high content of biomass and lipid (Rodolfi et al., 2009).

The effect of light and temperature on the fatty acid composition of *Nannochloropsis salina* was investigated under a light intensity of 5–850 μmol/m^2s and 13–40 °C. The maximum biomass accumulation was obtained at 250 μmol/m^2s light intensity at 23 °C. Furthermore, an abundance of palmitic and palmitoleic acid was found during the exponential growth phase, whereas low light intensity induces unsaturated fatty acid synthesis (Van Wagenen et al., 2012).

Yeesang and Cheirsilp (2011) have investigated the effect of light intensity on biomass and lipid production of four strains of *Botryococcus sp.* named TRG, KB, SK, and PSU. They observed that biomass concentration decreased with an increase in the light intensity under nitrogen deprived condition. Moreover, the maximum lipid content was observed under the moderate light intensity of 49.5 μE/m^2s whereas the lower (33 μE/m^2s) and higher (82.5 μE/m^2s) light intensities did not show any prominent effect on lipid accumulation.

2.3.2 Temperature

Temperature is a crucial factor for algal growth. It intensely influences cellular and chemical changes, the uptake of nutrients, CO_2 fixation and growth rate of microalgae. The discrepancies in optimal cultivation temperature of microalgae reduces the photosynthetic and respiration rate due to an imbalance in the ATP requirement for metabolic process and degradation of proteins in the active center of photosystem (PS II) machinery (Sheng et al.,

2011). The fatty acid profile of microalgae drastically changes with a change in temperature. Increase in temperature reduces the total unsaturated fatty acid of microalgae which is necessary to maintain the membrane fluidity (Wei et al., 2015).

Effect of temperature (25–40 °C) on three microalgae species *Chaetoceros sp.* FIKU035, *Tetraselmis suecica* FIKU032 and *Nannochloropsis sp.* FIKU036 for the growth, lipid content, lipid profile and biodiesel properties were examined. It was suggested that the growth and lipid content of microalgae decreases with increase in temperature. Contrastingly, the PUFA content increases with increase in temperature whereas, the saturated fatty acid (SFA) content decreases in *Tetraselmis suecica* FIKU032 and *Nannochloropsis sp.* FIKU036. The highest lipid productivity was observed in *Chaetoceros sp.* FIKU035 at 25 °C to up to 66.73 mg/L/day. The biodiesel properties of *Chaetoceros sp.* FIKU035 also showed resemblance to the standard biodiesel (Chaisutyakorn et al., 2017).

In another report, it was found that increase in temperature from 20 to 25 °C increases the lipid yield two folds in *N. occulata* (7.90 % to 14.92 %) whereas an increase in 25 to 30 °C decreases the lipid content from 14.7 % to 5.90 % in *Chlorella* (Converti et al., 2009).

Further, in a study of microalgae *Scenedesmus* sp. the optimum temperature was suggested to fall in between 30–40 °C. Moreover, it was suggested that temperature above 40 °C can be detrimental to microalgae growth (Sánchez et al., 2008).

Another *Scenedesmus* sp. was studied at temperatures of 15 to 36 °C and found that at lower temperatures the chlorophyll and protein levels were reduced, while levels of carotenoids, saccharides, and lipid were increased. Moreover, at higher temperature (36 °C) presence of high amount of sugars and lipid was observed (Christov et al., 2001).

Investigation of the effect of cultivation temperature (10 to 30 °C) on the growth and lipid accumulation properties of *Scenedesmus* was performed and suggested that 20 °C

temperature is the optimum temperature for the growth under batch cultivation. It has been established that modulation in cultivation temperature changes the lipid content and also significantly alters the fatty acid profile of microalgae such as reduction in the polyunsaturated fatty acid (PUFA) content with an increase in the cultivation temperature (Xin et al., 2011).

2.3.3 pH

pH variation in the culture medium can affect algal growth in a number of ways. It can change the distribution of CO_2 and carbon availability, alter the availability of trace metals and essential nutrients. Under phototrophic culture condition the uptake of CO_2 is very slow in microalgae which causes a decrease in partial pressure of CO_2 resulting an increase in pH of the medium (Juneja et al., 2013). Fluctuations of pH in the medium also found to alter the lipid composition of microalgae. In *Chlorella* CHLOR1 the alkaline pH stress provides flexibility to the microalgae cell wall and prevent the release of auto spores thereby increasing the length of the cell cycle. The increased duration in the cell cycle is directly proportional to increase in the TAG accumulation and a corresponding decrease in the membrane lipids (Guckert and Cooksey, 1990).

The effect of pH change on growth and lipid accumulation on *Nannochloropsis salina* and resistance towards invading organisms was studied under alkaline pH conditions. It was observed that pH 8 and 9 not only enhances the growth (95.6×10^6 cells/mL) and lipid accumulation (24.75 %) of *Nannochloropsis,* but also prevent the growth of other invading algae species. Furthermore, the mechanism of pH change with photoperiod was also discussed. The day/night pH fluctuations are driven by photosynthesis and respiration, creates an environment that exhibit changing pH range. During the day, photosynthesis and use of CO_2 increase the pH and during respiration in dark reverses this process and lowers the pH. Actually, low pH causes less utilization of carbon in the medium which is a major

factor of cellular constituent development. Slight change of pH can be easily observed in a medium under same conditions by changing the photoperiod (Bartley et al., 2014).

The high pH induced lipid accumulation in *Phaeodactylum tricornutum* has been investigated. The cultures have been maintained for low pH (pH 7) and high pH stress (pH 8.5 and 9) whereas the control *Phaeodactylum* cultivation was done at pH 7.8. They observed that both low and high pH stress reduces the specific growth rate whereas increases the corresponding nile red florescence intensity. An upsurge in lipid content from control (11.21 %) to alkaline pH stress at pH 9 (55.49 %) was observed on 5 day of cultivation and from 11.78 % to 74.39 % on 6 day of cultivation, respectively (Mus et al., 2013).

2.3.4 Salt

Recently, salt stress–mediated lipid accumulation has accomplished an overwhelming attention towards microalgae biofuel production (Kim et al., 2016; Talebi et al., 2013). It has been reported that salinity significantly enhances the synthesis of neutral lipids specifically triacylglycerides (TAGs) in the form of secondary metabolite to withstand adversarial environmental conditions (BenMoussa–Dahmen et al., 2016). It was hypothesized that salinity affects the metabolism of microalgae by altering respiration rate, assimilation of nutrients and carbon uptake from the surrounding environment (Sudhir and Murthy, 2004). There are numerous reports which highlight the significant presence of various compatible molecules such as proline, glycine etc. in response to stress conditions (BenMoussa–Dahmen et al., 2016; Mohan and Devi, 2014; Solovchenko, 2012).

A study on three microalgae species, *Microcystis, Chlorococcum* and *Chaetoceros* demonstrated an enhanced lipid accumulation within seven days of cultivation in the presence of high salt concentrations of sodium chloride (NaCl). *Microcystis* and

Chaetoceros showed the highest lipid contents of 8.4 and 8.0 mg/mL respectively, followed by *Chlorococcum* species of up to 6.6 mg/mL, albeit the growth was reduced and no significant pattern of growth was observed (Asulabh et al., 2012).

The directive discrimination of carbon fluxes between starch and glycerol corresponding to the cellular compartment is also regulated by salt stress as reported in some unicellular marine microalgae such as *Dunaliella salina.* Under the stressed condition, halotolerant microalgae species increases glycerol synthesis, massive beta–carotene accumulation and increased metabolism of abscisic acid (ABA) (Cowan et al., 1995).

In another study, the presence of NaCl was reported as an effective inducer for lipid accumulation in *Desmodesmus abundans* and showed the highest lipid accumulation of 34.59 % when treated with 20 g/L NaCl, and 34.98 % with 25 g/L sodium bicarbonate ($NaHCO_3$). However, the application of sodium acetate (NaAc) and sodium sulfite (Na_2SO_3) showed a relatively less lipid accumulation (Xia et al., 2014). Similarly, *Chlorella vulgaris* also had shown lipid enhancement of up to 58.6 % under NaCl mediated osmotic stress (Duan et al., 2012).

It has been reported that increasing salt concentrations from 0.5 M to 1.0 M increases the intracellular lipid accumulation in *Dunaliella* from 60 to 67 % respectively, whereas a further increase in salt concentration from 1.0 M to 1.5 M significantly reduces the cell growth by 42 %. It was expected that there must be the possibility of microalgae cell adaptation under high salt concentration, however, the clear mechanism of salt–induced lipid accumulation is not known (Takagi et al., 2006). Some microalgae species has been represented in following Table 2.2 for the salt induced lipid accumulation.

Table 2.2: Lipid content of microalgae under various salts.

Microalgae species	Salt	Lipid yield (% dcw)	References
Chlorella CG12	$CaCl_2$	40.02	Srivastava et al., (2017)
Desmodesmus GS12		45	
Chlorella	$NaNO_{3+}$ NaH_2PO_4	54.9	Cheng et al., (2016)
Desmodesmus abundans	NaCl	34.59	Xia et al., (2014)
	$NaHCO_3$	34.98	
Chlorella vulgaris	NaCl	58.6	Duan et al., (2014)
Chlorella vulgaris	$CaCl_2$ starved	40.3	Gorain et al., (2013)
Scenedesmus obliquus	NaCl	38.7	
Dunaliella	NaCl	67	Takagi et al., (2006)

2.3.5 Nutrients

Nutrients are the essential integral components responsible for the proper metabolic functioning and photosynthetic activity of microalgae. Remarkable changes in biochemical composition and physiochemical activities of microalgae can be seen under nutrient surplus and nutrient limitation conditions. Carbon (C), nitrogen (N) and phosphorous (P) are critical nutrients for microalgae growth, therefore, an imbalance in any of the nutrient can alter metabolic activity of microalgae. Excess or limitation of any of these element alters the metabolic machinery of microalgae, for example, ample amount of N and P enhances the biomass and cell division rate of microalgae whereas their limitation in the culture media tends to synthesize neutral lipid (Chen et al., 2011). In fact, nutrient limitation is a key strategy for enhancing carbohydrate and lipid accumulation in microalgae (Juneja et

al., 2013). Hence, for this reason generally, the nutrient of the culture media is outsourced which directly correspond to the increased production cost of microalgae biodiesel.

However, wastewater derived from urban, agronomic, and industrial activities are a good source of nutrients for microalgae cultivation (Mostafa et al., 2012; Rawat et al., 2011). The ability of microalgae to use inorganic N and P for their growth provides an efficient solution to tertiary and quaternary wastewater treatment and essentially can reduce the necessity for additional N and P sources by nearly 55 % (Yang et al., 2011). Therefore, an unique advantage to combine microalgae with nutrient–rich effluent streams reduces the processing cost by consuming polluting nutrients from wastewater and thus meet the goal of sustainable fuel production (Gokulan, 2014; Zhou et al., 2012). Additionally, it also offers the possibility to recondition these nutrients into algae biomass as a fertilizer and thus can offset treatment cost (Becker, 2004).

It has been suggested that microalgae biofuel integrated with wastewater treatment is the only economically feasible approach towards commercialization of microalgae biofuel (Pittman et al., 2011). Another recent report presented the recent progress in microalgae biofuel coupled with wastewater treatment (Salama et al., 2017). Hence, it can be concluded that integration of microalgae biofuel production with waste stabilization is an effective solution to develop cost–effective and sustainable microalgae biodiesel. Utilization of waste material as a nutrient source for microalgae can additionally offset the production cost. The microalgae biomass generated while treating wastewater streams can possibly be converted to various forms of biofuels such as biogas, biodiesel, bioethanol and bio–crude oil (Medeiros et al., 2015).

Various species of *Chlorella* and *Scenedesmus* are known for their simultaneous wastewater treatment and high biomass and lipid accumulation. Wang et al., (2010) have

investigated the biomass accumulation and lipid profile of *Chlorella* sp. grown on anaerobically digested dairy manure. They observed that biomass (1.47 g/L to 1.71 g/L) and lipid content (9 % to 13.7 %) varies with the concentration of the effluent and obtained a maximum lipid productivity up to 11 mg/L/day.

In another study of *Chlorella minutissima* grown on the raw sewage showed better compatibility and growth performance in mixotrophic condition under a wide range of pH and salt concentrations. Additionally, the highest biomass productivity of 379 mg/L was also found in mixotrophic condition compared to photoautotrophic condition (73.03 mg/L) (Bhatnagar et al., 2010).

Mandal and Mallick (2011) have reported the biodiesel production potential of *Scenedesmus* species cultivated in three different waste media. They have observed the highest biomass (2 g/L) and lipid content (1.049 g/L) in *Scenedesmus* sp. cultivated using 15 g/L of municipal secondary settling tank sludge supplemented with poultry litter. Further, investigation of the fatty acid composition of microalgae revealed the presence of high amount of palmitic acid deciphering its suitability for biodiesel production. Numerous studies have been reported in the literature where microalgae were co–cultivated with wastewater in a batch or continuous bioreactor for the biomass and lipid production are summarized in Table 2.3

Table 2.3: Various microalgae species reported for high biomass and lipid yield grown under waste streams.

Wastewater	Microalgae species	Biomass productivity (mg/L/day)	Lipid content (% dcw)	Lipid productivity (mg/L/day)	References
Municipal (centrate)	*Chlamydomonas reinhardtii* (biocoil–grown)	2000	25.25	505	Kong et al., (2010)
Agricultural (digested dairy manure, 20 dilution)	*Chlorella sp.*	81.4	13.6	11	Wang et al., (2010)
Industrial (carpet mill, untreated)	*B. braunii*	34	13.20	4.5	Chinnasamy et al., (2010)
	Chlorella saccharophila	23	18.10	4.2	
	Dunaliella tertiolecta	28	15.20	4.3	
	Pleurochrysis carterae	33	12	4	
Municipal (secondary treated)	*Botryococcus braunii*	345.6	17.85	62	Órpez et al., (2009)
Agricultural (fermented swine urine)	*Scenedesmus sp.*	6	0.9	0.54	Kim et al., (2007)
Agricultural (piggery manure with high NO_3–N)	*B. braunii*	700	–	69	An et al., (2003)
Municipal (secondary treated)	*Scenedesmus obliquus*	26	31.4	8	Martınez et al., (2000)
Artificial wastewater	*Scenedesmus sp.*	126.54	12.8	16.2	Voltolina et al., (1999)
Agricultural (dairy manure with polystyrene foam support)*	*Chlorella sp.*	2.6	9	230	Jacobson and Alexander, (1981)

* Biomass productivity and lipid productivity are represented as gm^2/day and $mg.m^2$/day respectively

2.4 Optimization strategies

Conclusively, all the aforementioned reports revealed the mechanistic insight on the effect of light intensity, temperature, pH, salt concentration and nutrient requirement on the growth and lipid accumulation in microalgae cultivation. However, there are limited reports available in the literature where a combinatorial effect of all the influential factors have been investigated (Breuer et al., 2013; Difusa et al., 2015). Therefore, to understand the effect of the medium, salt concentrations and environmental factors the use of statistical model based tool are becoming quite popular.

Earlier the optimization studies were preferably conducted by considering single parameter. This conventional method have very low accuracy level due to less experimental iterations and combinations. Moreover, considering only single factor in bioprocess system could not be able to define the exact expression or response (Figure 2.1). Additionally, it also faces irregular data representation and lacks reproducibility. Therefore, with time various advanced statistical optimization tools were incorporated in designing experiments for the better understanding on effect of multiple variables for output responses. Response surface methodology (RSM), Artificial neural network (ANN), Aspen, Hysys and Genetic algorithm (GA) are some statistical and mathematical tools commonly used in prediction of response under defined culture condition regime (Pankaj and Awasthi, 2014; Tran et al., 2010; Wu and Shi, 2007).

These mathematical tools are able to define both linear and non–linear interaction expression and can accurately defines the behavior of system. Some expression are used for local generalization such as RSM and ANN whereas some are used for global optimization of parameters such as GA.

The in–depth investigation of a physical and chemical phenomenon occurring in a process environment is the key to develop a successful design. The integrated biological system with the mathematical and statistical network would not only enhance the production yield but also reduces the overall production cost and time required for algae cultivation.

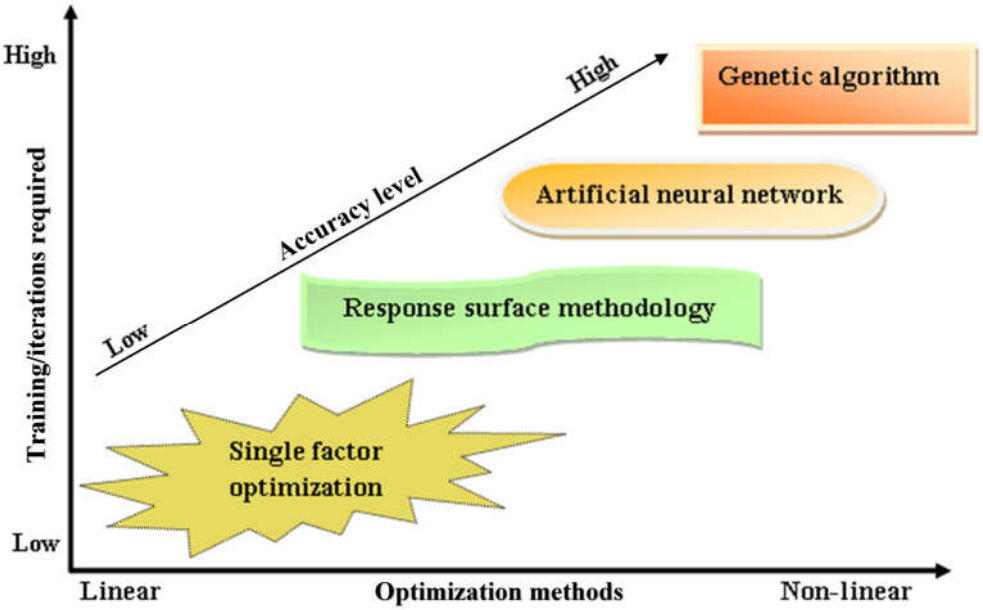

Figure 2.1: Various optimization methods used for response prediction.

Traditionally, optimization of single influential factor one at a time is usually performed during microalgae cultivation. However, the fact is, that the response of microalgae is a product of various physicochemical factors. Therefore, it is difficult to decide that among all the selected parameters which one is most significantly affecting the microalgae behavior. Moreover, single factor optimization is time–consuming, tedious process and gives erroneous results (Marudhupandi et al., 2016). Therefore, advanced integrated process system has been adopted to improve production yield of microalgae oriented products.

The advantage of integrated process system is that it accurately defines the problem in the form of the mathematical model and therefore provide a pool of best suitable

alternative responses (Seferlis and Georgiadis, 2004). In the algae culture system, RSM coupled with central composite design (CCD) is popularly used as a tool to model the probable curvatures as measured responses and provides good fitting to the linear responses (Saeidi et al., 2016). Additionally, RSM was used as a decision–making tool for optimization of culture conditions of green microalgae *Chlorella* sp. for biodiesel production where nitrate, phosphate, glucose, and pH of the medium are considered as effective parameters for lipid induction in microalgae. The most significant increase in lipid production (dry cell weight basis) occurred at limited concentrations of nitrate and phosphate, 1 % (wt.) glucose and pH 7.5. The addition of nitrates during the mid–lag and mid–exponential phase showed the maximum inhibitory effect on lipid accumulation and the presence of yeast extract led to a further enhancement of lipid accumulation. Among all the tested media, BG–11 was found to be the best medium for chlorophyll content and algal biomass production. A significant increase in algal biomass was observed in BG–11 supplemented with bicarbonate and 1 % (wt.) glucose (Kirrolia et al., 2014).

Cheng et al. (2013) have also done the statistical optimization of culture media for growth and lipid production in *Chlorella protothecoides* UTEX250. The concentration of $NaNO_3$, $MgSO_4.7H_2O$, and proteose, in the culture medium, was optimized by RSM using Box–Behnken design (BBD). The optimal concentrations found were 0.45 g/L of $NaNO_3$, 6 mg/L of $MgSO_4.7H_2O$, and 0.25 g/L of proteose for maximum biomass production of 1.19 g/L and 2 mg/L of $MgSO_4.7H_2O$ and no addition of $NaNO_3$ and proteose for lipid accumulation. At the optimal condition, biomass concentration obtained was 1.19 g/L, which was 1.8 times higher than obtained in the original medium. Whereas, in lipid production medium a lipid content obtained was 12.9 % dcw, which was three times higher than of original medium. The fatty acid profile of

algae grown in the optimized medium demonstrated a higher unsaturated fatty acid content of methyl linoleate (C18:2) and methyl linolenate (C18:3) than that of the algae grown in an original medium.

Although, RSM has been popularly used as a statistical and mathematical design tool. However, the limitations of RSM technique is that it requires some preliminary experiments to set the selection range, cannot predict non–linear relationship and response for the unseen data. Whereas, ANN can predict response to the unseen data and therefore, is being progressively applied in various bioprocess optimization systems to overcome the problems associated with RSM for both linear and non–linear responses (del Rio–Chanona et al., 2016).

ANN is the highly interconnected network of processing elements (neurons) capable of massive parallel computations, representing a data–centric modeling inspired by the biological nervous system. It fundamentally transforms the inputs that passes through a network of neurons with weighed interconnection into the output, predicted to the best of its ability (Ahmad et al., 2013). ANN is more flexible and does not impose any restriction on the type of relationship governing the dependence output parameters on various running conditions (Garcíaa-Gimeno et al., 2003). It can also perform a task which is unpredictable by linear programming. Therefore, in the last two decades for non–linear multivariate modeling ANN proved to be an effective tool. Conceptually, ANN requires a huge number of data sets for the model fitting, thus the data generated by RSM should be sufficient to build an effective ANN network.

In a comparative study for optimization of biodiesel from Mahua oil using RSM and ANN, ANN offered better prediction capability compared to RSM. It was also suggested that ANN can be chosen to optimize the process parameters and can accurately explain the non–linear relationship (Sarve et al., 2015).

Furthermore, Maran and Priya (2015) have selected RSM and ANN optimization for ultrasound–mediated intensification of biodiesel production in neem and muskmelon oil. They have observed high response prediction capability of ANN compared to RSM. Most of the optimization studies carried out so far are primarily on downstream processing of microalgae biodiesel. Still, limited reports are available in the literature, where, RSM and ANN models are developed and studied together for the optimization of the upstream process of microalgae culture conditions for biofuel production (Dineshkumar et al., 2015).

Uptill now, most of the biodiesel production optimization studies primarily conducted using RSM and ANN based approaches. Nevertheless, the problem with these two optimization methods (RSM and ANN) is their local approximation generalization. However, the individual experimental setup for local estimation is not feasible for the process system engineering due to the huge expense of energy and time. Therefore, GA is one such technique to provide a global optimum condition. It is a prerequisite for developing optimization model to look after local optimization problems. Furthermore, the genetic algorithm provides a condition for global optimization for both linear and non–linear programming. GA is used for stochastic optimization with an aim to minimize the objective function based on Darwinian Theory of "survival of the fittest" (Li et al., 2013). It creates solutions for the problem available in search space using its genetic operator, selection, crossing over and mutation (Fayyazi et al., 2015). In the recent years, GA based on RSM and ANN models (as an objective function) have been applied successfully to optimize the input space of a bioprocess where RSM and ANN generated second–order polynomial equation was used as a fitness function (Muthuraj et al., 2015; Prabhu and Jayadeep, 2016).

A genetic algorithm is not function optimization technique but it is a simple and powerful general purpose stochastic optimization. The main advantage of GA is that it uses stochastic operators instead of deterministic rules to reach the solution. Furthermore, GA considers many points in the search space simultaneously in–spite of determining a single point thereby reducing the chance of converging to local minima (Fayyazi et al., 2015). The input data processed by GA is used to create an initial population (set of a possible solution) either randomly or heuristically. The structure of the population is chosen by a randomized selection process which ensures that the expected number of times a structure chosen is approximately equal to the structure's performance (fitness) relative to the rest of the population. The less fit individuals in the population die during the selection process. Further, to search other points in space some variations are introduced into the new population by using idealized recombination (translational) operators (eg. Crossovers, mutation). Therefore, over the generation, the best fit individual population survives and the best suitable optimized condition is generated globally (Kadiyala et al., 2010).

Hence, from the above discussion it is proposed that computational intelligence techniques (artificial intelligence) are efficient modeling tools used in optimization, process intensification, supervision and control of biodiesel production centered on global optimization method. Nowadays, the process system engineering becomes essential for establishing sustainable and less energy intensive method (Nasir et al., 2013; Nicoletti et al., 2009).

2.5 Conversion of oil to fatty acid methyl ester

Fatty acid methyl esters (FAME) are a type of fatty acid ester that are derived by transesterification of fats with alcohol (methanol/ethanol). The molecules in biodiesel are primarily FAMEs, usually obtained from vegetable oils by transesterification.

Conventionally transesterification (vegetable oils) is carried out using homogeneous (sulfuric acid, sodium hydroxide, and potassium hydroxide), heterogeneous (sulfated zirconia, MgO, CaO, etc.) and enzymatic (lipase) catalysts (Meher et al., 2006). The transesterification process is the reaction of a triglyceride (fat/oil) with an alcohol to form esters and glycerol as shown in Figure 2.2. A successful transesterification reaction is signified by the separation of the methyl ester (biodiesel) and glycerol layers after the complete reaction. However, this crude biodiesel requires some purification prior to use.

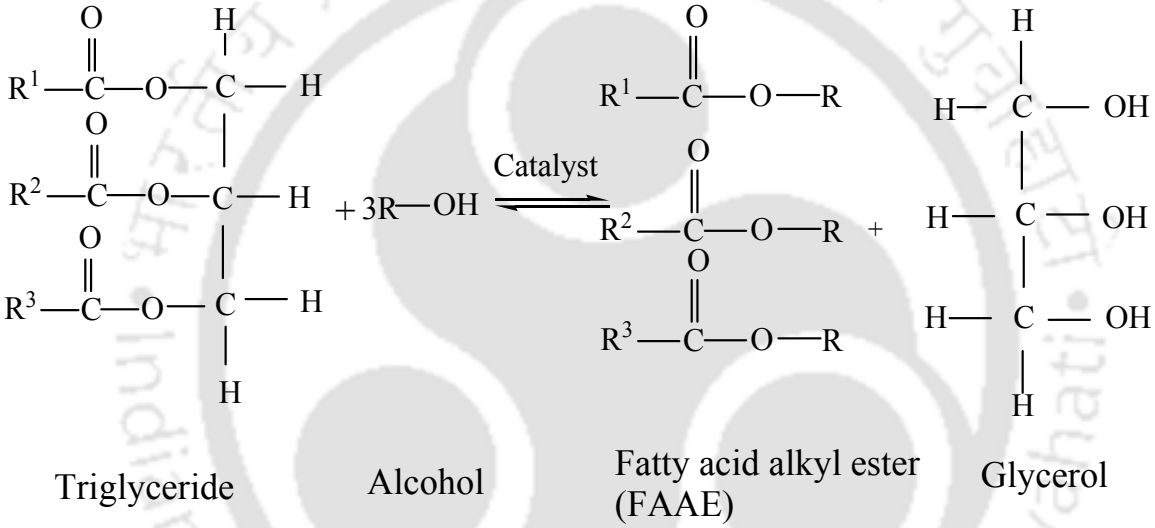

Figure 2.2: The empirical reaction of transesterification.

The conventional process of transesterification has several drawbacks such as usage of catalysts, high energy consumption, production cost, complicated purification and separation process, the necessity to reduce free fatty acid content and release of hazardous chemicals to the environment (Lee et al., 2012). Therefore, various technologies have been adopted for biodiesel production for improved recovery, intensification, and waste reduction by process system engineering (Banos et al., 2011; Nasir et al., 2013). Various transesterification methods used for conversion of microalgae oil to biodiesel has been represented in Table 2.4.

Table 2.4: Transesterification methods employed for conversion of microalgae oil to biodiesel.

Feedstock	Method	Transesterification yield (%)	References
Chlorococcum	Lipase	–	Prabakaran et al., (2018)
Chlorella	Lipase	98	Gumbytė et al., (2018)
Chlorella CG12	SCM	98.12	Srivastava et al., (2018)
Nannochloropsis	MW+US	48	Martinez-Guerra et al., (2018)
Chlorella minutissima	H_2SO_4 Nb_2O_5/SO_4	96.5 98	Loures et al., (2018)
Chlorella sp. BDUG 91771	H_2SO_4	44.9	Mathimani et al., (2015)
Chlorella protothecoides	SCM SCE	90.8 87.8	Nan et al., (2015)
Scenedesmus	MW+WO_3/ZrO_2 US+WO_3/ZrO_2	71 52	Guldhe et al., (2014)
Nannochloropsis	MW	–	Patil et al., (2012)
Nannochloropsis oculata	CaO/Al_2O_3	97.5	Umdu et al., (2009)

Application of microwave and ultrasound are explored for better results compared to conventional transesterification methods. A comparative study on the transesterification reaction of cotton seed oil using KOH catalyst (1.5 wt %) with 6:1 molar ratio of methanol to oil showed improved yield in a lesser duration in the case of microwave assisted process (92.4 % in 7 min reaction time) than conventional process, 91.4 % in 30 min. reaction time (Azcan and Danisman, 2007).

Due to the immiscible nature of reactant compounds alcohol and triglycerides of vegetable/algal oil, a contact surface area between the reactants is only at the interface and hence causes a lower reaction rate. An ultrasonic phenomenon in a reactive solution increases the liquid–liquid interfacial area, which is important to enhance the rate of transesterification reaction. During ultrasonic irradiations vapour bubble in methanol and cavitation in vegetable oil are generated ultrasonically. Mostafaei et al., (2013) have reported an improvement in the conversion of waste cooking oil to methyl esters using ultrasonic approach (89 % yield) compared to conventional stirrer technique (50 % yield).

Moreover, to overcome these limitations of conventional transesterification process recently a catalyst–free method of supercritical methanol (SCM) transesterification was introduced by Japanese researcher (Kusdiana and Saka, 2001). Under supercritical conditions, short chain alcohols such as methanol and ethanol are hydrophobic and triglyceride dissolves well in them (Qiang Li et al., 2013). Hence, there is no issue of soap formation, catalyst efficiency and consumption as well as yield of biodiesel (Borugadda and Goud, 2012; Warabi et al., 2004). The SCM for conversion of oil to FAME and is devoid of the usage of the catalyst. It also reduces the experimental runtime and processes high free fatty acid containing feedstock which was earlier not feasible to process by conventional base–catalyzed method (Wei et al., 2013).

Fluids above its critical temperature and pressure conditions, under compressed state, behave as a supercritical fluid and act as a good solvent for many substances. The critical temperature and pressure conditions for methanol are 239 ^{o}C and 8.09 MPa. At this supercritical state, methanol behaves as a non–polar solvent and is capable of dissolving oil sample uniformly (Kusdiana and Saka, 2001). Moreover, the conversion achieved by supercritical methanolysis is relatively higher than ethanolysis (Vieitez et

al., 2010). However, there are various reaction parameters that affect SCM transesterification process *viz.* reaction temperature, reaction pressure, residence time, MeOH: oil molar ratio and mixing intensity which has been illustrated in Table 2.5. Recently the advantages of SCM over standard homogenous base catalyzed method have been systematically studied by Sawangkeaw et al. (2010) and it has been proposed that extreme reaction conditions of high temperature (320–350 ^{o}C), pressure (19 to 45 MPa) and MeOH: oil molar ratio (40:1 to 42:1) should be maintained for high biodiesel yield.

Table 2.5: Effect of reaction process parameters on SCM transesterification.

Oil sample	**Temperature (^{o}C)**	**Time (min)**	**MeOH:oil (molar ratio)**	**FAME[#] (%)**	**References**
Chlorella CG12	285	26.57	23.47	98.12	Srivastava et al., (2018)
Tobacco	300	90	43:1	92.8	García et al., (2017)
Canola oil	350	15	40:1	96.5	Farobie and Matsumura, (2015)
Palm oil	400	20	12:1	90	Sakdasri et al., (2015)
Microalgae oil	320	31	19:1	90.8	Nan et al., (2015)
	340	35	33:1	87.8	
Jatropha oil	350	10	40.1	84.6	Samniang et al., (2014)
Algae	265	20	9:1*	67	Reddy et al., (2014)
Rapeseed oil	350	15	42:1	93	Micic et al., (2014)
WCO[$]	287	30	41:1	99.6	Demirbas (2009)

*wt./vol. ratio, [$]waste cooking oil, [#]conversion efficiency

However, another report suggests that extreme reaction conditions may lead to thermal degradation of FAME. SCM transesterification performed at extreme temperatures

between 325 °C to 420 °C with saturated (16:0 and 18:0) and unsaturated (18:1) fatty acids unveiled thermal decomposition of FAME due to isomerization, hydrogenation, and pyrolysis (Shin et al., 2011). Therefore, several researchers have suggested high MeOH: oil molar ratio to reduce this extreme temperature. Thus, in SCM transesterification process 42:1 molar ratio of MeOH: oil is preferred to avoid the excessive rise in temperature. However, excess methanol is the major nuisance for the development of SCM process at industrial scale. Therefore, development of techno–economical and eco–friendly SCM process is essential for the sustainable production of biodiesel.

2.6 Microalgae biorefinery

The biorefinery concept has been identified as the most promising way to create a biomass–based industry. Microalgae are classified as promising candidates in biorefinery processes because they are particularly important for obtaining multiple products. Algae are not only promising as waste converters and recyclers. The algal cell contains many useful substances and microalgae are cultivated increasingly for the production of valuable raw materials. For example, it is possible to produce oil, proteins, starch and pigments (e.g., beta–carotene). Applications of these materials are numerous, ranging from biodiesel and bioplastics to colorants and hamburgers. Indeed the key challenges toward commercial deployment from the technical and economical point of view have to be addressed. Biodiesel production from microalgae produces approximately 60–70 % of residual biomass as a byproduct. Therefore coupling of microalgae biodiesel with bioethanol or biogas production can be a better solution for commercialization of microalgae biofuel. Certainly, the microalgae residue remained

after lipid extraction is a competent raw material for methane production which recovers more energy than energy obtain only from microalgae oil (Sialve et al., 2009). A typical composition of microalgae biomass can be represented as $CO_{0.48}H_{1.83}N_{0.11}P_{0.01}$ (Chisti, 2007). However, this excessive amount of N and P do not add any benefits to environmental, economic and sustainable aspect towards biofuel production. Hence, if the anaerobic digestion is coupled to process algae waste generated from biodiesel production, it will not only reutilize nitrogen and phosphorous but also produces methane. The energetic balance of the microalgae biofuel process can be developed by the high calorific value of methane (Uggetti et al., 2017). Hence combining biodiesel production with biogas would definitely suffice the energy demand in an economically viable manner.

Nonetheless, in present time the microalgae anaerobic digestion (AD) is not a well–established technology as it faces many challenges, most significantly low concentration of substrate (due to less biomass accumulation of microalgae), poor cell wall degradability and low carbon to nitrogen (C/N) ratio (Ward et al., 2014). Golueke et al., (1957) have first reported a methane yield of 170–320 mL/g VS from AD of microalgae *Chlorella* and *Scenedesmus* grown on wastewater. They observed the low methane yield up to 30 days of hydraulic retention time (HRT) due to less biomass concentration and poor digestibility of microalgae cell wall.

Further, disconcerting in microalgae AD is lower C/N ratio. A typical C/N ratio in microalgae ranges from 4.16 to 7.82, however, an optimal C/N ratio of 20–30 is a prerequisite for anaerobic microflora for efficient biogas production. The disproportion of C/N ratio below 20 leads to noxious ammonia (NH_3) secretion in the digester that has the inhibitory effect on the methanogenic bacteria resulting in a discrepancy of volatile fatty acids (VFA) accumulation in the digester (Sreekrishnan et al., 2004; Wang

et al., 2012). Hence, to meet these challenges researchers have explored the anaerobic co–digestion (A–CoD) process, where microalgae have been co–digested with other waste streams or biomass to increase the substrate loading capacity and C/N ratio. The main idea of co–digestion is to mix different substrates and solve issues related to an AD on a single substrate (Table 2.6). The co–digestion of different environmental wastes showed that better methane generation potential can be achieved by using an optimum ratio of the substrates, than using a single organic material (Lee et al., 2013).

Yen and Brune (2007) have used paper waste to improve C/N ratio of the microalgae *Scenedesmus* and *Chlorella* from 6.7 to 36.4. They observed the best co–digestion with 1:1 ratio of paper and microalgae biomass with final C/N ratio of 18 resulting in 50 % increase in biogas production compared to digestion of only microalgae biomass. They also suggested that for better biogas production, the optimum C/N ratio must lie in between 20:1 to 25:1.

India, as one of the biggest agricultural country, produces millions of tons of rice residue each year. It is to be noted that for every ton of rice harvested, 1.35 tons of rice straw (RS) remain in field unutilized with high energy potential. Direct incorporation of rice residue into soil may lead to deteriorating the soil conditions and releases methane gas to the atmosphere which is 23 times more potent greenhouse gas than CO_2. Hence, this connexion of microalgae biomass with agriculture residues such as rice straw, wheat straw (WS), rice husk (RH) etc. will boost the net biogas yield. This assemblage upsurges the loading capacity, HRT, balances the C/N ratio and also decreases the NH_3 toxicity occurred in microalgae AD. Furthermore, the digested sludge can be reutilized for microalgae cultivation. Hence, the coupling of microalgae biodiesel with biogas generation will be a virtuous option for zero waste energy generation process. Co–digestion of microalgae biomass with agriculture residues

potentially paves a way not only for biogas production but also as microalgae biorefinery which involves utilization of microalgae as a raw material for various biofuel production (Cheng et al., 2014; Lee et al., 2013; Solé–Bundó et al., 2017).

Moreover, the organic matter composition has a profound effect on anaerobic digestion that delimits the relationship between the organic matter used and biomethane potential, which is based not only on its biodegradable fraction but also on the non–biodegradable fraction. There is an empirical relationship between the biochemical, organic and elemental composition of the substrate with the methane potential (Park and Li, 2012). Therefore, based on the elemental composition the theoretical methane potential can give a clear insight into maximum methane production from the specific substrate. Additionally, researchers have evolved various strategies of BMP co–digestion using mathematical models and expressions to save cost and experimental runtime. Mathematically, the degradation rate of each group of compounds can be described by a differential kinetic equation. The knowledge of the biodegradation kinetics and methane production could be helpful for the methane prediction from a specific substrate and can provide information for optimum mixing to improve bio–methane potential (Cecchi et al., 1991).

Table 2.6: Microalgae species co–digested with various biomass for methane production.

Microalgae	Co–digestion	HRT (days)	BMP (mL/g VS)	References
Spirulina platensis#	–	30	290	Sumprasit et al., (2017)
Chlorella sorokiniana#	–	42	253	Ayala–Parra et al., (2017)
Scenedesmus residue	–	–	100–140	Uggetti et al., (2017)
Chlorella vulgaris	Cattle manure	90	415	Mahdy et al., (2017)
Scenedesmus			163	
Scenedesmus#	Pig manure	70	192	Astals et al., (2015)
*Scenedesmus**			102	
Nannochloropsis	Corn sialge	225	280	Schwede et al., (2013)
Chlorella	WAS	45	262	Wang et al., (2012)
Taihu blue algae	Corn straw	30	325	Zhong et al., (2012)

defatted biomass, WAS waste activated sludge, RS rice straw, * protein extracted

From the above discussion, it is clear that huge efforts have been made for microalgae biodiesel production. All the major facets of culture condition optimization for increasing biomass and lipid productivity was investigated by several researchers. Most of the studies have been carried out in improvising the downstream processing steps and incorporation of the various novel and advanced process technologies to attain high biodiesel yield.

Moreover, it was proposed that an integration of phycoremediation with concurrent biodiesel production could be the only possible route for sustainable fuel synthesis. Hence, the other biofuel potentials of microalgae biomass were appraised in literature incorporating the concept of microalgae biorefinery. All the above discrete reports

showed immense efforts towards establishing the sustainable microalgae biodiesel production. Though, with that great efforts the microalgae biodiesel is not yet marketed and lag behind the conventional biodiesel production processes. Most of the studies do not consider the economic aspect of microalgae biofuel production process. The comprehensive review of the literature suggests that very few measures have been taken for microalgae biofuel marketing considering techno–economical aspect.

Till today no complete report has been presented where all the aspects of enhancement of productivity, reduction of processing steps and utilization of waste in a biorefinery concept have been dealt. The consolidation of all the aforementioned exertions can be a good measure to develop a technical, economical and sustainable microalgae biodiesel. Hence, the present thesis put the effort and tried the best to cover all the major challenges of microalgae biodiesel commercialization.

2.7 Research gap

Microalgae showed its immense application for biofuel synthesis. It has various added advantages such as fast growth rate, easy cultivation, independence of seasonal variation, waste remediation and synthesis of value–added chemicals and fuels. Still, the microalgae biofuel is not yet commercialized. The main reason for such techno–economical barrier is high processing cost of microalgae biofuel. There are several challenges to overcome to make microalgae biofuel economic and sustainable. The main hurdles of microalgae biodiesel commercialization can be overlooked by strategic planning. The major research gap of microalgae biodiesel commercialization are as follows:

1. Lack of information on upstream processing
2. Lack of careful hybrid optimization studies

3. Most of the study used artificial media for microalgae cultivation which unnecessarily increased the production cost.
4. Integration of co–product synthesis along with biodiesel is prerequisite to make sustainable microalgae biodiesel.

2.8 Objectives

Basically, the main motivation of this thesis is to design a zero waste energy production system in an economical and eco–friendly manner. The process developed in this thesis also provides a solution to potential microalgae biodiesel problems. Hence, to overcome the major limitation of microalgae biodiesel, the objectives of the present study have been designed as:

1a. Maintenance of axenic culture of microalgae, identification and growth study under various physical (light, temperature, and pH) and chemical conditions (BG–11, BBM, AM, Chu).

1b. Further, optimization of physical and chemical parameters using RSM to find out global optimum parameters and its validation using ANN.

2. Effect of various salts concentrations on growth and lipid accumulation in microalgae.

3. Scale up studies and conversion of microalgae oil to biodiesel via supercritical methanol transesterification.

4a. Comparative growth study of microalgae species grown in the waste medium for biomass and lipid production (biogas plant waste, cow dung, and vermicompost).

4b. Further, optimization of waste medium, physical and chemical parameters using RSM to find out global optimum parameters and its validation using ANN.

5. Reutilization of microalgae residues for sustainable biorefinery development.

2.9 Thesis organization

The work in this thesis has been presented in following chapters. Moreover, the potent problems and their possible solutions have also been suggested in this thesis.

Chapter 1 presents the general introduction of alternative energy demands, biofuels and suitable techniques for the production of biofuels from microalgae. The motivation to pursue the present work has been represented and background information on the major problem related to energy security and the present energy status of the country has been elaborated.

Chapter 2 involves a comprehensive review of literature considering following major aspects of microalgae biofuel production:

i. Present status of microalgae biofuel, advantages and applications,
ii. Factors affecting microalgae growth, biomass and lipid accumulation,
iii. Optimization strategies involved in the enhancement of lipid productivity,
iv. Conversion of microalgae oil to biodiesel,
v. Utilization of residual biomass for co–product synthesis.

Overall these chapters provides the complete direction of this Ph.D. research.

Chapter 3 includes the detailed list of material and methods applied during the thesis work. The methodology chosen for the study is solely based on the literature review. Standardization, optimization, statistical analysis, and product confirmatory analysis were done according to the experimental demand of the work.

Chapter 4 dealt with the isolation, characterization and a preliminary selection of potent species obtained from the wetland of Assam, India. The isolated strains were screened based on its dominancy, growth and biochemical compositions for potential utilization as renewable biomass feedstock for biofuel production. Further, preliminary experimentation strategy was discussed to study the growth profile of selected microalgae species under various physical (light, temperature, and pH) and chemical conditions (BG–11, BBM, AM, Chu). The study also involves further optimization of cultivation conditions (physicochemical parameters) obtained from preliminary experimentation by design of experiment to prepare an experimental matrix using RSM followed by CCD. The interactive effect of parameters on the lipid accumulation of microalgae and optimization of process parameters are also presented in this chapter.

Chapter 5 from the last chapter it was found that optimization of cultivation conditions (i.e. physicochemical parameters) could enhance the lipid in microalgae but the increase was not significant. In this chapter, attempts are made to study the impact of salt concentrations on lipid accumulation of microalgae.

Chapter 6 deals with the mass cultivation of high lipid content microalgae and conversion of microalgae oil to biodiesel using supercritical methanol transesterification.

Chapter 7 illustrates utilization of different waste streams (*viz.* biogas plant waste, cow dung and vermicompost) for microalgae cultivation for efficient growth and lipid production and simultaneous waste stabilization. This chapter provides a solution for simultaneous waste remediation and sustainable fuel production. With this facts present study discusses optimization of cultivation condition using the waste stream for enhanced lipid synthesis.

Chapter 8 addresses the issue related to microalgae residues generated as waste after extraction and transesterification the microalgae lipid. This chapter aims at the utilization of residual microalgae biomass for co–product synthesis in order to develop microalgae–based sustainable biorefinery.

Chapter 9 describes the Overall Conclusions and Scope of Future Work.

Schematic workflow of the thesis

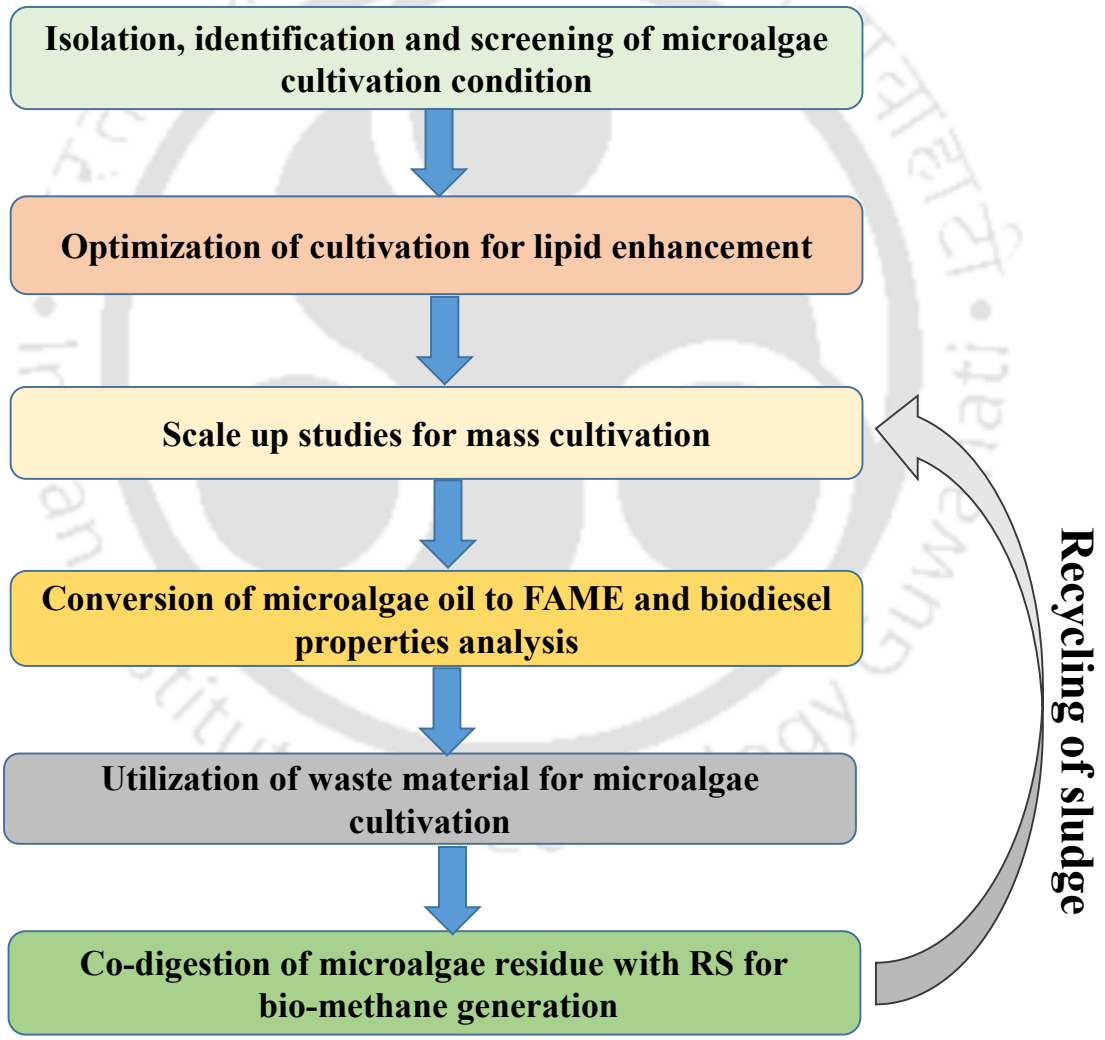

CHAPTER 3

MATERIALS AND METHODS

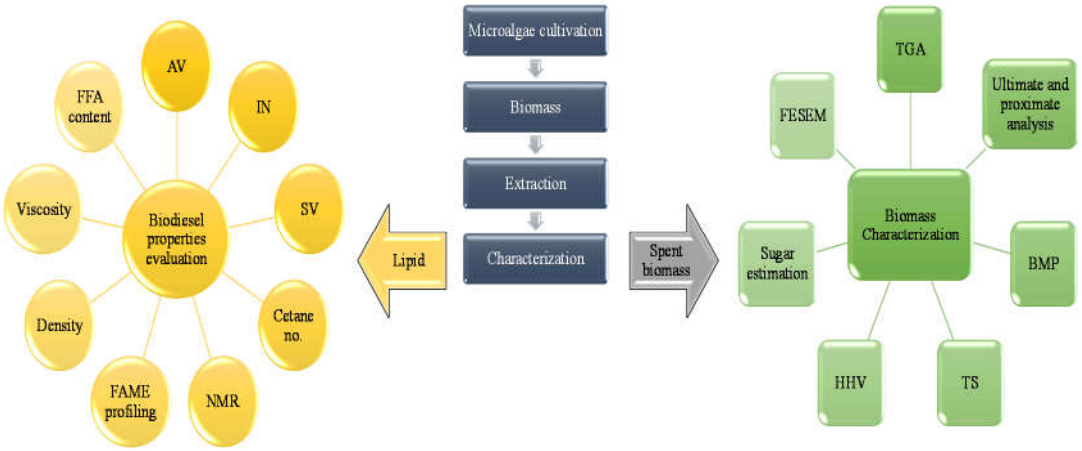

Materials and methods

In this chapter, the details of material used, experimental methods and procedures are described. During growth study of microalgae and transesterification process, response surface methodology (RSM) with central composite design (CCD) and artificial neural network (ANN) was applied for parameter optimization. The analytical techniques such as ^{1}H NMR, GC–MS, TGA, FTIR, and acid value are extensively used for product confirmation and quality assessment.

3.1 Materials

3.1.1 Chemicals

The chemicals employed for the present study were procured from M/s Merck India Pvt. Ltd. and M/s Himedia. Various salts such as NaCl, KCl, $MgCl_2$, and $CaCl_2$ used for stress study and solvents for lipid extraction such as chloroform and methanol were also procured from M/s Merck India Pvt. Ltd. with 99.4 % purity. Nile red dye (9–diethylamino–5H–benzo [alpha] phenoxazine–5–one) (catalog no. RM9734) was purchased from M/s Himedia. $CDCl_3$ for NMR analysis was procured from M/s Merck India Pvt. Ltd.

3.1.2 Media composition

Four different medium blue–green medium–11 (BG–11), Bold's basal medium (BBM), Allen medium (AM) Chu–13 medium prescribed by Culture Collection of Algae and Protozoa (CCAP) was chosen to cultivate microalgae in order to achieve high lipid production. Out of these only two media, BG–11 and BBM were found supportive of microalgae growth and lipid accumulation and hence, used for further study. These media components include all the macro and micro nutrients which are responsible for

the luxuriant growth of both the microalgae. The media compositions of BG–11 and BBM used in this study are as follows:

Table 3.1: Media composition of BG–11 and BBM medium used for microalgae cultivation.

Macro–nutrients	**BG–11 Stock (g/500mL)**	**BBM Stock (g/400mL)**	**Working volume (mL/L)**	
			BG–11	**BBM**
$NaNO_3$	7.5	10	100	10
$MgSO_4.7H_2O$	3.75	3	10	10
NaCl	–	1	–	10
K_2HPO_4	2	3	10	10
KH_2PO_4	–	7	–	10
$CaCl_2.2H_2O$	1.80	1	10	10
Citric acid	0.30	–	10	–
Ammonium ferric citrate green	0.30	–	10	–
Na_2EDTA	0.05	–	10	–
Na_2CO_3	1	–	10	–
Micro–nutrients				
$ZnSO_4.7H_2O$	0.22	8.82	1mL	
$MnCl_2.4H_2O$	1.81	1.44		
MoO_3	–	0.71		1mL
$CuSO_4.5H_2O$	0.08	1.57		
$Co(NO_3)_2.6H_2O$	0.05	0.49		
H_3BO_3	2.86	11.43		1mL
EDTA	–	50		1mL
KOH		31		
$FeSO_4.7H_2O$	–	4.98		1mL
H_2SO_4 (conc.)		1mL		

3.1.3 Samples collection from waste stream

Instead of using synthetic medium some waste materials such as cow–dung (CD), biogas plant digested sludge (BPD) and vermicompost (VM) were used for media formulations. The effect of these media compositions on the cell growth and lipid accumulation of selected microalgae strains was carried out at various dilution from 10 % to 30 %. The cow dung used in this study was collected near K.V. gate of IIT Guwahati. Biogas plant digested sludge was obtained from the anaerobic digestor unit, technology complex, IIT Guwahati, and vermicompost samples were obtained from Civil Engineering Department, IIT Guwahati. All the sample obtained were in semi–dried form.

3.1.4 Isolation of microalgae

The freshwater microalgae samples were collected from water bodies near Gauhati University, 26.1539° N 91.6622° E India. The mixed consortia of algae and bacteria present in water samples were serially diluted to obtain axenic microalgae strains. The 1 mL inoculum of the sample was diluted into 9 mL of distilled water up to 10^5 dilutions and plated on agar plates depicted in Figure 3.1. The single microalgae colonies observed on plates were used for further examination and confirmation of single microalgae.

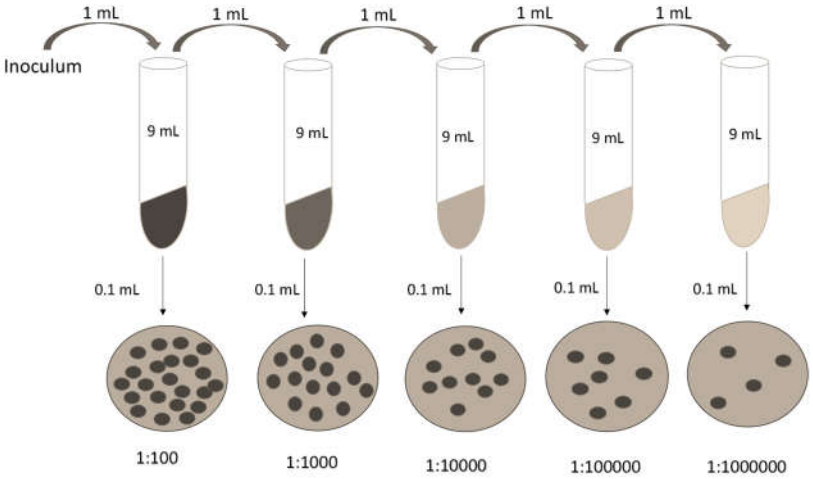

Figure 3.1: Isolation of microalgae by serial dilution method.

3.2 Experimental techniques

3.2.1 Species identification

The species identification was performed on cellular, biochemical and genetic organization. The morphological identification was done by light microscope (Labomed TCM 400) and Field–Emission Scanning Electron microscope (FESEM, Carl Zeiss SIGMA VP, Germany). Species identification was performed on the growth pattern, pigmentation, cell size, and shapes, however, shape and size of the cell usually vary with nutrition, age and other environmental factors. Therefore, for molecular identification the pure cultures of microalgae were sent to Zeal Biologicals, Hyderabad, India for 18S rDNA sequencing. The presence of conserved and variable regions in the ribosomal genes (rDNA) has paved a possible way of species identification and phylogenetic relationship (Ghosh et al., 2016; Wu et al., 2001). The sequences obtained were further processed by multiple sequence alignment tool and based on sequence similarity phylogenetic tree was constructed using MEGA 6.0 software.

3.2.2 Growth study

Optical density was measured at 680 nm for monitoring the algal growth in batch culture up to 21 days. Each sample was measured three times and the average value was processed in the analysis. The growth rate (μ) was calculated with the following equation (Eq. 3.1):

$$\mu = \ln \frac{(X_2 - X_1)}{(t_2 - t_1)} \quad 3.1$$

Where, X_1 and X_2 are cell densities at time t_1 and t_2, respectively.

The time required to achieve a doubling of the number of viable cells is termed as doubling time (T_2), which was calculated by using Eq. 3.2.

$$t_g = \frac{0.6931}{\mu} \quad 3.2$$

3.2.3 Total chlorophyll content

Total chlorophyll content was estimated by Mackinney method (Mackinney, 1941). Cells were centrifuged and washed with distilled water. After the removal of water, 1 mL of methanol was added. The sample was homogenized, kept in a water bath at 60 °C for 10 min and centrifuged afterward. The optical density of the supernatant was measured at 665 nm and the total chlorophyll content was calculated using the following equation:

$$\text{Chl } (\mu g/ml) = O.D._{665} \times 13.9 \quad 3.3$$

3.2.4 Nile red staining

Nile red staining was practiced for localization of intracellular lipids in microalgae as it is considered an excellent staining dye for lipid detection through fluorescence microscopy (Carl Zeiss AXIO SCOPE A1, Germany). The stock concentration of 1

mg/mL was prepared in DMSO which was diluted accordingly for the final working concentration of 1 µg/mL. In staining procedure, 1:100 ratio of dye and algal cells was maintained throughout all the measurements.

3.2.5 Lipid extraction and quantification

The lipid extraction for all the experiments was performed by Bligh and Dyer (1959) method with slight modifications. The dried microalgae biomass was soaked overnight in the solvent mixture of $CHCl_3$: MeOH: H_2O (1:2:0.8 v/v). The oil extraction was performed manually in a pestle mortar and centrifuged at 6000 rpm for 10 min. The lower heavy $CHCl_3$ and oil phase recovered at the bottom was washed with 0.9 % NaCl solution to remove all debris. Subsequently, the oil samples were poured in pre–weighed dried vials and vacuum dried to remove the trace of solvents. The total lipid quantification was done gravimetrically based on the lipid obtained from the respective dry cell biomass. All the experiments were repeated thrice to assess the reproducibility of the results.

$$\text{Lipid content (\% dcw)} = \left(\frac{\text{lipid wt.}}{\text{dry biomass}}\right) \times 100 \qquad 3.4$$

3.2.6 Transesterification

The oil samples were transesterified according to Christie (2009). The oil samples were mixed with methanol in 1:10 (v/v) ratio under constant stirring at 60 °C. Consequently, sulphuric acid (1 v %) was added to the oil–methanol mixture and constant mixing was done for 6–8 h to overnight. Once the phase separation occurred between the fine biodiesel and thick glycerol, the reaction was stopped and washed with lukewarm water. Further, the corresponding methyl esters were recovered in hexane. The composition analysis of fatty acid methyl ester (FAME) was performed by gas chromatography (GC).

3.2.7 Supercritical methanol transesterification (SCM)

To overcome the limitations of conventional transesterification process such as huge reaction time and low conversion efficiency an advanced and cleaner method of transesterification i.e. SCM transesterification was used in this study. Microalgae oil and MeOH were premixed in a beaker at 60°C for 5 min and poured into the 200 mL autoclave batch reactor (Model no. 1734, Amar equipment, India) depicted in (Figure 3.2). The pressure inside the autoclave reactor was maintained by N_2 gas and the mixing speed was kept at 400 rpm/min. The major process parameters were reaction temperature (°C), reaction time (min) and MeOH: oil molar ratio (MR). The range of selected process parameters conditions was temperature 240, 270 and 300 °C; reaction time 15, 30 and 45 min.; and MeOH: oil molar ratio 15, 30, and 45. Once the desired conditions were reached in a reactor sample were drawn after every 15 min time interval. At the end of the reaction, a small layer of glycerol was observed at the bottom of the reactor. However, the upper light phase of the sample was used for NMR analysis for the calculation of percentage conversion efficiency of oil to FAME.

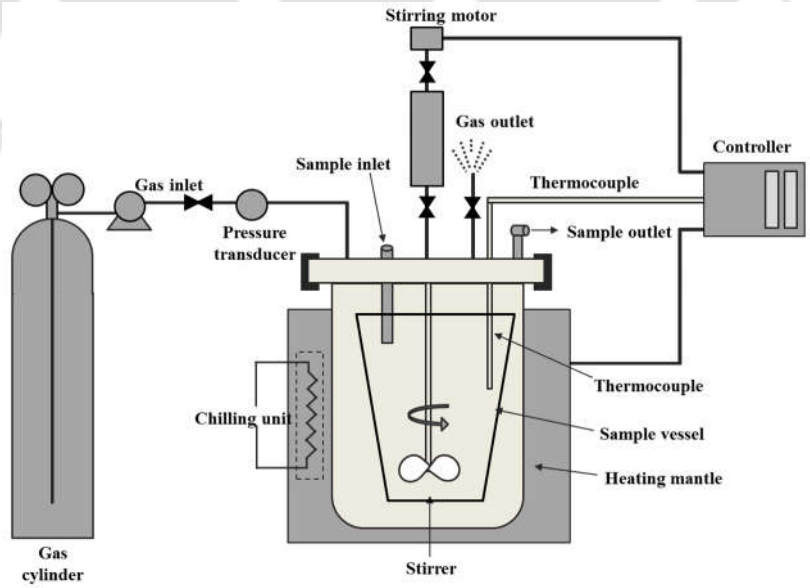

Figure 3.2: Supercritical methanol reactor used for conversion of microalgae oil to FAME.

3.2.8 Anaerobic digestion reactor assembly

The batch reactor of 500 mL capacity was prepared to study the rate and extent of A–CoD of microalgae and rice straw (RS). The mouth openings of the bottles were sealed with a rubber cork and Teflon tape. Each bottle was equipped with a definite aspirator bottle with long silicon tubing containing 1.5 N NaOH solution and few drops of Thymol indicator solution. The daily generated methane was measured through water displacement method as depicted in Figure 3.3 till 40 days of hydraulic retention time (HRT). The NaOH solution was replaced regularly depending on the rate of change of solution color from dark blue to light blue due to the reaction of CO_2 with NaOH solution (Dhamodharan et al., 2015).

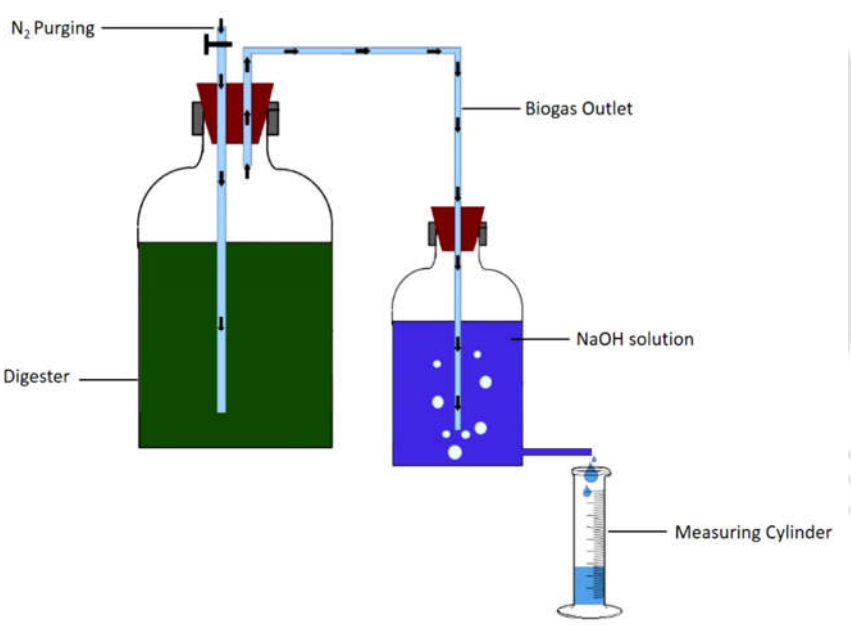

Figure 3.3: Anaerobic digester assembly to study the biomethane potential.

3.2.9 Biochemical methane potential (BMP)

In the present study two different microalgae biomass *viz.* CG12 and GS12 with RS were used as substrate whereas, the CD was used as an inoculum. Moreover, the essential macro and micronutrients were provided to the BMP setup for the luxuriant

growth of microbes present in the inoculum. A control reactor solely with RS was established to compare the BMP changes due to the addition of microalgae biomass as a nitrogen source. Further, the pH of the BMP setup was maintained by adding 1 % phosphate buffer within the limits of anaerobic digestion process and the final volume in all the bottles was equilibrated with deionized water. Moreover, the anaerobic conditions were maintained by nitrogen gas purging for 3–5 min at a mesophilic temperature condition of 37–38 °C using room heater with continuous monitoring of pH, volatile solids (VS), and soluble chemical oxygen demand (sCOD), respectively. The reactors were connected to aspirator bottles having 1.5 N NaOH as mentioned above in sludge activity test and the methane produced was measured on daily basis up to 40 days.

3.2.10 Theoretical methane yield (TMY)

The theoretical methane yield (TMY) of the co–digestion process was calculated on the elemental composition basis using the Buswell formula illustrated in Eq. 3.5 and 3.6. Additionally, the anaerobic biodegradability of the substrate can be calculated by dividing the experimental methane yield (EMY) to theoretical methane yield (TMY) (Buswell and Mueller, 1952).

$$CnHaObNc+(n-\frac{a}{4}-\frac{b}{2}+\frac{3c}{4})H_2O \rightarrow (\frac{n}{2}+\frac{a}{8}-\frac{b}{4}+\frac{3c}{8})CH_4+(\frac{n}{2}+\frac{a}{8}+\frac{b}{4}+\frac{3c}{8})CO_2+cNH_3 \quad 3.5$$

$$TMY(\frac{mlCH_4}{gVS})=\frac{22400\,(\frac{n}{2}+\frac{a}{8}-\frac{b}{4}-\frac{3c}{8})}{12n+a+16b+14c} \quad 3.6$$

3.2.11 Specific methanogenic activity (SMA) and biodegradability (BD)

SMA can be accomplished by dividing the highest methane production rate to the quantity of VS reduction in the co–digestion mixtures. The methanogenic activity assay was performed using 2 g VS content of inoculum in serum bottles, and acetic acid with mineral media was added as a substrate. The organic loading rate was maintained at 1.0 g COD/g VS. The final volume of each reactor was made to 500 mL. The anaerobic condition was maintained by purging N_2 gas for 2–3 min. The bottles were connected to aspirator bottles containing 1.5 N NaOH solution. The quantification of methane was done by measuring the displaced NaOH solution.

3.3 Optimization strategies

Three major optimization strategies were involved in this study to obtain the local and global optimization conditions for microalgae cultivation and the conversion of microalgae oil to methyl ester. Hence, to attain high process yield the following optimization procedures have been adopted.

3.3.1 Response surface methodology (RSM)

Response surface methodology is a statistical tool to analyze problems, where the response depends on several independent factors with an objective to obtain optimum yield (Myers et al., 2016). The optimum levels of variables having a significant effect on response were analyzed by CCD. It follows three major steps consisting of carrying out statistically designed experiments, evaluating the coefficient in a mathematical model with a prediction of response and examine the adequacy of the model (Pankaj and Awasthi, 2014).

The Central Composite Design with three coded levels for all 20 runs was used to analyze the combined effect of physicochemical parameters on lipid production,

utilization of waste material for microalgae cultivation and supercritical methanol transesterification. The experimental data were analyzed using Design Expert software (version 7.0.0) and the results of a variance, significance level and lack of fit were carried out by analysis of variance (ANOVA). The second order polynomial equation was fitted with the experimental results obtained from CCD analysis. The coefficient of all the three coded values was determined using the following equation

$$Y = \beta_0 + \sum_{i=1}^{n} \beta ixi + \sum_{i=1}^{n} \beta iix_i^2 + \sum_{i=1}^{n} \sum_{j>1}^{n} \beta_{ij} x_i x_j \qquad 3.7$$

Where Y is the response variable and β_0 is the constant. The β_0, βixi, βix^2, $\beta_{i,j}x_ix_j$ are coefficients for intercept, linear, quadratic and interactive terms, respectively for the three independent variables A, B, and C (Shahum, 2014). The overall optimized conditions are stated to predict the maximization of lipid content and high conversion efficiency of microalgae oil to FAME under optimized process conditions (Dhawane et al., 2015).

3.3.2 Artificial neural network (ANN)

The artificial neural network has been progressively applied in a number of optimization works. ANN was applied to the same data obtained from RSM for model comparison and validation, to understand the significance of the factors in a more interactive way. MATLAB [version R2014b (8.4.0.150421)] was used to predict the lipid content using artificial neural network toolbox (version 8.2.1). It was chosen to conduct the pattern recognition on similar data set subjected to RSM analysis. ANN can be used as an alternative to polynomial regression–based modeling tool which provides the modeling of complex non–linear relationships. ANN having a highly interconnected structure consists of a large number of simple processing elements called neurons, which are arranged in different layers in the network such as input layer,

an output layer, and all other intermediate units, called hidden layers. In this study, a three–layered neural network with log sigmoid transfer function (logsig) at the hidden layer and a linear transfer function (purely) at output layer was used. The sigmoid transfer function was given by

$$Y_i = \frac{1}{(1 + \exp(-net_i))} \quad 3.8$$

The linear activation function is used as output layer activation function

$$Y_i = (net_i) \quad 3.9$$

Where is the output from node *i* and net_i is the input to the node $i = \sum w_i \times x_i$

Where w is total weights for unit *i* and x is activation value for unit *i*.

Training a network consists of an iterative process in which the network is given the desired inputs along with the correct output for those inputs. The network then tries to alter its weight to attempt and create the right output (subtle error margin). After successful training, it has learned the training set and is prepared to perform previously unseen data (Lahiri and Ghanta, 2008). The back propagation algorithm (BPA) and Levenberg–Marquardt (LM) was used for network training (Mohamed et al., 2013). The learning weights are slightly adjusted during each and every iteration of the training cycle until the appropriate weight was attained.

3.3.3 Genetic algorithm (GA)

A genetic algorithm is a straightforward and powerful general purpose stochastic optimization method, inspired by the Darwinian evolution of population genetics. It is subjected to duplicate, crossover the alteration in a particular environment where only fittest can survive. Second order polynomial equation generated by RSM and ANN was

used as an objective function for GA. GA preferably combines with genetic operators to create an artificial survival of fittest obtained from given search space to form a very robust mechanism that is suitable for the variety of optimization problems (Kana et al., 2012). The input data of GA creates an initial population (set off a possible solution) either indiscriminately or learning through experience (heuristically). The less fit individuals in the population die and to search other points in space some variations are introduced into the new population by using idealized recombination (translational) operators (e.g. crossovers, mutation). Thus over the generation, the best fit of an individual population survives, in other words, the best suitably optimized condition will be generated globally.

3.4 Analytical techniques

3.4.1 Proximate and ultimate analysis

The proximate and ultimate analysis was carried out to evaluate the major characteristics of initial microalgae biomass. The moisture content and ash content were determined by NREL method. The elemental composition of biomass was analyzed by CHNS analyzer (Euro EA Elemental Analyser) and EDX (Carl Zeiss SIGMA VP, Germany).

3.4.2 Fourier transform–infrared (FTIR) spectroscopy

The FTIR analysis of dried algal biomass was carried out before and after the of oil extraction using FTIR spectrometer (SHIMADZU, Model: 01722, Japan). The biomass was ground with potassium bromide (KBr) powder and pressed into pellets for analysis. A spectrum from 400 nm to 4000 nm was scanned and analyzed for functional groups

of various biomolecules. The corresponding FTIR peak assignment for biomolecule has been given in the appendix A.1.

3.4.3 Calorific value (CV)

The calorific values estimation was carried out in a bomb calorimeter; a sealed Parr 1108 (Parr, USA), using NREL method. Sample pellets of 0.5 g were used for each analysis. A cotton thread was attached to the platinum ignition wire and placed in contact with the pellet. The bomb was filled with oxygen at 25 °C with 2.0 cm^3 of water added to the bomb. The calorimeter was placed in an isothermal jacket with an air gap separation of 10 mm between all surfaces. The electrical energy for ignition was determined from the change of potential across a capacitor when discharged from about 40 V through a platinum wire. The bomb calorimeter was submerged in a calorimeter cane filled with distilled water.

$$\text{CV (Calorie/gm)} = \frac{tw\text{-}e_1\text{-}e_2\text{-}e_3}{m} \qquad 3.10$$

e_1= correction in calories for heat of formation of HNO_3= 10

e_2= correction of calories for heat of formation of H_2SO_4= 0

e_3= correction in calories for heat of combustion of fused wire= 40

3.4.4 Thermogravimetric analysis (TGA)

Thermogravimetric analysis of the biomass samples was performed using TG/DTG (Perkin Elmer, Pyris Diamond) instrument at inert (nitrogen) atmosphere. The purpose of TGA is to understand the devolatilization characteristics of the biomass samples with temperature. The non–thermal analysis was performed at a heating rate of 10 °C/min from room temperature to 800 °C.

A high purity nitrogen gas (99.99 %) was fed at a constant flow rate of 10 mL/min as an inert purge gas to avoid the unwanted oxidation of sample. The weight loss vs

temperature data was recorded and obtained data were used to plot the TG and DTG curves. TG and derivative of TG (DTG) curves were used to determine the onset temperature of samples which indicate the thermal behavior of samples.

3.4.5 Thin layer chromatography (TLC)

The extracted microalgae lipid was purified by thin layer chromatography (TLC) to obtain TAG molecules for the fatty acid characterization by proton (^{1}H) NMR as depicted in Figure 3.4. The solvent system used for separation of the TAG from the other fatty acid molecule was hexane: diethyl ether: acetic acid (70:30:1 v/v/v). The 100–150 mg of crude microalgae oil sample was spotted on silica plates (TLC Silica Gel 60 F254, Merck) and run using the above–mentioned solvent system. The presence of TAG band was developed by iodine (I_2) fumes.

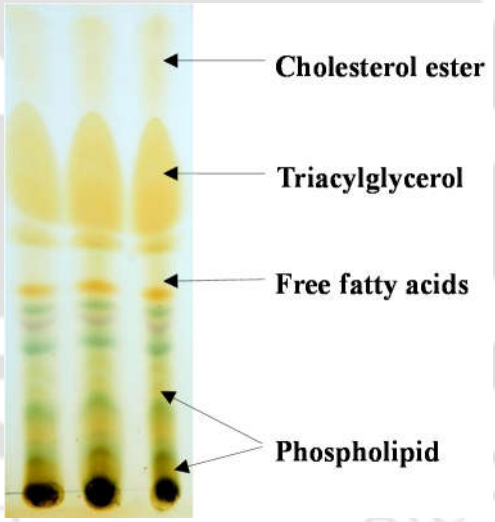

Figure 3.4: Thin layer chromatography of microalgae lipid.

3.4.6 Nuclear magnetic resonance (NMR)

NMR experiments were performed on a Bruker Avance III spectrometer operating at 600.13 MHz NMR proton frequencies. Extracted lipid was dissolved in $CDCl_3$ (deuterated chloroform) and relaxation time (T1) measurement and ^{1}H spectra were

acquired using 5 mm inverse triple resonance probe. The total number of scans were 16–32 in a time interval of 24 seconds. Echo time (TE) measurements were performed at 25 °C. The chemical shift of TMS (tetra methylsilane) peak was set to 0 ppm. The $CDCl_3$ peak was assigned as 7.20 for baseline correction. All NMR data were processed and analyzed through a version of Mnova 11.0.2 (Mestrelab Research).

3.4.7 Gas chromatography (GC)

The fatty acid composition of algae methyl ester was determined using Shimadzu QP–2010 Plus gas chromatograph equipped with a ame ionization detector and SP–2560 column 100 m × 0.25 mm × 0.20 µm). A sample of 0.6 µl (0.5 mg of algae biodiesel in 1 mL of hexane) was injected under the split mode of 80:1 and injector temperature was maintained at 260 °C using nitrogen as a carrier gas at a ow rate of 45 ml/min, air and hydrogen ow rates were 30 ml/min and 300 ml/min, respectively. The oven was kept at 140 °C for 5 min. and then heated up to 240 °C at the rate of 4 °C/min. with the holding time of 20 min. The detector temperature was set to 270 °C. Supelco™ 37 Component fame mix was used as a standard for identification and quantification of the peaks obtained in the methyl ester sample.

3.4.8 Gas chromatography–mass spectroscopy (GCMS)

The composition of FAME samples was analyzed by a gas chromatography–mass spectroscopy (GC–MS) (Varian GC 450 and MS 420) system equipped with 30 x 25 µm VF–5MS column. The detection system was equipped with a flame ionization detector. GC analysis was performed using the following temperature program; start–up injection at 50 °C, hold for 1 min, followed by 10 °C/min oven temperature ramp to 230 °C; hold for 3 min., followed by 5 °C/min. ramp to 300 °C holds for 10 min. Injection temperature was set at 250 °C with a hold time of 5 min, and the sample

injection volume was 2.0 µl. Split mode of 1:20 was selected using helium as a carrier gas at a flow rate of 1.1 mL/min, and the solvent delay was 8 min. The concentration of individual fatty acids was calculated based on their peak areas with respect to the total peak area of FAME, and the relative percentage of the corresponding fatty acid component was calculated and used to estimate various physicochemical properties of prepared methyl esters using biodiesel analyzer (Talebi et al., 2014).

3.5 Miscellaneous methods

Different physicochemical properties such as soluble total solids (TS), volatile solids (VS), ash content and chemical oxygen demand (COD) were calculated using standard protocols (Federation and Association, 2005). For the initial pH measurement around 10 gm of was taken in a conical flask with 100 mL of Millipore water and mixed in a horizontal shaker for 2 h at 150 rpm. The sample was centrifuged at 13500 rpm and the supernatant was used for pH measurement. Sampling from the reactors was done after every seven days and the samples were stored at 4 ºC prior to the analysis. Analysis of volatile fatty acids (VFAs) was performed by pH titration method (Dilallo and Albertson, 1961). All the experiments were conducted in triplicates and average values were used for data interpretation.

3.5.1 Total solids (TS)

The total solids content of a biomass sample is the amount of solids remaining after all volatile matter has been removed by heating the sample at 105 °C ± 3 °C to constant weight. Around 1 gm of predried biomass was taken in a crucible and then placed in a hot air oven for 4 h. Then after the samples were removed from the oven and placed in a desiccator; cool to room temperature. The samples were weighed and again kept in

the oven for 1 h. The process was repeated till the constant weight was achieved. The total solid content was calculated using the following equation.

$$\% \text{ TS} = \frac{\text{Total wt. - crucible wt.}}{\text{Sample wt. - crucible wt.}} \times 100 \quad 3.11$$

3.5.2 Volatile solids (VS)

The volatile solids content is a measure of biodegradability of the organic matter. The dried and finely ground 500 mg sample was placed into electric muffle furnace at 550 ± 25 °C for 4 h. The samples were placed in a desiccator; cool to room temperature and the corresponding weight was measured. The VS % was calculated using Eq. 3.12.

$$\text{VS (mass \%)} = \frac{\text{initial mass - final mass}}{\text{initial mass}} \times 100 \quad 3.12$$

3.5.3 Chemical oxygen demand (COD)

The chemical oxygen demand was measured using titration method. Freshly prepared standard reagents such as 0.25N $K_2Cr_2O_7$, concentrated H_2SO_4, 0.1N $Fe(NH_4)_2(SO_4)_2$, $HgSO_4$ were used for analysis whereas ferroin was used as an indicator. 0.4 g $HgSO_4$ was placed in the reflux tube and then add 20 mL of diluted sample. Further, 10 mL of $K2Cr_2O_7$ was added followed by slow addition of concentrated H_2SO_4 (with added silver sulfate). The samples were mixed thoroughly until blue–green color appears. The COD vials were then connected to COD digester (Hach DRB200) and refluxed for 2 h at 150 °C. The samples were cool to room temperature and titrated against $Fe(NH_4)_2(SO_4)_2$ using ferroin indicator. A sharp color change from blue–green to reddish–brown and should be taken as the end point although the blue–green color may

reappear within minutes. Simultaneously, the blank sample was also run under the similar reaction condition. The COD estimation was performed using equation 3.13.

$$\text{COD (mg/L)} = \frac{\text{(A-B) Normality of } Fe(NH_4)_2(SO_4)_2 \times 8000}{\text{Volume of sample taken}} \quad 3.13$$

Where,

A = ml of FAS used for titration of blank; B = mL of FAS used for titration of sample

3.5.4 Volatile fatty acid (VFA)

The VFA content was calculated according to the method described by Dilallo and Albertson (1961). The co–digested samples were centrifuged and the supernatant was used for analysis by following the acid titration method. Initially, 50 mL of samples were taken and the pH of the sample maintained to pH 4 using conc. H_2SO_4. Further, H_2SO_4 was added to maintain the pH to up to 3.5 and then 3.2. The volume of H_2SO_4 used to maintain the pH 3.5 and 3.2 from pH 4 was noted and then the samples were boiled for 3 min. and cooled down to room temperature. Finally, the samples were titrated with 0.05N NaOH to up to pH 4 with a known volume of NaOH solution. Again the pH was raised to up to 7 with the volume of NaOH was noted down and the volatile acid–alkalinity was calculated between pH 4 to pH 7.

$$\text{VFA} = \frac{\text{Vol. of sample} \times 0.05 \text{ N NaOH} \times 2500}{\text{Vol. of sample}} \quad 3.14$$

The volatile fatty acid can be calculated as

1. >180 mg/L volatile acid–alkalinity

   Volatile fatty acid= volatile acid–alkalinity 1.5

2. < 180 mg/L volatile acid–alkalinity

   Volatile fatty acid= volatile acid–alkalinity 1.0

CHAPTER 4

ISOLATION, IDENTIFICATION, GROWTH STUDY AND LIPID ACCUMULATION OF MICROALGAE UNDER VARYING CULTURE CONDITIONS AND FURTHER OPTIMIZATION AND VALIDATION USING RSM AND ANN

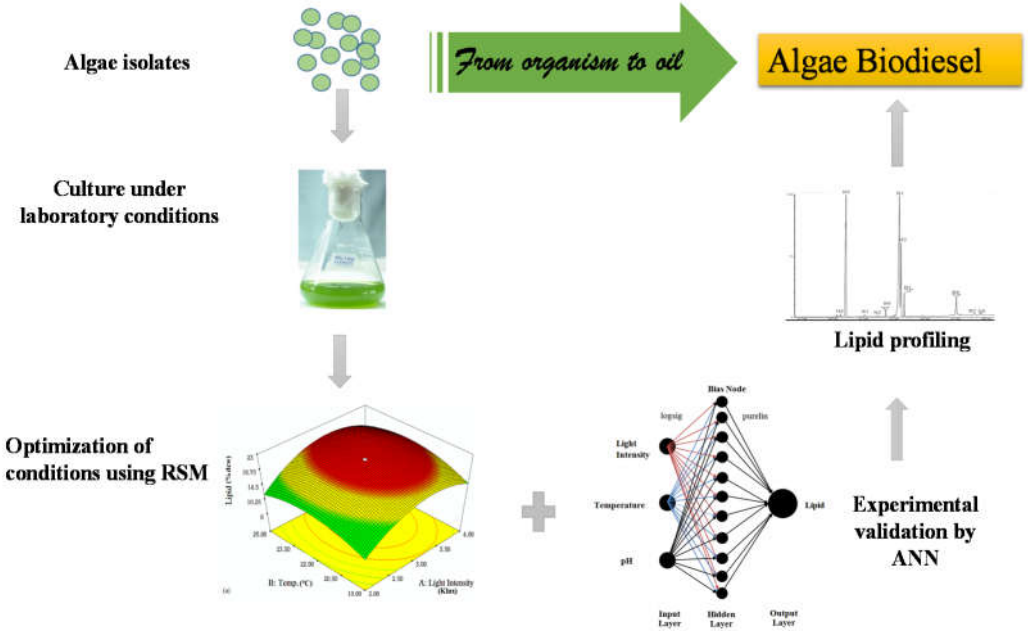

Isolation, identification, growth study and lipid accumulation of microalgae under varying culture conditions and further optimization and validation using RSM and ANN

This chapter includes the isolation, identification, preliminary growth study and estimation of lipid content in microalgae. The initial identification of microalgae was done on the morphological and biochemical basis and the axenic cultures were sent to Zeal Biologicals, Hyderabad, India for 18S rDNA sequencing. Further the microalgae were grown under the various physicochemical condition and optimization studies were performed for enhanced lipid accumulation.

4.1 Isolation and identification of microalgae

The freshwater microalgae culture were isolated from water bodies near Gauhati University, 26.1539° N 91.6622° E India. The isolation of microalgae was carried out by serial dilutions and subsequently cultivated under laboratory conditions in the BG–11 medium. The freshwater microalgae were subjected to the light microscope and identified for the corresponding genera. Morphological identification was done by simple light and FESEM which reveals the size and shape of both the species. The CG12 cells were a green colour, non–motile and spherical in shape. The size ranges from 3–6 µm in diameter, circular to spherical in shape whereas GS12 were slightly elongated, ellipsoid with a rough surface. Cells remain in single, double and quadruple stages and cell size varies from 3–10 µm based on the cell stage. Terminal and axial spines were observed on GS12 (Figure 4.1). Furthermore, identification of microalgae class was performed based on their pigmentation system. The whole cell homogenate of microalgae was extracted in methanol and analyzed the absorption spectrum in UV–

Visible (200–700 nm) region peculiar to the pigments. An intense peak near 680–682 nm was observed corresponding to photosystem II (PS–II) of the chlorophyll molecule. Additionally, minor peaks near 450 nm were observed due to the presence of certain secondary pigments such as carotenoids (Figure 4.2). However, no significant peaks were observed in the UV region. Hence, based on the pigmentation and structural integrity the microalgae has been considered as members of class Chlorophyceae.

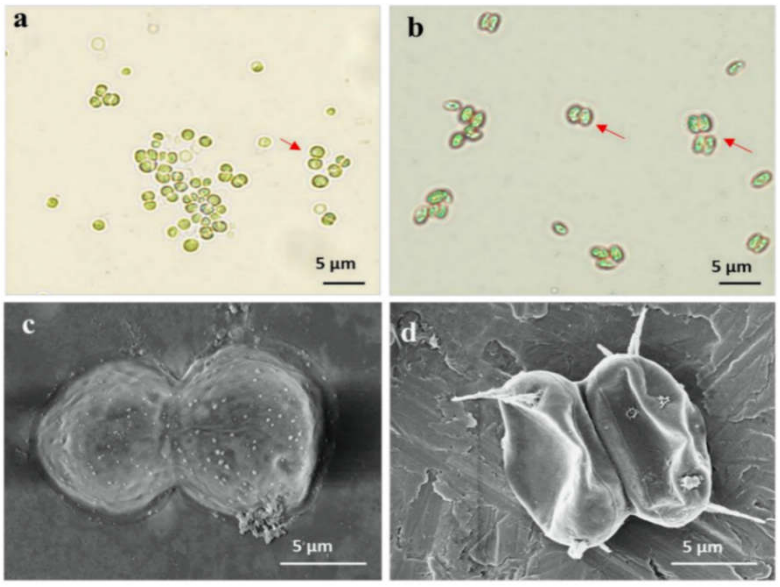

Figure 4.1: Morphological identification of microalgae under a light microscope of (a) CG12, (b) GS12 and under FESEM (c) CG12, (d) GS12.

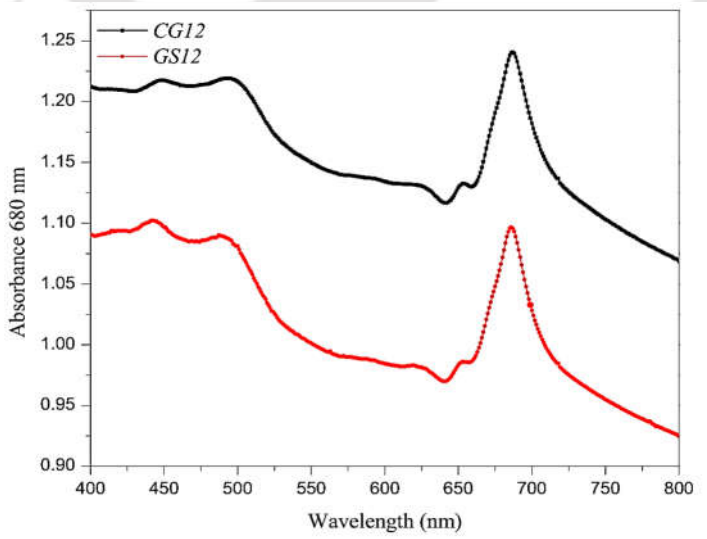

Figure 4.2: Biochemical pigment analysis of microalgae cell homogenate under U.V–Vis spectrophotometer.

Subsequently, the microalgae cultures were outsourced for DNA sequencing for the further confirmation of microalgae genus and species. The partial 18S rDNA sequencing was performed in Zeal Biologicals, Hyderabad, India for both the species. Sequence analysis and pre–processing were carried out by DNASTAR software (https://www.dnastar.com). The partially sequenced data of 522 nucleotides for CG12 (https://www.ncbi.nlm.nih.gov/nuccore/KR905186) and 629 nucleotides for GS12 (https://www.ncbi.nlm.nih.gov/nuccore/KR905187) were analyzed through the BLAST (Basic Local Alignment Search Tool) in NCBI (National Center for Biotechnology Information) for sequence similarity.

The multiple sequence alignment of the nine most related species were generated through a MUSCLE program for both CG12 and GS12 and a phylogenetic tree was constructed by software MEGA 6.0 (Figure 4.3). The evolutionary distance was calculated by neighbor end joining method and maximum similar sequences were chosen for dendrogram assembly. An overall insignificant sequence difference was observed (0.001) in CG12 when compared with nine other most aligned 18S rDNA sequences of *Chlorella* and 99–100 % similarity was recorded. The complete sequence alignment (0.000) of CG12 was obtained with different *Chlorella* strains, namely KU219, ZSLD–2–1, SGH–6, XZL–1 and MAT–2008b. However, other *Chlorella* strains, KU207, UTEX2805, CB4 and UTEX2714 depicted 98.0 %, 98.6 %, 97.7 % and 99.8 % sequence similarities respectively with CG12 (Figure 4.3 a).

On the other hand, GS12 showed 95–96 % similarity with other nine *Desmodesmus* descendants with a maximum sequence difference of 0.004. Amongst the nine most aligned 18S rDNA sequences of *Desmodesmus,* M1–20 was found to have the most sequence similarity while that of AKS–11 had the least similarity of 97.1 % with GS12 (Figure 4.3 b).

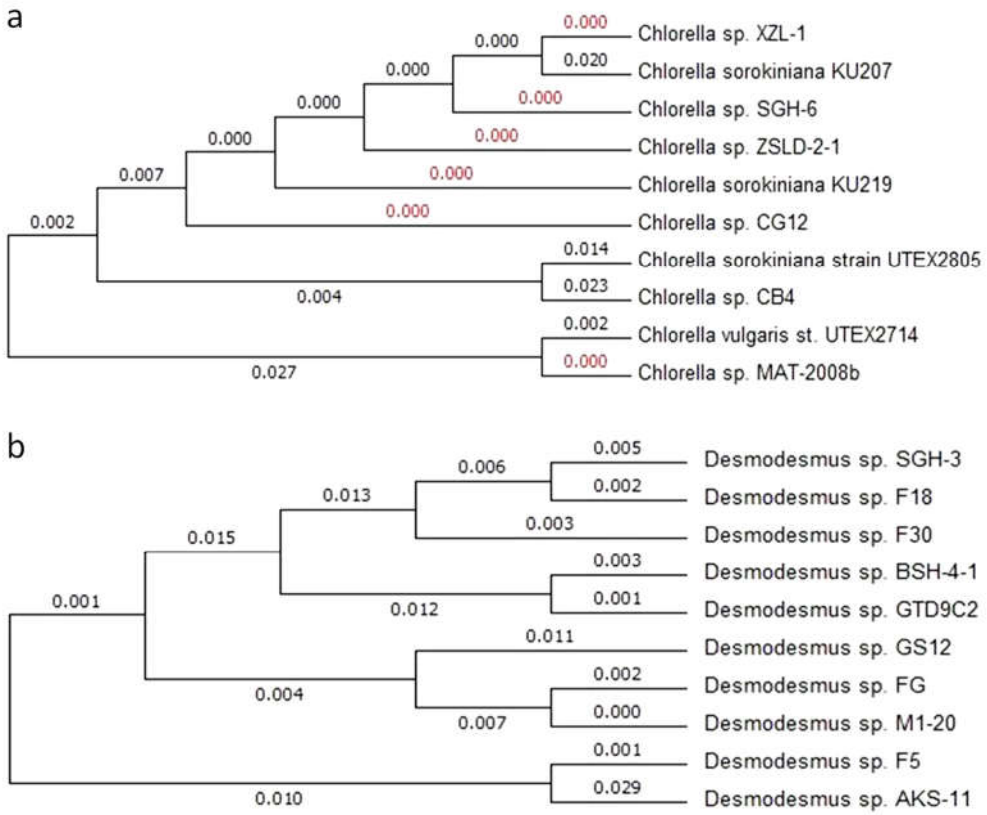

Figure 4.3 Phylogenetic tree of closely related species of (a) CG12 and (b) GS12.

4.2 Growth study

The freshwater microalgae CG12 and GS12 were grown in standard BG–11 and BBM medium, respectively up to 21 days from the day of inoculation under laboratory culture conditions. Growth parameters were studied in terms of cell density on a particular time interval based on absorbance at 680 nm. Absorbance at 680 nm is actually, directly related with the photosynthetic ability of photosystem II which gives a clear cut information about cell density. It was observed that, the lag phase remains up to 3 days, exponential phase of growth for CG12 lies between 4–15 days and reached stationary phase by 20 days. GS12 species follow the same trend of lag and log phase but it reaches stationary phase by the 17 day of cultivation. CG12 took lesser time for its cell division compared to GS12 (Figure 4.4). The specific growth rate and the doubling time was calculated and depicted in (Table 4.1). The initial biomass productivity, lipid content

and lipid productivity were estimated for both the species. Lipid content refers to the lipid accumulation within the microalgae cells for the corresponding dry cell weight (dcw) of microalgae biomass. Whereas, lipid productivity takes into account both the lipid content of the cells and the biomass productivity.

Table 4.1: Growth analysis of microalgae.

Organism	Specific growth rate (μ)	Doubling time (h)	Biomass productivity (gm/L/day)	Lipid content (%dcw)	Lipid Productivity (mg/L/day)
CG12	0.0904	7.67	0.0618	10.2	0.402
GS12	0.0816	8.5	0.1047	10.72	1.122

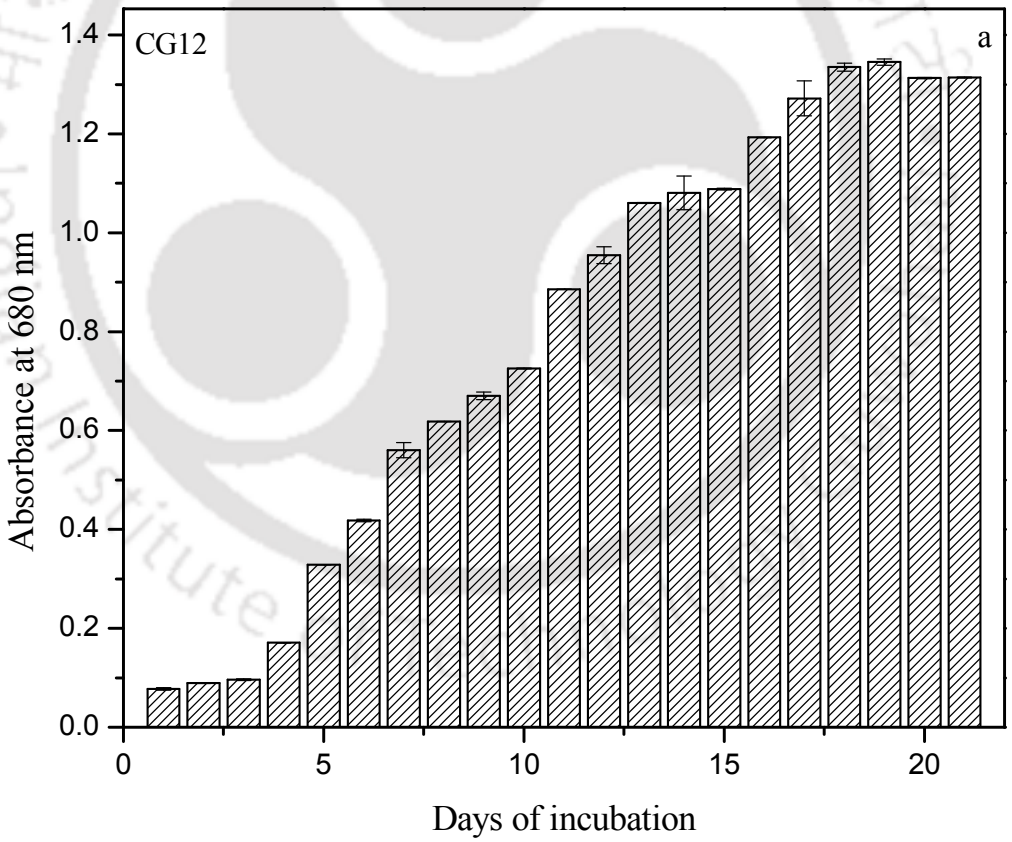

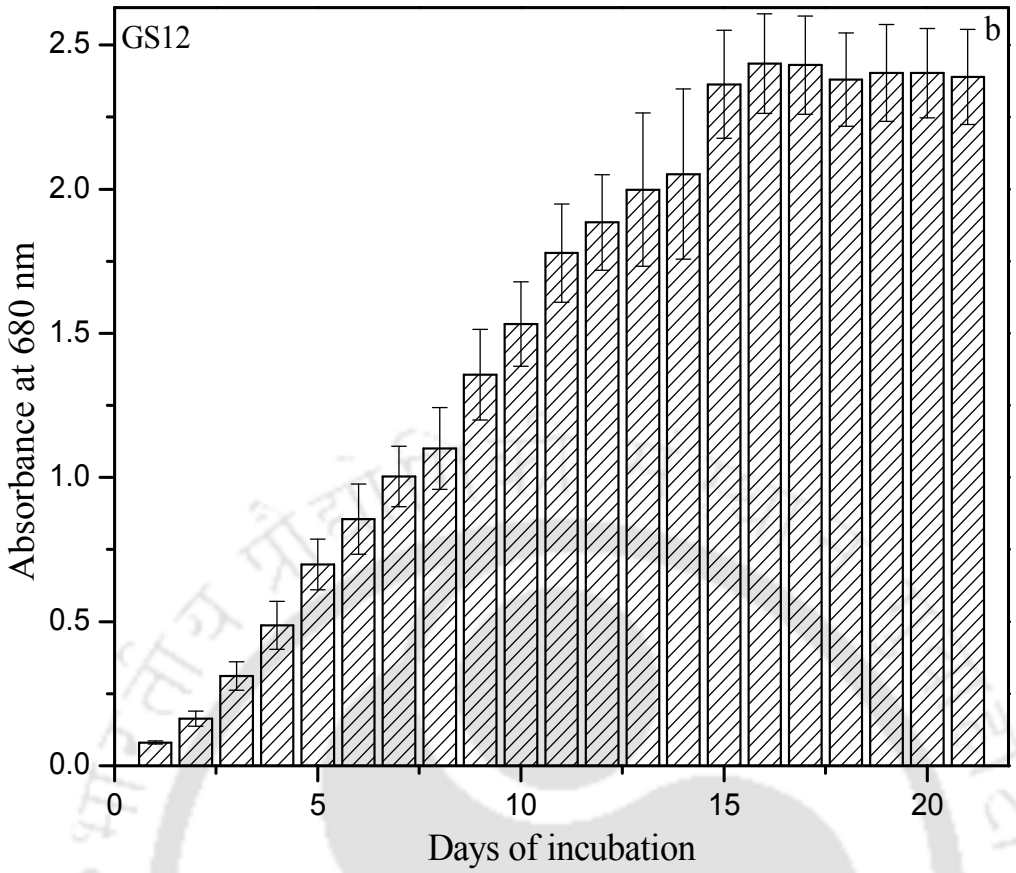

Figure 4.4: The growth rate of microalgae CG12 and GS12 estimated by measuring cell density at 680 nm.

4.3 Microalgae cultivation under varying culture conditions for enhanced lipid accumulation

Indeed, not only biomass and lipid in fact all the biochemical composition of microalgae was assessed for finding the best suitable condition for its growth and especially lipid accumulation. Effect of light intensity on the growth and lipid content of CG12 and GS12 species were investigated. Microalgae growth can be directly related to the chlorophyll content. Different light intensities from 1 Klux to 4 Klux were used for evaluating the growth of CG12 and GS12. It has been observed that at 3 Klux of light intensity has positive effect on both the chlorophyll and lipid content (Ifeanyi et al., 2011). In a similar study, the effect of light and salt concentrations on Aphanocapsa

algal population was examined. Several other reports showed that by changing the light intensity a drastic change in lipid accumulation may occur (Al–Qasmi et al., 2012).

Effect of temperature on the growth and lipid content of CG12 and GS12 species were investigated from 19–31 °C. A temperature range was found favorable between 22 to 25 °C for growth and lipid accumulation. The maximum lipid content was obtained in CG12 at 22 °C however, In case of a GS12 maximum of lipid yield obtained at 25 °C was 21.6 % dcw. The growth and lipid content of CG12 increased with an increase in temperature from 19 to 22 °C whereas slightly decrease thereafter i.e. 25 °C.

Effect of pH on growth and lipid accumulation of CG12 and GS12 were studied. A range of pH was selected initially from 3–12, but no observable growth obtained in cultures. Thus a range of 5–9 was selected and observed that pH 7–9 was the optimum pH range for both biomass and lipid production. It was observed that CG12 showed high lipid yield at pH 8 however, in GS12 maximum lipid accumulation was obtained at pH 7. The reason of such fluctuation of pH change and lipid accumulation may be the distribution of inorganic carbon and another nutrient in the culture medium of microalgae (Moheimani, 2013).

4.4 Optimization of physiochemical parameters using RSM and its validation using ANN

4.4.1 Single factor optimization

The preliminary study was conducted to find out the best suitable condition for microalgae growth and lipid accumulation. The three most influential environmental conditions considered *viz.* light intensity, temperature and pH. The range of all the influential factors was studied independently and in a combinatorial manner. Both the microalgae were grown in the light intensity from a minimum range of 1 Klux to a

maximum of 4 Klux, temperature from 19 °C to 31 °C and pH from 5 to 9. Initially, one parameter at a time was varied considering the remaining parameters constant, by following traditional optimization approach. A huge disparity was observed in lipid accumulation of microalgae varying from 2–9 % in CG12 and 2–20 % in GS12. The maximum lipid accumulation in CG12 was recorded in BG–11 medium up to 8.97 % dcw at 3 Klux light intensity. Whereas, in GS12 highest lipid content of 20 % dcw was obtained in BBM medium at light intensity 3 Klux however, further increase in light intensity to 4 Klux decreases the lipid content by 3 % and reached to 17 % dcw in GS12. Furthermore, to screen out the optimum temperature on lipid accumulation 19 °C to 31 °C temperature range was chosen, based on the available literature (Breuer et al., 2013; Cassidy, 2011). The main reason for selecting this temperature range is that, it should not make any subtle changes to the fatty acid profile during lipid accumulation. Some microalgae decreased their growth with increasing temperature and also increase the ratio of unsaturated to saturated fatty acid. Higher temperature induces accumulation of monounsaturated fatty acids and reduces the polyunsaturated fatty acids (PUFA) (Renaud et al., 2002). The average temperature of Northeast India usually stays between 25–35 °C. Therefore, a moderate temperature range almost favorable to most of the microalgae in the tropical region such as in India was selected. As a result, highest lipid accumulation of 8.97 % and 21.6 % dcw was obtained at the moderate temperatures (22 °C and 25 °C) in CG12 (BG–11 medium) and GS12 (BBM), respectively.

Moreover, another determining physicochemical factor, pH of the culture media was also investigated. The highest lipid accumulation of was obtained at pH 8 and pH 7 for CG12 and GS12 to up to 8.97 % and 20 % respectively. A regular subculture of cells was done after 7 days interval to maintain high cell density. All the experiments were conducted in triplicates and the average value was used for statistical optimization.

Mathematical modelling was performed with the optimum response obtained using single parameter optimization technique.

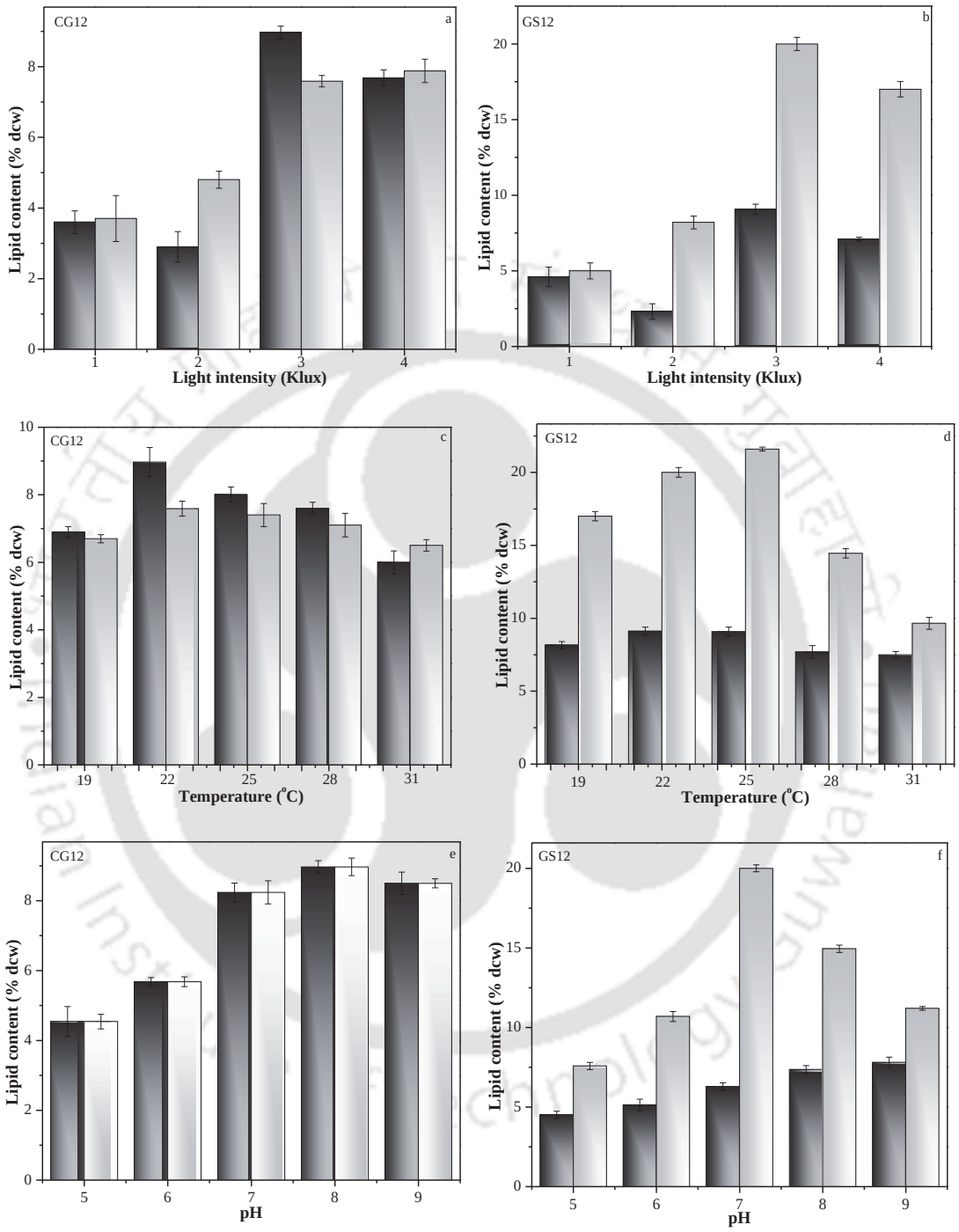

Figure 4.5: The effect of various physicochemical factors (light intensity, temperature and pH) on lipid accumulation property of microalgae CG12 and GS12 in BG–11 (black column) and BBM media (grey column) respectively.

4.4.2 Response surface methodology

The range of light intensity, temperature, and pH obtained from preliminary experiments were selected as input parameters for the process optimization. These independent process variables and their levels have been depicted in Table 4.2 (a) for CG12 and (b) GS12, respectively.

Table 4.2 (a): Independent variables and their levels of response surface design of lipid production for CG12.

Independent variables	Symbol	Unit	Variable levels		
			–1	0	+1
Light Intensity	A	Klux	2	3	4
Temperature	B	°C	19	22	25
pH	C	–	7	8	9

Table 4.2 (b): Independent variables and their levels of response surface design of lipid production for GS12.

Independent variables	Symbol	Unit	Variable levels		
			–1	0	+1
Light Intensity	A	Klux	2	3	4
Temperature	B	°C	19	22	25
pH	C	–	6	7	8

In CCD three coded levels for all 20 runs was used to analyze the combined effect of all physicochemical parameters on lipid accumulation and the response was recorded as lipid content on % dcw, illustrated in Table 4.3 (a and b). Light intensity, temperature, and pH were designed as coded factors A, B, and C, respectively. ANOVA performed the results of a variance, significance level and lack of fit. The second order polynomial equation was used to fit the model response. A quadratic polynomial equation derived from the experimental data was used to predict the lipid content in microalgae as depicted in Eq. 4.1 and 4.2.

$$\text{CG12 Lipid (\% dcw)} = 9.46+(1.79\times A)+(0.41\times B)+(0.37\times C)+(0.23\times A\times B)+(0.30\times A\times C)-(0.36\times B\times C)-(1.56\times A^2)-(1.34\times B^2)-(1.12\times C^2) \quad 4.1$$

$$\text{GS12 Lipid (\% dcw)} = 21.73+(2.64\times A)+(1.00\times B)+(1.93\times C)+(0.18\times A\times B)+(1.54\times A\times C)+(0.65\times B\times C)-(4.99\times A^2)-(3.10\times B^2)-(4.59\times C^2) \quad 4.2$$

All the designed experimental runs were performed under laboratory conditions and the results were analyzed by multiple regression analysis for CG12 (Table 4.3 a) and GS12 (Table 4.3 b).

Table 4.3 (a): Effect of parameters on lipid accumulation of microalgae CG12 as observed experimentally, RSM and ANN models.

CG12	Light Intensity (Klux)	Temperature (°C)	pH	Lipid content (% dcw)		
				Exp.	RSM	ANN
1	2	19	7	2.59	3.04	2.23
2	4	19	7	4.93	5.57	5.07
3	2	25	7	2.98	4.12	2.60
4	4	25	7	6.84	7.57	7.75
5	2	19	9	3.21	3.91	5.23
6	4	19	9	7.32	7.62	7.25
7	2	25	9	2.73	3.53	2.74
8	4	25	9	7.19	8.17	7.78
9	1.32	22	8	3.19	2.04	1.72
10	4.68	22	8	8.95	8.07	8.67
11	3	16.95	8	5.54	4.99	5.70
12	3	27.05	8	7.84	6.36	7.81
13	3	22	6.32	6.74	5.67	6.72
14	3	22	9.68	7.87	6.91	7.88
15	3	22	8	9.41	9.46	9.46
16	3	22	8	9.43	9.46	9.46
17	3	22	8	9.42	9.46	9.46
18	3	22	8	9.40	9.46	9.46
19	3	22	8	9.39	9.46	9.46
20	3	22	8	9.38	9.46	9.46

Table 4.3 (b): Effect of parameters on lipid accumulation of GS12 observed experimentally, RSM and ANN models.

GS12	Light intensity (Klux)	Temperature (˚C)	pH	Lipid content (% dcw)		
				Exp.	RSM	ANN
1	2	19	6	3.11	5.86	4.37
2	4	19	6	5.87	7.7	7.99
3	2	25	6	4.59	6.2	6.29
4	4	25	6	7.13	8.76	7.25
5	2	19	8	3.71	5.34	5.33
6	4	19	8	11.67	13.33	15.76
7	2	25	8	6.84	8.28	7.93
8	4	25	8	16.47	16.99	17.71
9	1.32	22	7	6.03	3.19	5.71
10	4.68	22	7	13.85	12.07	15.00
11	3	16.95	7	14.38	11.28	14.62
12	3	27.05	7	16.16	14.64	11.08
13	3	22	5.32	8.58	5.51	8.76
14	3	22	8.68	13.53	11.99	14.54
15	3	22	7	21.60	21.73	21.10
16	3	22	7	21.56	21.73	21.10
17	3	22	7	21.65	21.73	21.10
18	3	22	7	21.54	21.73	21.10
19	3	22	7	21.57	21.73	21.10
20	3	22	7	21.69	21.73	21.10

The highest predicted lipid content from RSM model was 9.46 % dcw and 21.73 % dcw, in the proximity of experimentally observed value of 9.43 % dcw and 21.69 % dcw for CG12 and GS12 respectively, obtained from CCD matrix. The coefficient of determination, (R^2) defines the ratio of predicted variables to the total variables to envisage the model precision, is another measure of significance of regression, i.e. R^2_{CG12}= 0.9113 R^2_{GS12}= 0.9357 not only indicate excellent fit of the model to the experimental data but shows that 91.1 % and 93.5 % of the effect on the lipid enhancement was explained by variation of the process parameters.

ANOVA analysis was performed to estimate the F and p–value for the model accuracy and significance evaluation. The lower p–value and higher F value indicate that model is highly acceptable. The model F–value of 11.42 CG12 and 16.18 for GS12 implies the model is significant (Chellamboli and Perumalsamy, 2014). The estimated p–value for CG12 and GS12 were <0.0004 and <0.0001 indicates that there is only 0.004 % and 0.001 % chance that this high "Model F–Value" is due to noise and model is capable for prediction of most of the variations. The probability value less than <0.0001 present that model terms are significant. However, their corresponding interactions cannot be explained by a linear relationship. The lack of fit of the sum of squares of the model was calculated as 11.32 for CG12 (Table 4.4 a) and 58.91 for GS12 (Table 4.4 b) that signifies the model fitting.

Table 4.4 (a): ANOVA performed for microalgae CG12.

CG12	**Sum of Squares**	**Degree of freedom**	**Mean Square**	**F Value**	**p–value**
Model	116.42	9	12.94	11.42	<0.0004
A–Light Intensity (Klux)	43.8	1	43.8	38.67	<0.0001
B–Temperature (°C)	2.26	1	2.26	2	0.188
C–pH	1.84	1	1.84	1.62	0.2315
AB	0.44	1	0.44	0.39	0.5484
AC	0.7	1	0.7	0.62	0.4494
BC	1.06	1	1.06	0.93	0.3565
A^2	35.02	1	35.02	30.92	0.0002
B^2	25.87	1	25.87	22.84	0.0007
C^2	18.15	1	18.15	16.02	0.0025
Residual	11.33	10	1.13	–	–
Lack of Fit	11.32	5	2.26	6471.36	
Pure Error	1.75E–03	5	3.50E–04	–	–
Cor Total	127.74	19	–	–	–

Table 4.4 (b) ANOVA performed for the GS12.

GS12	Sum of Squares	Degree of freedom	Mean Square	F Value	p–value
Model	857.64	9	95.29	16.18	< 0.0001
A–Light Intensity (Klux)	95.12	1	95.12	16.15	0.0024
B–Temperature (°C)	13.67	1	13.67	2.32	0.1586
C–pH	50.71	1	50.71	8.61	0.0149
AB	0.26	1	0.26	0.045	0.837
AC	18.88	1	18.88	3.21	0.1037
BC	3.37	1	3.37	0.57	0.4671
A^2	358.13	1	358.13	60.79	< 0.0001
B^2	138.54	1	138.54	23.52	0.0007
C^2	303.72	1	303.72	51.56	< 0.0001
Residual	58.91	10	5.89	–	–
Lack of Fit	58.91	5	11.78	–	–
Pure Error	0	5	0	–	–
Cor Total	916.55	19	–	–	–

The PRESS (predicted residual sum of squares) value of the model showed a good measure of its relative recision. Further the adequate precision measures the signal to noise ratio and a ratio above 4 is desirable. The present model showed a correspondingly high value of adeqaute precision of 9.47 for CG12 and 10.80 for GS12 respectively. However a high CV value was observed due to incorpation of some insignificant terms into the model. The final optimized model value has been represented in Figure 4.6. Moreover, the experimental yield obtained at optimized condition was 13.36 % dcw in CG12 and 25.85 % in GS12.

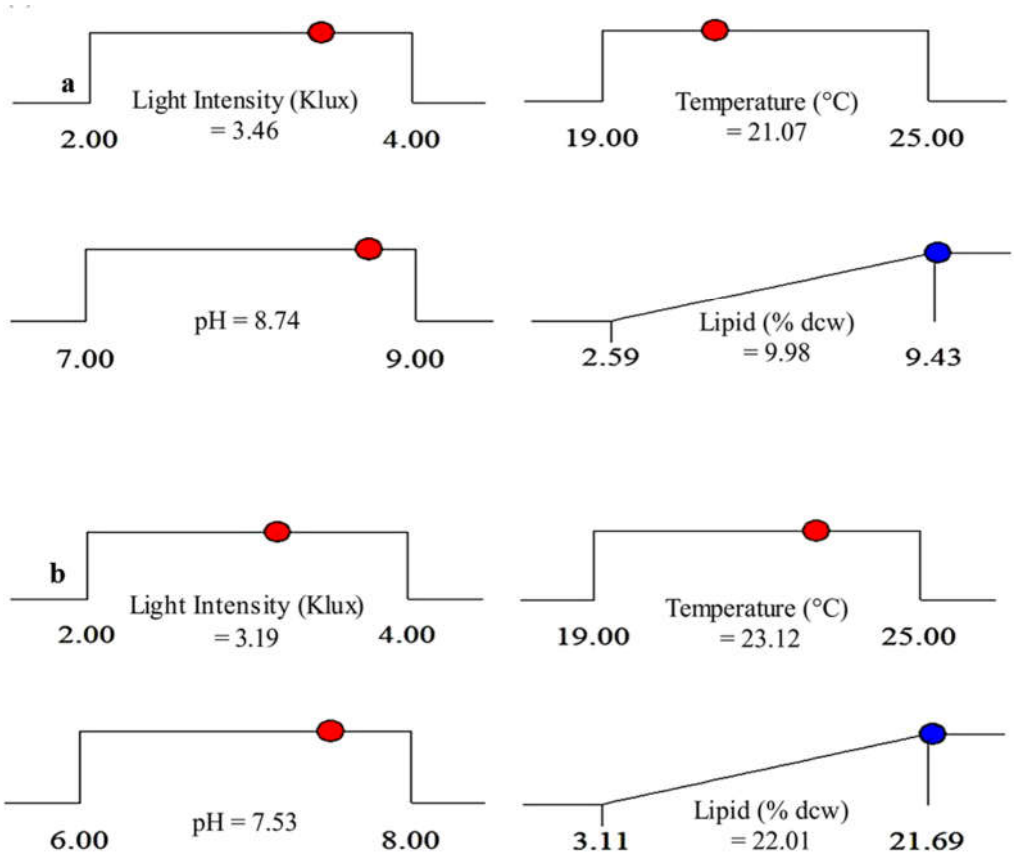

Figure 4.6: Final optimized RSM condition for lipid accumulation in (a) CG12 and (b) GS12.

4.4.2.1 Response of light on lipid accumulation

The response of light on lipid accumulation of microalgae was investigated, based on the preliminary study, the light intensity of 1 to 4 Klux was selected to maximize the lipid accumulation. Initially, the light intensity was varied from 1 Klux to 4 Klux keeping other parameters (pH and temperature) constant. Later from the selected parameters 2 to 4 Klux was selected as lower and upper boundaries for RSM optimization. All the CCD matrix generated experiments were conducted and to check the prediction accuracy ANOVA analysis was performed which revealed the significant probability values for light intensity in CG12 and GS12 as <0.0004 and <0.0024, respectively. The ANOVA results showed that among all three influential factors, light intensity had a prominent effect on lipid accumulation for both the species.

The highest experimental lipid yield at final RSM optimised light intensity of 3.46 and 3.19 Klux in CG12 and GS12 was found to be 13.36 % and 25.85 % dcw whereas the model predicted response was 9.98 % and 22.01 % dcw (Table 4.5). This observed response of lipid accumulation in microalgae was due to the dependence of microalgae on light intensity for cell growth, biomass productivity, utilization of minerals and synthesis of essential compounds. However, high light intensity (4 Klux) reduces the lipid content whereas, low light intensity (2 Klux) did not show any significant increase in the lipid content depicting the non–linear behaviour of microalgae system. Furthermore, low light intensity also did not provide sufficient energy packets to carry out metabolic process and thus did not contribute much to lipid accumulation in CG12 (3.19 % dcw). Therefore, in case of inadequate light intensity the metabolic activity of microalgae ceases which results in less utilization of inorganic nutrients and thereby did not show any strong response towards lipid accumulation. However incerasing the light intensity enhances the lipid accumulation in CG12 to up to 9.43 % dcw depicted in Figure 4.7 (a and b) whereas a further increase in light intensity above 3 Klux showed a slight decrease in lipid accumulation (8.95 % dcw) as depicted in Table 4.3 a.

An increase in the light intensity from 1.32 Klux to 3 Klux increased the lipid accumulation by 3.5 folds (6.03 % dcw) in GS12, Figure 4.7 (d and e). However, further increase in light intensity from 3–4 Klux reduced lipid accumulation to 13.85 % dcw (Table 4.3 b). High light intensity reduces the growth of microalgae by damaging the photosynthetic machinery. This may be a probable cause of decreased lipid content in CG12 and GS12 due to photoinhibition and photosaturation effect reflected by non–linear behaviour of microalgae.

Here it is clear that up to some extent light is directly related with lipid accumulation means incerasing the light intesnsity increases the lipid yield (linear relationaship)

wheras after a threshold level or photosaturation increase in light intensity decreases the lipid content (non–linear response). This phenomenon may be due to damgae in photosynthetic machinery represented by curvatures of response surface model and showed quadratic interactions more prominently.

Additionally, it is evident from the steepness of 3D response surface plot that impact of light intensity on lipid accumulation is more prominent compared to temperature and pH (Figure 4.7). The profound effect of light intensity has masked the corresponding inteaction and influence of temperature and pH. Therefore, the interaction terms for light with temperature (AB) and pH (AC) found insignificant. It is also speculated that high light intensity may substaintialy generate heat which may result in lower lipid accumulation and hence a combination of light (A) and temperature (B) showed an insigficant response in microalgae.

The high light intensity results in frequent photo–oxidation of PUFA due to damage of the chlorophyll antenna system. Also, reactive oxygen species (ROS) arising under high light intensity play a role of signal molecules inducing and controlling many biosynthetic processes, including the biosynthesis of secondary carotenoid and neutral lipids (Solovchenko, 2012).

Hence, from the above discussion, it can be concluded that a moderate light intensity supports both growth and lipid accumulation in microalgae, whereas extreme high and low light conditions may cause a detrimental effect. Therefore an optimum light condition is a prerequisite for proper microalgae culture cultivation where both lipid accumulation and biomass productivity of microalgae could not be compromised by each other. The present study illustrated that CG12 and GS12 require 3.46 and 3.19 Klux, respectively of light intensity for their adequate growth and lipid accumulation and thus provide optimum conditions.

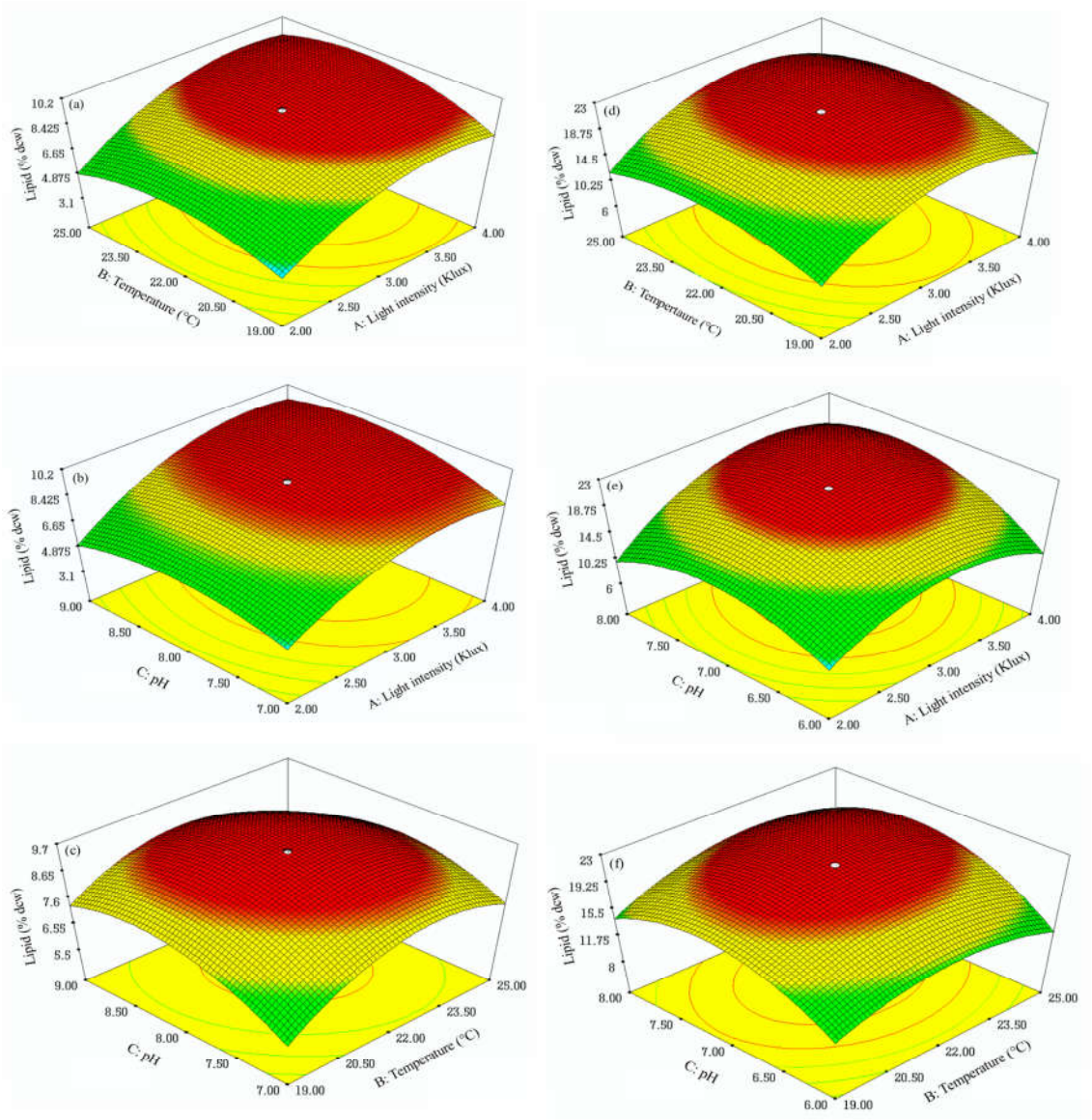

Figure 4.7: 3D Response surface plots for process parameter and its effect on lipid accumulation of microalgae (a,b,c) CG12 and (d,e,f) GS12.

4.4.2.2 Response of temperature on lipid accumulation

Temperature is a crucial factor targeting lipid accumulation in microalgae, especially lipid profile. Initially a temperature region from 19 °C to 31 °C was selected and based on the response of preliminary experiments a region from 19 °C to 25 °C was chosen for RSM optimization as lower and upper boundaries. All 20 CCD designed experimental runs performed with a various combination of temperature with light intensity and pH depicted in Table 4.2 (a and b). However, from the conditions as

mentioned above, an insignificant linear effect of temperature was observed in both the species. Moreover, no significant two factor interactions (2FI) were observed whereas, the quadratic terms for temperature were found significant. This observation suggests that though the temperature may have a significant impact on lipid accumulation if it comes in critically intense form. Since, the temperature range is so lenient for any microalgae to grow therefore it has not exerted much effect on microalgae lipid accumulation and composition, which was the major criteria for designing an experiment for qualitative lipid yield. The favorable temperature for growth and lipid accumulation lies more or less around 22±2 °C (Figure 4.7). The optimum temperature obtained for CG12 and GS12 were 21.07 and 23.12 °C, respectively. A similar response was also reported by Xin et al., (2011) that 20 °C as the optimum temperature for *Scenedesmus* growth. Moreover, lower temperature induces PUFA (22:3) synthesis whereas higher temperature increases the SFA (16:0) and MUFA (18:1) fatty acids.

In the present study, for CG12 and GS12 optimum microalgae growth temperature was found to be 21.07 and 23.12 °C, respectively having with a high amount of oleic (17.16 % in CG12 and 41.43 % in GS12) and palmitic acid (31.82 % in CG12 and 36.27 % in GS12) has been discussed in the subsequent section.

4.4.2.3 Response of pH on lipid accumulation

pH is an important parameter which affects the lipid accumulation in microalgae. In a batch culture, continuous cell growth results in the depletion of nutrients and accumulation of toxic materials and gaseous products which affect the pH of culture medium. In the preliminary study slightly acidic to alkaline pH from 5 to 9 range was considered to grow both the microalgae. Apparently, pH is an important factor regulating lipid accumulation in microalgae but it did not exert its prominent effect in combination to light intensity and temperature. An insignificant linear and 2FI effect of

pH was observed in CG12, Figure 4.7 (b and c) and GS12 4.7 (d and e) however, quadratic terms were found significant. The optimum pH was recorded as 8.74 and 7.53 respectively for CG12 and GS12 respectively. It was reported earlier that neutral to alkaline pH favor lipid accumulation as well as improve the resistance towards invading organisms (Bartley et al., 2014). Furthermore, similar results of enhanced lipid accumulation under alkaline condition were also reported in *Scenedesmus* and *Coelastrella saipanensis* (Gardner et al., 2011). The day/night pH fluctuations are driven by photosynthesis and respiration, also create an environment that exhibits varying pH range. During day time, photosynthesis and use of CO_2 increase the pH, whereas respiration in dark reverses this process and lowers the pH (Bartley et al., 2014). Most of the available reports suggested that neutral to alkaline pH supports the lipid accumulation in microalgae. In accordance with the previous studies, the present study also observed that neutral to slightly alkaline pH of 8.74 and 7.53 are the optimum pH for lipid maximization in CG12 and GS12, respectively. Light intensity, pH and temperature are although independent factors but their effective response is someway regulated by each other. The inefficiency of any of the regulatory factor can lead to increase or decrease lipid accumulation in microalgae.

All the process parameters were evaluated for their active contribution towards lipid accumulation and the optimum process conditions obtained were light intensity 3.46 and 3.19 Klux, temperature 21.07 °C and 23.12 °C, pH 8.74 and 7.53 for CG12 and GS12, respectively. The RSM predicted lipid content under the above–mentioned conditions were 9.98 % and 22.01 % dcw in CG12 and GS12, respectively. The observed experimental value of lipid content for the same experimental conditions was (CG12 13.36 % dcw GS12 25.85 % dcw) showed very less deviation from the predicted values which indicates that the model is accurate and precise.

Table 4.5: Cross validation of optimized conditions.

Microalgae	LI (Klux)	Temp.(° C)	pH	Lipid (% dcw)		
				RSM	ANN	Exp.
CG12	3.46	21.07	8.74	9.50	9.98	13.36
GS12	3.19	23.12	7.53	22.01	23.01	25.85

*LI= light intensity, Exp.= experimental

4.4.3 Artificial neural network

The artificial neural network is extensively used for predicting algal blooms and ecological modelling for last two decades (Lee et al., 2003). However, lack of available literature on the statistical optimization of physicochemical parameters for microalgae lipid enhancement using ANN is a major aspect that has not been explored (Li et al., 2013). The present study aims to develop ANN for physicochemical parameter optimization with an objective to maximize lipid yield. A feed–forward back propagation network structure was designated for maximizing the lipid yield. The network architecture (3–13–1) was developed with 3 nodes in the input layer, 13 nodes in the hidden layer and 1 node in output layer for CG12 (Figure 4.8). Likewise, for GS12 the selected architecture was 3–13–1. Three inputs (light intensity, temperature and pH) were given to ANN model to come up with a single output (lipid content). The LM algorithm is often regarded as the most efficient learning algorithm regarding speed and accuracy in finding the optimal point compared to other algorithms and thereby selected to train the network. Adjustment of network parameters encompassed with the number of neurons (or node) in the hidden layer (logsig) and the output layer (purelin) (Li et al., 2013).

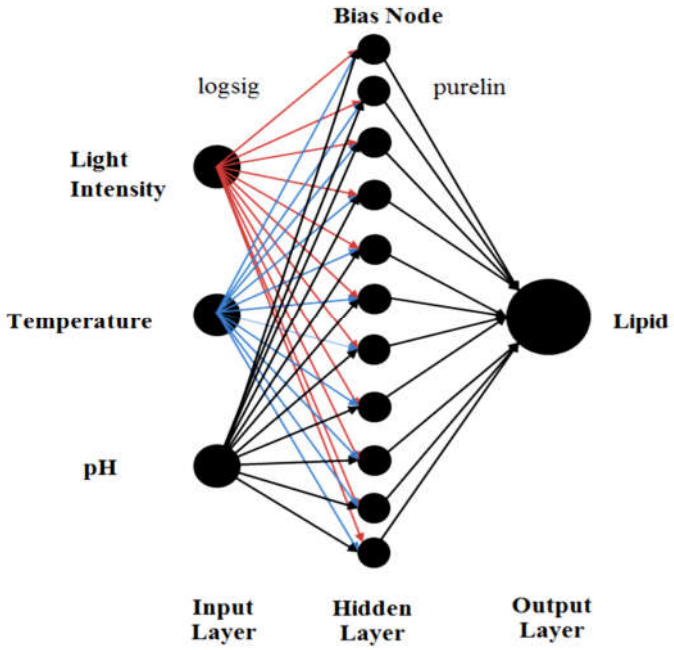

Figure 4.8: Finalized neural network architecture trained via LM.

The changes in output parameter with the relative change in input parameter was studied by sensitivity analysis using leaving each time one parameter out approach. The change in root means square error (RMSE) percentage with a change in sensitivity parameter was evaluated and compared with all input parameters. The withdrawal of any of the significant input parameter among all the influential parameter resulted in higher RMSE value, which revealed more sensitivity of network output for the specific parameter (Nasir et al., 2013). Herein, the sensitivity analysis showed that light intensity has a prominent role in microalgae growth and lipid accumulation which was earlier established by RSM. Light intensity contribution to lipid accumulation was around 87.78 % and 49.09 % in CG12 (Table 4.6 a) and GS12 (Table 4.6 b), respectively. The network output regarding RMSE value increases from 0.62 to 2.51 for CG12 and 1.99 to 5.17 for GS12 after eliminating light intensity from the input parameters.

Table 4.6 (a): Sensitivity analysis of each parameter for CG12.

CG12	RMSE	RMSE Diff.	Contribution (%)
All Parameters (3)	0.6223	–	–
L–Light Intensity	2.5171	1.8948	87.78
L–Temp.	0.8544	0.2321	10.75
L–pH	0.6541	0.0318	01.47
Total	–	2.1587	100

L: leave one out

Table 4.6 (b): Sensitivity analysis of each parameter for GS12.

GS12	RMSE	RMSE Diff.	Contribution (%)
All Parameters (3)	1.9997	–	–
L–Light Intensity	5.1779	3.1782	49.09
L–Temp.	3.3456	1.3459	20.79
L–pH	3.9493	1.9496	30.11
Total	–	6.4737	99.99

L: leave one out

The iteration of each data point was performed for several times untill the lowest RMSE value obtained. The gradient is a value of back propagation algorithm on each iteration in logarithmic scale. The gradient value of $5.9001e^{-11}$ for CG12 and $1.0043e^{-9}$ for GS12 suggests that it has reached the bottom of a local minimum of goal function at epoch 5 as depicted in Figure 4.9 (a and b). The best validation of the model was determined by 2 epoch whereas total 5 iterations were run and stopped at 6 cycle. However, consequent validation failure means more repetition required to train the model (Beale et al., 2010).

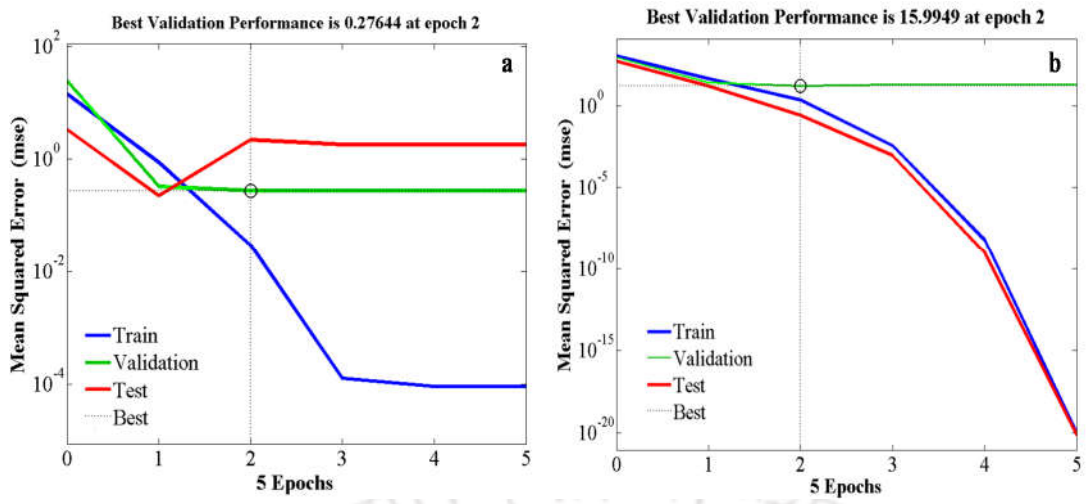

Figure 4.9: The best performance validation check plot for (a) CG12 and (b) GS12.

4.5 Comparison of estimation capabilities of RSM and ANN

In the present study optimization of physicochemical parameters to maximize lipid yield was assessed and compared using two statistical optimization techniques such as RSM and ANN. All the three parameters were independent and showed a good approximation of response for predicting the lipid yield. RSM optimization, however, provided a good fit in the present study, but failed to explain the nonlinear behaviour under such envrionmental condition. It was also observed that at times RSM was incabale of explaining the linear and 2FI of the model. Moreover, during ANOVA analysis RSM failed to define the insignificant corresponding interaction among all the studied parameters and did not provide good fitting. Therefore, validation of the RSM model becomes necessary to figure out the unseen interaction responsible for lipid accumulation which was conducted by ANN. ANN provided a better approximation of physicochemical condition for lipid accumulation in microalgae.

During the sensitivity analysis, it was clearly observed that light had a prominent role in lipid accumulation compared to other two parameters of temperature and pH. ANN corroborate with the ANOVA showing that the significant response for light $p<0.0001$

and <0.0024 for CG12 and GS12. Sensitivity analysis also suggested the 88 % and 49 % contribution was given by light intensity which might have concealed the impact of other pameters when analyzedin a combinitorial manner. These observations of percent contribution and exact response of each parameter were not properly explained by RSM. Thus ANN becomes an efficient tool to develop more understanding about the interaction of process parameters.

Moreover, the evaluation based on models coefficient of determination (Eq. 6) showed satisfactory convergence between the actual and predicted response. The observed regression coefficient R^2_{CG12} and R^2_{GS12} obtained from RSM model was 0.91 and 0.93, respectively shown in Figure 4.10 (a and b). Whereas ANN predicted values for R_{CG12} 0.97 and R_{GS12} 0.95 as presented in Figure 4.10 (c and d) depicted that prediction capability of ANN was higher as compared to RSM. Therefore, it is believed that both the models can efficiently perform data fitting and offered a stable response, however, ANN prediction is comparatively more accurate. The variability existence of the sample was determined by RMSE (Eq. 4.2) value. The adequacy of RMSE value describes the good fitting of model equation. It was used to define the system's behavior and is applicable to experimental condition.

$$R^2 = 1 - \sum_{i=1}^{n} \left(\frac{(y_{pre,i} - x_{ex,i})^2}{(x_{av,exp} - x_{ex,i})^2} \right) \quad 4.1$$

$$RMSE = \sqrt{\frac{1}{n} \sum_{i=1}^{n} (x_{ex,i} - y_{pre,i})^2} \quad 4.2$$

$$AAD = \left(\frac{1}{n} \sum_{i=1}^{n} \left(\frac{y_{pre,i} - x_{ex,i}}{x_{ex,i}} \right) \right) \times 100 \quad 4.3$$

$x_{ex,i}$ = experimental data, $y_{pre,i}$ =predicted data, n= number of experimental data, x_{av}= experimental average value

The RMSE value was calculated for the models and the least RSME value was chosen to train the model for higher prediction accuracy. The comparative analysis of RMSE also revealed that ANN can provide better assumption with minimum errors. The RMSE value for GS12 obtained by RSM and ANN were 1.82 and 1.74, respectively whereas, in CG12 the RMSE value was 0.62. It can be clearly seen that ANN predicted response has less deviation as compared to RSM. Furthermore, the cross–validation of the experimental results was also compared to the absolute average deviation (AAD) which shows less deviation of an experimental value and ANN predicted response. Similar results were reported earlier during optimization of biodiesel from Mahua oil where ANN offered better prediction capability compared to RSM. It was also suggested that ANN can be chosen to optimise the process parameters and can accurately explain the non–linear relationship (Sarve et al., 2015).

From the above discussion, it can be concluded that though ANN is highly efficient in response prediction of linear and non–linear relationship. However, to reduce the experimental run and data point redundancy ANN can be used in combination with RSM. In other words, to explain the non–linear and unseen data points of RSM a hybrid optimization with ANN can be applied.

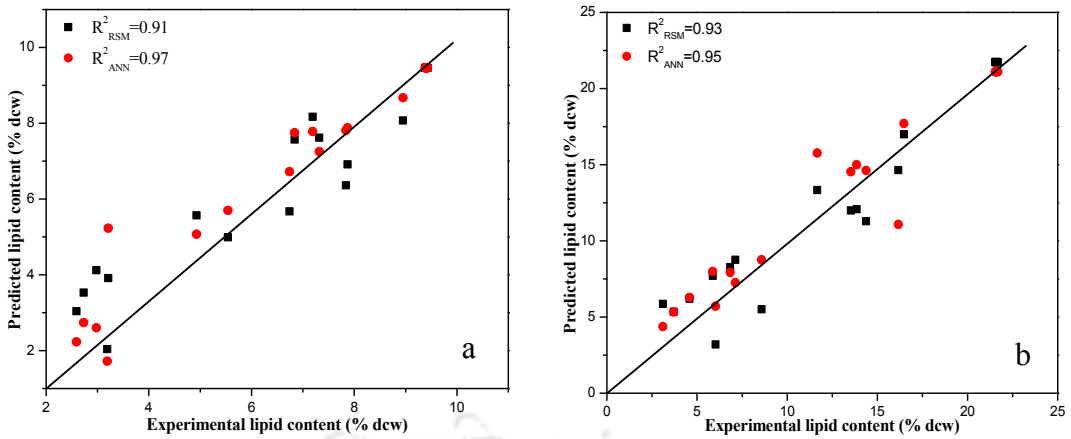

Figure 4.10 Regression analysis of the data obtained from RSM for (a) CG12, (b) GS12 and from ANN for (c) CG12, (d) GS12 respectively.

4.6 Fatty acids compositions

The fatty acid composition of transesterified microalgae oil was estimated by GC–MS analysis and depicted in Figure 4.11. In the CG12 the most abundant fatty acid was palmitic acid (16:0) up to 31.82 % compared to other fatty acids such as oleic acid (17.16 %), linoleic acid (15.14 %), linolenic acid (9.31 %) and arachidonic acid (5.10 %). Whereas, GS12 exhibits maximum content of oleic acid (18:1) about 41.43 % followed by 36.27 % palmitic acid (16:0), 13.49 % linoleic acid (18:2), 3.7 % linolenic acid (18:3) and stearic acid 1.10 % (18:0). Other fatty acids such as a palmitoleic acid (16:1), arachidonic acid (20:0) were observed in trace amount. There is a direct correlation between the fatty acid composition and biodiesel properties (Borugadda and Goud, 2014; Refaat, 2009; Singh and Singh, 2010). Moreover, Lang et al. (2011) reported that presence of saturated and mono–unsaturated fatty acids in oil sample provide more oxidative stability to biodiesel. Similar kind of behaviour was also noticed during the growth characteristic study of *Chlamydomonas* in industrial wastewater (Wu et al., 2012). In the present study, the lipid profiling of CG12 and GS12 displayed a high content of saturated and monounsaturated fatty acids which corresponds to their

immense importance for biofuel application (Knothe, 2005; Ramírez–Verduzco et al., 2012; Talebi et al., 2013).

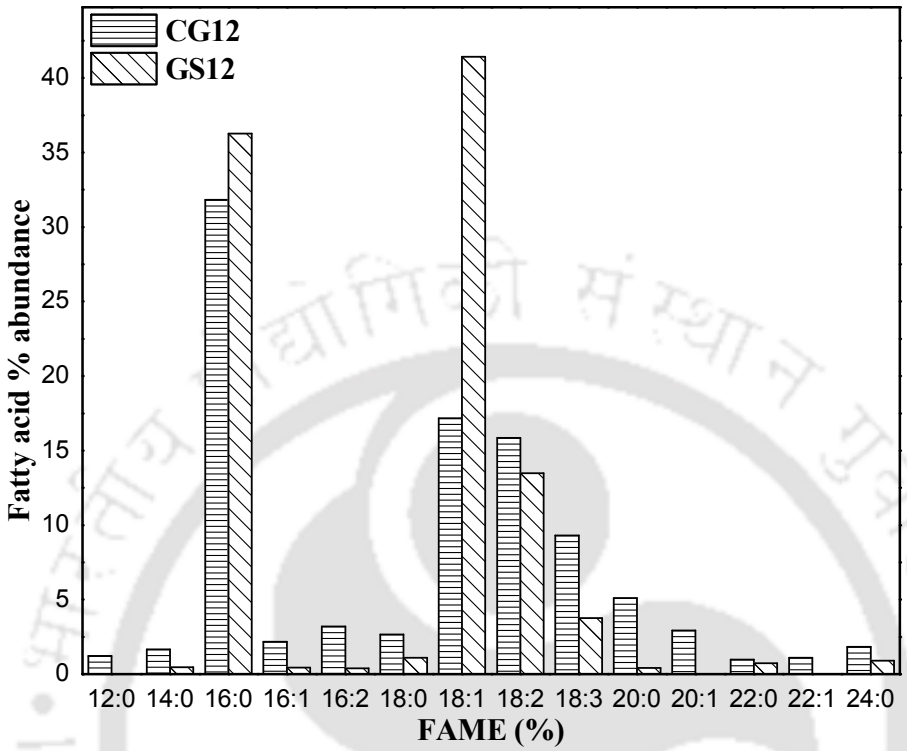

Figure 4.11: The fatty acid composition of microalgae species based on its weight percentage (wt. %).

4.7 Evaluation of biodiesel properties of microalgae oil

Physicochemical properties of microalgae oil were evaluated based on its fatty acid composition using empirical formulae from biodiesel analyzer software (Talebi et al., 2014). Hoekman et al. (2012) have suggested that biodiesel properties such as acid value, saponification value, iodine value, cetane no, density, viscosity, cloud point and pour point depends on the fatty acid composition and its structure.

Biodiesel properties of microalgae oil were estimated and compared with ASTM D6751 biodiesel standard (Table 4.7). However, the acid value of microalgae biodiesel was estimated by a standard method and observed as 0.44 mg KOH/g for CG12 and 0.47 mg KOH/g for GS12, which was comparable with standard ASTM D6751.

Saponification value was calculated as 197.05 mg KOH/g and 204.53 mg KOH/gm for CG12 and GS12, respectively. The degree of unsaturation was estimated using Wijs' Iodine method which reveals the unsaturation content in CG12 and GS12 as 79.51 gI_2/100g and 78.43 gI_2/100g, respectively.

Table 4.7: Biodiesel properties characterization of microalgae.

Properties	**CG12**	**GS12**	**ASTM D6751**
Acid value (mg KOH/g)	0.44	0.47	< 0.5
Saponification Value (mg KOH/g)	197.05	204.53	–
Iodine Value (gI_2/100g)	79.51	78.434	>120
Cetane Number (CN)	56.10	56.05	46–52
Cloud Point (°C)	11.75	14.09	–3 to –12
Higher Heating Value (MJ/Kg)	38.21	39.28	37.528
Kinematic Viscosity (mm^2/s)	3.75	3.84	1.9–6
Density (ρ) (g/Cm^3)	0.84	0.87	0.875–.90
Pour point (^oC)	5.93	8.47	–15 to 16
Oxidative stability (h)	7.27	9.42	–

High cetane no. is a desired quality for the diesel engine to avoid obnoxious gas emission. The cetane number of CG12 (56.10) and GS12 (56.05) biodiesel sample indicates the presence of long chain saturated and unsaturated fatty acids. Cetane no. increases with an increase in the carbon chain length and decreases with the branching of carbon chains. In the case of microalgae, it was observed that long chain fatty acids such as palmitic and oleic acid were abundant and are devoid of carbon chain branching. Chen et al. (2012) have reported compatible fuel properties of microalgae *Chlorella* with biodiesel and its blend which suggest its applicability for biodiesel production. The cloud point is the temperature at which fatty acid methyl ester becomes cloudy due to a formation of wax crystals, whereas pour point is considered as that temperature below which the biodiesel loses its flow properties. Cloud point increases with an

increase in the saturated fatty acid content. The cloud point obtained for CG12 and GS12 were 11.75 °C and 14.09 °C, respectively due to the presence of high monounsaturated and saturated fatty acid contents. The pour point of microalgae oil methyl esters was obtained as 5.93 °C and 8.47 °C for CG12 and GS12, correspondingly. Additionally, high heating value (HHV) is the gross calorific value of fuel released during combustion and was found to be 38.21 MJ/Kg for CG12 and 39.28 MJ/Kg for GS12 biodiesel, respectively. Besides that, density and viscosity of methyl esters are another equally important parameters of biodiesel. The observed density and kinematic viscosity of CG12 and GS12 biodiesel were 0.84 (g/cm^3) and 0.87 (g/cm^3) and 3.75 (mm^2/s) 3.84 (mm^2/s), respectively. The results of the present study were also comparable with those inherited by biodiesel obtained from oil crops and comparable with ASTM D6751 biodiesel standards (Mazumdar et al., 2012).

The increase in long chain saturated fatty acid content increases cloud point, cetane no., viscosity, oxidative stability and prevents obnoxious gas emission, whereas not suitable for the colder climatic region due to its poor cold flow properties. Thus the balanced saturated and unsaturated fatty acid mixture is a prerequisite for biodiesel production (Mazumdar et al., 2012). Therefore, monounsaturated fatty acids (MUFA) are favored as raw material for an alternative fuel. In the present study, it was found that microalgae CG12 and GS12 showed a balanced SFA and PUFA content whereas, higher MUFA percentage was observed in their fatty acid profile which improves the biodiesel properties and hence can be used as potential source for biodiesel production.

4.8 Summary

This chapter concludes that the two freshwater microalgae are CG12 and GS12 belongs to division *Chlorellaceae*. Both the species have peculiar green color due to the

abundance of the chlorophyll molecule. Growth study reveals that growth rate of CG12 is faster compared to GS12 however, the biomass and lipid productivity is higher for GS12. Moreover, high lipid content was observed in the high light intensity of 3–4 Klux, temperature 22–25 °C and pH 7–8 in microalgae isolates.

Statistical optimization of RSM and ANN provided best model fitting and resulted with enhanced lipid accumulation in microalgae to up to 13.36 % and 25.85 % in CG12 and GS12 respectively. ANOVA and sensitivity analysis clearly revealed the huge impact of light intensity on qualitative lipid accumulation. Fatty acids composition of microalgae has shown high saturated (45 % and 39.15 %) and unsaturated fatty acids (51 % and 59 % and) content in CG12 and GS12, respectively. Physicochemical characterization of fatty acid methyl esters ensures that both the microalgae CG12 and GS12 are well–suited organisms for biodiesel production.

However, this systematic optimization study of RSM and ANN has not been able to increase significant lipid content, in microalgae. Hence, to further enhance the lipid accumulation another strategy of addition of mineral salt has been investigated. The effect of mineral salt addition on microalgae lipid accumulation has been described in the following chapter (Chapter 5).

CHAPTER 5

SALINITY INDUCED LIPID PRODUCTION

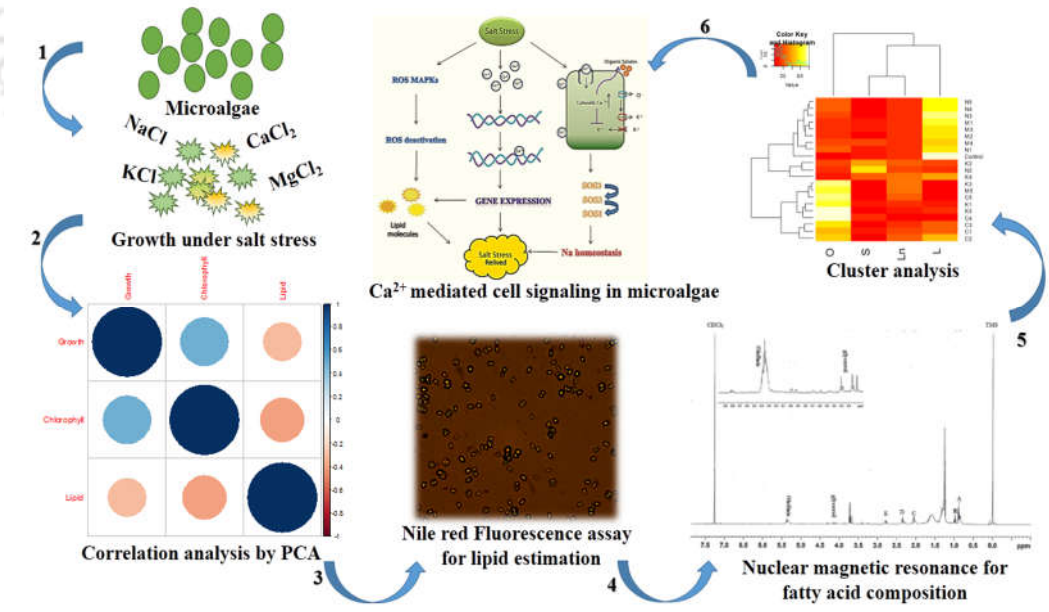

Salinity Induced Lipid Production

This chapter is intended to increase the lipid accumulation in microalgae. The effects of various salts such as NaCl, KCl, $MgCl_2$ and $CaCl_2$ were investigated on quantitative and qualitative lipid yield. Furthermore, the correlation was built between the salt concentration and lipid profile to gain the mechanistic insights into the salt induced lipid accumulation in microalgae.

5.1 Growth study of microalgae species in various salt concentration

The growth response was measured in terms of biomass yield in gm/L up to 21 days of cultivation under various salt concentrations. In the control condition, 1.77 gm/L and 1.97 gm/L dry biomass were recorded in CG12 and GS12, respectively (Figure 5.2). However, a gradual reduction in biomass concentration was observed under NaCl treatment. It was reported that the biomass reduction might be prevailed by salinity induced osmotic stress in microalgae (Mohan and Devi, 2014). The biomass concentration reduced from 1.65 (5 mM) to 1.32 gm/L (25 mM) in CG12, whereas a substantial reduction in total biomass was observed in GS12 and reaches to 1.91 gm/L at 25 mM NaCl concentration.

In case of $CaCl_2$ treatment, biomass concentration was increased from 5 mM (1.27 gm/L) to 20 mM (1.41 gm/L) in CG12, whereas further increase in $CaCl_2$ concentration decreased the biomass concentration up to 1.32 gm/L (Figure 5.2 a). Furthermore, no significant difference was observed in GS12 in 5 mM (1.22 gm/L) and 10 mM (1.21 gm/L) $CaCl_2$ concentration. A further increase in $CaCl_2$ concentrations from 15 mM to 20 mM showed a sharp decline in biomass concentration up to 1.15 and 1.87 gm/L,

respectively. Additionally, an increase from 20 mM to 25 mM corresponds to further increase in biomass up to 2.24 gm/L GS12 (Figure 5.2 e).

In KCl treatment, no specific pattern of biomass yield was obtained in CG12. Maximum biomass concentration 1.71 gm/L was reported in presence of 20 mM KCl whereas the least biomass concentration 0.82 gm/L was found in the presence of 25 mM KCl in CG12. However, another microalgae species GS12 demonstrated higher biomass yield of 2.05 gm/L in 20 mM and 1.99 gm/L in 25 mM KCl concentrations respectively under similar culture conditions (Figure 5.2 e).

Moreover, $MgCl_2$ also exerted its effect on biomass concentration of microalgae where an increase was obtained from 0.81 gm/L and 1.46 gm/L in the presence of 5 to 15 mM concentration of $MgCl_2$, respectively. However, a further increase in concentrations of $MgCl_2$ from 20 to 25 mM resulted in the reduction of biomass from 1.41 to 1.10 gm/L, respectively in CG12. However, no specific pattern of biomass accumulation was observed in GS12 and coincides with the estimated chlorophyll content. It was hypothesized that GS12 has better stress responsive adaptations and can acquire various morphological shapes under stress conditions. These features play a pivotal role in the protection of its photosynthetic machinery and thereby able to resist against increased salt concentration. Therefore, it is believed that this could be a reason for high biomass accumulation in GS12 as compared to CG12 under similar culture conditions (Lürling, 2003).

5.2 Estimation of chlorophyll content

Chlorophyll is the most abundant pigment present in green microalgae. In previous reports it has been elucidated that microalgae have potential to use their pigmentation system as a defense mechanism under various stress conditions. Hence, it was

suggested that salt stress in microalgae can be measured by quantitative estimation of several pigments such as xanthophyll and chlorophyll (Ahmad et al., 2013). Therefore, chlorophyll quantification was considered a growth responsive parameter and was correlated with growth kinetics associated with diverse *in vitro* conditions (Demetriou et al., 2007). Microalgae grown under different salts concentrations indicated a significant reduction in chlorophyll concentration and displayed similar trends with previous reports (Hiremath and Mathad, 2010; Kirroliaa et al., 2011).

A gradual reduction in chlorophyll content was observed from 5 to 25 mM concentration of salts in CG12 as compared to control (Figure 5.2 b). The chlorophyll content declined from control 2.54 to 2.35 µg/mL in 5 mM NaCl. The chlorophyll reduction trend in was followed as 2.36, 1.12, 0.77 and 0.47 µg/mL with an increase in NaCl concentration from 10 to 25 mM. Similarly in $CaCl_2$, a gradual reduction in chlorophyll content was observed from 2.09 to 0.66 µg/mL, followed by KCl and $MgCl_2$ from 1.43 to 0.8 µg/mL and 0.78 to 0.11 µg/mL, respectively. However, in GS12, less significant chlorophyll reduction was observed compared to control (Figure 5.2 f). In GS12, control cultures showed chlorophyll content of 2.87 µg/mL whereas NaCl salt treated cultures depicted slight reduction of 2.60, 2.49, 2.26, 2.19 and 2.11 µg/mL of chlorophyll when treated with 5, 10, 15, 20 and 25 mM concentrations, respectively.

In $CaCl_2$, KCl and $MgCl_2$, similar trends of chlorophyll reduction were observed with GS12. However, the minimum chlorophyll content recorded in CG12 was 0.47 µg/mL under 25 mM NaCl concentration and 1.3 µg/mL in GS12 after treatment with 25 mM $CaCl_2$ depicted in Figure 5.2 (b and f). It has been observed that CG12 is prone to salt mediated chlorophyll reduction as compared to GS12.

It was observed that reduction in chlorophyll contents can be attributed to the modification in the metabolic system of microalgae. Under saline conditions, the rate of CO_2 and nutrients utilization are reduced with an accelerated rate of formation of NADPH. In the presence of these stress conditions, a small fraction of the absorbed light energy only enters into the photosystem pathways and subsequently decreases the total quantum yield. These induced outcomes subsequently reduce the chlorophyll synthesis and biomass accumulation. Moreover, a significant fraction of the absorbed light energy released in the form of heat due to non–photochemical quenching (Sudhir and Murthy, 2004). The role of sodium (Na^+) and potassium (K^+) are well studied and considered as major components for the maintenance of cellular osmolarity. However, the imbalance of any of these salts leads to an osmotic stress and formation of reactive oxygen species (ROS). It has been postulated that ROS presence is crucial for the cellular defence mechanism and are inevitable to the whole algal life cycle.

The change in microalgae chlorophyll concentration, as discussed above, is attributed to the inhibitory effect of accumulated salt ions (Rai et al., 2015; Rao et al., 2007). The reduction in chlorophyll contents as well as in photosynthesis rate is usually considered as one of the key symptoms of oxidative stress mediated by salinity (Affenzeller et al., 2009). Conclusively, oxidative stress mediates the formation of ROS along with reduced growth due to photo inhibition. Additionally, an elevated rate of lipid synthesis was also reported under similar stress conditions (Yilancioglu et al., 2014). It has been reported that lipids, specifically neutral lipids are considered as a key player in quenching of the accumulated ROS (Pancha et al., 2015).

Magnesium (Mg^{2+}) is a structural part of a chlorophyll molecule, therefore the presence and absence of Mg^{2+} significantly affect the chlorophyll biogenesis which ultimately affects microalgae growth and lipid production. An absence of Mg^{2+} results in hindered

cell growth and cell division which ultimately decline the accumulation of cellular lipid and subsequently reduce the total biomass yield (Gorain et al., 2013). Furthermore, K^+ are also key components in modulating the properties of lipid membranes and are known to control the phosphatidylethanolamine contents (Gurtovenko and Vattulainen, 2008).

Calcium (Ca^{2+}) is crucial in perceiving the light energy through chlorophyll molecules, however in the absence of nitrogen in culture media or any other stress condition, the excess reducing power use to channelize towards the lipid synthesis by compromising cell growth (Chen et al., 2014). Ca^{2+} also play a significant role as a secondary messenger that activates the cellular machinery through the activation of various receptors associated with metabolic activities against stress induced ROS generation (Chen et al., 2015; Wheeler and Brownlee, 2008). Therefore, the absence of any of these salts subsequently cause osmotic stress to the microalgae and lead to the generation of ROS (Yilancioglu et al., 2014).

It is assumed that in the present study, the reduction in chlorophyll content was due to the oxidative stress resulted from salinity. The gradual reduction in chlorophyll content was obtained with increasing salt concentrations in consistency with the previous reports (Rao et al., 2007). In comparison to CG12, GS12 depicted better adaptability and tolerance to salt stress conditions as illustrated in Figure 5.2 (b and f). Therefore, this could be a reason for high chlorophyll, biomass and lipid content in GS12 as compared to CG12 grown under similar salt stress conditions.

5.3 Lipid estimation

Numerous theories have been proposed to explain the mechanism of lipid accumulation in microalgae under various stress conditions (Solovchenko, 2012). It was observed that various salts and their respective concentrations affect microalgae metabolism not

only in terms of growth but also in lipid accumulation and modulation in lipid profile (Gurtovenko and Vattulainen, 2008). Under the stress condition, microalgae system enhances the intracellular lipid that acts as a storage energy material till the favorable conditions are attained (Mohan and Devi, 2014). In the present study, the intracellular lipid accumulation and localization on microalgae were investigated by nile red fluorescence assay. Nile red is a lipophilic fluorescent dye that selectively binds to triacylglycerol (TAG). The fluorescence intensity counts were measured for both the microalgae culture grown under various salt treatments. High fluorescence intensity counts were observed under a saline condition in comparison to control and the cells were visualized under a microscope. The lipid droplets in microalgae cells were reflected by red–yellow fluorescence depicted in Figure 5.1. The neutral lipid accumulation was marked by golden yellow fluorescence in both the microalgae.

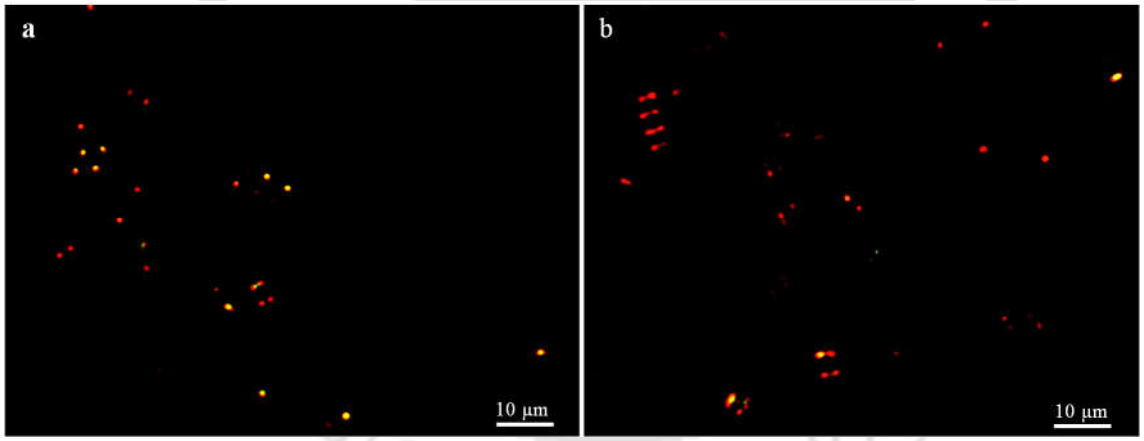

Figure 5.1: Nile red stained microalgae visualized under a fluorescent microscope for lipid localization (a) CG12 and (b) GS12.

However, total lipid quantification was performed gravimetrically for all the samples and was estimated on a % dcw. It was observed that though Na^+, K^+, and Mg^{2+} play an important role in cellular metabolism and lipid accumulation, Ca^{2+} role was more decisive. Maximum lipid accumulation was observed in Ca^{2+} treated microalgae cells. Maximum lipid content up to 40.02 % was observed in case of 25 mM calcium (C5)

concentration in CG12 and 44.97 % in GS12 with 5 mM Ca^{2+} concentration (C1) as depicted in Figure 5.2 (c and g). Ca^{2+} is crucial to cell growth and lipid production. Further, it also helps in maintaining the stability of the membrane by generating adaptive responses to stress conditions.

However, a contrasting behavior of both the microalgae was observed in $CaCl_2$ treatment. Increasing Ca^{2+} salt concentration from 5 mM to 25 mM increases the lipid content in CG12 from 12.56 % (5 mM) to 40.02 % (25 mM) but decreases in GS12 from 44.97 % (5 mM) to 8.94 % (25 mM). Similar observation of Ca^{2+} induced lipid production was also reported in *Chlorella C2* suggesting that Ca^{2+} plays a significant role in the signaling pathway for neutral lipid accumulation. It is hypothesized that this increase in cellular lipids can be accounted as a defense mechanism towards the cell injury caused by osmotic stress (Chen et al., 2014).

The cytoplasmic level of Ca^{2+} rises in response to osmotic stress. Higher concentration of cytoplasmic Ca^{2+} exerts signal transductions through various Ca^{2+} binding proteins for the up or down regulation of cellular responses (Chen et al., 2014; Wheeler and Brownlee, 2008; Yilancioglu et al., 2014). Ca^{2+} binding with these proteins activate the calmodulin and other calcium binding proteins and regulate the cyclic electron flow in microalgae necessitated for photophosphorylation and respiratory oxidative phosphorylation. The regulation of energy flow is typically encompassed the synthesis of neutral lipid and provide ATP to microalgae for various metabolic activities. Under the limited presence of nitrogen, the rate of cyclic electron flow is increased near photosystem I to compensate the decreased rate of photophosphorylation and promote the biosynthesis of neutral lipid through supplying ATP (Chen et al., 2015).

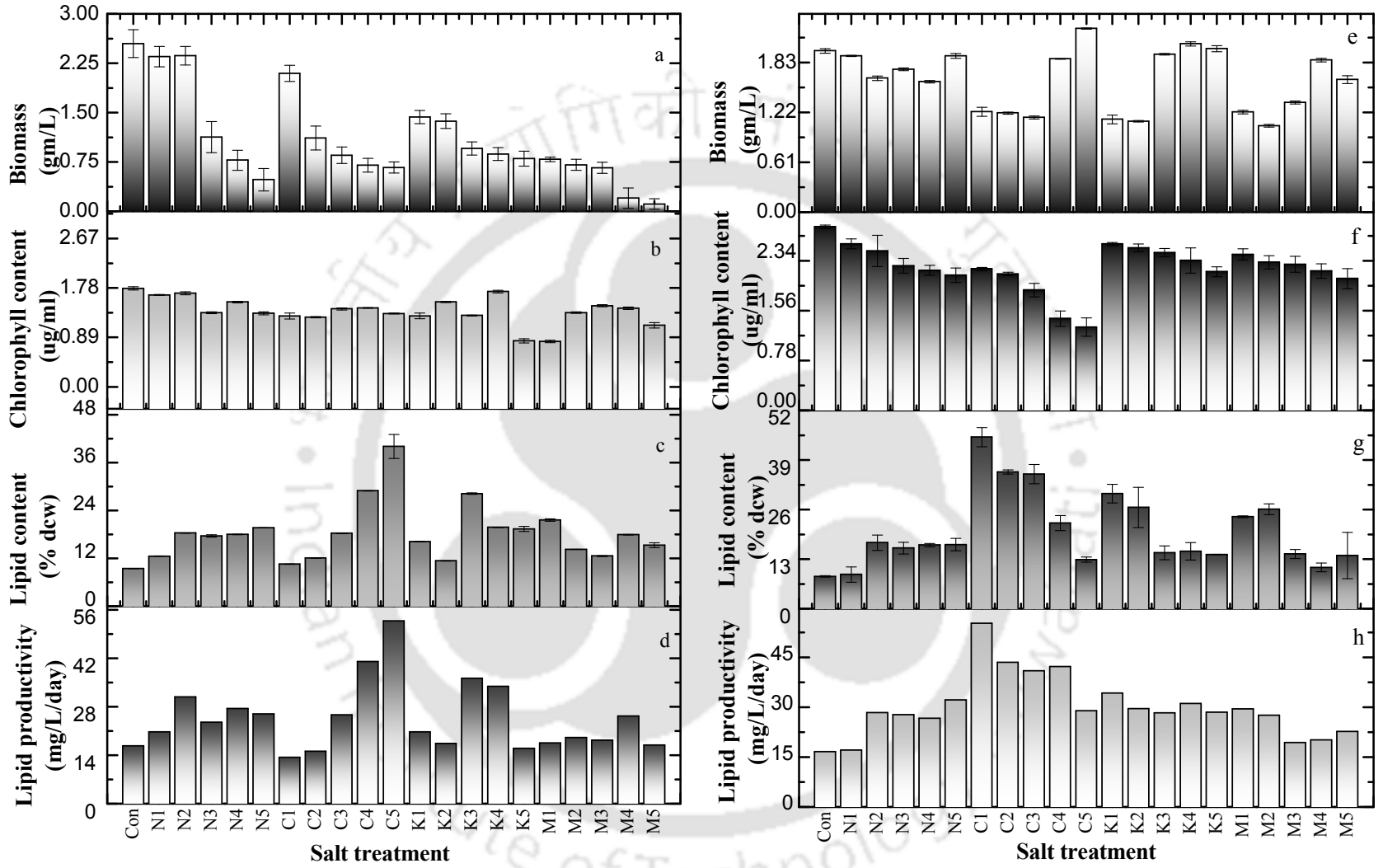

Figure 5.2: Biomass concentration, chlorophyll content, lipid content and lipid productivity of microalgae CG12 (a,b,c,d) and GS12 (e,f,g,h) obtained under various salt treatment.

An appropriate concentration of Ca^{2+} ions also triggers the activity of Acetyl–CoA carboxylase that catalyzes the conversion of acetyl–coenzyme A (CoA) to malonyl–CoA during the biosynthesis of fatty acid (Gorain et al., 2013). Hence, the outcomes of the present study also corroborate with the previous reports that highlights the Ca^{2+} induce intracellular lipid accumulation over the due course of cultivation in nitrogen–depleted condition, is in accordance with previous reports (Chen et al., 2015; Chen et al., 2014). The present study also suggested that Ca^{2+} is a key regulator of neutral lipid accumulation in microalgae as illustrated in Figure 5.2 (c and g). A relative increase of lipid content was observed under $CaCl_2$ treatment, 4.25 fold (25 mM) increase was observed in CG12 and 5.33 fold in GS12 (5 mM). This was further followed by 3.03 (20 mM) and 4.25 (10 mM) folds in CG12 and GS12, respectively.

Furthermore, in other salt treatments an increase in lipid content was also observed. In NaCl treated CG12, the lipid content enhanced from 12.56 % to 19.62 % with increasing salt concentration from 5 mM to 25 mM, whereas in GS12 it reached from 8.94 % (5 mM) to 16.81 % (25 mM). In KCl treated CG12, lipid content increases from 5 mM to 15 mM and attained up to 28.23 % while a further increase in KCl concentration from 20 to 25 mM reduced the lipid content to 19.38 %. Similarly, in GS12 the high lipid content of 30.17 % was observed at lower KCl concentration (5mM), whereas a further increase in salt concentration decreased the lipid content by 14.21 %.

Therefore, in $MgCl_2$ treatment no significant response for lipid enhancement was observed. However, it was found that the lower concentration of $MgCl_2$ favored a substantial lipid accumulation of up to 21.57 and 24.08 % in CG12 and GS12, respectively, as depicted in Figure 5.2 (c and g).

Additionally, an overall lipid yield was also estimated as a product of total biomass and lipid content that was represented as lipid productivity. A subsequent increase in lipid productivity was obtained in both microalgae species as compared to control. In control, the lipid productivity was reported as 16.63 % in CG12 and 16.69 % in GS12, illustrated in Figure 5.2 (d and h). Approximately, 1.5 to 2 fold increase in lipid productivity was observed in both microalgae species in the presence of NaCl. A corresponding increase in lipid productivity 30.90 (10 mM) and 32.14 (25 mM) mg/L/day was obtained in CG12 and GS12, respectively by varying concentration of NaCl.

Furthermore, CG12 showed 3.16 fold increase (52.83 mg/L/day) in lipid productivity in the presence of 25 mM of $CaCl_2$ followed by 2.45 fold increase (41.02 mg/L/day) in the presence of 20 mM of $CaCl_2$ (Figure 5.2 d). In contrast to CG12, GS12 showed a subsequent increase in lipid productivity with decreasing concentrations of $CaCl_2$ from 25 mM to 5 mM. The increase lipid productivity of GS12 were reported as 55.18 (25 mM), 43.45 (20 mM), 40.86 (15 mM), 42.12 (10 mM) and 28.92 (5mM) mg/L/day depicted in Figure 5.2 (h). In the present study, a substantial increase in lipid productivity was observed in KCl and $MgCl_2$ treated microalgae which is comparatively higher than reported in the literature (Mohan and Devi, 2014; Xia et al., 2013).

The previous studies in literature also suggested the application of high salt concentration to induce the lipid accumulation (Xia et al., 2014). In the present study we proposed that salts can exert the similar response at low concentration under nitrogen deficient conditions. Beside the quantity, a qualitative lipid yield can also be obtained by wise discrimination of salt type applied for lipid enhancement. It is assumed that probably the presence of KCl and $MgCl_2$ provides structural integrity to microalgae and subsequently help in biomass accumulation, whereas the introduction

of NaCl and $CaCl_2$ induce various metabolite synthesis process in order to maintain cellular homeostasis.

5.4 Determination of fatty acid composition

The extracted lipid was purified by TLC (Figure 3.5) in order to obtain pure TAG and was subsequently characterized by proton (^1H) NMR. The composition of major fatty acids such as a linolenic acid (Ln), linoleic acid (L), oleic acid (O) and other saturated fatty acids (S) was calculated according to Yeung et al., (2008) equations as depicted in Eq. 5.1–5.4. The alphabets A, B, C, D and E correspond to different NMR peak positions (Figure 5.3) and their corresponding chemical shifts have been represented in appendix A.2.

$$\text{Ln}\,(\%) = 100\left(\frac{B}{A+B}\right) \quad 5.1$$

$$\text{L}\,(\%) = 100\left(\frac{E}{D}\right) - 2\left(\frac{B}{A+B}\right) \quad 5.2$$

$$\text{O}\,(\%) = 100\left(\frac{C}{2D}\right) - \left(\frac{E}{D}\right) + \left(\frac{B}{A+B}\right) \quad 5.3$$

$$\text{S}\,(\%) = 100\left(1 - \frac{C}{2D}\right) \quad 5.4$$

The NMR data was further applied for correlation and cluster analysis. The correlation analysis of various salt treatments on growth, chlorophyll content and lipid accumulation in microalgae were analyzed by R, version 3.3.0 (https://www.r–project.org/) and the extracted lipid composition was represented by function ggplot2 (https://www.r–project.org/) through hierarchical cluster analysis (HCA).

The major objective of NMR based fatty acid characterization was that all fatty acids in TAG formed by esterification of the three fatty acid moieties with a glycerol molecule. Therefore, measuring the presence of different hydrogen in the sample would better explain the composition of fatty acid considering the glycerol molecule as a backbone reference.

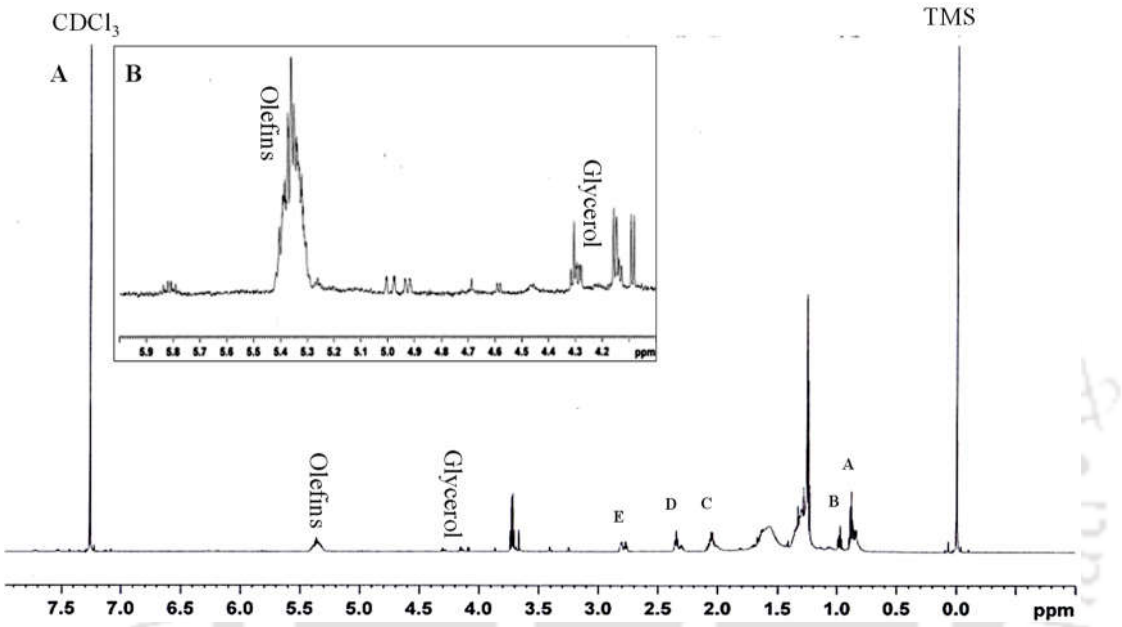

Figure 5.3: NMR various peak assignments for estimating the fatty acid composition of oil.

The integrated area under NMR peak is directly proportional to the number of hydrogen atoms present in the sample and fatty acid quantity can be determined by finding the area underneath the specified peak. The hydrogen of glycerol moiety resulted in distinct peaks at 4.12, 4.37 and 5.4 ppm. All the different chemical shifts for various hydrogen atoms were taken from previous reports available in the literature (Yeung et al., 2008).

The quantity of linolenic acid was determined through the area calculation underneath the peak obtained at 0.98 ppm that was exclusive from the hydrogen of a methyl group from linolenic acid. In relation to the area of one of these signals from the alpha (α)

hydrogen of the glycerol backbone, the percentage of linoleic acid was determined by integrating the signal at ~2.74 ppm that was due to the hydrogen of a methylene group between two double bonds or olefins (signal E in Figure 5.3). The content of oleic acid obtained by measuring the area of the signal at ~2.02 ppm that corresponds to the alpha hydrogen of a methylene group from all unsaturated fatty acids (signal C in Figure 5.3). Finally, the content of saturated fatty acids was determined by the ratio between the areas of one of these signals from the alpha hydrogen of glycerol and the signal at ~2.34 ppm from six alpha hydrogen of carbonyl of all fatty acids esterified to the glycerol moiety (signal D, Figure 5.3). The signal A of the NMR peak corresponds to the trace amount of linoleic acid, oleic acid as well as for saturated fatty acids.

Based on the observations, the fatty acid composition of microalgae under various salt treatment was calculated by ^{1}H proton NMR. The concentration of major fatty acids, linolenic acid, linoleic acid, oleic acid and saturated fatty acid were assessed by their peak area integration at their corresponding peaks of 0.98, 2.74, 2.02, 2.34 ppm. The corresponding composition of untreated control cultures of CG12 and GS12 were linolenic acid 15.2 and 24.29, linoleic acid 38.26 and 19.06, oleic acid 40.06 and 41.94, and total saturated fatty acids were 6.0 and 14.71 respectively. Among all the fatty acids, oleic acid is considered as the most suitable fatty acid for biodiesel production (Singh and Mallick, 2014).

The maximum oleic acid content was witnessed in KCl at 25 mM concentration in CG12 which was around 1.94 fold compared to control. Albeit, in GS12 not much variation in fatty acid profile was observed, however maximum oleic acid was obtained in NaCl at 25 mM concentration up to 53.45 %. Furthermore, the second highest oleic acid content was found in $CaCl_2$ at 25 mM concentration in CG12 and 5 mM concentration in GS12 up to 64.18 % and 51.46 % respectively. The maximum statured

fatty acid content was found in 10 mM NaCl concentration in CG12, whereas a significant amount of saturated fatty acid content was obtained in GS12 32.44 % in KCl at 5 mM concentration. Although, an insignificant variation of lipid composition was observed in GS12 under varied salt concentrations.

Under different salt concentrations, the observed variations in NMR response were due to the chemical heterogeneity and hence, it was further subjected to cluster analysis for data comparison and representation. The multivariate analysis of fatty acid composition alteration due to variation in salts and its concentration helps in reproducing the most prominent variation pattern in the data (Verma et al., 2016). The hierarchical heat map enables the conception of comparisons between samples and the establishment of clusters that were built depending on the type of salt and its concentration on the fatty acid profile of microalgae (Quispe et al., 2016). The major fatty acids namely linolenic acid, linoleic acid, oleic acid and saturated fatty acid were measured through various NMR peaks and quantified by its area underneath and designed as heat map as by hierarchical cluster analysis (Figure 5.4).

Based on these results, it is hypothesized that Ca^{2+} is transported into the cells through Ca^{2+} transmembrane channels. An excess amount of intracellular calcium triggers numerous metabolic pathways. Subsequently, intracellular concentrations of Ca^{2+} into the cells influence Na^{+} transportation in microalgae, thereby changing the fatty acid composition and quantity as well (Karimova et al., 2000).

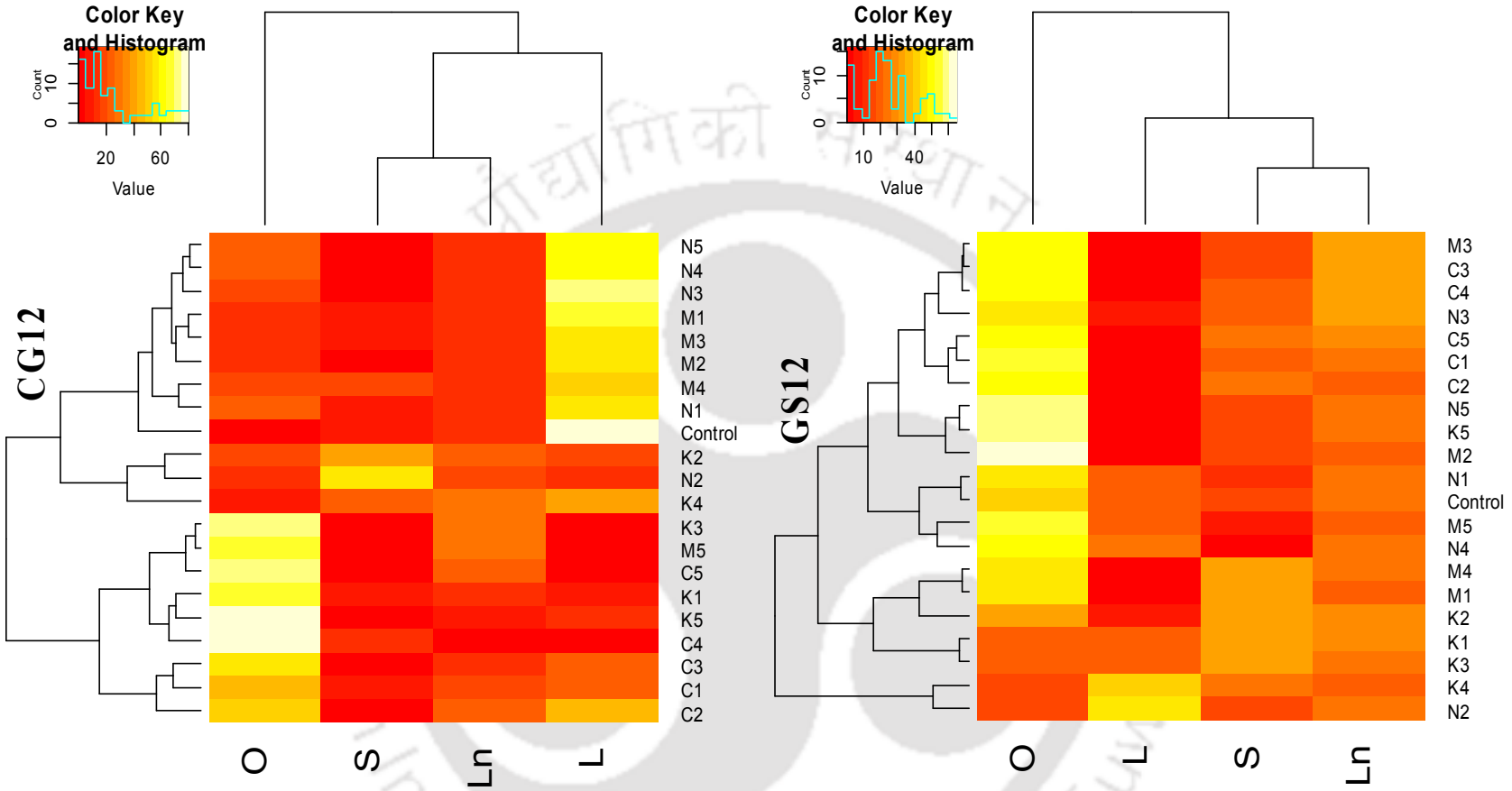

Figure 5.4: Heat map of microalgae based on the correlation of fatty acid profile and various salt treatments.

The mechanistic reason for a high lipid accumulation in the presence of Ca^{2+} is possibly due to its involvement in cell signaling pathways of microalgae (Chen et al., 2014; Zhu, 2016). It has been reported that there are various Ca^{2+} channels participating in metabolic pathways of microalgae required for light perceptions, circadian oscillations and motor response that cause Na^{+} exclusion and K^{+} accumulation inside the cellular system (Wheeler and Brownlee, 2008). It also helps in maintaining Ca^{2+}/H^{+} pump and enhances permeability to calcium ions thereby maintaining the cell integrity (Campbell, 2014).

However, in the microalgae system, numerous alternative pathways have been evolved to coordinate with various ion transporters in diverse stress conditions and thereby maintaining homeostasis in the cytoplasm. The Salt Overly Sensitive (SOS) pathway is one the most studied pathway that comprises three major proteins SOS1, SOS2 and SOS3 and plays a pivotal role in Na^{+} homeostasis. Higher Ca^{2+} level inside the cell activates the SOS3 and SOS2 proteins where SOS2 protein plays a central role in regulations of various other associated reactions including the blockage of plasma membrane localized Na^{+}/H^{+} antiporter and activation of Na^{+}/H^{+} antiporter localized on vacuole. Additionally, Ca^{2+} also binds with DNA molecule through DNA binding motifs and activates the expression of various stress related genes in response to sustain under stress conditions. Several other enzymatic and non–enzymatic regulations mediated by carotenoids, catalase and peroxidase also play an important role in stress conditions through reaction with ROS in order to release the excess stress caused by numerous environmental factors (Zhu, 2016), Figure 5.5.

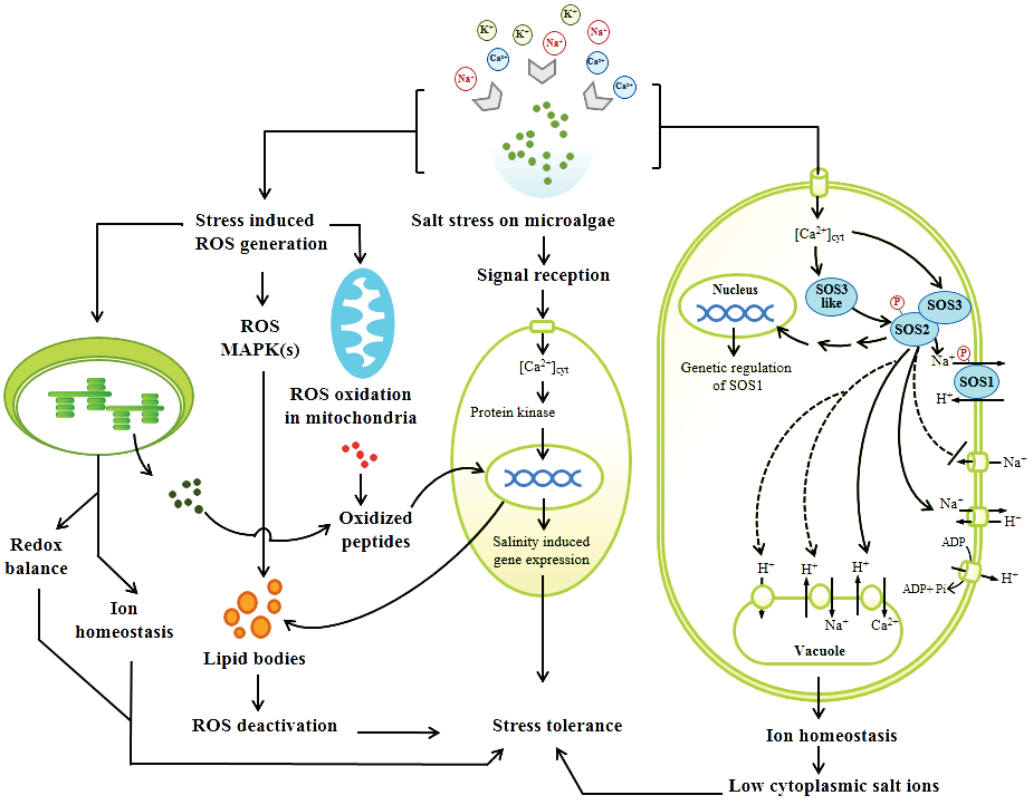

Figure 5.5: Mechanism of lipid accumulation under salt induced condition.

5.5 Summary

The role of various salts concentrations on the two freshwater microalgae CG12 and GS12 were investigated. The maximum lipid content was obtained in $CaCl_2$ treated microalgae up to 40.02 % and 44.97 % in CG12 and GS12 respectively with a retarded growth. The fatty acid profile of extracted lipids was quantified by NMR and demonstrated significant changes in the presence of salt treatment. A correlation was built between fatty acid composition and salt treatment by hierarchical cluster analysis. The mechanistic model for Ca^{2+} ion mediated lipid accumulation suggest a holistic base for salt study in microalgae and its subsequent application for biofuel production.

The most imperative inference of this chapter is application of $CaCl_2$ enhances the lipid accumulation in microalgae by two folds as compared to untreated cell (refer

Chapter 4). Hence, after attaining such high lipid content in CG12 (40.02 %) and GS12 (44.97 %) the lab scale (100-200 mL) culture has been extended to 100 L in serially connected 10 L photobioreactors for scale up studies. The scale-up studies was conducted to accumulate significant amount of lipid and further its extraction and transesterification. Moreover, the next chapter also provide brief insight on supercritical methanol transesterification.

CHAPTER 6

SCALE UP STUDIES AND CONVERSION OF MICROALGAE OIL TO BIODIESEL VIA SUPERCRITICAL METHANOL TRANSESTERIFICATION

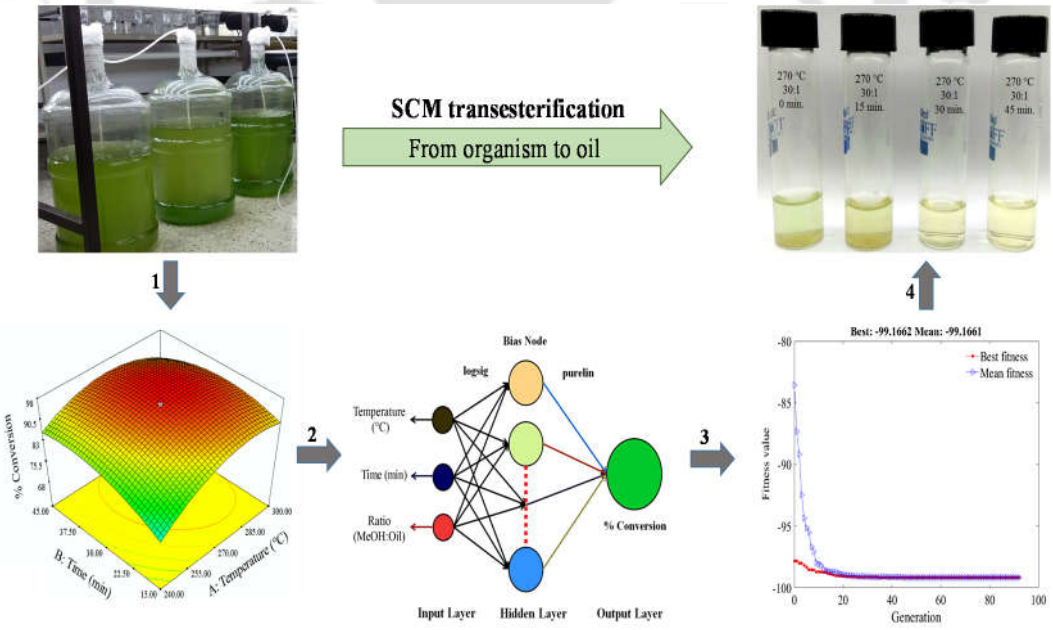

Scale up studies and transesterification of microalgae oil to biodiesel *via* supercritical methanol

After attaining the high lipid content in microalgae the scale up studies were performed to extract huge amount of lipid from microalgae biomass. The conventional method of biodiesel production is less effective and releases hazardous waste into the environment. Therefore, this chapter has focused to explore advanced transesterification process to overlook the problems of conventional transesterification method that can provide a holistic model for industrial scale biodiesel production. Additionally, the process must have a global or standard conditions so that variety of feedstock can be process through this method. Hence, SCM transesterification method was chosen with sequential hybrid optimization of RSM, ANN and GA to generate an effective biodiesel production process.

6.1 Scale up studies

The microalgae cultivation of CG12 was performed under laboratory optimized conditions of light intensity 3460 lux, temperature 21.07 °C and pH 8.74 in a standard BG–11 medium. The details of optimized culture conditions have been extensively described in the earlier chapter 4. Photobioreactors for large–scale microalgae cultivation up to 100 L were established in a serially connected 10 L batch mode for biomass accumulation (Figure 6.1). After the completion of cultivation period (21 days), the biomass was harvested by flocculation (using trivalent metal ion solution of $FeCl_3$), centrifuged (6000 rpm for 10 min.), dried overnight at 60 °C and subsequently employed for lipid extraction.

Figure 6.1: Mass cultivation and scale up studies performed for microalgae cultivation (a) harvested microalgae paste, (b) dried biomass and (c) bioreactor used for mass cultivation.

6.2 Conversion of microalgae oil to FAME

The extracted microalgae lipid was initially transesterified by acid catalyzed method (Christie, 2009). However, the biodiesel yield obtained was only 80 % hence, for further upgrading and high biodiesel yield an advanced method of SCM transesterification was employed for conversion of microalgae oil to FAME. The efficiency of SCM transesterification process depends on several intrinsic operating parameters such as reaction temperature, reaction time and MeOH: oil molar ratio (MR) etc. Therefore, to optimize the process conditions an integrated approach of stepwise hybrid optimization was followed using RSM, ANN and GA.

6.3 Evaluation of significant factors using CCD design

A three–level, three–factor CCD was applied for carrying out the optimization studies to maximize the oil to FAME conversion process. For this study, the input variables (factors) and their levels were selected, based on the reported literature and preliminary experiments carried out in the laboratory. Temperature, time and MeOH: oil molar ratio was designed as coded factors A, B, and C, respectively (Table 6.1).

Table 6.1: Independent process variables and their response on lipid accumulation on microalgae.

Independent variables	Symbol	Unit	Variable levels		
			–1	0	+1
Temperature	A	°C	240	270	300
Time	B	Min	15	30	45
MeOH: oil	C	MR	15	30	45

MR= molar ratio

A matrix of 20 experimental runs were performed to find out the optimum combination and the effect of process parameters on FAME conversion efficiency analyzed by ^{1}H NMR (Table 6.2). The second order polynomial equation obtained with the experimental results from CCD is depicted in Eq. 6.1.

$$\% \text{ Conversion} = 96.47+(3.55\times A)+(1.85\times B)-(3.82\times C)-(2.99\times A\times B) + (3.38\times B\times C)-(6.55\times A^2)-(4.61\times B^2)-(2.51\times C^2) \quad 6.1$$

The experimental observation showed closed proximity with the model predicted assumptions having a regression coefficient of 0.97 which not only indicate an excellent fit of the model to the experimental data. It also shows that 97 % effect on the yield of SCM transesterification can be explained by the variation of the process parameters. Moreover, the probability value (p–value) of the model was 0.0001 which shows that the model is highly accurate and precise to explain all the variables.

Table 6.2: RSM generated matrix condition for experimentation and validation through ANN.

S.no.	Temp. (°C)	Time (min.)	MeOH: oil (molar ratio)	% Conversion of oil to FAME		
				Exp.	RSM	ANN
1	240	15	15	85.01	81.62	84.86
2	300	15	15	93.23	94.70	92.10
3	240	45	15	86.64	84.53	90.26
4	300	45	15	87.60	85.65	87.60
5	240	15	45	67.36	67.21	67.38
6	300	15	45	81.33	80.29	81.32
7	240	45	45	85.22	83.65	85.15
8	300	45	45	84.54	84.78	84.54
9	219.55	30	30	68.48	71.98	68.44
10	320.45	30	30	85.13	83.92	85.13
11	270	4.77	30	79.26	80.32	79.25
12	270	55.23	30	85.30	86.53	85.29
13	270	30	4.77	94.22	95.80	94.22
14	270	30	55.23	82.24	82.95	82.21
15	270	30	30	95.89	96.47	96.23
16	270	30	30	97.11	96.4	96.23
17	270	30	30	95.67	96.47	96.23
18	270	30	30	97.15	96.4	96.23
19	270	30	30	96.26	96.47	96.23
20	270	30	30	97.14	96.47	96.23

All the single coded factors for temperature (A), time (B) and MeOH: oil ratios (C), two–factor interactions AB, BC and quadratic interactions such as A^2, B^2, and C^2 were found significant. Further, the significance of the model was justified by high F value and low p–value. The model F–value of 46.22 also indicates that all the model terms are independent and important (Table 6.3). It should be noted that the quadratic regression model valid only within the experimental range applied in the present study.

Table 6.3: ANOVA analysis performed for SCM transesterification.

Source	Sum of Squares	Df	Mean Square	F Value	p–value Prob > F
Model	1460.21	8	182.53	46.22	< 0.0001
A–Temperature (°C)	172.04	1	172.04	43.57	< 0.0001
B–Time (min.)	46.60	1	46.60	11.80	<0.0056
C–MeOH:Oil	199.35	1	199.35	50.48	< 0.0001
AB	71.46		71.46	18.10	<0.0014
BC	91.60	1	91.60	23.20	<0.0005
A^2	617.74	1	617.74	156.44	< 0.0001
B^2	306.46	1	306.46	77.61	< 0.0001
C^2	90.63	1	90.63	22.95	<0.0006
Residual	43.44	11	3.95	–	–
Lack of Fit	41.12	6	6.85	14.80	0.0048
Pure Error	2.31	5	0.46	–	–
Cor Total	1503.65	19	–	–	–

6.4 Effect of process parameters on transesterification conversion efficiency

6.4.1 Effect of temperature

The present study indicates that the temperature has the most significant role in SCM conversion of microalgae oil to FAME. In a supercritical state, at a higher temperature, the intramolecular hydrogen bonding in the MeOH molecule decreased significantly, due to high energy molecular vibrations. As a result, the polarity and dielectric constant of MeOH reduce and allowed to behave as a free monomer. In this condition, MeOH can solvate the non–polar triglycerides to form a single phase of oil/MeOH mixture and results in FAME and diglycerides. Similarly, diglycerides react with SCM to form monoglyceride and FAME, and subsequently, monoglyceride will again react with SCM to form FAME and glycerol (Biktashev et al., 2011; Marulanda, 2012).

Moreover, it was observed that at lower temperatures of 220 to 240 °C the percentage conversion efficiency of FAME hardly reaches to 67–85 %. Whereas, a further increase in the temperature to 270 °C, increased the conversion efficiency to 97.15 % (Table 6.2). It is believed that the lower temperature may not be able to create significant variation in the weakening of intermolecular hydrogen bonding resulting in low conversion efficiency. However, at 270 °C the sufficient intermolecular vibrational energy was exhibited to efficiently convert microalgae oil to FAME. A similar observation was also reported while producing biodiesel from waste canola oil (Lee et al., 2012). Conversely, further increase in the temperature from 270 to 300 °C and 320 °C reduces the conversion efficiency to 85 % (Table 6.2). Previously, it was suggested that higher temperatures may cause the degradation of FAMEs due to thermal decomposition which could be a reason for less conversion efficiency of microalgae oil to FAME (Imahara et al., 2008; Quesada–Medina and Olivares–Carrillo, 2011).

Hence, from the above experimental observations it can be concluded that temperature has most profound effect on percent conversion efficiency of microalgae oil to FAME. Furthermore, the higher F–value (43.57) and lower p–value (0.0001) for temperature also represents the significant impact of temperature on the percentage conversion efficiency of microalgae oil to FAME.

6.4.2 Effect of reaction time

Reaction time plays a significant role in SCM transesterification compared to MeOH: oil molar ratio. The effect of reaction time on FAME yield was investigated by varying the reaction time from 15 to 45 min. Experiments were conducted with various MeOH: oil molar ratio for the above–mentioned conditions (Table 6.2). SCM transesterification converts fatty acids to their corresponding FAME within few min. (Samniang et al., 2014). It is expected that longer reaction time offers transesterification reaction to

progress towards completion and may result in higher yield of FAMEs. However, higher reaction time beyond the particular limit in supercritical transesterification may lead to loss of unsaturated FAME due to degradation reaction (Reddy et al., 2014) Similarly, in the present study, a low conversion efficiency (85.30 %) was observed at longer reaction time of 55.23 min. whereas, maximum conversion of microalgae oil to FAME was obtained at a moderate reaction time of 30 min. (Table 6.2).

Moreover, the corresponding interaction of reaction time with other process parameters on FAME yield has been examined and represented in 3D response surface plots (Figure 6.2). Temperature and reaction time showed a strong interaction which can be easily observed by the steepness of response surface curvatures. It was also observed that increasing the temperature from 240 to 270 °C with increase in reaction time from 15 to 30 min increases the conversion efficiency whereas a further increase in temperature and reaction time to 300 °C and 45 min. respectively, decreases the conversion efficiency (Figure 6.1 a). In addition to that reaction time also had strong interaction with MeOH: oil molar ratio. The smaller reaction time could not allow the oil and MeOH molecule to react completely and therefore decrease the conversion efficiency. Hence, it can be concluded that effective MeOH molecules to oil and sufficient interaction time needed for the efficient conversion of microalgae oil to FAME which has been observed at approximately 30 min. time at 30:1 MeOH: oil molar ratio resulting in yield of 97.15 % (Figure 6.2 b). Similarly, Samniang et al., (2014) have reported high conversion efficiency of oil to FAME due to induced intramolecular hydrogen bond collision in a short reaction time.

Further, no significant interaction between temperature and MeOH: oil molar ratio was observed and therefore to maintain the model adequacy the non–significant terms have been removed.

6.4.3 Effect of MeOH: oil molar ratio

The MeOH: oil molar ratio considered as another effective parameter for efficient conversion of microalgae oil to FAME. Conventionally three moles of methanol are required to convert one mole of the TAG into FAME, however, in SCM transesterification high MeOH: oil molar ratio is favored for effective conversion. It is suggested that high MeOH: oil molar ratio is a prerequisite to push the reaction in the forward direction by increasing the contact area of oil with MeOH and maintaining a lower critical temperature for SCM transesterification (Hegel et al., 2008). However, with this assumption many studies in the literature have reported the use of high MeOH: oil molar ratio during SCM transesterification, which is a major concern in sustainable development due to the non–renewable nature of MeOH (Bunyakiat et al., 2006; Lee et al., 2012; Samniang et al., 2014). Therefore, recent studies were mostly focused on the usage of lower molar ratio of methanol in SCM transesterification (Sakdasri et al., 2015). Hence, considering this fact, the present study also employed low MeOH: oil molar ratio and achieved maximum conversion of 97.15 % with 30:1 MeOH: oil molar ratio (Table 6.2). However, low conversion of 87.01 % was obtained in 15:1 MeOH: oil molar ratio. It is assumed that lower MeOH: oil molar ratio might not provide effective free MeOH molecules to interact with oil, additionally high MeOH: oil molar ratio 55.23:1 must have diluted the oil molecule that may also lead to lower conversion (82.24 %) of FAME (Table 6.2). This interpretation was further supported by high F–value of 50.48 for 30:1 MeOH: oil molar ratio and low p–value 0.0001 which suggest that the model is sufficient to build reaction conditions for efficient percentage conversion of microalgae oil to FAME (Table 6.3).

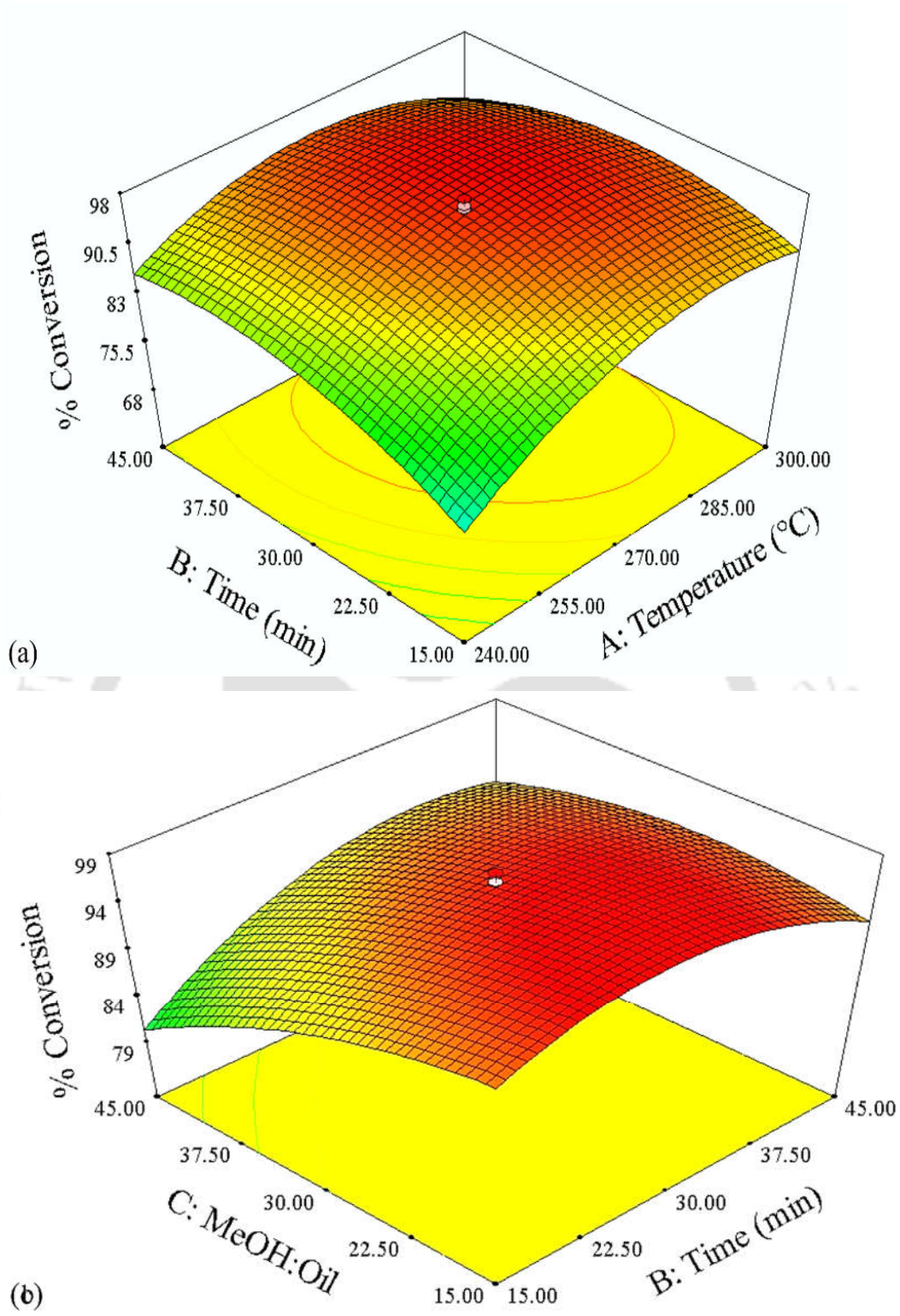

Figure 6.2 3D response surface plots obtained for % conversion efficiency of microalgae oil to FAME.

6.5 Artificial neural network

In the current scenario, artificial neural networks have been applied successfully in various bioprocess optimization systems to overcome the problems associated with RSM for both linear and non–linear responses (Betiku et al., 2014; del Rio–Chanona et al., 2016; Sarve et al., 2015). The RSM generated matrix conditions were applied to ANN for model comparison and validation. A sequential training was given to ANN network from input layer to hidden layer and from hidden layer to output layer. The network architecture was constructed with feed forward back propagation (3–7–1) and trained by trainlm training algorithm (Figure 6.3).

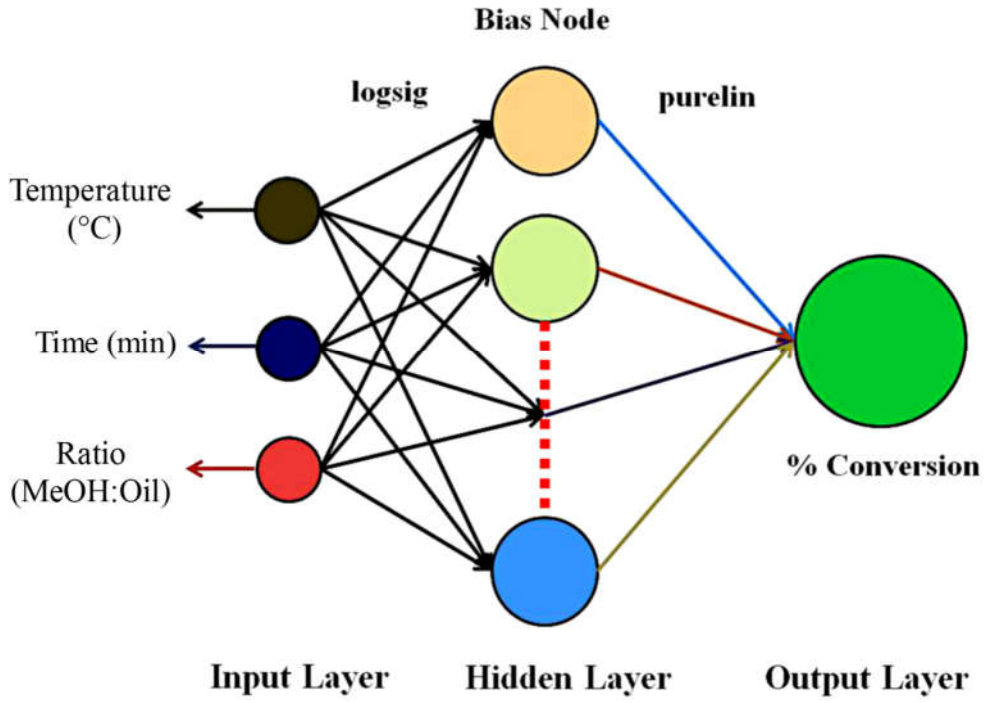

Figure 6.3: Finalized artificial neural network architecture for SCM transesterification.

After several iterations, the best–optimized reaction condition was selected based on a minimum RMSE value. A successive training of neural network requires extensive dataset for higher accuracy. Therefore 70 % of total data generated by ANN was used

to train the model, while 15 % data was used for testing and 15 % for validation (Figure 6.4). Regression analysis of ANN model showed the R^2 value of 0.994, exhibiting the higher accuracy and significance of ANN model compared to RSM.

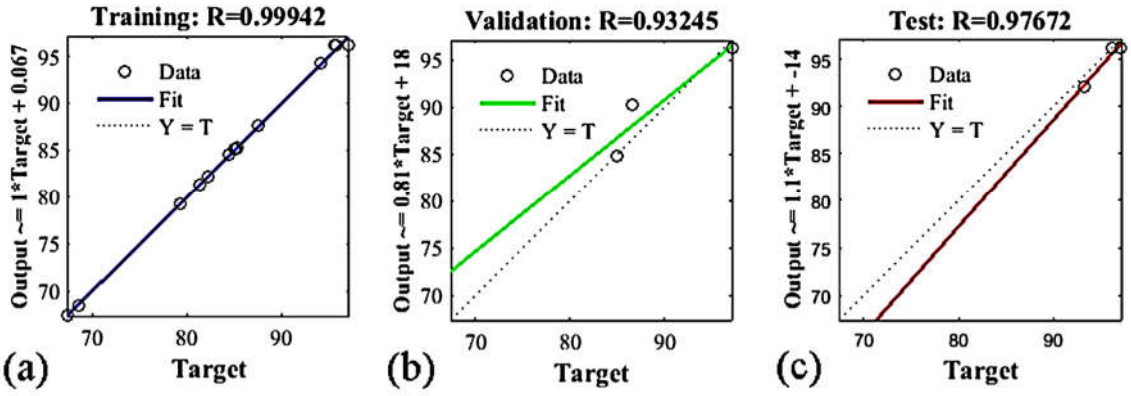

Figure 6.4: ANN state plot for training, validation and test analysis of SCM transesterification.

Furthermore, the subsequent iteration cycles were carried out till the best–optimized condition attained. The best–optimized condition was generated in 4 epoch whereas 6 epochs were run to confirm the model accuracy (Figure 6.5).

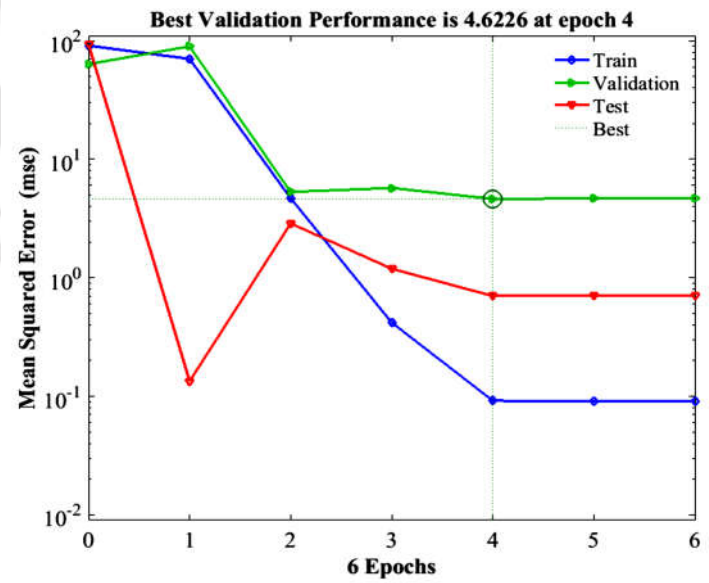

Figure 6.5: The best performance validation check for SCM transesterification.

Moreover, the sensitivity analysis revealed the valuable contribution of each process parameter for the successful conversion of microalgae oil into FAME under SCM transesterification condition (Table 6.5). The leave one out approach was considered for estimating the sensitivity of each process parameters, which revealed that temperature had the most significant effect on percentage conversion of microalgae oil to FAME. The similar observation was earlier established by RSM model.

Table 6.4: Sensitivity analysis of the effective parameters of SCM transesterification.

SCM transesterification	RMSE	RMSE difference	Contribution (%)
All Parameters (3)	0.9289	–	
L–Temperature	9.5572	8.6283	51.11
L–Time	5.5226	4.5937	27.22
L–MeOH:oil	4.5865	3.6576	21.67
Total	–	16.8796	100.00

L: leave one out

6.6 Genetic algorithm

Though, both the RSM and ANN models were adequately predicted the optimization conditions, but the problem associated with these models is their local convergence of generalization. Therefore, researchers have developed an optimization tool i.e. GA which is capable of predicting the optimization conditions globally. The response obtained from ANN optimized process conditions were used as fitness function for GA. GA depicts the constraints for temperature, time and MeOH: oil molar ratio with lower (Temp. – 219.5 °C, Time – 4.7 min. and MeOH:oil – 4.7) and the upper bound (Temp. –320.4 °C, Time – 55.2 min., MeOH:oil –55.2) of process parameters selected for optimization. Concurrently 50 generations were analyzed to find the best–fit individual. The best–optimized condition generated by GA with temperature – 285.21 °C, time – 26.5 min., and MeOH: oil –23.4:1 resulted with 99.16 % conversion efficiency (Figure

6.6) after 51 iterations (reproduction) and crossovers. It was also observed that during the selection of the best fitness value almost 95 generation were analyzed by GA however the experimental yield obtained at the optimum condition was 98.12 % conversion efficiency. Moreover, GA response also showed that temperature played a significant role in the conversion of microalgae oil to FAME compared to the time and MeOH: oil molar ratio.

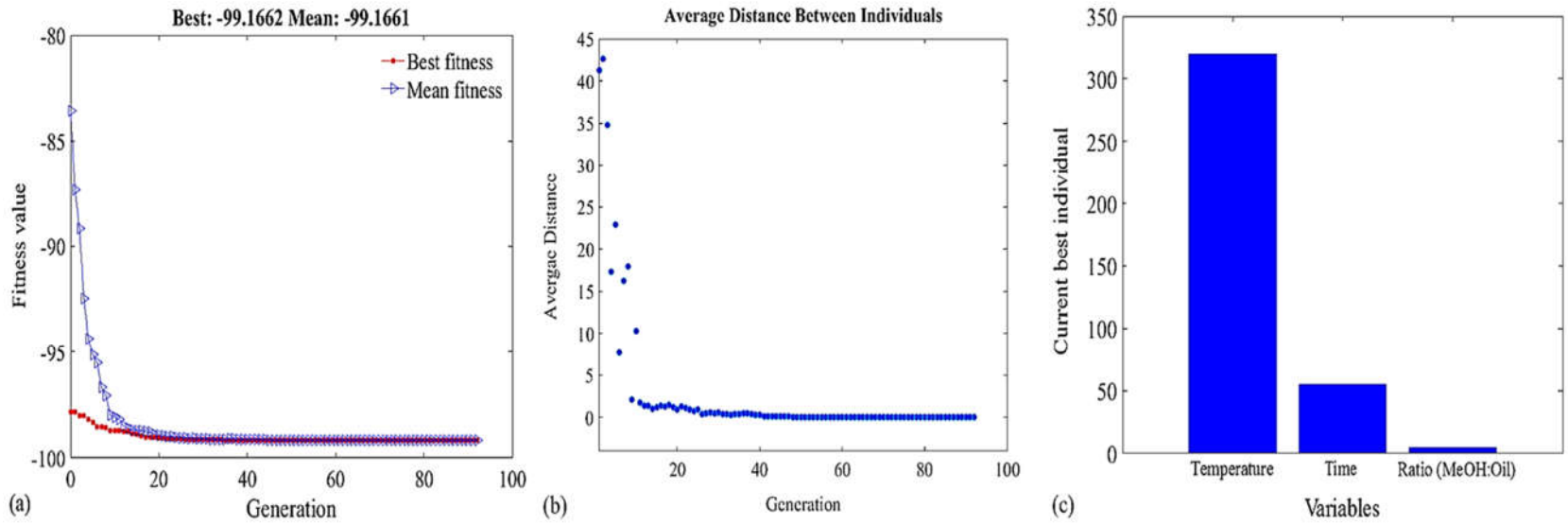

Figure 6.6: Genetic algorithm performed to create global optimum condition (a) selection of best–fit individual (b) average distance between the selected individual and (c) % contribution of effective parameters.

6.7 Integrated hybrid modelling for SCM transesterification

From the above discussion, it is concluded that an integrative hybrid modeling approach is useful in predicting global response for process optimization. Firstly, the experimental boundary conditions were defined by selecting preliminary experiments. The three most influential parameters selected for SCM transesterification such as temperature, time and MeOH: oil molar ratio. Further, based on the primary study the experimental matrix conditions were designed by RSM using CCD matrix. ANOVA analysis evaluated the accuracy and significance level of the model. Subsequently, the data set was validated through ANN so that the non–linear equations can be defined precisely which was not explained by RSM. ANN being a more advanced optimization method was chosen to select the best model based on the minimum RMSE value. Further, both the predicted models were compared for high accuracy centered on their regression coefficient, RMSE value and average standard deviation (SD). Regression analysis showed 0.97 and 0.99 R^2 value of RSM and ANN suggesting more accuracy of ANN predicted model compared to RSM. Furthermore, a huge difference in RMSE value and standard deviation of the predicted models were also observed. The RSM predicted RMSE value was 1.46 while ANN predicted 0.92. Moreover, SD of experimental and predicted response of the model showed the less deviation of 1.37 for RSM and 0.95 for ANN. The comparative study of both the model suggested the prediction performance of the ANN model for the validation data set confirmed its superior generalization capacity for the given case over the RSM (Figure 6.7).

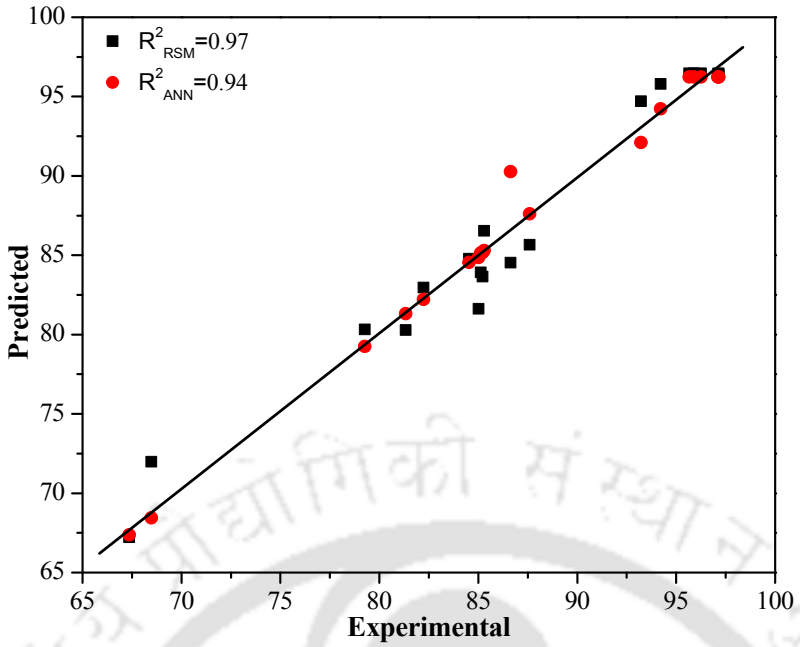

Figure 6.7: Regression analysis performed for comparative analysis between RSM and ANN predicted model.

Furthermore, as discussed earlier that RSM and ANN models are good for their predictive and generalization capacity locally, but fail to develop global optimum conditions. Therefore, the polynomial equation generated by the ANN model was selected as a fitness function and integrated to GA for building a global optimization condition. Hence, in the present study, a subsequent stepwise hybrid optimization of RSM–ANN–GA showed a dependence of all the optimization methods on each other for global prediction of response more accurately. RSM was employed to reduce the data redundancy and to provide a precise matrix of closely interacting parameters. RSM was followed by ANN to ensure the validity of a predicted model and to explain the non–linear interaction unleashed by RSM. Additionally, the coupling of the GA network with ANN was used to represent the global optimum condition for SCM of microalgae oil. The less fit individual data point died in generation cycle, and only the best individual was selected. In this study, at the end of 51 generation, the best–optimized condition was created with 99.16 % conversion efficiency of oil to FAME (Table 6.5). Further,

experimentation on the GA optimized condition yielded 98.12 % conversion of oil to FAME. Hence, this integrative hybrid modeling and optimization methodology provides a better understanding of the process parameters on the outcomes of SCM transesterification process and thus helped in sustainable biodiesel process development.

Table 6.5: Final optimized local and global generalized performance yield of FAME obtained from SCM transesterification.

	Input Parameters			Output Value
Models	Temp. (°C)	Time (min.)	MeOH:oil (MR)	% Conversion
RSM	280.41	28.55	24.32	98.01
ANN	280.41	28.55	24.32	98.15
GA	285.21	26.57	23.47	99.16
Exp.	285.21	26.57	23.47	98.12

6.8 Evaluating the transesterification conversion efficiency

A ratio of protons of the methyl esters (3.6 ppm) to the α–methylene proton (2.34 ppm) was used to determine the percentage (%) conversion efficiency of FAME (Figure 6.8). The corresponding reduction of the α–methylene triplet peak at 2.34 ppm and an increase in methyoxy proton singlet peak near 3.6 ppm was used to establish the percentage conversion efficiency of oil to FAME using following equation (Meher et al., 2006).

$$\% \text{ Conversion} = \frac{2\text{Me}}{3\text{CH}_2} \times 100 \qquad 6.1$$

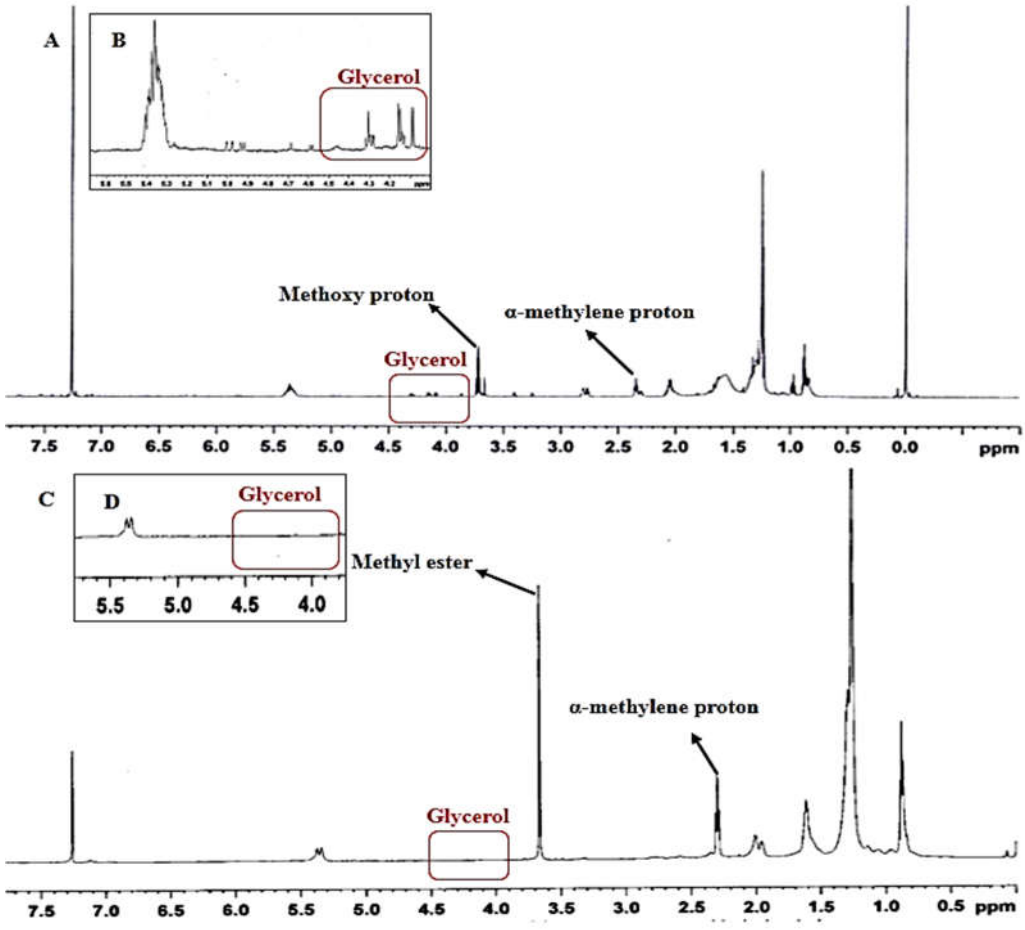

Figure 6.8: Conversion of microalgae oil to fatty acid methyl ester.

NMR is a high throughput, non–destructive technique used to calculate the conversion of oil to FAME. The chemical shifts for methoxy protons and methylene protons were analyzed for each experimental run. Conversion efficiency was calculated by peak integration at 3.6 ppm and 2.3 ppm, respectively. The peak at 2.3 ppm corresponds to a methylene proton, and a singlet at 3.6–3.7 ppm represents methyl esters peak. Furthermore, these two peaks were multiplied by a factor of 2 and 3, respectively. The corresponding increase in 3.6 ppm peak and a decrease in 2.3 ppm peak corroborate the conversion of microalgae oil to FAME (Knothe et al., 2015). Moreover, the peak at 2.7–2.8 ppm also diminishes with increased conversion of FAME. From NMR analysis it is quite evident that most of the oil converted to FAME in SCM transesterification. The disappearance of glycerol peak at 4.2 ppm after SCM transesterification indicates

the high conversion efficiency of microalgae oil to FAME. Additionally, the insignificant quantity of glycerol was observed at the bottom of a reactor and remain undetected in the NMR analysis. However, both biodiesel and the remaining glycerol were obtained in its approximately pure form. Therefore, SCM transesterification yield with almost 99 to 100 % conversion efficiency is considered as a zero waste generation process of biodiesel production (Demirbas, 2009). The biodiesel obtained after SCM process showed that after 30 and 45 min. pure biodiesel can be obtained along with glycerol. However, insuffcicient reaction time of 15 min. showed unreacted fatty acids and particulate material (Figure 6.9).

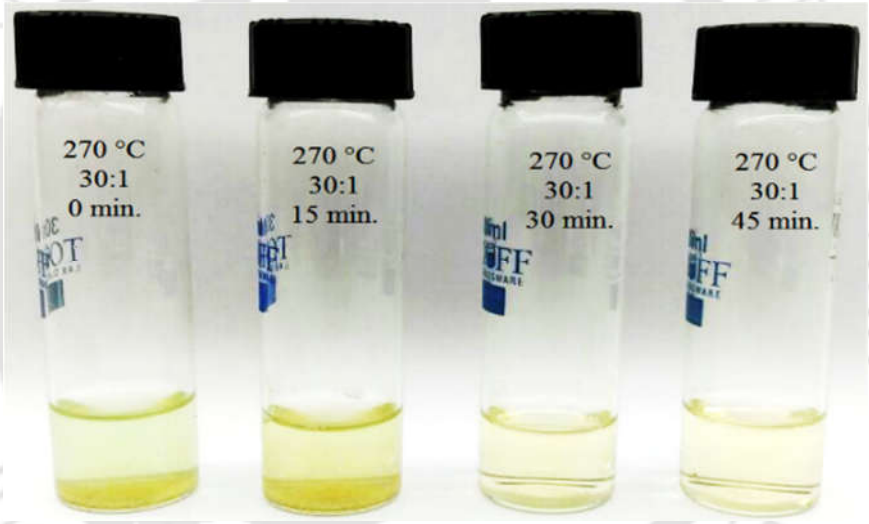

Figure 6.9: Biodiesel quality assessment obtained after SCM transesterification at different time intervals.

6.9 Product characterization

Evaluation of methyl esters properties was carried out by biodiesel analyzer software using FAME composition (Talebi et al., 2014). The fatty acid composition of microalgae oil majorly showed the presence of palmitic acid 28.13 %, palmitoleic acid 8.02 %, oleic acid 33.8 %, linoleic acid 8.15 %, linolenic acid 2.25 % and margaric acid 4.86 % accounting 85 % of total fatty acids. Moreover, the remaining 15 % of fatty acid profile showed the presence of some other fatty acids such as tridecanoic acid 12 ME

(2.79 %), 9,12 octadecanoic acid (6.44 %), 7 dimethyl–4–(1–methylethyl) cyclodecane (4.72 %). Among the major fatty acids, the total saturated and unsaturated fatty acid contents were found to be 32.99 % and 52.25 %, respectively. Whereas, monounsaturated fatty acid content was 41.85 %. Several researchers have reported that biodiesel properties such as acid value, saponification value, iodine number, cetane number and oxidation stability, etc. depend on the fatty acid composition of oil (Knothe, 2005; Ramírez–Verduzco et al., 2012). It was reported that high monounsaturated fatty acid content favors high cetane number, cloud point, viscosity, and oxidation stability (Mazumdar et al., 2012).

Other properties of microalgae FAME such as saponification value, iodine value, and cetane number were estimated to be 178.64 mg/g, 76.89, and 59.55, respectively. High cetane number is desirable to reduce obnoxious gas emissions. The oxidation stability of microalgae biodiesel was 12.7 hr., HHV 33.94 MJ/Kg, viscosity 3.07 mm^2/s and density 0.756 g/cm^3. The above mentioned fuel properties of microalgae oil were comparable with biodiesel ASTM D6571 standard. The results of the study reveal that SCM transesterification process can efficiently convert microalgae oil to FAME in a single–step and can act as attractive solutions to reduce chemical and energy consumption in the overall biodiesel production process.

6.10 Summary

Supercritical methanol transesterification is an efficient and eco–friendly process for industrial–scale biodiesel production. Sequential optimization of the process conditions using integrated hybrid modeling of RSM–ANN–GA showed a comparably high prediction ability of the model. A globally best–optimized condition generated by GA for SCM transesterification with temp.–285.21 °C, time – 26.5 min., and MeOH: oil

molar ratio 23.4 displayed 99.16 % conversion efficiency. The experimental yield obtained at this optimized condition was 98.12 % with 1 % deviation from the predicted model. Furthermore, GC–MS analysis showed higher palmitic and oleic acid content which revealed the compatibility of algal biodiesel with ASTM D6751 standard. Hence, it is encouraged that computational intelligence based hybrid optimization is an efficient approach to model the process conditions to obtain high SCM transesterification conversion efficiency to attain qualitative biodiesel from microalgae oil.

From the above discussion it can be concluded that SCM transesterification can be a cost effective process for industrial scale microalgae biodiesel production. However, the major problem is the need of huge microalgae biomass. Moreover, to cultivate such large amount of microalgae biomass excessive amount of nutrient will be required. The need of purchased nutrient additionally add expenses on the microalgae biodiesel production cost. Therefore, an alternative nutrient resource is prerequisite for large scale microalgae cultivation. The unconventional nutrient source for microalgae cultivation has been described in the following chapter (Chapter 7).

CHAPTER 7

MICROALGAE CULTURE CONDITION OPTIMIZATION UNDER WASTE STREAMS FOR BIOMASS AND LIPID PRODUCTION USING RSM AND ANN

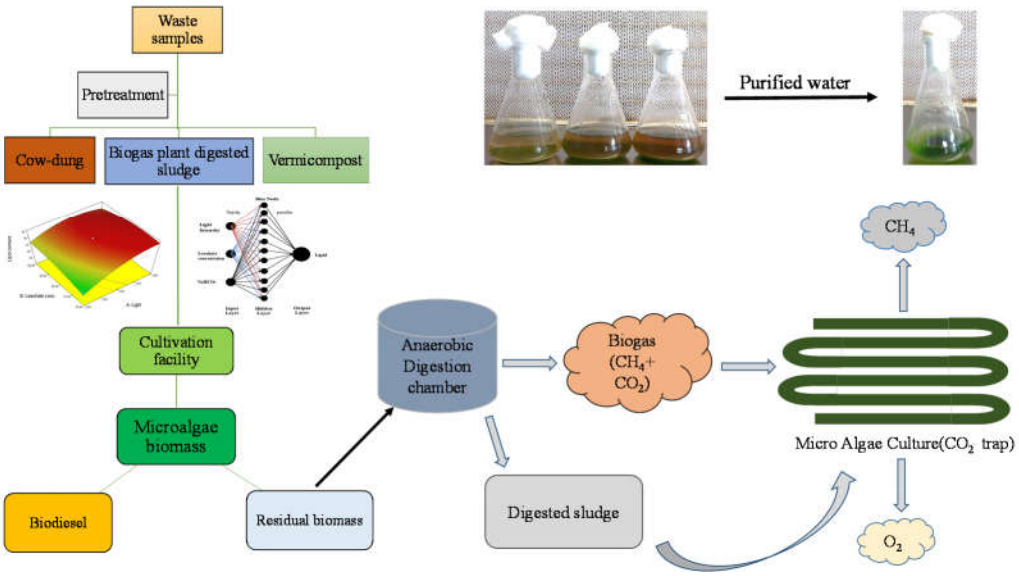

Microalgae culture condition optimization under waste streams for biomass and lipid production using RSM and ANN

Waste disposal today loom as a major concern worldwide. If we look around our environment the disposal of agricultural, domestic and industrial waste are contaminating soil, water and air in a number of ways. According to World Bank group by the next 15 years, 1.2 to 1.4 kg per capita waste will be generated daily. India alone generate 100000 million solid waste every day. It is high–time that we realize waste management is not only essential from a public welfare perspective but it can also contribute to economic growth. If the recycling industry is promoted alongside eco–industrial production, this integrated approach would put India at an advantage while managing its growing solid wastes. With this facts and figures the present study was carried to use three different solid waste streams *viz.* cow–dung (CD), biogas plant digested sludge (BPW) and vermicompost (VM) for microalgae cultivation for efficient growth and lipid production and simultaneous waste stabilization. Moreover, as discussed in the previous chapters that the purchased nutrients increases the production cost of microalgae cultivation which therefore lag behind the marketing of microalgae biodiesel. Therefore, this chapter provides a solution to both of the above said problems. Microalgae provide an effective solution for simultaneous waste remediation and sustainable fuel production.

7.1 Characterization of samples

The elemental analysis of the three waste samples *viz.* CD, BPW and VM were performed by EDX and CHNS. EDX analysis of waste material revealed the presence of macroelements such as Na, K,Mg,Ca, P etc., that supports the growth of microalgae (Table 7.1). Highest nitrogen concentration was observed in CD (3.4 wt %) followed

by BPW 2.6 wt. % and 2.09 wt. % in VM. The CHNS elemental analysis shows that BPW and CD can be directly used as cheap media source whereas VM requires certain additional salts to cope up with microalgae growth. However maximum carbon content was observed in vermicompost 50.81 followed by cow dung 36.93 %. It is believed that the low carbon content in BPW might be because most of the carbon content has been liberated in form of methane (CH_4) and CO_2 during biogas production.

Table 7.1: Elemental analysis of the waste sample.

Elements	CD	BPW	VM
C	36.93	17.67	50.81
H	5.31	2.52	5.68
N	3.44	2.63	2.09
S	0.50	0.62	0.02
Si	2.56	18.83	14.33
Al	0.23	7.40	3.33
P	0.15	3.06	1.8
Fe	0.23	3.43	2.2
Ca	0.40	2.53	3.1
Mg	0.20	2.53	1.47
K	0.46	1.87	2.5
S	0.15	0.50	0.7
Na	0.10	0.43	–
Mn	0.10	0.43	–
Cl	0.16	–	0.70
Ni	0.10	–	0.15

7.2 Preliminary study

Initially, the dried powder of waste samples were mixed in 1:10 ratio with distilled water, continuously stirred for 24 hr. at 60 °C. The extracts were filtered and centrifuged to remove all the particulate matter and subsequently autoclaved to 121 °C at 15 psi to

avoid microbial contamination. The autoclaved extract/leachate was used as culture medium for subsequent microalgae cultivation. The three different concentrations of leachate 10 % (A), 20 % (B) and 30 % (C) were used for succeeding experiments.

The preliminary study was conducted under laboratory conditions of 3 Klux light intensity, 22±2 °C temperature, pH range varies from 7–7.5. Initially, the growth response of microalgae was recorded based on the biomass concentration (g/L) and lipid content (% dcw) in all the three waste dilutions of 10 %, 20 % and 30 % for all three solid waste. In CG12 the highest biomass accumulation was observed in 10 % leachate concentration of BPW whereas the comparable lipid accumulation was observed in both 10 % and 20 % leachate concentration of BPW (Figure 7.1 a). Similarly, in GS12 the maximum biomass was obtained in 10 % leachate concentration whereas highest lipid content was observed in 20 % BPW extract. The present finding showed coherence with most of the previous reports suggesting that 15–20 % waste dilution is effective for microalgae cultivation (Bohutskyi et al., 2016; Wang et al., 2010). Moreover, during the study it was also observed that BPW grown microalgae have better growth response and lipid accumulation compared to CD and VM. Therefore, only BPW was carried forward for the optimization studies. Moreover, it was also found that microalgae were capable of removing the contaminants and can purify water in a due course of time. The nutrient removal efficiency of microalgae was about 99–100 % and can be used for tertiary or quaternary wastewater treatment as it removes all the impurities and provide clear water (Figure 7.2)

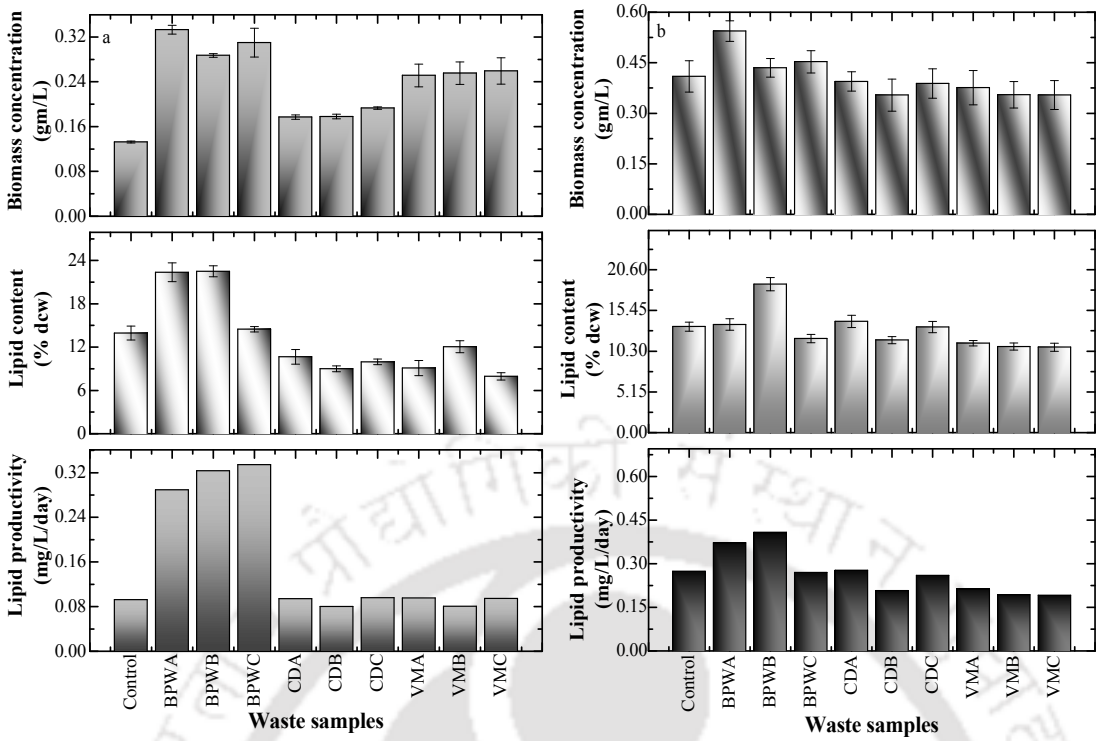

Figure 7.1: Biomass, lipid content and lipid productivity of microalgae (a) CG12 and (b) GS12.

Figure 7.2: Growth of microalgae under different dilution of biogas plant digestate.

7.3 Optimization of culture condition

RSM experiments were designed to obtain enhanced lipid yield from waste grown microalgae under varying environmental conditions. The three different process variables light intensity, leachate concentration and $NaHCO_3$ were selected as process variables. Ranges of the process variables involved in this study has been depicted Table 7.2. The reason for selecting these variables are that light is an intrinsic factor for

growth and survival of phototrophic microalgae. The other imperative factor is nutrient availability which has been provided by the BPW. The excess and limitation of nutrients in the culture medium strappingly influences the microalgae growth as well as lipid accumulation. Hence, maintenance of appropriate concentration of nutrient is essential for proper microalgae growth. Therefore, different dilutions of the waste stream has been selected as important parameter. Finally, as stated above that the carbon concentration in BPW is lesser than CD and VM due to release of CH_4 and CO_2 during anaerobic digestion. Hence, to provide additional inorganic carbon supplementation $NaHCO_3$ has been selected as another parameter, as it is easily utilizable by microalgae. All these three factors have been studied individually for their effect on lipid accumulation on microalgae during preliminary studies.

Table 7.2: Independent process variables and their response on lipid accumulation.

Independent variables	Symbol	Unit	Variable levels		
			–1	0	+1
Light Intensity	A	Klux	2	3	4
Leachate conc.	B	v/v %	10	20	30
$NaHCO_3$	C	wt./v %	0.5	1	1.5

The response was calculated on the basis of percent lipid content obtained after each set of experiment. Light intensity, leachate concentration and $NaHCO_3$ were designed as coded factors A, B and C respectively. The second order polynomial equation was fitted with the experimental results. A quadratic polynomial equation was obtained from the experimental data was used to predict the optimum lipid content for microalgae depicted in equation 7.1 and 7.2.

$$\text{Lipid content (\% dcw)} = 44.94+4.25*A+1.30*B+4.61*C+1.66*A*B +7.39*A*C-0.093*B*C-6.30*A^2-5.31*B^2-8.24*C^2 \quad 7.1$$

$$\text{Lipid content (\% dcw)} = 41.16 + 5.46*A + 1.08*B + 0.99*C - 2.66*A*B + 0.70*A*C + 1.02*B*C - 4.73*A^2 - 1.86*B^2 - 7.30*C^2 \quad (7.2)$$

All the designed experimental runs were performed under laboratory conditions and the results were analyzed by multiple regression analysis for CG12 and GS12 depicted in Table 7.3 (a and b). The lipid content obtained from RSM predicted model was 44.94 % dcw and 41.16 % dcw whereas the experimentally observed value was 44.88 % dcw and 41.13 % dcw for CG12 and GS12 respectively. The model precision was evaluated by the regression coefficient i.e., R^2. The regression values for lipid content were represented as R^2_{CG12}= 0.9946 and R^2_{GS12}= 0.9914 (Figure 7.3). The adjusted R^2 for the model were R^2_{CG12}= 0.9897 and R^2_{GS12} = 0.9837 whereas the corresponding predicted R^2 were 0.9592 and 0.9336. The predicted R^2 has a good agreement with the adjusted R^2 depicting model's good fitting to the experimental observation.

Table 7.3 (a): RSM based CCD generated matrix condition for experimentation and their corresponding experimental yield and validation through ANN in CG12.

CG12	Light intensity (Klux)	Leachate conc. (%)	$NaHCO_3$ (%)	Lipid content Exp.	RSM	ANN
1	2	10	0.5	23.29	23.89	23.29
2	4	10	0.5	12.77	14.29	12.77
3	2	30	0.5	23.05	23.37	23.05
4	4	30	0.5	19.42	20.38	19.42
5	2	10	1.5	18.04	18.51	18.04
6	4	10	1.5	37.36	38.48	37.36
7	2	30	1.5	17.70	17.62	17.70
8	4	30	1.5	43.37	44.21	44.24
9	1.32	20	1	20.07	19.98	20.07
10	4.68	20	1	36.22	34.27	37.26
11	3	3.18	1	29.24	27.73	29.24
12	3	36.82	1	32.63	32.11	37.49
13	3	20	0.16	15.21	13.88	15.21
14	3	20	1.84	30.10	29.40	30.10
15	3	20	1	44.88	44.94	44.88
16	3	20	1	44.88	44.94	44.88
17	3	20	1	44.88	44.94	44.88
18	3	20	1	44.88	44.94	44.88
19	3	20	1	44.88	44.94	44.88
20	3	20	1	44.88	44.94	44.88

Table 7.3 (b): RSM based CCD generated matrix condition for experimentation and their corresponding experimental yield and validation through ANN in GS12.

GS12	Light intensity (Klux)	Leachate conc. (%)	$NaHCO_3$ (%)	Lipid content		
				Exp.	RSM	ANN
1	2	10	0.5	19.03	18.80	19.03
2	4	10	0.5	32.06	33.64	32.05
3	2	30	0.5	24.69	24.24	24.67
4	4	30	0.5	28.61	28.43	28.57
5	2	10	1.5	16.58	17.34	14.41
6	4	10	1.5	33.94	34.98	33.97
7	2	30	1.5	27.88	26.88	28.02
8	4	30	1.5	33.05	33.86	33.04
9	1.32	20	1	17.79	18.61	17.88
10	4.68	20	1	38.61	36.96	38.61
11	3	3.18	1	35.69	34.09	35.60
12	3	36.82	1	36.95	37.72	36.92
13	3	20	0.16	18.98	18.83	19.09
14	3	20	1.84	22.85	21.17	22.98
15	3	20	1	41.13	41.16	41.12
16	3	20	1	41.13	41.16	41.12
17	3	20	1	41.13	41.16	41.12
18	3	20	1	41.13	41.16	41.12
19	3	20	1	41.13	41.16	41.12
20	3	20	1	41.13	41.16	41.12

7.4 Evaluating the significance of factors using CCD design

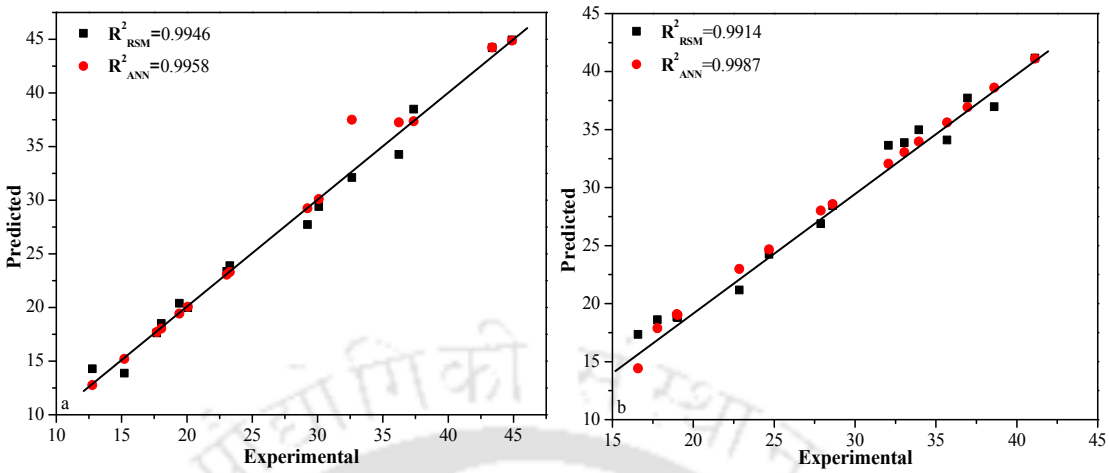

Figure 7.3: The regression analysis performed for microalgae (a) CG12 and (b) GS12.

Moreover, from ANOVA analysis high model F value was obtained for CG12 and GS12 to up to 204.75 and 128.35 respectively whereas the p value signifies to 0.0001 level suggesting the high model adequacy and fitting. Lower p value and higher F value indicates that model is highly considerable. It was found that there is only a 0.0001 % chance of the model fitting error in CG12 and GS12 may be due to noise. Values of "Prob > F" less than 0.0500 indicate model terms for CG12 *viz.* A, B, C, AB, AC, A^2, B^2, C^2 are significant. Simmilarly in GS12 A, B, C, AB, BC, A^2, B^2 and C^2 were significant. The lack of fit of the sum of squares of the model must be non–significant for the model fit which was obsered in the present study. The lack of fit for the model was calculated as 14.48 and 13.32 for CG12 and GS12. Moreover, the high adequate precision 36.40 and 29.40 and low coefficient of variance for the model prediction and corresponding experimental observations (CV %) with 3.83 and 3.62 showed that there is very rare chance of experimental error.

Table 7.4 (a): ANOVA analysis performed for CG12.

CG12	Sum of Squares	Degree of freedom	Mean Square	F Value	p–value Prob > F
Model	2668.23	9	296.47	204.75	< 0.0001
A–Light	246.37	1	246.37	170.15	< 0.0001
B–Leachate conc.	23.12	1	23.12	15.97	0.0025
C–$NaHCO_3$	290.58	1	290.58	200.68	< 0.0001
AB	21.91	1	21.91	15.13	0.0030
AC	437.30	1	437.30	302.01	< 0.0001
BC	0.068	1	0.068	0.047	0.8322
A^2	571.37	1	571.37	394.60	< 0.0001
B^2	406.09	1	406.09	280.46	< 0.0001
C^2	977.70	1	977.70	675.22	< 0.0001
Residual	14.48	10	1.45		
Lack of Fit	14.48	5	2.90		
Pure Error	0	5	0		
Cor Total	2682.71	19			

Table 7.4 (b): ANOVA analysis performed for GS12

GS12	Sum of Squares	Degree of freedom	Mean Square	F Value	p–value Prob > F
Model	1515.35	9	168.37	128.35	< 0.0001
A–Light	406.51	1	406.51	309.89	< 0.0001
B–Leachate conc.	15.90	1	15.90	12.12	0.0059
C–NaHCO3	13.46	1	13.46	10.26	0.0094
AB	56.73	1	56.73	43.25	< 0.0001
AC	3.90	1	3.90	2.97	0.1156
BC	8.40	1	8.40	6.41	0.0298
A^2	322.23	1	322.23	245.64	< 0.0001
B^2	49.68	1	49.68	37.87	0.0001
C^2	768.46	1	768.46	585.81	< 0.0001
Residual	13.12	10	1.31		
Lack of Fit	13.12	5	2.62		
Pure Error	0	5	0		
Cor Total	1528.47	19			

7.4.1 Effect of light intensity

The effect of light intensity was studied on lipid accumulation of microalgae. Among all three influential factor light intensity showed a profound effect on lipid accumulation on both the species. The calculated p–value was obtained 0.0001 for both CG12 and GS12 respectively. The preliminary study was conducted with an initial light intensity of 3 Klux at temperature 22±2 °C under laboratory condition. The range of light intensity for RSM designing was taken from 2–4 Klux. It was expected the switching of nutrient assimilation mode of microalgae from phototrophic to heterotrophic and/or mixotrophic and vice versa may induce the lipid accumulation.

Microalgae itself can adjust to assimilate excess amount of C, N and P shifting the phototrophic assimilation of nutrients towards heterotrophic mode. Microalgae require light for cell growth, biomass enhancement and synthesis of essential compounds for its growth. The green microalgae especially absorb light energy through chlorophyll and convert the radiation energy into chemical energy such as NADPH and ATP involved in the metabolic activity (Blair et al., 2014; Přibyl et al., 2013). During the photosynthesis process the oxygen evolved is utilized by the microorganism for the oxidation of waste which converts the macromolecules into simple organics. Subsequently, these simpler molecules were utilized by microalgae to synthesize the biomass in presence of sunlight. The mechanism of waste stabilization has been presented in Figure 7.4. In the present study it was found that increasing the light intensity increases lipid accumulation in microalgae and reaches a maximum at 3 Klux. The maximum lipid accummulation obtained at 3 Klux light intensity and 20 % leachate concentration was 44.88 % and 41.13 % dcw, CG12 and GS12 correspondingly.

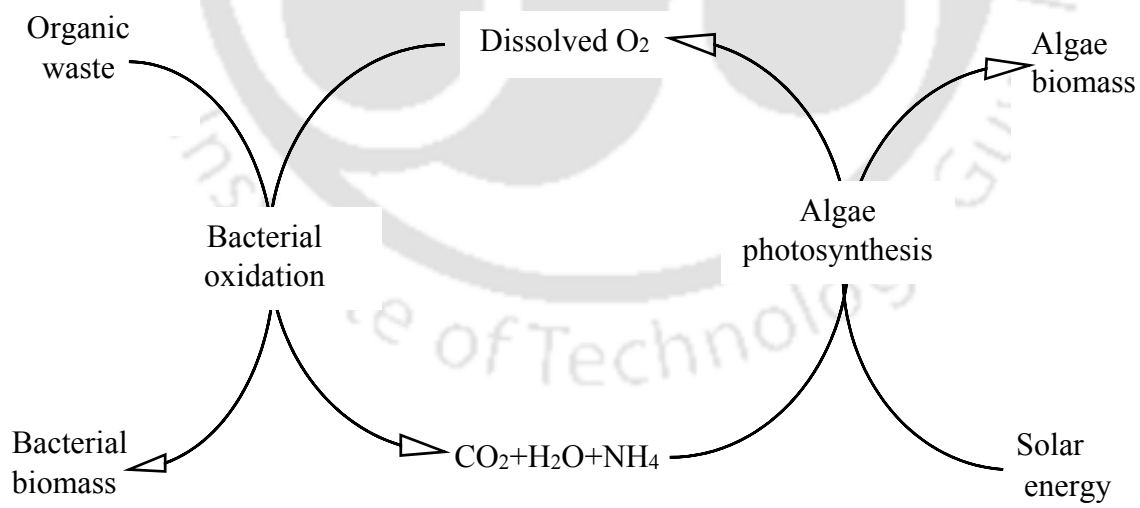

Figure 7.4: The phototrophic mechanism of waste stabilization by microal_

The steepness of 3D response surface plot clearly reveals the contribution of light intensity towards lipid accumulation compared to leacahate concentation and $NaHCO_3$

in CG12 and GS12 (Figure 7.5). In CG12 the lipid accumulation was obtained 20.07 % dcw under the low light intensity of 1.32 Klux. The maximum lipid accumulation acheived at 3 Klux was 44.88 % dcw. Further increament of light intensity to 4.68 Klux decreases lipid accumulation in CG12 to 36.22 % dcw (Table 7.3 a). Whereas in GS12 increasing the light intensity from 1.32 Klux (17.79 % dcw) to 3 Klux enhances the lipid accumulation 2 folds, whereas a further increase of light intensity of 4.68 slightly reduces lipid content 38.61 % dcw (Table 7.3 b). It was clearly observed that moderate light intensity favors lipid accumulation while high and low light intensity did not show high impact. The RSM optimized condition for light intensity was obtained 3.68 Klux for both CG12 and GS12 resulting in 45.42 % dcw and 41.71 % dcw lipid accumulation (Figure 7.6).

7.4.2 Effect of Leachate concentration

In the present study three different leachate concentrations were used to examine the role of leachate concentration on lipid accumulation of both the microalgae. Leachate concentration of 10 %, 20 % and 30 % were used for all the RSM designed experiments. It was found that higher concentration above 30 % hinders light to pass through into the culture medium due to its dark colour reducing the microalgae growth. A significant effect of leachate concentration was observed with linear (B) and quadratic interaction terms (B^2) in both the microalgae. However, in GS12 the interaction of leachate concentration with light intensity (AB) and $NaHCO_3$ (BC) were significant whereas in CG12 only interaction of leachate concentration with light intensity (AB) was significant. It was assumed that indeed the photoautotrophic nature of microalgae plays a significant role in nutrient assimilation and synthesizes biomass under high leachate concentration and sufficient light energy. The interaction of leachate concentration with

light is highly desirable for microalgae growth and lipid accumulation as it was observed from response surface plots of CG12 depicted in Figure 7.5 (b and c) and GS12 Figure 7.5 (e and f). The p value for leachate concentration was observed 0.0025 and 0.0059 for CG12 and GS12 respectively. The optimized leachate concentration for maximized lipid yield of 45.42 % and 41.71 % obtained at 19.27 % and 11.12 % for CG12 and GS12 respectively (Figure 7.6).

Furthermore, the simplest form of macro and micro nutrient are present in BPW than any other waste material which is essential microalgae growth and metabolism. The volume of the sludge produced daily is extremely large with no availability problem all year round, and the sludge needs to be recycled for further treatment to avoid environmental contamination. Thus, the use of the biogas plant digested sludge for algae cultivation could serve the dual role of waste reduction and biomass/bioenergy production.

7.4.3 Effect of $NaHCO_3$

Microalgae have an ability to switch the mode of nutrition to phototrophic to heterotrophic, sometime mixotrophic and vice versa based on the environmental condition. Generally, during the photosynthesis, microalgae use CO_2 as an inorganic carbon source, while water acts as an electron donor for production of glucose, which is further transformed to various complex sugar forms such as carbohydrate, starch etc. Many microalgae species are able to utilize carbonates such as Na_2CO_3 and $NaHCO_3$ for cell growth (Wang and Lan, 2011). Some studies have indicated that about 25–50 % of the algal carbon in high rate algal ponds (HRAP) is derived from heterotrophic utilization of organic carbon. The organic carbon sources can be assimilated either chemo or photo–heterotrophically (Marudhupandi et al., 2016). In the present study,

this nutritional fluctuation can be easily observed with the significant interaction of light intensity and leachate concentration (AB) in CG12 and with less significant interaction (BC) in $NaHCO_3$ and leachate. From ANOVA analysis it was observed that $NaHCO_3$ have a significant role in lipid accumulation and showed a p–value of 0.0001 and 0.0094 in CG12 and GS12 respectively. Moreover, the optimized concentration of $NaHCO_3$ for high lipid yield was observed at 1.04 % and 1.09 % concentration for CG12 and GS12 respectively (Figure 7.6).

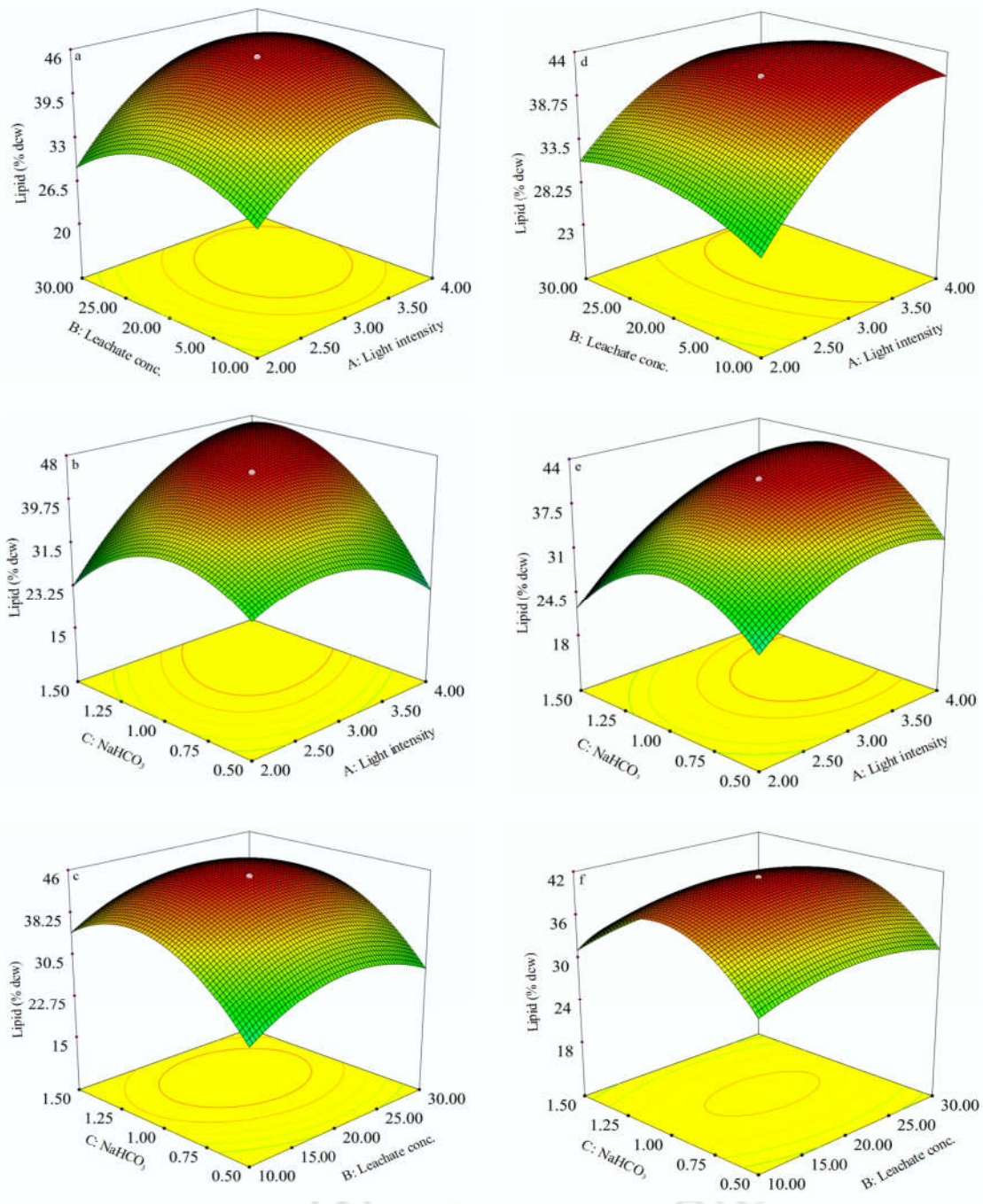

Figure 7.5: The 3D response surface plots obtained for microalgae (a,b,c) CG12 and (d,e,f) GS12.

7.5 Artificial neural network

The response of artificial neural network was analyzed using same process parameters, used in RSM. A feed–forward back propagation network structure was selected for modelling the lipid accumulation. The network architecture was developed with 3

nodes in the input layer, 13 nodes in the hidden layer and 1 node in output layer for CG12 (3–13–1). Likewise for GS12 the selected architecture was 3–11–1. The three inputs given to ANN were light intensity, leachate concentration and $NaHCO_3$ wheras lipid content was selected as an output (Figure 7.6)

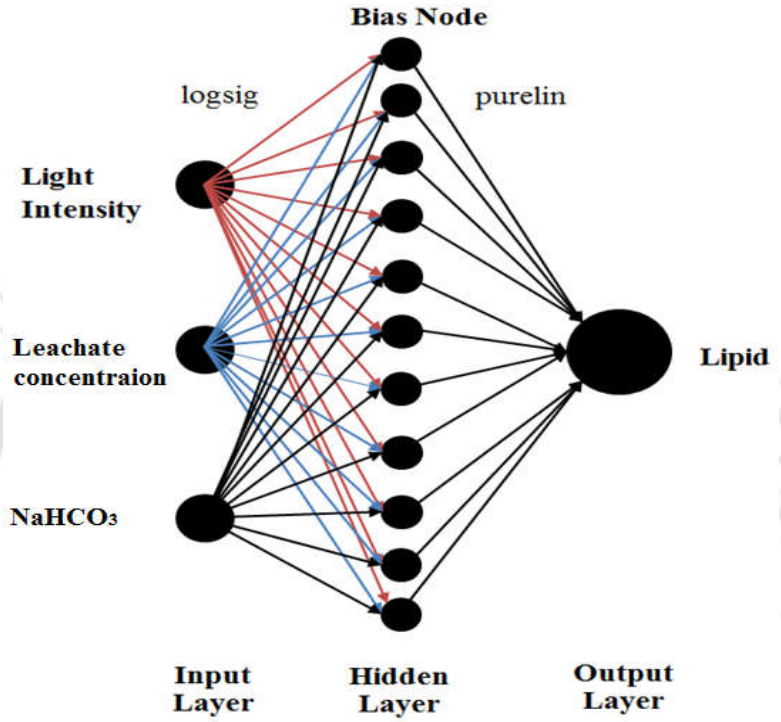

Figure 7.6: Finalized neural network architecture for microalgae.

The changes of output parameter with the relative change in input parameter was studied by sensitivity analysis. It shows the corresponding dependence of an output parameter sensitivity over an input. Further, to evaluate the effect of each input parameter on output parameter by leave one out approach was employed. By leaving each input parameter the percentage change of RMSE value was calculated with respect to the RMSE value while considering all the input parameters (Nasir et al., 2011). The withdrawal of significant input parameter resulted in a higher RMSE value, which revealed the greater sensitivity of network output to that parameter. From the senstivity analysis it was observed that light intensity plays a crucial role in algae growth and lipid accumulation. Light intensity contribution to lipid accumulation were

observed 45.73 % and 42.61 % in CG12 and GS12 respectively as depicted in Table 7.5 (a and b). The RMSE value increases from 0.9958 to 10.1452 and 0.9987 to 7.3254 while eliminating light intensity from the other input parameters in CG12 and GS12, respectively. Next to the light intensity the other sensitive parameter for lipid accumulation was $NaHCO_3$ concentration followed by leachate concentration.

Table 7.5 (a): Sensitivity analysis performed for CG12.

CG12	RMSE	RMSE difference	Contribution (%)
All Parameters (3)	0.9958	–	–
L: Light intensity	10.1452	9.1494	45.73
L: Leachate conc.	4.9952	3.9994	19.99
L: $NaHCO_3$	7.8544	6.8586	34.28
Total		20.0074	100.0

L: leave out

Table 7.5 (b): Sensitivity analysis performed for GS12.

GS12	RMSE	RMSE difference	Contribution (%)
All Parameter	0.9987	–	–
Light intensity (Klux)	7.3254	6.3267	42.61
Leachate conc. (%)	4.1157	3.1170	21.00
$NaHCO_3$ (%)	6.4012	5.4025	36.39
Total		14.8462	100.0

L: leave out

Moreover, ANN requires a large number of data sets as compared to RSM. Therefore 70 % of data was used to train the model, 15 % was used for validation of the predicted model and 15 % data was used for testing the model (Figure 7.7). The gradient is a value of back propagation algorithm on each iteration in logarithmic scale. The gradient value $5.8503e^{-14}$ and $5.4074e^{-9}$ for CG12 and GS12 respectively suggests that it reached

the bottom of the local minimum of goal function at epoch 7 and epoch 4 (Figure 7.8). Hence, the model was stopped at a 7 and 4 cycle for CG12 and GS12 respectively.

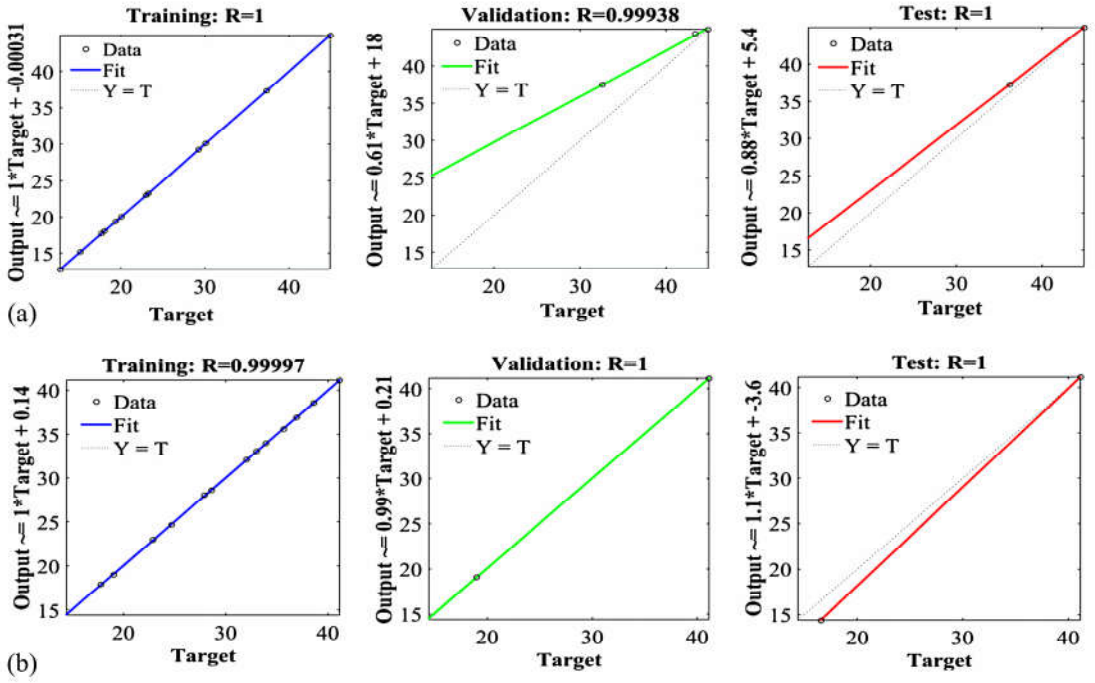

Figure 7.7: Training validation and test plot for microalgae (a) CG12 and (b) GS12.

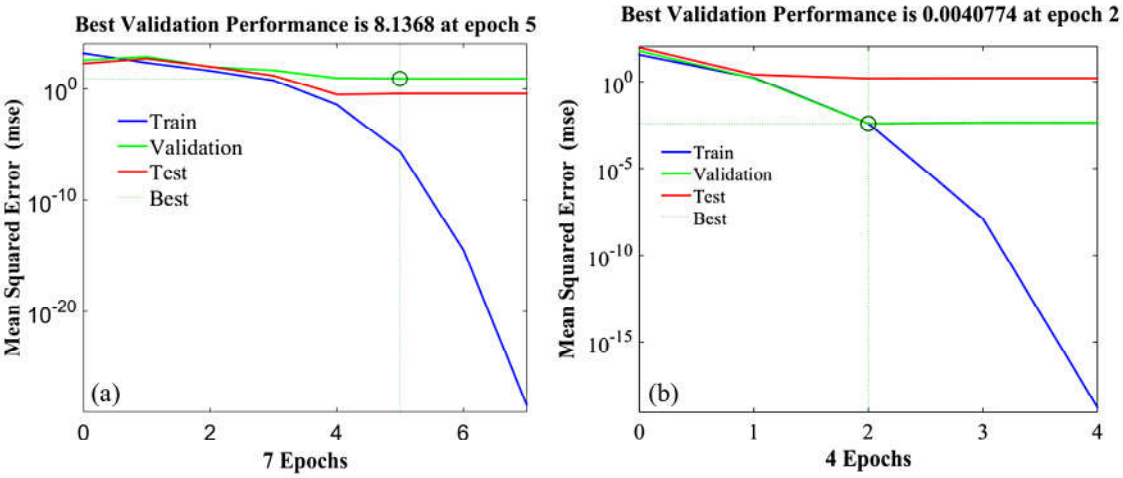

Figure 7.8: Validation performance check for microalgae (a) CG12 and (b) GS12.

7.6 Comparison of estimation capabilities of RSM and ANN

The predicted response computed by RSM and ANN are presented for CG12 and GS12 respectively presented in Table 7.2 (a and b). Evaluation based on the models'

coefficient of determination actually showed the satisfactory convergence between the actual and predicted response. Thus both the models can be considered to perform data fitting and offered a stable response. Therefore, from the above study it can be suggested that both the models can be used either in combination or distinctly. The observed regression coefficient R^2_{CG12} and R^2_{GS12} obtained from RSM were 0.9946 and 0.9914 (Figure 7.3), respectively. Whereas ANN predicted values were R_{CG12} 0.9958 and R_{GS12} 0.9987 (Figure 7.3), respectively. These values are very close to 1 showed that both the models worked well for this study of lipid accumulation in microalgae influenced by physicochemical parameters. ANOVA analysis of the process parameters revealed that the model terms are significant. Light intensity showed the greatest impact on lipid accumulation with a p value of 0.0001 for CG12 and GS12. Further validation by ANN also proved the significant contribution of light intensity up to 45.73 % and 42.61 % in CG12 and GS12. Moreover, the final optimum condition obtained from both the model showed very less average standard deviation from the experimental observation (Table 7.6). Further, to minimize the number of experiments and for the better understanding of inter–interaction of all process parameters both the methods can be chosen. The preliminary observation of selected parameters by RSM reduces the number of experiments, while using the same data set for validation by ANN (different nodal signals) clearly revealed their inter–interaction. On the basis of accuracy ANN is more reliable, but requires huge number of the dataset. While RSM is preferred technique for statistical analysis with small data points. Thus, it has been suggested that for a better model prediction both the methods can be chosen together.

Table 7.6: Final optimized conditions obtained for microalgae from RSM and ANN predicted models and experimental observation.

Microalgae	LI (Klux)	LC (%)	$NaHCO_3$ (%)	RSM	ANN	Exp.
CG12	3.68	19.27	1.04	45.42	45.18	44.56
GS12	3.68	11.12	1.09	41.71	42.04	41.89

LI: light intensity, LC: leachate conc.

7.7 Summary

The present chapter summarizes that BPW can be an efficient source of nutrient for microalgae growth. The optimized process condition obtained for CG12 and GS12 were light intensity (3.68 Klux), leachate concentration (19.27 and 11.12 %) and $NaHCO_3$ (1.04 and 1.09 %) for CG12 and GS12 respectively. The optimized process condition yielded with high lipid content of 44.56 % in CG12 and 41.89 % in GS12 correspondingly. Hence, it is suggested that phycoremediation is not only helpful in mitigating environmental pollution but also reduces the production cost of microalgae biofuel.

During the whole study it has been observed that after the oil extraction from microalgae (includes chapter 4, 5, 6 and 7) the residual biomass has been discarded as waste. Though, it has a huge energy potential and can be exploited for synthesis of other forms of biofuel. Therefore, the defatted microalgae residue was used for the co-digestion with rice straw for biogas production and discussed in the following chapter (Chapter 8).

CHAPTER 8

REUTILIZATION OF MICROALGAE RESIDUES FOR SUSTAINABLE BIOREFINERY DEVELOPMENT

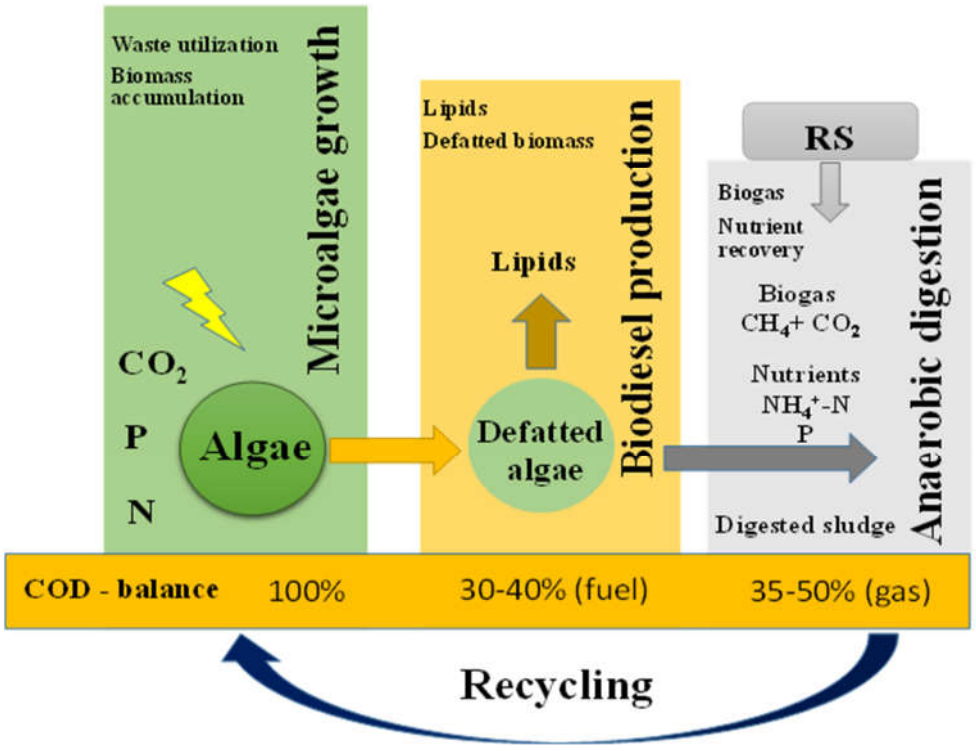

Reutilization of microalgae residues for sustainable biorefinery development

After the extraction and transesterification of microalgae oil to biodiesel, the residual microalgae biomass was utilized for anaerobic co-digestion (AcoD). Utilization of the microalgae residue for biomethane production recovers more energy than energy obtained from biodiesel alone. Due to low solid loading capacity and high C/N ratio of microalgae biomass, the defatted microalgae were co-digested with rice straw (RS). RS was chosen as co-digestion substrate due to its abundance and availability throughout the year in agriculture country like India. The batch study for bio-methane potential experiments was conducted to study the cooperative effects of both the substrates (RS and defatted microalgae) on bio-methane production. The co-digestion of microalgae and RS not only enhances the biogas yield but also provide a platform for the development of microalgae-based sustainable biorefinery.

8.1 Physicochemical properties analysis

The primary motivation of the present study was to extract the additional energy content available in the defatted microalgae residue. The physicochemical analysis was conducted to evaluate the biomethane production potential of defatted microalgae biomass. The FTIR analysis of raw and defatted microalgae clearly showed that even after lipid extraction other functional molecules still present in the microalgae biomass with high energy potential as depicted in Figure 8.1. Initially, biomass characterization performed by CHNS analysis revealed the percentage composition of elements present in the microalgae CG12, GS12, RS and cow-dung inoculum (Table 8.1). The calculated C/N values for CG12, GS12, and RS were found to be 4.89, 7.02 and 43, respectively. The discrepancy in C/N ratio is the main influential factor for establishing high

biomethane production potential. The high C/N ratio increases the uptake of nitrogen by methanogens, whereas lower C/N ratio tends to accumulate ammonia, any of the above-mentioned conditions can be unfavorable for the rate of methane production. It is believed that high C/N ratio in RS and low C/N ratio in defatted microalgae can together balance the effective C/N ratio. Hence, during all the experimentation an effective C/N ratio of 30 was maintained. The C/N of CD inoculum was excluded from the calculation because an equal amount of CD was inoculated in all the reactors assuming that it imparts equal C/N to all the reactors.

The observed total solid (% TS) content for all the three substrates CG12, GS12 and RS was 89.49 %, 92.47 %, and 94.09 %, respectively. The low TS content in CG12 is may be due to the tiny microalgae structure of CG12. The bio-methane potential is a function of both microalgae structural and biochemical composition and therefore, the corresponding volatile solid (VS) content was measured on % TS basis which revealed 54.85 %, 80.5 % and 84.80 % of VS in CG12, GS12, and RS, respectively, depicting the high biodegradability and suitability of aforementioned biomass for efficient biogas production (Divya et al., 2015). The gross calorific value for all the biomass was measured and showed the correspondingly high energy content of 19.50, 22.94, 15.57 and 15.51 MJ/kg in CG12, GS12, RS and cow dung, supporting the claim of its utilization as an organic matter in anaerobic co-digestion (Table 8.1).

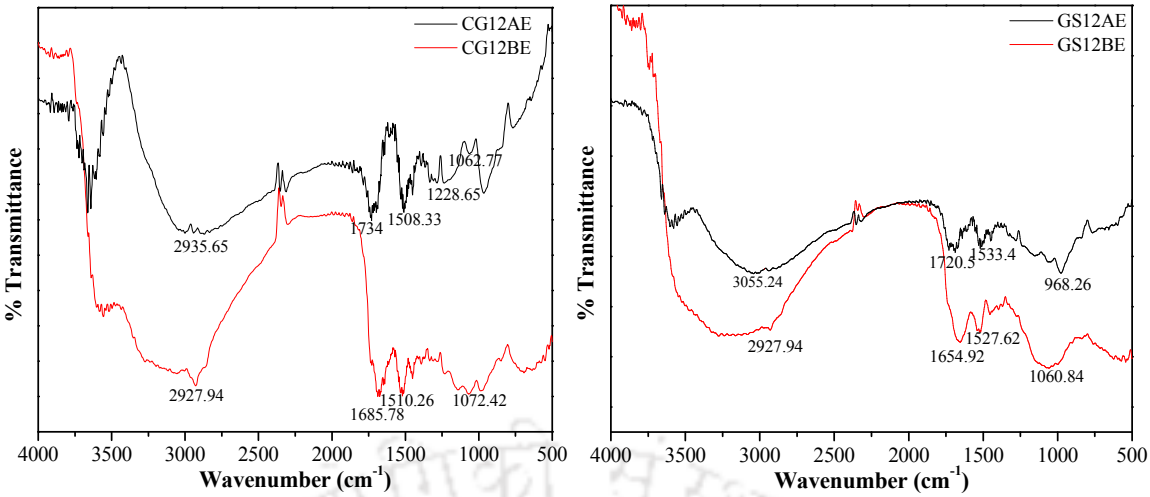

Figure 8.1: FTIR analysis of microalgae biomass for the presence of biomolecules.

Table 8.1: Physicochemical parameter analysis for rice straw, cow-dung, and microalgae.

Parameters	CD	RS	CG12	GS12
C	36.93	31.39	47.39	51.49
H	5.313	ND	6.964	7.448
N	3.446	0.73	9.692	7.334
S	ND	ND	ND	ND
C/N	10.71	43	4.89	7.02
pH	6.88	7.08	7.42	7.53
TS (%)	94.09	19.8	89.49	92.47
VS (%TS)	84.80	65.02	54.85	80.5
VS/TS	0.901	3.28	1.65	6.62
sCOD (g/L)	5.6	8.13	3.2	2.4
VFA (mg/L)	452.5	504	1875	1575
CV (MJ/kg)	15.57	15.51	19.50	22.94
Ash (%)	12.5	25.9	33.20	12.15
Cellulose	62.46	ND	64.32	66.94
Hemicellulose	17.68	ND	27.12	26.30
Lignin	19.81	ND	8.53	6.75

*ND: not determined

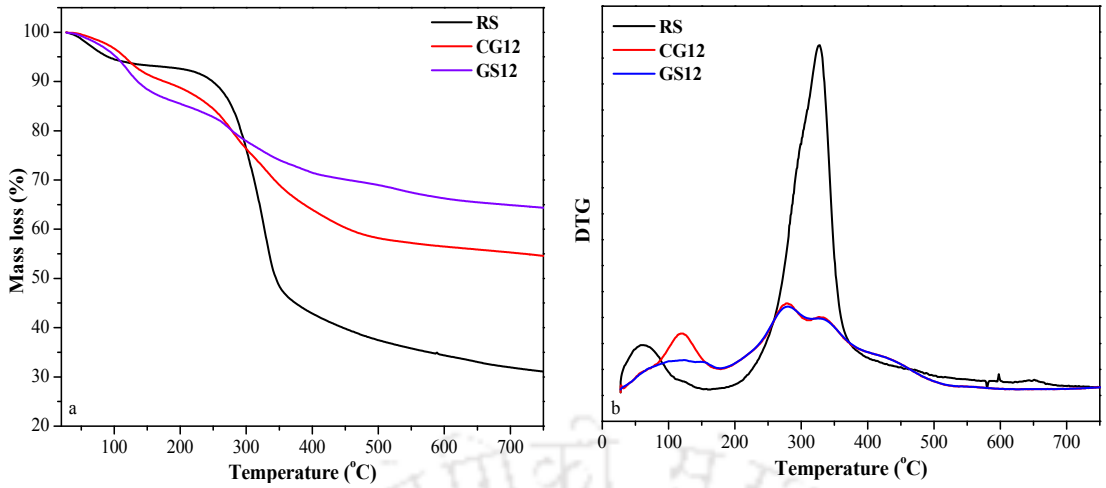

Figure 8.2: Thermo-gravimetric analysis of biomass (a) weight loss due to thermal degradation and (b) derivative of TG kinetics.

The cellulose, hemicellulose, and lignin content in the biomass sample were determined by thermo-gravimetric analysis (TGA) technique based on their thermal decomposition profile as depicted in Figure 8.2. The initial mass loss was observed between 40-100 °C due to vaporization of water. Further, degradation of bio-fillers such as cellulose, hemicellulose, and lignin was observed between 150-550 °C. The degradation of hemicellulose starts at 150 °C and continues up to 350 °C, whereas the cellulose degradation occurs between 275-350 °C. Moreover, due to huge structural complexity lignin degradation require higher temperature region and lies between 250 to 500 °C (Doan et al., 2016). The high cellulose and hemicellulose content of microalgae made it an efficient raw material for biogas production. However, high lignin content in RS is expected to be a reason for poor degradability, resulting in less biomethane production.

The high sCOD and wide range of VS/TS of substrates and inoculum advocated the appropriateness of above-mentioned substrates for effective AcoD. The pH of the sample was adjusted neutral to slightly alkaline (7.5) to support the methanogenic

activity. Additionally, the high VFA accumulation in the digester showed fast decomposition of substrates and its accessibility for the methanogens.

8.2 Effect of intracellular lipid on anaerobic digestion

Lipids are the attractive substrates for the AD and have a higher theoretical methane potential as compared to proteins and carbohydrates (Park and Li, 2012). However, due to lower alkalinity and buffering capacity, lipids can cause inhibitory effect due to the production of inhibitory compounds such as long chain fatty acids (LCFA) and volatile fatty acids (VFAs) produced during acidogenesis and acetogenesis. It has been suggested that the conversion of microalgae biomass to methane-rich biogas is energetically more promising than the removal of lipid molecules from microalgae biomass having lipid content less than 40 %. Cirne et al. (2007) reported that there was no inhibition for the AD at a lipid concentration of 5 %, 10 %, and 18 %, however, the inhibitory effect was observed for lipid concentration of 31 %, 40 %, and 47 %. The microalgae, CG12 and GS12 used in the present study showed lipid content approximately from 40-45 %, respectively as discussed earlier (Srivastava et al., 2017). As stated above, oil content more than 40 % is not favorable for biogas production, thus, the defatted microalgae biomass was used for the biomethane production. The biomethane yield obtained was 382 mL/g VS and 311 mL/g VS for CG12 and GS12, respectively which was higher than the control bio-methane yield of 255 mL/g VS. A similar observation was reported by Uggetti et al., (2017) for co-digestion of defatted CG12 biomass with lipid-rich fat, oil, and grease with a methane yield varying from 0.15 L CH_4/g VS to 0.54 L CH_4/g VS.

8.3 Biochemical methane potential assay

The biochemical methane production assay was performed to determine the extent of biomethane obtained from anaerobic degradation of biomass. Further, to evaluate the feasibility of microalgae with RS as a substrate, different weights of CG12 and GS12 were mixed to a fixed amount of RS (5 g) maintaining a C/N ratio 30 for a period of 40 days. In anaerobic biodegradation, C/N is the most significant parameter that helps in the determination of bio-methane yield and the process kinetics (Ramos-Suárez and Carreras, 2014). Initially, the hydrolytic bacteria break down the complex organic molecules into soluble monomers by releasing extracellular enzymes by the process called hydrolysis. This is the rate determining step for biogas production. Further, the hydrolyzed product acts as a substrate for acidogenic bacteria. Subsequently, the intermediate products are converted into simpler compounds like acetate, carbon dioxide, hydrogen and formate by secondary fermentation with a final decrease in the pH of the digester (Figure 8.3). The acid production can be visualized by increased VFA production.

Finally, methanogenic archaea which are highly specific to these substrates converts them to biogas (Kumar et al., 2016). The degradation of the lignocellulosic substrate tends to increase the organic material which successively causes an increase in the sCOD. Indeed, the inoculum plays a decisive role in initiating the anaerobic condition in the reactor by balancing the microbial population of *Syntrophobacter* and methanogens. The inoculum also sustains the syntrophic metabolism for the thermodynamic feasibility of the reactor.

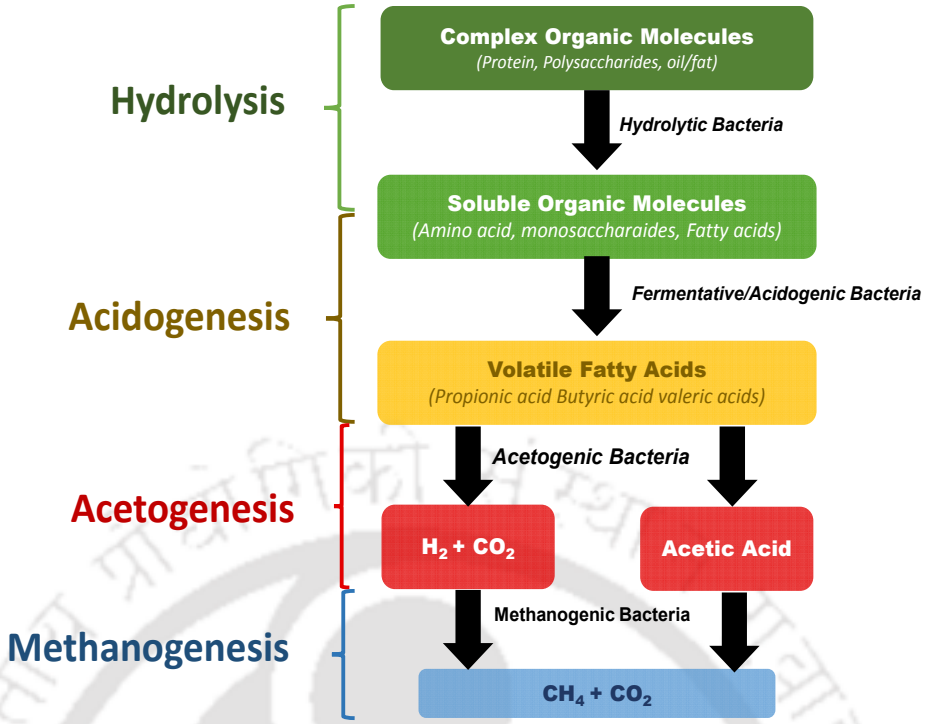

Figure 8.3: Mechanism of microbial bio-methane production.

Once the AD process starts the response of daily and cumulative biogas potential was recorded and represented in figure 4. The relative biogas production was measured in mL/g VS degraded. The bio-methane production declined after the 10th day and increased sharply at 15th day in the RS digester with a maximum of 92 mL/g VS. However, after 15th day no significant biogas production was observed and it was believed that highest solubilization or degradation of substrate might have achieved by the methanogens. However, in case of microalgae CG12 and GS12, the maximum daily bio-methane production of 80 mL and 53 mL/g VS was obtained at 21st and 25th day suggesting that microalgae biomass required more time for degradation. Initially, the cumulative bio-methane was comparatively same for CG12 and RS whereas, it was less for GS12, (Figure 8.4). The maximum cumulative methane production of 382 mL/g VS was obtained for CG12 and 311 mL/g VS for GS12. However, 255 mL/g VS bio-methane was recorded for control. After 40th day negligible fluctuation was observed

in all the reactors (figure 8.4). The comparative analysis of biogas production showed 49.87 % and 22.26 % enhancement in CG12 and GS12, respectively than control.

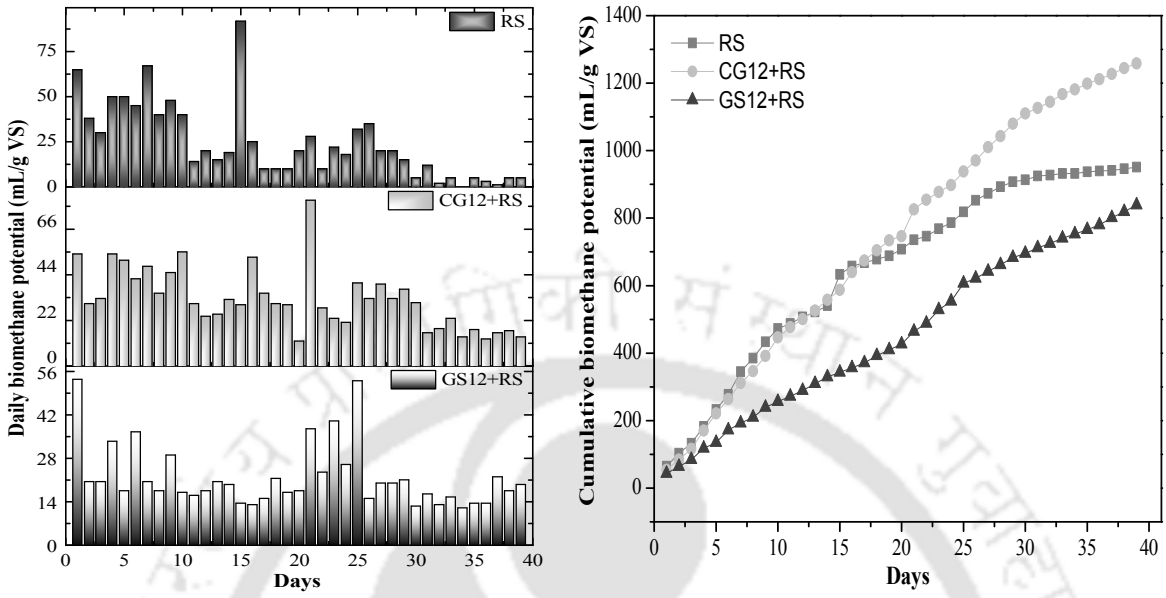

Figure 8.4: The daily and cumulative biomethane potential of RS, CG12+RS, and GS12+RS.

It is believed that the main reason for overall low gas yield in microalgae may be due its complex cellular structure. The presence of tough cell wall and sporopollenin hinders the decomposition of biomass and thus decreases the bio-methane potential. Hence, the present study also suggests that for better bio-methane potential microalgae necessitate further pretreatment (González-Fernández et al., 2012; Ramos-Suárez et al., 2014; Veluchamy and Kalamdhad, 2017). However, overall lower gas yield in all the reactor including control was due to the lignocellulosic complexity of RS. The utilization efficiency of overall digestibility of substrate is the primary function of lignin content. Several species of *Chlorella* and *Scenedesmus* have been reported earlier for their different BMP range and also finds similarity with the present study.

8.4 Effect of VFA and pH on volatile solid degradation

In the AD technology, pH and VFA are one of the simple tests to experience the symbiotic relation between acetogens and methanogens at the well-balanced condition. The change in VFA gives an indication of hydrolytic-acidogenic stage evaluation whereas the change in pH is an indication of solubilization or digestion of organic matter. An appropriate pH range of 6.8 to 7.2 is required for efficient biogas production. During acetogenesis phase, the higher accumulation of VFAs reduces the pH and affects the overall methanogenic activity and subsequently decrease the biogas yield. Therefore, for satisfactory biogas production maintaining pH to the optimum range is crucial.

In the AD process, mass loss is an indication of a considerable decrease in the concentration of total VFAs in the sample and can be directly correlated with the biogas production. The VS gives an approximate correlation of substrate that can potentially be turned into methane. An estimate can be made which refers to the higher solubilization of substrate. In general, the reduction of VS is an indication of microbial activity for the conversion of complex organics to simpler molecules which can be further converted to biogas. In the present study, maximum VS reduction of 21.62 % was observed for CG12 followed by 19.28 % for GS12 with cumulative biogas production of 1261 mL and 997.5 mL, respectively. The overall VS reduction of 15.85 % in case of control was lower with respect to CG12 and GS12, illustrated in Figure 8.5. The pH and VFA also affect the biochemical reactions by altering the reaction rate and reaction pathways, substrate utilization, microbial community, and the degree of acidification.

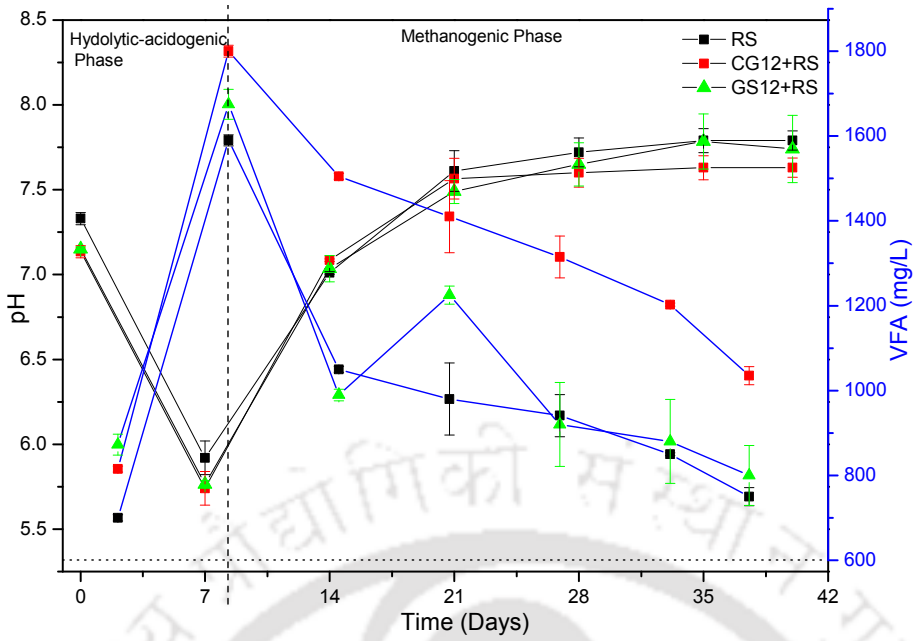

Figure 8.5: Effect of VFA and pH on volatile solid degradation.

The initial decrease in pH was observed prominently from 0 to 7 day due to higher production of VFAs. On the other hand, acidogens were not affected by this wide pH range from 5.0 to 8.5 and can continue to produce acids, which fluctuates the pH in the wider range. The pH of the digester was maintained by the addition of 1 N $NaHCO_3$ solution on the 7 day. Further, increase in pH was recorded up to 25 day and stabilized by 32 day which may be due to the utilization of VFA by methanogens. Thereafter, no further fluctuations were observed from 32 to 40 day. The effect of pH and VFA on VS degradation for the different reactor setups have been depicted in figure 8.5. The maximum VFAs accumulation of 1800±14.14 mg/L at pH drop of 5.74±0.09 and 1675±35.35 mg/L at pH of 5.76±0.02 was observed for CG12 and GS12, respectively after the 7 day of digestion.

Generally, the VS reduction of 15.85 % in RS was lower with respect to CG12 and GS12. It has been reported that higher biogas production can be achieved even though the VS reduction is low (Cheng et al., 2014). Furthermore, the VFAs are also influenced by temperature and HRT of the reactor (Cavinato et al., 2017). In a similar observation,

it was stated that an increased concentration of VFA in the digester decreases the pH which is inhibitory to the methanogens (Veluchamy and Kalamdhad, 2017). In an optimization study of alkali treatment for bio-methane enhancement similar trend of decrease in pH was reported on the 3 day. Further, it was suggested that neutral pH is favorable for the luxuriant growth of methanogens and the corresponding enhancement of bio-methane (Shetty et al., 2017).

8.5 Specific methanogenic activity and biodegradability test

The specific methanogenic activity (SMA) of the microflora and the extent of biodegradability (BD) of the substrate defines the methane production potential of the specific substrate. The present study evaluated the SMA activity of microalgae co-digested with rice straw with relation to its biodegradability. It was observed that the lignocellulosic constituents of the substrate were digested by the active anaerobic microorganisms by secreting the extracellular polymeric substances (EPS). It was observed that the SMA of the reactor was increased sharply by the addition of microalgae residues and resulted in biomethane production up to 290 mL/VS and 210 mL/g VS in CG12 and GS12, respectively (Table 8.2).

Table 8.2 Bio-methane production potential and biodegradability of substrates.

Digester	SMA (mL/g VS)	EMY (mL/g VS)	TMY (mL/g VS)	BD (%)
RS	187	254.95	412.13	61.86
CG12+RS	290	382.12	440.03	86.83
GS12+RS	210	311.71	436.04	71.48

It is to be noted that the co-digestion mixture of CG12 with RS act as an active ingredient that provides sufficient and maximal SMA for enhanced methane yield. The possible reason may be the efficient solid-liquid separation at optimum mixture which

must have provided the increased food source to the methanogens for quick assimilation and subsequent methane production. The SMA of CG12 was found to be 28 % higher with respect to GS12 substrate mixture. The high lignin content may suppress the anaerobic digestion activity which might be the reason for low SMA in RS. Therefore, the biodegradability analysis is crucial to estimate the methane yield potential of microalgae residue with RS or any substrate. The correlation between the SMA and biodegradability pattern of the co-digested substrates is illustrated in Table 8.3. The presence of active methanogens in the bioreactor increases the SMA activity. The present study also showed coherence with the previous reports where an increase in the SMA was reported with the high food to microorganism ratio using several lignocellulosic substrates (Le Hyaric et al., 2011; Pommier et al., 2007).

8.6 Summary

The most imperative conclusion of the present study is that the lipid-exhausted algae biomass can be a viable substrate for biogas production. The bio-methane production depends on various factors that affect the yield such as solid loading, methanogenic activity, biodegradability and more importantly, the C/N ratio. The co-digestion of microalgae biomass with RS improves C/N ratio of the AD process and thereby enhanced the biogas yield in CG12 (382 mL/g VS) and GS12 (311 mL/g VS) as compared to control (255 mL/g VS). The mathematical bio-kinetic modeling is the good measures to evaluate the theoretical biomethane yield and design the experiments to save both time and energy. Hence, the co-digestion of microalgae and RS could make a sustainable pathway to microalgae biorefinery.

CHAPTER 9

OVERALL CONCLUSION AND FUTURE SCOPE

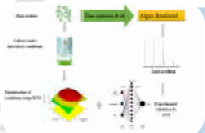

- ✓ Microalgae isolates : Chlorella CG12 (KR905186) and Desmodesmus GS12 (KR905187)
- ✓ Lipid yield: 13.36 % (CG12) and 25.85 % (GS12)

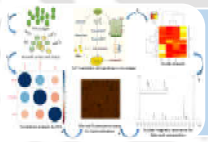

- ✓ Ca2+ induces the lipid accumulation under nitrogen deprived condition
- ✓ Lipid yield : 40.02 % and 44.97

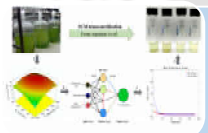

- ✓ Optimum process conditions: Temperature 285.21, Time 26.5 min and MeOH: oil molar ratio 23.4
- ✓ Conversion efficiency : 98.12 %

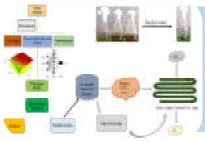

- ✓ Optimum culture conditions: For CG12 Light intensity 3.68 Klux, leachate concentration 19.27 % and $NaHCO_3$ 1.04 % and for GS12 Light intensity 3.68 Klux, leachate concentration 11.12 % and $NaHCO_3$ 1.09 %
- ✓ Lipid yield: 44.56 % (CG12) and 41.89 % (GS12)

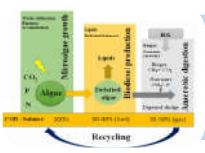

- ✓ Substrate loading capacity and C/N ratio are two important factors for BMP
- ✓ Biogas yield: CG12+RS (382 mL/g VS), GS12+RS (311 mL/g VS) and RS (255 mL/g VS).

Overall Conclusions and future scope

9.1 Salient features of the present study

The chapter summarizes the major conclusions of this study and discusses the scope for future research work which can be carried out. The present work basically dealt with the isolation of native microalgae strain, optimization of culture conditions for lipid enhancement, salt-induced lipid increment, scale-up studies, transesterification of microalgae oil to biodiesel, utilization of waste stream as a nutrient source for microalgae cultivation and reuse of residual microalgae biomass for biogas production. The major finding of the study has been highlighted in the following points.

- The present study is probably the first comprehensive report considering the major shortcomings of microalgae biofuel commercialization and its potential solutions. The freshwater isolates CG12 and GS12 are the native and robust species which can survive under a wide range of environmental conditions. Moreover, the microalgae isolates can also accumulate a substantial amount of lipid content.
- Optimization of culture conditions (light intensity, temperature, and pH) was performed in order to enhance the lipid content in microalgae. It was found that light plays a significant role in microalgae cultivation and lipid accumulation with a relative importance of 87.78 % and 49.09 % in CG12 and GS12, respectively
- The highest lipid content obtained in CG12 and GS12 under optimized physicochemical conditions were 13.25 and 25.85 % dcw.
- Salt-induced lipid accumulation in microalgae resulted in 40 % and 45 % lipid content in CG12 and GS12, respectively.

- The high lipid yielding strain were subjected to mass cultivation and scaled up to 100 liters bioreactor. Subsequently, lipid extraction and transesterification were performed from the harvested biomass by the advanced supercritical methanol (SCM) technique in order to achieve maximum microalgae biodiesel.
- Moreover, the quality characterization of microalgae biodiesel showed analogous trends with the ASTM D6751 standards.
- Further, to improve the process efficiency optimization of effective process parameters of SCM process such as reaction temperature, reaction time and MeOH: oil molar ratio were optimized via hybrid optimization tools of RSM-ANN-GA to generate a global optimum condition.
- The GA based final optimized SCM transesterification process conditions of temperature 285.21 ^{o}C, time 26.57 min and MeOH: oil molar ratio 23.47 resulted in a 98.12 % conversion of microalgae oil to biodiesel.
- With the advent concern of waste management and reduction in the production cost various waste resources have been used for microalgae cultivation such as CD, BPW, and VM where BPW showed its profound effect on lipid enhancement in microalgae.
- Hence, the culture condition optimization studies were carried only for BPW which resulted in 44.56 % and 41.89 % lipid accumulation in CG12 and GS12, respectively. Indeed, the light was the main driving force of microalgae growth and lipid accumulation.
- Due to high energy potential of residual microalgae biomass, the microalgae residues remained after lipid extraction was co-digested with RS and showed a high bio-methane yield of 382 mL/g VS in CG12 and 311 mL/g VS in GS12.

- The sludge obtained after ACoD was reutilized as a growth medium for microalgae cultivation in order to recycle the available nutrients.
- The most imperative inference of the study was to develop a sustainable, cost-effective and eco-friendly biorefinery without any discharge of waste.

9.2 Future prospects

Though, the present study tries to resolve all the issues of microalgae biofuel commercialization. However, some refinements can be made to improve the process. The major implementation can be made in following directions:

- Reduction in microalgae cultivation time.
- Harvesting process can be improved for suspended cultures.
- Biofilm–based microalgae cultivation system can be incorporated.
- Designing of photobioreactor with the controlled condition is definitely a prerequisite.
- In spite of oil extraction and then transesterification, a single pot biodiesel synthesis would be a better option.
- Implementation of hydrothermal liquefaction could be a better approach to obtain single pot microalgae biofuel.
- Improvement and up-gradation of biomethane production process.

REFERNCES


ResearchGate
Contents lists available at ScienceDirect
Energy Conversion and Management
journal homepage: www.elsevier.com/locate/enconman
ELSEVIER
Optimization of non-catalytic transesterification of microalgae oil to biodiesel under supercritical methanol condition
Garima Srivastava, Atanu Kumar Paul, Vaibhav V. Goud
ScienceDirect | Scopus
Google scholar
Contents lists available at ScienceDirect
Bioresource Technology
journal homepage: www.elsevier.com/locate/biortech
Salinity induced lipid production in microalgae and cluster analysis (ICCB 16-BR_047)
Garima Srivastava, Nishchal, Vaibhav V. Goud
Scopus
The largest abstract and citation database of peer-reviewed literature from more than 5,000 publishers

References

Affenzeller, M.J., Darehshouri, A., Andosch, A., Lütz, C., Lütz-Meindl, U., 2009. Salt stress-induced cell death in the unicellular green alga *Micrasterias denticulata*. J Exp Bot, 60, 939-954.

Ahmad, P., Azooz, M.M., Prasad, M.N.V. 2013. Salt stress in plants: signalling, omics and adaptations. Springer Science & Business Media.

Al-Qasmi, M., Raut, N., Talebi, S., Al-Rajhi, S., Al-Barwani, T. 2012. A review of effect of light on microalgae growth. Proceedings of the world congress on engineering. pp. 4-6.

An, J.-Y., Sim, S.-J., Lee, J.S., Kim, B.W., 2003. Hydrocarbon production from secondarily treated piggery wastewater by the green alga Botryococcus braunii. J Appl Phycol, 15, 185-191.

Astals, S., Musenze, R., Bai, X., Tannock, S., Tait, S., Pratt, S., Jensen, P., 2015. Anaerobic co-digestion of pig manure and algae: impact of intracellular algal products recovery on co-digestion performance. Bioresour Technol, 181, 97-104.

Asulabh, K., Supriya, G., Ramachandra, T. 2012. Effect of Salinity Concentrations on Growth Rate and Lipid Concentration in *Microcystis Sp., Chlorococcum Sp. and Chaetoceros Sp*. National Conference on Conservation and Management of Wetland Ecosystems. School of Environmental Sciences, Mahatma Gandhi University, Kottayam, Kerala.

Ayala-Parra, P., Liu, Y., Field, J.A., Sierra-Alvarez, R., 2017. Nutrient recovery and biogas generation from the anaerobic digestion of waste biomass from algal biofuel production. Renew Energ, 108, 410-416.

Azcan, N., Danisman, A., 2007. Alkali catalyzed transesterification of cottonseed oil by microwave irradiation. Fuel, 86(17-18), 2639-2644.

Banos, R., Manzano-Agugliaro, F., Montoya, F., Gil, C., Alcayde, A., Gómez, J., 2011. Optimization methods applied to renewable and sustainable energy: A review. Renew Sustain Energy Rev, 15, 1753-1766.

Bartley, M.L., Boeing, W.J., Dungan, B.N., Holguin, F.O., Schaub, T., 2014. pH effects on growth and lipid accumulation of the biofuel microalgae *Nannochloropsis salina* and invading organisms. J Appl Phycol, 26, 1431-1437.

Beale, M.H., Hagan, M.T., Demuth, H.B. 2010. Neural Network Toolbox 7.

Becker, W., 2004. 21 Microalgae for Aquaculture. Handbook of microalgal culture: Biotechnology and applied phycology, 380.

BenMoussa-Dahmen, I., Chtourou, H., Rezgui, F., Sayadi, S., Dhouib, A., 2016. Salinity stress increases lipid, secondary metabolites and enzyme activity in *Amphora subtropica* and *Dunaliella* sp. for biodiesel production&&. Bioresour Technol, 218, 816-825.

Betiku, E., Omilakin, O.R., Ajala, S.O., Okeleye, A.A., Taiwo, A.E., Solomon, B.O., 2014. Mathematical modeling and process parameters optimization studies by artificial neural network and response surface methodology: a case of non-edible neem (Azadirachta indica) seed oil biodiesel synthesis. Energ, 72, 266-273.

Bhandari, R., Sharma, P.K., 2006. High-light-induced Changes on Photosynthesis, Pigments, Sugars, Lipids and Antioxidant Enzymes in Freshwater (Nostoc spongiaeforme) and Marine (Phormidium corium) Cyanobacteria. J Photochem Photobiol, 82, 702-710.

Bhatnagar, A., Bhatnagar, M., Chinnasamy, S., Das, K., 2010. Chlorella minutissima—a promising fuel alga for cultivation in municipal wastewaters. Appl Biochem Biotechnol, 161, 523-536.

Biktashev, S.A., Usmanov, R., Gabitov, R., Gazizov, R., Gumerov, F., Gabitov, F., Abdulagatov, I., Yarullin, R., Yakushev, I., 2011. Transesterification of rapeseed and palm oils in supercritical methanol and ethanol. Biomass Bioenergy, 35, 2999-3011.

Blair, M.F., Kokabian, B., Gude, V.G., 2014. Light and growth medium effect on Chlorella vulgaris biomass production. J Environ Chem Eng, 2, 665-674.

Bligh, E.G., Dyer, W.J., 1959. A rapid method of total lipid extraction and purification. Can J Biochem Physiol, 37, 911-917.

Bohutskyi, P., Kligerman, D.C., Byers, N., Nasr, L.K., Cua, C., Chow, S., Su, C., Tang, Y., Betenbaugh, M.J., Bouwer, E.J., 2016. Effects of inoculum size, light intensity, and dose of anaerobic digestion centrate on growth and productivity of Chlorella and Scenedesmus microalgae and their poly-culture in primary and secondary wastewater. Algal Res, 19, 278-290.

Borugadda, V.B., Goud, V.V., 2012. Biodiesel production from renewable feedstocks: status and opportunities. Renew Sustain Energy Rev, 16, 4763-4784.

Borugadda, V.B., Goud, V.V., 2014. Thermal, oxidative and low temperature properties of methyl esters prepared from oils of different fatty acids composition: A comparative study. Thermochim Acta, 577, 33-40.

Breuer, G., Lamers, P.P., Martens, D.E., Draaisma, R.B., Wijffels, R.H., 2013. Effect of light intensity, pH, and temperature on triacylglycerol (TAG) accumulation induced by nitrogen starvation in Scenedesmus obliquus. Bioresour Technol, 143, 1-9.

Bunyakiat, K., Makmee, S., Sawangkeaw, R., Ngamprasertsith, S., 2006. Continuous production of biodiesel via transesterification from vegetable oils in supercritical methanol. Energ Fuel, 20, 812-817.

Buswell, A., Mueller, H., 1952. Mechanism of methane fermentation. Ind Eng Chem Res, 44, 550-552.

Campbell, A.K. 2014. Intracellular calcium. John Wiley & Sons.

Cassidy, K.O. 2011. Evaluating algal growth at different temperatures. in: *Biosystems and Agriculture Engineering*, Vol. M.Sc. Thesis, University of Kentucky.

Cecchi, F., Mata-Alvarez, J., Marcomini, A., Pavan, P., 1991. First order and step-diffusional kinetic models in simulating the mesophilic anaerobic digestion of complex substrates. Bioresour Technol, 36, 261-269.

Chaisutyakorn, P., Praiboon, J., Kaewsuralikhit, C., 2017. The effect of temperature on growth and lipid and fatty acid composition on marine microalgae used for biodiesel production. J Appl Phycol, 1-9.

Chellamboli, C., Perumalsamy, M., 2014. Application of response surface methodology for optimization of growth and lipids in *Scenedesmus abundans* using batch culture system. RSC Adv, 4, 22129-22140.

Chen, H., Hu, J., Qiao, Y., Chen, W., Rong, J., Zhang, Y., He, C., Wang, Q., 2015. Ca^{2+}regulated cyclic electron flow supplies ATP for nitrogen starvation-induced lipid biosynthesis in green alga. Sci Rep, 5, 15117.

Chen, H., Zhang, Y., He, C., Wang, Q., 2014. Ca^{2+} signal transduction related to neutral lipid synthesis in an oil-producing green alga *Chlorella sp. C2*. Plant Cell Physiol, 15.

Chen, M., Tang, H., Ma, H., Holland, T.C., Ng, K.S., Salley, S.O., 2011. Effect of nutrients on growth and lipid accumulation in the green algae Dunaliella tertiolecta. Bioresour Technol, 102, 1649-1655.

Chen, Y.-H., Huang, B.-Y., Chiang, T.-H., Tang, T.-C., 2012. Fuel properties of microalgae (*Chlorella protothecoides*) oil biodiesel and its blends with petroleum diesel. Fuel, 94, 270-273.

Cheng, J., Lu, H., Huang, Y., Li, K., Huang, R., Zhou, J., Cen, K., 2016. Enhancing growth rate and lipid yield of Chlorella with nuclear irradiation under high salt and CO 2 stress. Bioresour Technol, 203, 220-227.

Cheng, J.J., Liu, Z., Gontupil, J., Kwon, O.-S., 2014. Anaerobic co-digestion of rice straw and digested swine manure with different total solid concentration for methane production. Int J Agri Bio Eng, 7, 79.

Cheng, K.-C., Ren, M., Ogden, K.L., 2013. Statistical optimization of culture media for growth and lipid production of Chlorella protothecoides UTEX 250. Bioresour Technol, 128, 44-48.

Chinnasamy, S., Bhatnagar, A., Hunt, R.W., Das, K., 2010. Microalgae cultivation in a wastewater dominated by carpet mill effluents for biofuel applications. Bioresour Technol, 101, 3097-3105.

Chisti, Y., 2007. Biodiesel from microalgae. Biotechnol Adv, 25, 294-306.

Chng, L.M., Chan, D.J.C., Lee, K.T., 2016. Sustainable production of bioethanol using lipid-extracted biomass from *Scenedesmus dimorphus*. J Clean Prod, 130, 68-73.

Christie, W.W. 2009. Methylation of fatty acids—a beginner's guide.

Christov, C., Pouneva, I., Bozhkova, M., Toncheva, T., Fournadzieva, S., Zafirova, T., 2001. Influence of temperature and methyl jasmonate on *Scenedesmus incrassulatus*. Biol plantarum, 44, 367-371.

Chuah, L.F., Klemeš, J.J., Yusup, S., Bokhari, A., Akbar, M.M., 2017. A review of cleaner intensification technologies in biodiesel production. J Clean Prod, 146, 181-193.

Clark, J.H., Luque, R., Matharu, A.S., 2012. Green chemistry, biofuels, and biorefinery. Annu Rev Chem Biomol Eng, 3, 183-207.

Converti, A., Casazza, A.A., Ortiz, E.Y., Perego, P., Del Borghi, M., 2009. Effect of temperature and nitrogen concentration on the growth and lipid content of *Nannochloropsis oculata* and *Chlorella vulgaris* for biodiesel production. Chem Eng Process, 48, 1146-1151.

Cowan, A., Logie, M., Rose, P., Phillips, L., 1995. Stress Induction of Zeaxanthin Formation in the β-Carotene Accumulating Alga *Dunaliella salina Teod*. J Plant Physiol, 146, 554-562.

Cuellar-Bermudez, S.P., Garcia-Perez, J.S., Rittmann, B.E., Parra-Saldivar, R., 2015. Photosynthetic bioenergy utilizing CO_2: an approach on flue gases utilization for third generation biofuels. J Clean Prod, 98, 53-65.

del Rio-Chanona, E.A., Manirafasha, E., Zhang, D., Yue, Q., Jing, K., 2016. Dynamic modeling and optimization of cyanobacterial C-phycocyanin production process by artificial neural network. Algal Res, 13, 7-15.

Demetriou, G., Neonaki, C., Navakoudis, E., Kotzabasis, K., 2007. Salt stress impact on the molecular structure and function of the photosynthetic apparatus—the protective role of polyamines. Biochim Biophys Acta (BBA)-Bioenerg, 1767, 272-280.

Demirbas, A., 2009. Biodiesel from waste cooking oil via base-catalytic and supercritical methanol transesterification. Energ Converg Manage, 50, 923-927.

Demirbas, A., 2008. Biofuels sources, biofuel policy, biofuel economy and global biofuel projections. Energ Converg Manage, 49, 2106-2116.

Dhamodharan, K., Kumar, V., Kalamdhad, A.S., 2015. Effect of different livestock dungs as inoculum on food waste anaerobic digestion and its kinetics. Bioresour Technol, 180, 237-241.

Dhawane, S.H., Kumar, T., Halder, G., 2015. Central composite design approach towards optimization of flamboyant pods derived steam activated carbon for its use as heterogeneous catalyst in transesterification of Hevea brasiliensis oil. Energ Converg Manage, 100, 277-287.

Difusa, A., Talukdar, J., Kalita, M.C., Mohanty, K., Goud, V.V., 2015. Effect of light intensity and pH condition on the growth, biomass and lipid content of microalgae Scenedesmus species. Biofuels, 6, 37-44.

Dilallo, R., Albertson, O.E., 1961. Volatile acids by direct titration. Journal Water Pollution Control Federation, 356-365.

Dineshkumar, R., Dhanarajan, G., Dash, S.K., Sen, R., 2015. An advanced hybrid medium optimization strategy for the enhanced productivity of lutein in *Chlorella minutissima*. Algal Res, 7, 24-32.

Duan, X., Ren, G.Y., Liu, L.L., Zhu, W.X., 2014. Salt-induced osmotic stress for lipid overproduction in batch culture of Chlorella vulgaris. Afr J Biotechnol, 11, 7072-7078.

Duan, X., Ren, G.Y., Liu, L.L., Zhu, W.X., 2012. Salt-induced osmotic stress for lipid overproduction in batch culture of *Chlorella vulgaris*. Afr J Biotechnol, 11, 7072-7078.

Farobie, O., Matsumura, Y., 2015. A comparative study of biodiesel production using methanol, ethanol, and tert-butyl methyl ether (MTBE) under supercritical conditions. Bioresour Technol, 191, 306-311.

Fayyazi, E., Ghobadian, B., Najafi, G., Hosseinzadeh, B., Mamat, R., Hosseinzadeh, J., 2015. An ultrasound-assisted system for the optimization of biodiesel production from chicken fat oil using a genetic algorithm and response surface methodology. Ultrason Sonochem, 26, 312-320.

Federation, W.E., Association, A.P.H., 2005. Standard methods for the examination of water and wastewater. American Public Health Association (APHA): Washington, DC, USA.

Forero, C.L.B., 2004. Biodiesel from castor oil: a promising fuel for cold weather. Department of Hydraulic, Fluids and Thermal Sciences Francisco de Paula Santander University Avenida Gran Colombia(12E-96).

García-Martínez, N., Andreo-Martínez, P., Quesada-Medina, J., de los Ríos, A.P., Chica, A., Beneito-Ruiz, R., Carratalá-Abril, J., 2017. Optimization of non-catalytic transesterification of tobacco (Nicotiana tabacum) seed oil using supercritical methanol to biodiesel production. Energ Converg Manage, 131, 99-108.

Garcíaa-Gimeno, R., Hervás-Martíanez, C., Barco-Alcalá, E., Zurera-Cosano, G., Sanz-Tapia, E., 2003. An artificial neural network approach to Escherichia coli O157: H7 growth estimation. J Food Sci, 68, 639-645.

Gardner, R., Peters, P., Peyton, B., Cooksey, K.E., 2011. Medium pH and nitrate concentration effects on accumulation of triacylglycerol in two members of the chlorophyta. J Appl Phycol, 23, 1005-1016.

Ghosh, A., Khanra, S., Mondal, M., Halder, G., Tiwari, O., Saini, S., Bhowmick, T.K., Gayen, K., 2016. Progress toward isolation of strains and genetically engineered strains of microalgae for production of biofuel and other value added chemicals: A review. Energ Converg Manage, 113, 104-118.

Gokulan, R., 2014. Best dilution ratio and GC-MS analysis for the removal of nutrient from municipal wastewater by microalgae. Int J Chem Tech Res, 6, 663-672.

Golueke, C.G., Oswald, W.J., Gotaas, H.B., 1957. Anaerobic digestion of algae. Appl micro, 5, 47.

Gorain, P.C., Bagchi, S.K., Mallick, N., 2013. Effects of calcium, magnesium and sodium chloride in enhancing lipid accumulation in two green microalgae. Environ Technol, 34, 1887-1894.

Goswami, R.C.D., Kalita, M., 2011. *Scenedesmus dimorphus* and *Scenedesmus quadricauda*: Two potent indigenous microalgae strains for biomass production and CO_2 mitigation-A study on their growth behavior and lipid productivity under different concentration of urea as nitrogen source. J. Algal Biomass Utln, 2, 42-49.

Guckert, J.B., Cooksey, K.E., 1990. Triglyceride Accumulation And Fatty Acid Profile Changes In Chlorella (Chlorophyta) During High Ph-Induced Cell Cycle Inhibition1. J Phycol, 26, 72-79.

Guldhe, A., Singh, B., Rawat, I., Bux, F., 2014. Synthesis of biodiesel from Scenedesmus sp. by microwave and ultrasound assisted in situ transesterification using tungstated zirconia as a solid acid catalyst. Chem Eng Res Des, 92, 1503-1511.

Gumbytė, M., Makareviciene, V., Skorupskaite, V., Sendzikiene, E., Kondratavicius, M., 2018. Enzymatic microalgae oil transesterification with ethanol in mineral diesel fuel media. J Renew Sustain Eng, 10, 013105.

Gurtovenko, A.A., Vattulainen, I., 2008. Effect of NaCl and KCl on phosphatidylcholine and phosphatidylethanolamine lipid membranes: insight from atomic-scale simulations for understanding salt-induced effects in the plasma membrane. J Phys Chem B, 112, 1953-1962.

Hegel, P., Andreatta, A., Pereda, S., Bottini, S., Brignole, E.A., 2008. High pressure phase equilibria of supercritical alcohols with triglycerides, fatty esters and cosolvents. Fluid Phase Equilib, 266, 31-37.

Hiremath, S., Mathad, P., 2010. Impact of salinity on the physiological and biochemical traits of *Chlorella vulgaris Beijerinck*. J Algal Biomass Ultn, 1, 51-59.

Hoekman, S.K., Broch, A., Robbins, C., Ceniceros, E., Natarajan, M., 2012. Review of biodiesel composition, properties, and specifications. Renew Sustain Energy Rev, 16, 143-169.

Ifeanyi, V., Anyanwu, B., Ogbulie, J., Nwabueze, R., Ekezie, W., Lawal, O., 2011. Determination of the effect of light and salt concentrations on Aphanocapsa algal population. Afr J Micro Res, 5, 2488-2492.

Imahara, H., Minami, E., Hari, S., Saka, S., 2008. Thermal stability of biodiesel in supercritical methanol. Fuel, 87, 1-6.

Jacobson, S.N., Alexander, M., 1981. Enhancement of the microbial dehalogenation of a model chlorinated compound. Appl Environ Micro, 42, 1062-1066.

Juneja, A., Ceballos, R.M., Murthy, G.S., 2013. Effects of environmental factors and nutrient availability on the biochemical composition of algae for biofuels production: a review. Energies, 4607-4638.

Kadiyala, A., Kaur, D., Kumar, A., 2010. Application of MATLAB to select an optimum performing genetic algorithm for predicting in-vehicle pollutant concentrations. Environ Prog Sus Energ, 29, 398-405.

Kana, E.G., Oloke, J., Lateef, A., Adesiyan, M., 2012. Modeling and optimization of biogas production on saw dust and other co-substrates using artificial neural network and genetic algorithm. Renew Energ, 46, 276-281.

Karimova, F.G., Kortchouganova, E.E., Tarchevsky, I.A., Iagoucheva, M.R., 2000. The oppositely directed Ca^{2+} and Na^{+} transmembrane transport in algal cells. Protoplasma, 213, 93-98.

Kaur, S., Sarkar, M., Srivastava, R.B., Gogoi, H.K., Kalita, M.C., 2012. Fatty acid profiling and molecular characterization of some freshwater microalgae from India with potential for biodiesel production. New Biotechnol, 29, 332-344.

Kim, B.-H., Ramanan, R., Kang, Z., Cho, D.-H., Oh, H.-M., Kim, H.-S., 2016. *Chlorella sorokiniana* HS1, a novel freshwater green algal strain, grows and hyperaccumulates lipid droplets in seawater salinity. Biomass Bioenergy, 85, 300-305.

Kim, M., Park, J., Park, C., Kim, S., Jeune, K., Chang, M., Acreman, J., 2007. Enhanced production of Scenedesmus spp.(green microalgae) using a new medium containing fermented swine wastewater. Bioresour Technol, 98, 2220-2228.

Kirrolia, A., Bishnoi, N.R., Singh, R., 2014. Response surface methodology as a decision-making tool for optimization of culture conditions of green microalgae Chlorella spp. for biodiesel production. Ann Micro, 64, 1133-1147.

Kirroliaa, A., Bishnoia, N.R., Singh, N., 2011. Salinity as a factor affecting the physiological and biochemical traits of *Scenedesmus quadricauda*. J Algal Biomass Utln, 2, 28-34.

Knothe, G., 2005. Dependence of biodiesel fuel properties on the structure of fatty acid alkyl esters. Fuel Process Technol, 86, 1059-1070.

Knothe, G., Krahl, J., Van Gerpen, J. 2015. The biodiesel handbook. Elsevier.

Kong, Q.-x., Li, L., Martinez, B., Chen, P., Ruan, R., 2010. Culture of microalgae Chlamydomonas reinhardtii in wastewater for biomass feedstock production. Appl Biochem Biotechnol, 160, 9-18.

Kusdiana, D., Saka, S., 2001. Methyl Esterification of Free Fatty Acids of Rapeseed Oil as Treated in Supercritical Methanol. J Chem Eng Japan, 34, 383-387.

Lahiri, S.K., Ghanta, K.C., 2008. Development of an artificial neural network correlation for prediction of hold-up of slurry transport in pipelines. Chem Eng Sci, 63, 1497-1509.

Lang, I., Hodac, L., Friedl, T., Feussner, I., 2011. Fatty acid profiles and their distribution patterns in microalgae: a comprehensive analysis of more than 2000 strains from the SAG culture collection. BMC Plant Biol, 11, 124.

Lee, J.H., Huang, Y., Dickman, M., Jayawardena, A.W., 2003. Neural network modelling of coastal algal blooms. Ecol Model, 159, 179-201.

Lee, K., Chantrasakdakul, P., Kim, D., Kim, H.S., Park, K.Y., 2013. Evaluation of methane production and biomass degradation in anaerobic co-digestion of organic residuals. Int J Biol Ecol Environ Sci, 2, 2277-4394.

Lee, S., Posarac, D., Ellis, N., 2012. An experimental investigation of biodiesel synthesis from waste canola oil using supercritical methanol. Fuel, 91, 229-237.

Li, Q., Xu, J., Du, W., Li, Y., Liu, D., 2013. Ethanol as the acyl acceptor for biodiesel production. Renew Sustain Energy Rev, 25, 742-748.

Li, T., Zheng, Y., Yu, L., Chen, S., 2013. High productivity cultivation of a heat-resistant microalga *Chlorella sorokiniana* for biofuel production. Bioresour Technol, 131, 60-67.

Liao, Q., Sun, Y., Huang, Y., Xia, A., Fu, Q., Zhu, X., 2017. Simultaneous enhancement of Chlorella vulgaris growth and lipid accumulation through the synergy effect between light and nitrate in a planar waveguide flat-plate photobioreactor. Bioresour Technol, 243, 528-538.

Lürling, M. 2003. Phenotypic plasticity in the green algae *Desmodesmus* and *Scenedesmus* with special reference to the induction of defensive morphology. International Journal of Limnology. Cambridge Univ Press. pp. 85-101.

Ma, F., Hanna, M.A., 1999. Biodiesel production: a review. Bioresour Technol, 70, 1-15.

Mackinney, G., 1941. Absorption of light by chlorophyll solutions. J. biol. Chem, 140, 315-322.

Mahdy, A., Fotidis, I.A., Mancini, E., Ballesteros, M., González-Fernández, C., Angelidaki, I., 2017. Ammonia tolerant inocula provide a good base for anaerobic digestion of microalgae in third generation biogas process. Bioresour Technol, 225, 272-278.

Mandal, S., Mallick, N., 2011. Waste utilization and biodiesel production by the green microalga Scenedesmus obliquus. Appl Environ Micro, 77, 374-377.

Maran, J.P., Priya, B., 2015. Modeling of ultrasound assisted intensification of biodiesel production from neem (Azadirachta indica) oil using response surface methodology and artificial neural network. Fuel, 143, 262-267.

Martinez-Guerra, E., Howlader, M.S., Shields-Menard, S., French, W.T., Gude, V.G., 2018. Optimization of wet microalgal FAME production from Nannochloropsis

sp. under the synergistic microwave and ultrasound effect. Int J Energy Res, DOI: 10.1002/er.3989, 16.

Martınez, M., Sánchez, S., Jimenez, J., El Yousfi, F., Munoz, L., 2000. Nitrogen and phosphorus removal from urban wastewater by the microalga Scenedesmus obliquus. Bioresour Technol, 73, 263-272.

Marudhupandi, T., Sathishkumar, R., Kumar, T.T.A., 2016. Heterotrophic cultivation of *Nannochloropsis salina* for enhancing biomass and lipid production. Biotechnol Rep, 10, 8-16.

Marulanda, V.F., 2012. Biodiesel production by supercritical methanol transesterification: process simulation and potential environmental impact assessment. J Clean Prod, 33, 109-116.

Mascarelli, A.L., 2009. Algae: fuel of the future? Environ Sci Tech, 43, 7160-7161.

Mata, T.M., Martins, A.A., Caetano, N.S., 2010. Microalgae for biodiesel production and other applications: a review. Renew Sustain Energy Rev, 14, 217-232.

Mazumdar, P., Borugadda, V.B., Goud, V.V., Sahoo, L., 2012. Physico-chemical characteristics of *Jatropha curcas L.* of North East India for exploration of biodiesel. Biomass Bioenergy, 46, 546-554.

Medeiros, D.L., Sales, E.A., Kiperstok, A., 2015. Energy production from microalgae biomass: carbon footprint and energy balance. J Clean Prod, 96, 493-500.

Meher, L., Sagar, D.V., Naik, S., 2006. Technical aspects of biodiesel production by transesterification—a review. Renew Sustain Energy Rev, 10, 248-268.

Micic, R.D., Tomić, M.D., Kiss, F.E., Nikolić-Djorić, E.B., Simikić, M.Đ., 2014. Influence of reaction conditions and type of alcohol on biodiesel yields and process economics of supercritical transesterification. Energ Converg Manage, 86, 717-726.

Mohamed, M.S., Tan, J.S., Mohamad, R., Mokhtar, M.N., Ariff, A.B., 2013. Comparative analyses of response surface methodology and artificial neural network on medium optimization for *Tetraselmis sp*. FTC209 grown under mixotrophic condition. Scientific World J, 2013.

Mohan, S.V., Devi, M.P., 2014. Salinity stress induced lipid synthesis to harness biodiesel during dual mode cultivation of mixotrophic microalgae. Bioresour Technol, 165, 288-294.

Moheimani, N.R., 2013. Inorganic carbon and pH effect on growth and lipid productivity of Tetraselmis suecica and Chlorella sp (Chlorophyta) grown outdoors in bag photobioreactors. J Appl Phycol, 25, 387-398.

Mostafa, S.S., Shalaby, E.A., Mahmoud, G.I., 2012. Cultivating microalgae in domestic wastewater for biodiesel production. Not Sci Biol, 4, 56-65.

Mostafaei, B., Ghobadian, B., Barzegar, M., Banakar, A., 2013. Optimization of ultrasonic reactor geometry for biodiesel production using response surface methodology. Journal of Agricultural Science and Technology 15, 697-708.

Mus, F., Toussaint, J.-P., Cooksey, K.E., Fields, M.W., Gerlach, R., Peyton, B.M., Carlson, R.P., 2013. Physiological and molecular analysis of carbon source supplementation and pH stress-induced lipid accumulation in the marine diatom Phaeodactylum tricornutum. Appl Micro Biotechnol, 97, 3625-3642.

Mussgnug, J.H., Klassen, V., Schlüter, A., Kruse, O., 2010. Microalgae as substrates for fermentative biogas production in a combined biorefinery concept. J biotechnol, 150, 51-56.

Muthuraj, M., Chandra, N., Palabhanvi, B., Kumar, V., Das, D., 2015. Process Engineering for High-Cell-Density Cultivation of Lipid Rich Microalgal Biomass of Chlorella sp. FC2 IITG. Bioenerg Res, 8, 726-739.

Myers, R.H., Montgomery, D.C., Anderson-Cook, C.M. 2016. Response surface methodology: process and product optimization using designed experiments. John Wiley & Sons.

Naderi, G., Znad, H., Tade, M.O., 2017. Investigating and modelling of light intensity distribution inside algal photobioreactor. Chem Eng Process.

Naik, S., Goud, V.V., Rout, P.K., Dalai, A.K., 2010. Production of first and second generation biofuels: a comprehensive review. Renew Sustain Energy Rev, 14, 578-597.

Nan, Y., Liu, J., Lin, R., Tavlarides, L.L., 2015. Production of biodiesel from microalgae oil (Chlorella protothecoides) by non-catalytic transesterification in supercritical methanol and ethanol: Process optimization. J Supercrit Fluid, 97, 174-182.

Nasir, M.F.M., Juahir, H., Roslan, N., Mohd, I., Shafie, N.A., Ramli, N., 2011. Artificial Neural Networks Combined with Sensitivity Analysis as a Prediction Model for Water Quality Index in Juru River, Malaysia. IJEP.

Nasir, N.F., Daud, W.R.W., Kamarudin, S.K., Yaakob, Z., 2013. Process system engineering in biodiesel production: A review. Renew Sust Energ Rev, 22, 631-639.

Nautiyal, P., Subramanian, K., Dastidar, M., 2014. Production and characterization of biodiesel from algae. Fuel Process Technol, 120, 79-88.

Nicoletti, M., Jain, L., Giordano, R. 2009. Computational intelligence techniques as tools for bioprocess modelling, optimization, supervision and control. in: Computational Intelligence Techniques for Bioprocess Modelling, Supervision and Control, Springer, pp. 1-23.

Órpez, R., Martínez, M.E., Hodaifa, G., El Yousfi, F., Jbari, N., Sánchez, S., 2009. Growth of the microalga Botryococcus braunii in secondarily treated sewage. Desalination, 246, 625-630.

Pancha, I., Chokshi, K., Maurya, R., Trivedi, K., Patidar, S.K., Ghosh, A., Mishra, S., 2015. Salinity induced oxidative stress enhanced biofuel production potential of microalgae Scenedesmus sp. CCNM 1077. Bioresour Technol, 189, 341-348.

Pankaj, V.P., Awasthi, M., 2014. Optimization of Growth Condition for *Chlorella vulgaris* using Response Surface Methodology (RSM). Int J Eng Sci Adv Technol, 4, 492-500.

Park, S., Li, Y., 2012. Evaluation of methane production and macronutrient degradation in the anaerobic co-digestion of algae biomass residue and lipid waste. Bioresour Technol, 111, 42-48.

Patil, P.D., Gude, V.G., Mannarswamy, A., Cooke, P., Nirmalakhandan, N., Lammers, P., Deng, S., 2012. Comparison of direct transesterification of algal biomass under supercritical methanol and microwave irradiation conditions. Fuel, 97, 822-831.

Phukan, M.M., Chutia, R.S., Konwar, B., Kataki, R., 2011. Microalgae *Chlorella* as a potential bio-energy feedstock. Appl Energy, 88, 3307-3312.

Piemonte, V., Di Paola, L., Iaquaniello, G., Prisciandaro, M., 2016. Biodiesel production from microalgae: ionic liquid process simulation. J Clean Prod, 111, 62-68.

Pittman, J.K., Dean, A.P., Osundeko, O., 2011. The potential of sustainable algal biofuel production using wastewater resources. Bioresour Technol, 102, 17-25.

Prabakaran, P., Pradeepa, V., Selvakumar, G., Ravindran, A.D., 2018. Efficacy of Enzymatic Transesterification of Chlorococcum sp. Algal Oils for Biodiesel Production. Waste Biomass Valorization, 1-9.

Prabhu, A.A., Jayadeep, A., 2016. Optimization of enzyme-assisted improvement of polyphenols and free radical scavenging activity in red rice bran: A statistical and neural network-based approach. Prep Biochem Biotechnol, 1-9.

Pradhan, A., Shrestha, D.S., Van Gerpen, J., Duffield, J., 2008. The energy balance of soybean oil biodiesel production: a review of past studies. T ASABE, 51, 185-194.

Přibyl, P., Cepák, V., Zachleder, V., 2013. Production of lipids and formation and mobilization of lipid bodies in Chlorella vulgaris. J Appl Phycol, 25, 545-553.

Purkayastha, J., Bora, A., Gogoi, H.K., Singh, L., 2017. Growth of high oil yielding green alga Chlorella ellipsoidea in diverse autotrophic media, effect on its constituents. Algal Res, 21, 81-88.

Quesada-Medina, J., Olivares-Carrillo, P., 2011. Evidence of thermal decomposition of fatty acid methyl esters during the synthesis of biodiesel with supercritical methanol. J Supercrit Fluid, 56, 56-63.

Quispe, C.F., Sonderman, O., Khasin, M., Riekhof, W.R., Van Etten, J.L., Nickerson, K.W., 2016. Comparative genomics, transcriptomics, and physiology distinguish symbiotic from free-living *Chlorella* strains. Algal Res, 18, 332-340.

Rai, M.P., Gautom, T., Sharma, N., 2015. Effect of salinity, ph, light intensity on growth and lipid production of microalgae for bioenergy application. OJBS, 15, 260.

Rajvanshi, S., Sharma, M.P., 2012. Micro algae: a potential source of biodiesel. JSBS, 2, 49.

Ramírez-Verduzco, L.F., Rodríguez-Rodríguez, J.E., del Rayo Jaramillo-Jacob, A., 2012. Predicting cetane number, kinematic viscosity, density and higher heating value of biodiesel from its fatty acid methyl ester composition. Fuel, 91, 102-111.

Rao, A.R., Dayananda, C., Sarada, R., Shamala, T., Ravishankar, G., 2007. Effect of salinity on growth of green alga Botryococcus braunii and its constituents. Bioresour Technol, 98, 560-564.

Rawat, I., Kumar, R.R., Mutanda, T., Bux, F., 2013. Biodiesel from microalgae: a critical evaluation from laboratory to large scale production. Appl Energy, 103, 444-467.

Rawat, I., Kumar, R.R., Mutanda, T., Bux, F., 2011. Dual role of microalgae: phycoremediation of domestic wastewater and biomass production for sustainable biofuels production. Appl Energy, 88, 3411-3424.

Reddy, H.K., Muppaneni, T., Patil, P.D., Ponnusamy, S., Cooke, P., Schaub, T., Deng, S., 2014. Direct conversion of wet algae to crude biodiesel under supercritical ethanol conditions. Fuel, 115, 720-726.

Refaat, A., 2009. Correlation between the chemical structure of biodiesel and its physical properties. IJEST, 6, 677-694.

Renaud, S.M., Thinh, L.-V., Lambrinidis, G., Parry, D.L., 2002. Effect of temperature on growth, chemical composition and fatty acid composition of tropical Australian microalgae grown in batch cultures. Aquacult, 211, 195-214.

Richardson, K., Beardall, J., Raven, J., 1983. Adaptation of unicellular algae to irradiance: an analysis of strategies. New Phytol, 93, 157-191.

Rodolfi, L., Chini Zittelli, G., Bassi, N., Padovani, G., Biondi, N., Bonini, G., Tredici, M.R., 2009. Microalgae for oil: Strain selection, induction of lipid synthesis and outdoor mass cultivation in a low-cost photobioreactor. Biotechnol bioeng, 102, 100-112.

Saeidi, S., Jouybanpour, P., Mirvakilli, A., Iranshahi, D., Klemeš, J.J., 2016. A comparative study between Modified Data Envelopment Analysis and Response Surface Methodology for optimisation of heterogeneous biodiesel production from waste cooking palm oil. J Clean Prod, 136, 23-30.

Sakdasri, W., Sawangkeaw, R., Ngamprasertsith, S., 2015. Continuous production of biofuel from refined and used palm olein oil with supercritical methanol at a low molar ratio. Energ Converg Manage, 103, 934-942.

Salama, E.-S., Kurade, M.B., Abou-Shanab, R.A., El-Dalatony, M.M., Yang, I.-S., Min, B., Jeon, B.-H., 2017. Recent progress in microalgal biomass production coupled with wastewater treatment for biofuel generation. Renew Sustain Energy Rev, 79, 1189-1211.

Samniang, A., Tipachan, C., Kajorncheappun-ngam, S., 2014. Comparison of biodiesel production from crude Jatropha oil and Krating oil by supercritical methanol transesterification. Renew Energ, 68, 351-355.

Sánchez, J., Fernández-Sevilla, J., Acién, F., Cerón, M., Pérez-Parra, J., Molina-Grima, E., 2008. Biomass and lutein productivity of Scenedesmus almeriensis: influence of irradiance, dilution rate and temperature. Appl Micro Biotechnol, 79, 719-729.

Sarve, A.N., Varma, M.N., Sonawane, S.S., 2015. Response surface optimization and artificial neural network modeling of biodiesel production from crude mahua

(*Madhuca indica*) oil under supercritical ethanol conditions using CO_2 as co-solvent. RSC Adv, 5, 69702-69713.

Sawangkeaw, R., Bunyakiat, K., Ngamprasertsith, S., 2010. A review of laboratory-scale research on lipid conversion to biodiesel with supercritical methanol (2001-2009). J Supercrit Fluid, 55, 1-13.

Schenk, P.M., Thomas-Hall, S.R., Stephens, E., Marx, U.C., Mussgnug, J.H., Posten, C., Kruse, O., Hankamer, B., 2008. Second generation biofuels: high-efficiency microalgae for biodiesel production. Bioenerg Res, 20-43.

Schwede, S., Kowalczyk, A., Gerber, M., Span, R., 2013. Anaerobic co-digestion of the marine microalga Nannochloropsis salina with energy crops. Bioresour Technol, 148, 428-435.

Seferlis, P., Georgiadis, M.C. 2004. The integration of process design and control. Elsevier.

Shahum, S. 2014. International Conference on Energy and Power Engineering (EPE2014). DEStech Publications, Inc.

Sheehan, J., Dunahay, T., Benemann, J., Roessler, P., 1998. A look back at the US department of energy's aquatic species program-biodiesel from algae, National Renewable Energy Laboratory, Golden, CO.

Sheng, J., Kim, H.W., Badalamenti, J.P., Zhou, C., Sridharakrishnan, S., Krajmalnik-Brown, R., Rittmann, B.E., Vannela, R., 2011. Effects of temperature shifts on growth rate and lipid characteristics of Synechocystis sp. PCC6803 in a bench-top photobioreactor. Bioresour Technol, 102, 11218-11225.

Shin, H.-Y., Lim, S.-M., Bae, S.-Y., Oh, S.C., 2011. Thermal decomposition and stability of fatty acid methyl esters in supercritical methanol. J Anal Appl Pyrolysis, 92, 332-338.

Sialve, B., Bernet, N., Bernard, O., 2009. Anaerobic digestion of microalgae as a necessary step to make microalgal biodiesel sustainable. Biotechnol Adv, 27, 409-416.

Singh, D.K., Mallick, N., 2014. Accumulation potential of lipids and analysis of fatty acid profile of few microalgal species for biodiesel feedstock. J Micro Biotechnol Res, 4, 37-44.

Singh, R.S., Pandey, A., Gnansounou, E. 2016. Biofuels: Production and Future Perspectives, CRC Press.

Singh, S., Singh, D., 2010. Biodiesel production through the use of different sources and characterization of oils and their esters as the substitute of diesel: a review. Renew Sustain Energy Rev, 14, 200-216.

Snow, N., 2017. BP Energy Outlook: Global energy demand to grow 30% to 2035. OIL & GAS JOURNAL, 115, 30-31.

Solé-Bundó, M., Eskicioglu, C., Garfí, M., Carrère, H., Ferrer, I., 2017. Anaerobic co-digestion of microalgal biomass and wheat straw with and without thermo-alkaline pretreatment. Bioresour Technol, 237, 89-98.

Solovchenko, A.E., 2012. Physiological role of neutral lipid accumulation in eukaryotic microalgae under stresses. Russ J Plant Physiol, 59, 167-176.

Sreekrishnan, T., Kohli, S., Rana, V., 2004. Enhancement of biogas production from solid substrates using different techniques—a review. Bioresour Technol, 95, 1-10.

Srirangan, K., Akawi, L., Moo-Young, M., Chou, C.P., 2012. Towards sustainable production of clean energy carriers from biomass resources. Appl Energy, 100, 172-186.

Srivastava, G., Nishchal;, Goud, V.V., 2017. Salinity Induced Lipid Production in Microalgae and Cluster Analysis (ICCB 16-BR_047). Bioresour Technol, 242, 244-252.

Srivastava, G., Paul, A.K., Goud, V.V., 2018. Optimization of non-catalytic transesterification of microalgae oil to biodiesel under supercritical methanol condition. Energ Converg Manage, 156, 269-278.

Sudhir, P., Murthy, S.D.S., 2004. Effects of salt stress on basic processes of photosynthesis. Photosynthetica, 42, 481-486.

Sumprasit, N., Wagle, N., Glanpracha, N., Annachhatre, A.P., 2017. Biodiesel and biogas recovery from Spirulina platensis. Int Biodeter Biodegrad, 119, 196-204.

Takagi, M., Karseno, Yoshida, T., 2006. Effect of salt concentration on intracellular accumulation of lipids and triacylglyceride in marine microalgae *Dunaliella* cells. J Biosci Bioeng, 101, 223-226.

Talebi, A.F., Mohtashami, S.K., Tabatabaei, M., Tohidfar, M., Bagheri, A., Zeinalabedini, M., Mirzaei, H.H., Mirzajanzadeh, M., Shafaroudi, S.M., Bakhtiari, S., 2013a. Fatty acids profiling: a selective criterion for screening microalgae strains for biodiesel production. Algal Res, 2, 258-267.

Talebi, A.F., Tabatabaei, M., Chisti, Y., 2014. BiodieselAnalyzer: a user-friendly software for predicting the properties of prospective biodiesel. Biofuel Res J, 1, 55-57.

Talebi, A.F., Tabatabaei, M., Mohtashami, S.K., Tohidfar, M., Moradi, F., 2013b. Comparative salt stress study on intracellular ion concentration in marine and salt-adapted freshwater strains of microalgae. Not Sci Biol, 5, 309-315.

Talukdar, J., Kalita, M., Bhatnagar, S., Saxena, A., Kraan, S., 2011. Prospects of microalgae of North East India for biodiesel production. Algae biofuel, 69-90.

Talukdar, J., Kalita, M.C., Goswami, B.C., 2013. Characterization of the biofuel potential of a newly isolated strain of the microalga *Botryococcus braunii Kützing* from Assam, India. Bioresour Technol, 149, 268-275.

Tran, H.-L., Kwon, J.-S., Kim, Z.-H., Oh, Y., Lee, C.-G., 2010. Statistical optimization of culture media for growth and lipid production of *Botryococcus braunii LB572*. Biotechnol Biopro Eng, 15, 277-284.

Uggetti, E., Passos, F., Solé, M., Garfí, M., Ferrer, I., 2017. Recent Achievements in the Production of Biogas from Microalgae. Waste Biomass Valorization, 8, 129-139.

Umdu, E.S., Tuncer, M., Seker, E., 2009. Transesterification of Nannochloropsis oculata microalga's lipid to biodiesel on Al2O3 supported CaO and MgO catalysts. Bioresour Technol, 100(11), 2828-2831.

Van Wagenen, J., Miller, T.W., Hobbs, S., Hook, P., Crowe, B., Huesemann, M., 2012. Effects of light and temperature on fatty acid production in *Nannochloropsis salina*. Energies, 5, 731-740.

Verma, P., Kumar, M., Mishra, G., Sahoo, D., 2016. Multivariate Analysis of Fatty Acid and Biochemical Constitutes of Seaweeds to characterize their potential as Bioresource for Biofuel and Fine Chemicals. Bioresour Technol, 226, 132-144.

Vieitez, I., da Silva, C., Alckmin, I., Borges, G.R., Corazza, F.C., Oliveira, J.V., Grompone, M.A., Jachmanián, I., 2010. Continuous catalyst-free methanolysis and ethanolysis of soybean oil under supercritical alcohol/water mixtures. Renew Energ, 35, 1976-1981.

Voltolina, D., Cordero, B., Nieves, M., Soto, L.P., 1999. Growth of Scenedesmus sp. in artificial wastewater. Bioresour Technol, 68, 265-268.

Wang, B., Lan, C.Q., 2011. Biomass production and nitrogen and phosphorus removal by the green alga Neochloris oleoabundans in simulated wastewater and secondary municipal wastewater effluent. Bioresour Technol, 102, 5639-5644.

Wang, L., Li, Y., Chen, P., Min, M., Chen, Y., Zhu, J., Ruan, R.R., 2010. Anaerobic digested dairy manure as a nutrient supplement for cultivation of oil-rich green microalgae Chlorella sp. Bioresour Technol, 101, 2623-2628.

Wang, X., Yang, G., Feng, Y., Ren, G., Han, X., 2012. Optimizing feeding composition and carbon–nitrogen ratios for improved methane yield during anaerobic co-digestion of dairy, chicken manure and wheat straw. Bioresour Technol, 120, 78-83.

Warabi, Y., Kusdiana, D., Saka, S., 2004. Reactivity of triglycerides and fatty acids of rapeseed oil in supercritical alcohols. Bioresour Technol, 91, 283-287.

Ward, A., Lewis, D., Green, F., 2014. Anaerobic digestion of algae biomass: a review. Algal Res, 5, 204-214.

Wei, C.-Y., Huang, T.-C., Chen, H.-H., 2013. Biodiesel production using supercritical methanol with carbon dioxide and acetic acid. J Chem.

Wei, L., Huang, X., Huang, Z., 2015. Temperature effects on lipid properties of microalgae Tetraselmis subcordiformis and Nannochloropsis oculata as biofuel resources. Chinese J. Oceanol. Limnol., 33, 99-106.

Wheeler, G.L., Brownlee, C., 2008. Ca^{2+} signalling in plants and green algae–changing channels. Trends Plant Sci, 13, 506-514.

Wu, H.-L., Hseu, R.-S., Lin, L.-P., 2001. Identification of Chlorella spp. isolates using ribosomal DNA sequences. Bot Bull Acad Sinica, 42.

Wu, L.F., Chen, P.C., Huang, A.P., Lee, C.M., 2012. The feasibility of biodiesel production by microalgae using industrial wastewater. Bioresour Technol, 113, 14-18.

Wu, Z., Shi, X., 2007. Optimization for high-density cultivation of heterotrophic *Chlorella* based on a hybrid neural network model. Lett Appl Microbiol, 44, 13-18.

Xia, L., Ge, H., Zhou, X., Zhang, D., Hu, C., 2013. Photoautotrophic outdoor two-stage cultivation for oleaginous microalgae Scenedesmus obtusus XJ-15. Bioresour Technol, 144, 261-267.

Xia, L., Rong, J., Yang, H., He, Q., Zhang, D., Hu, C., 2014. NaCl as an effective inducer for lipid accumulation in freshwater microalgae *Desmodesmus abundans*. Bioresour Technol, 161, 402-409.

Xin, L., Hong-Ying, H., Yu-Ping, Z., 2011. Growth and lipid accumulation properties of a freshwater microalga Scenedesmus sp. under different cultivation temperature. Bioresour Technol, 102, 3098-3102.

Xu, X.-Q., Beardall, J., 1997. Effect of salinity on fatty acid composition of a green microalga from an antarctic hypersaline lake. Phytochemistry, 45, 655-658.

Yang, J., Xu, M., Zhang, X., Hu, Q., Sommerfeld, M., Chen, Y., 2011. Life-cycle analysis on biodiesel production from microalgae: water footprint and nutrients balance. Bioresour Technol, 102, 159-165.

Yeesang, C., Cheirsilp, B., 2011. Effect of nitrogen, salt, and iron content in the growth medium and light intensity on lipid production by microalgae isolated from freshwater sources in Thailand. Bioresour Technol, 102, 3034-3040.

Yen, H.-W., Brune, D.E., 2007. Anaerobic co-digestion of algal sludge and waste paper to produce methane. Bioresour Technol, 98, 130-134.

Yen, H.-W., Hu, I.-C., Chen, C.-Y., Ho, S.-H., Lee, D.-J., Chang, J.-S., 2013. Microalgae-based biorefinery–from biofuels to natural products. Bioresour Technol, 135, 166-174.

Yeung, D.K., Lam, S.L., Griffith, J.F., Chan, A.B., Chen, Z., Tsang, P.H., Leung, P.C., 2008. Analysis of bone marrow fatty acid composition using high-resolution proton NMR spectroscopy. Chem Phys Lipids, 151, 103-109.

Yilancioglu, K., Cokol, M., Pastirmaci, I., Erman, B., Cetiner, S., 2014. Oxidative stress is a mediator for increased lipid accumulation in a newly isolated *Dunaliella salina* strain. PloS one, 9, e91957.

Zhong, W., Zhang, Z., Luo, Y., Qiao, W., Xiao, M., Zhang, M., 2012. Biogas productivity by co-digesting Taihu blue algae with corn straw as an external carbon source. Bioresour Technol, 114, 281-286.

Zhou, W., Min, M., Li, Y., Hu, B., Ma, X., Cheng, Y., Liu, Y., Chen, P., Ruan, R., 2012. A hetero-photoautotrophic two-stage cultivation process to improve wastewater nutrient removal and enhance algal lipid accumulation. Bioresour Technol, 110, 448-455.

Zhu, J.-K., 2016. Abiotic stress signaling and responses in plants. Cell, 167, 313-324.

Appendix

A.1 FTIR peak assignment of microalgae biomass

S no.	Wave no. range	Assignments	Functional group	Reference
1	2809-3012	$\nu_{as}CH_2$	Lipids	(Liu et al., 2013)
2	1745-1734	νC=O of esters	Membrane Lipids, fatty acids	(Liu et al., 2013)
3	1389-1452	δCH_3 and δCH_2	Proteins	(Duygu et al., 2014)
4	1191-1356	ν_{as}(>P=O)	Nucleic acids, Phosphoryl group	(Dean et al., 2010)
5	980-1072	ν(=C-O-C=)	Polysaccharides	(Ponnuswamy et al., 2013)

A.2 ^{1}H NMR spectral peak assignment

Signal	Chemical shift (ppm)	Functional group
1	0.82–0.94	–CH_3(terminal methyl protons (saturated, oleic and linoleic)
2	0.94–1.03	–CH_3(terminal methyl protons (linolenic)
3	1.20–1.43	–$(CH_2)_n$–(methylene protons (saturated)
4	1. 55–1.69	–OCO–CH_2–CH_2–(β–methylene protons (carbonyl)
5	1.93–2.13	–CH2–CH=CH– (allyl methylene protons)
6	2.25–2.36	–OCO–CH_2–(α–methylene protons)
7	2.73–2.87	=HC–CH_2–CH= (divinyl methylene protons)
8	4.10–4.35	–CH_2OCOR (methylene protons (glyceryl)
9	5.23–5.29	–CH_2OCOR (methylene protons (glyceryl)
10	5.29–5.43	–CH=CH– (olefinic protons)

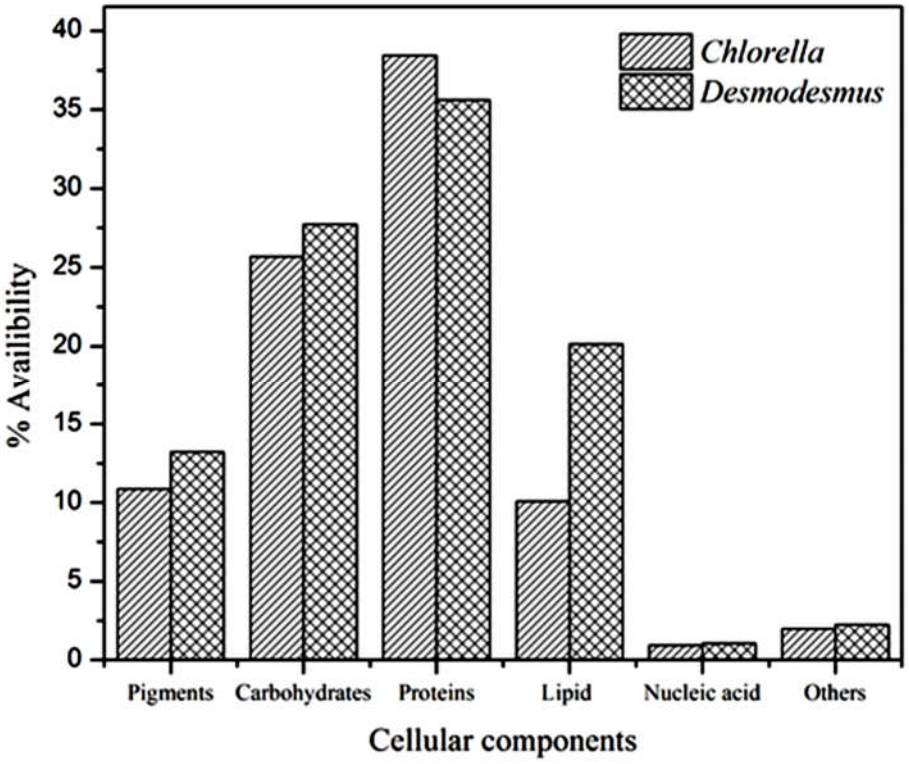

A.4 Total cellular component measured after culture condition optimization.

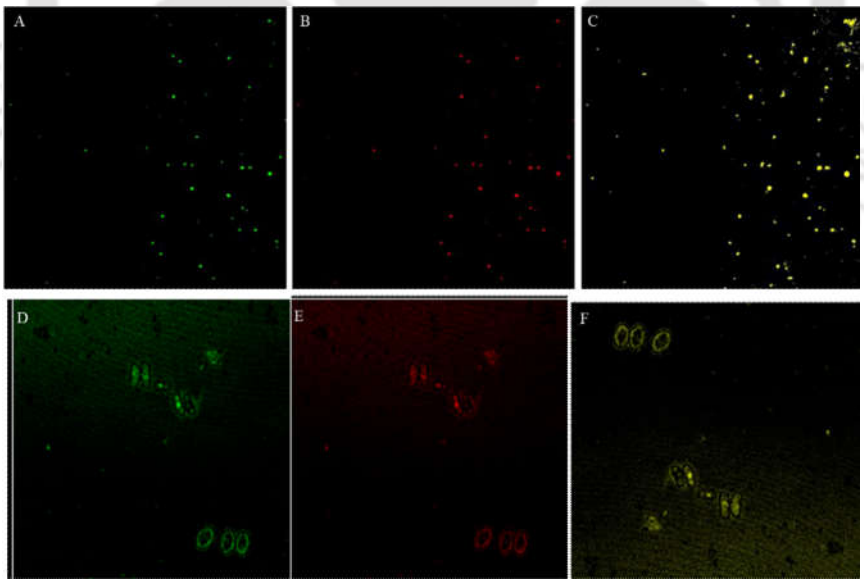

A.5 Lipid localization of microalgae of microalgae as observed under confocal laser scanning microscope for (A,B) CG12 and (D,E) GS12 under green and red filters respectively. The merged view was also captured for (C) CG12 and (F) GS12 respectively.

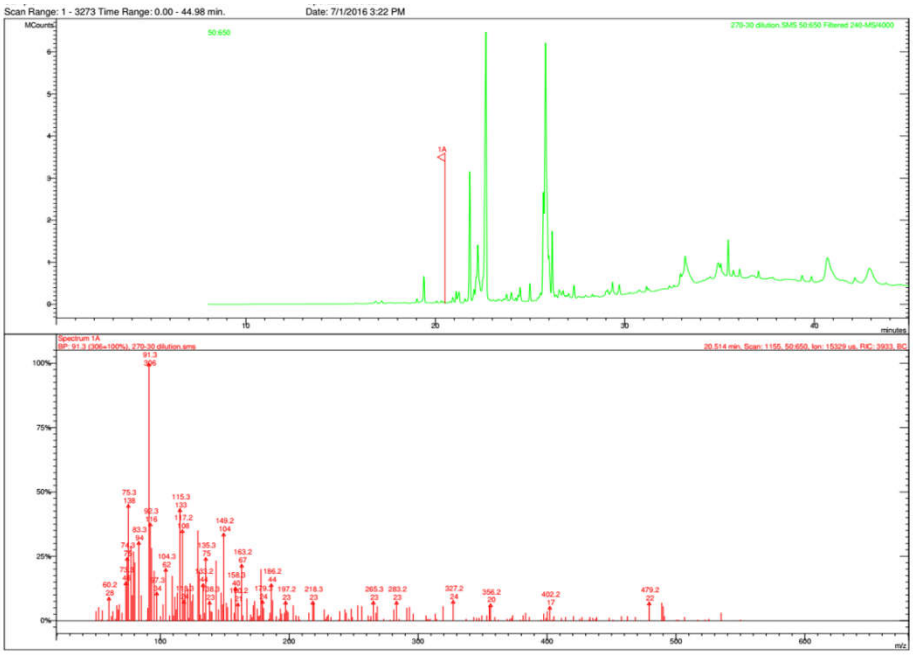

A.6 GCMS analysis was performed for SCM transesterification under optimum condition for determining the fatty acid composition.

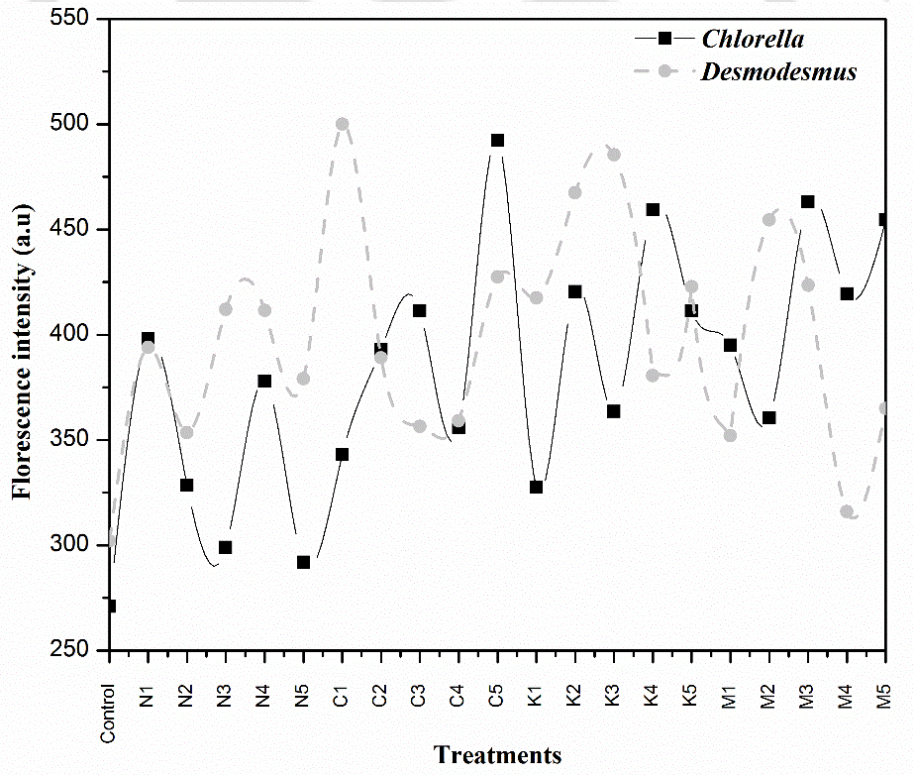

A.7 Florescence intensity measurement was done with flourimeter for salt treated microalgae cells (Chapter 5).

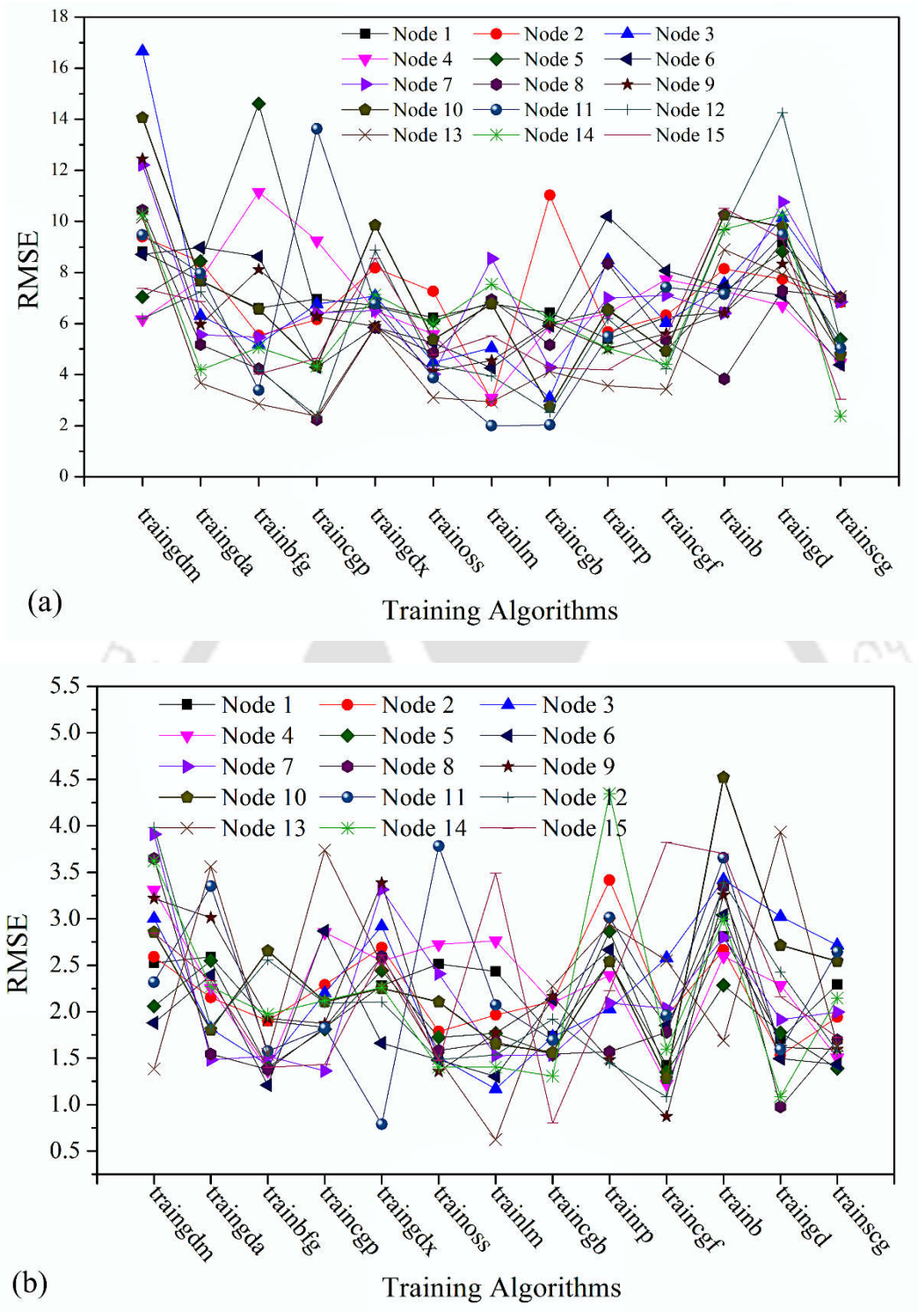

A.8 Different transfer functions used to train the ANN model for (a) CG12 and (b) GS12 (Chapter 4).

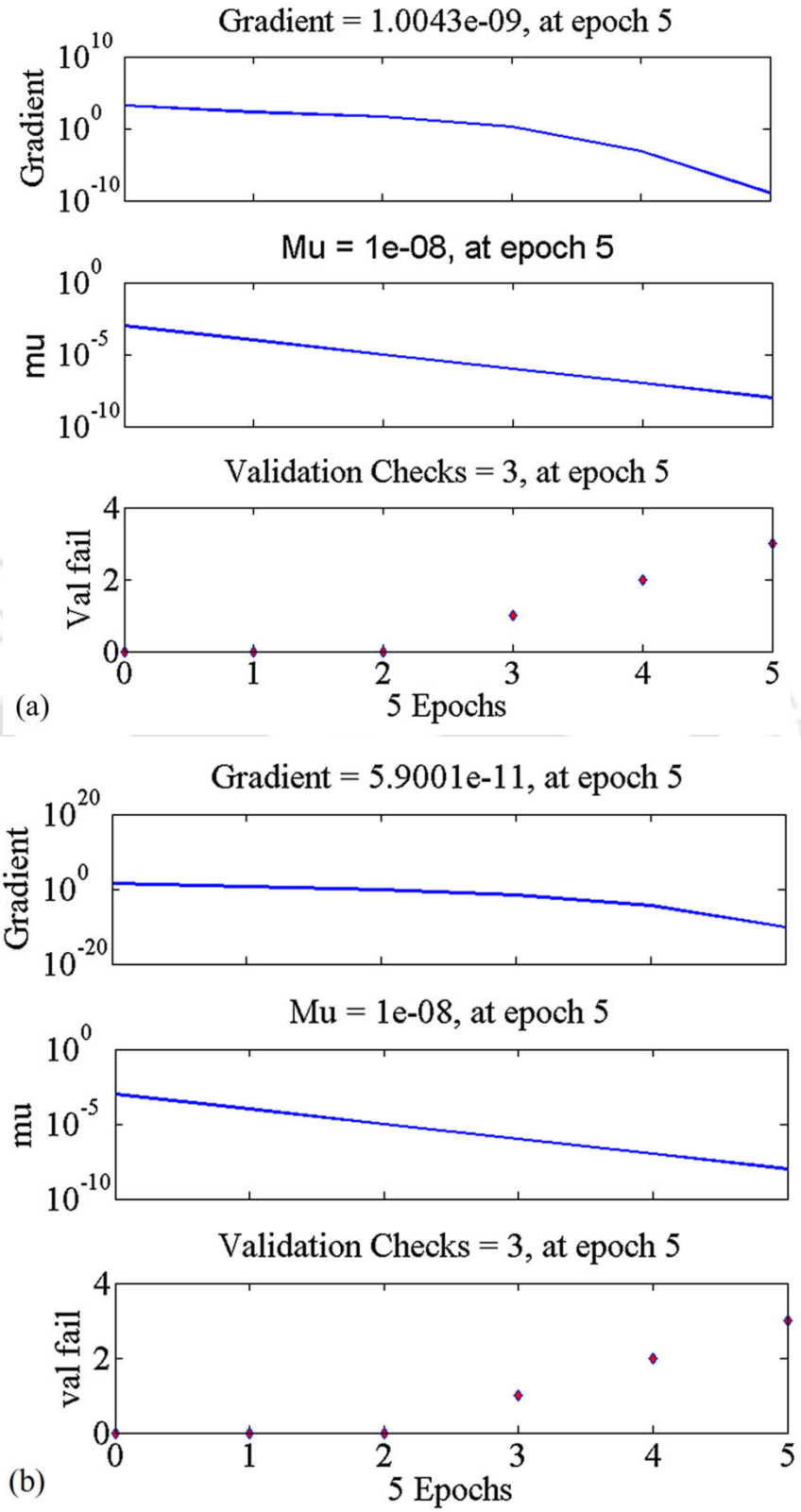

A.9 ANN validation check plot and gradient value for (a) CG12 and (b) GS12 (Chapter 4).

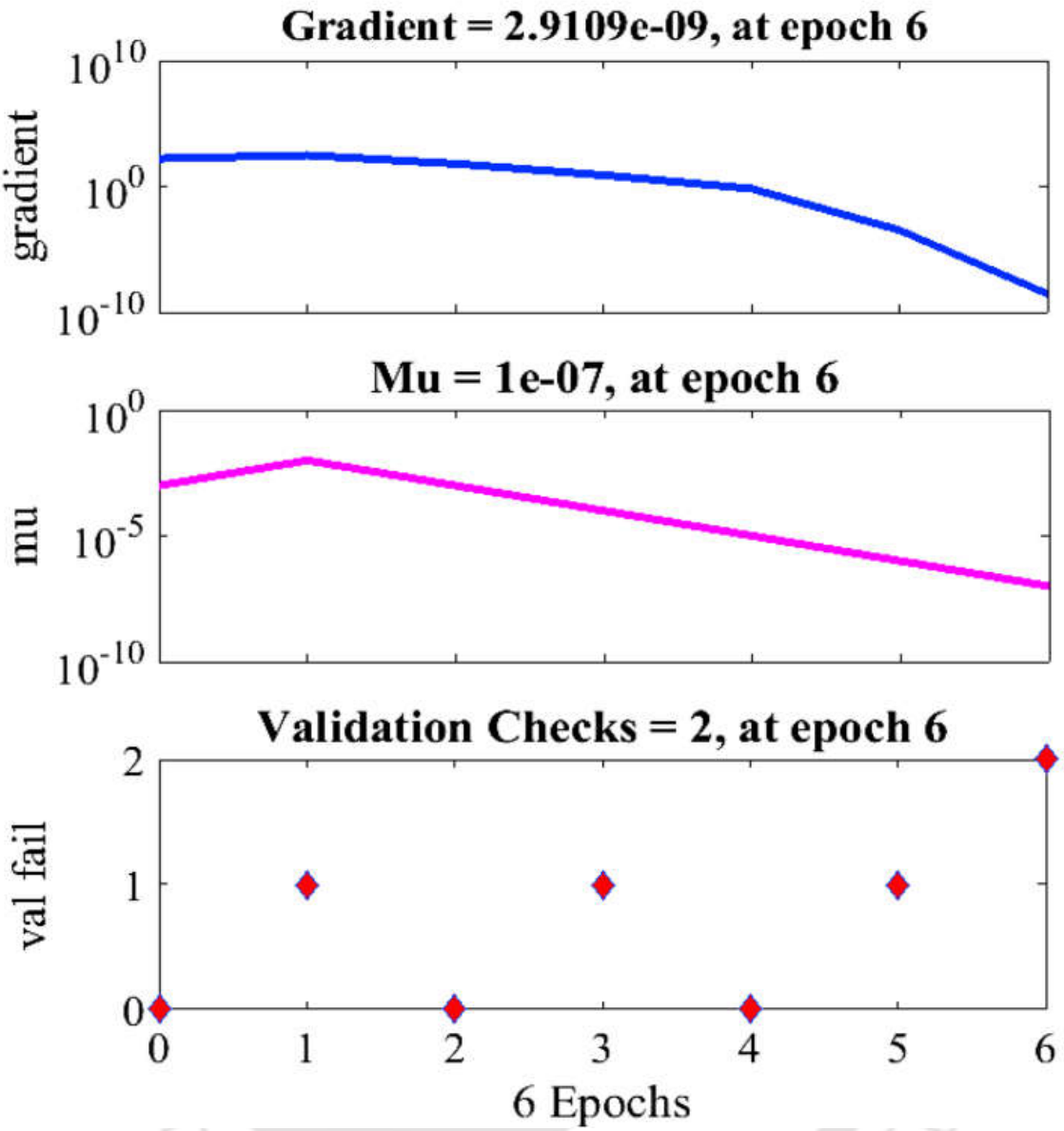

A.10 ANN validation check plot and gradient value for SCM transesterification (Chapter 6).

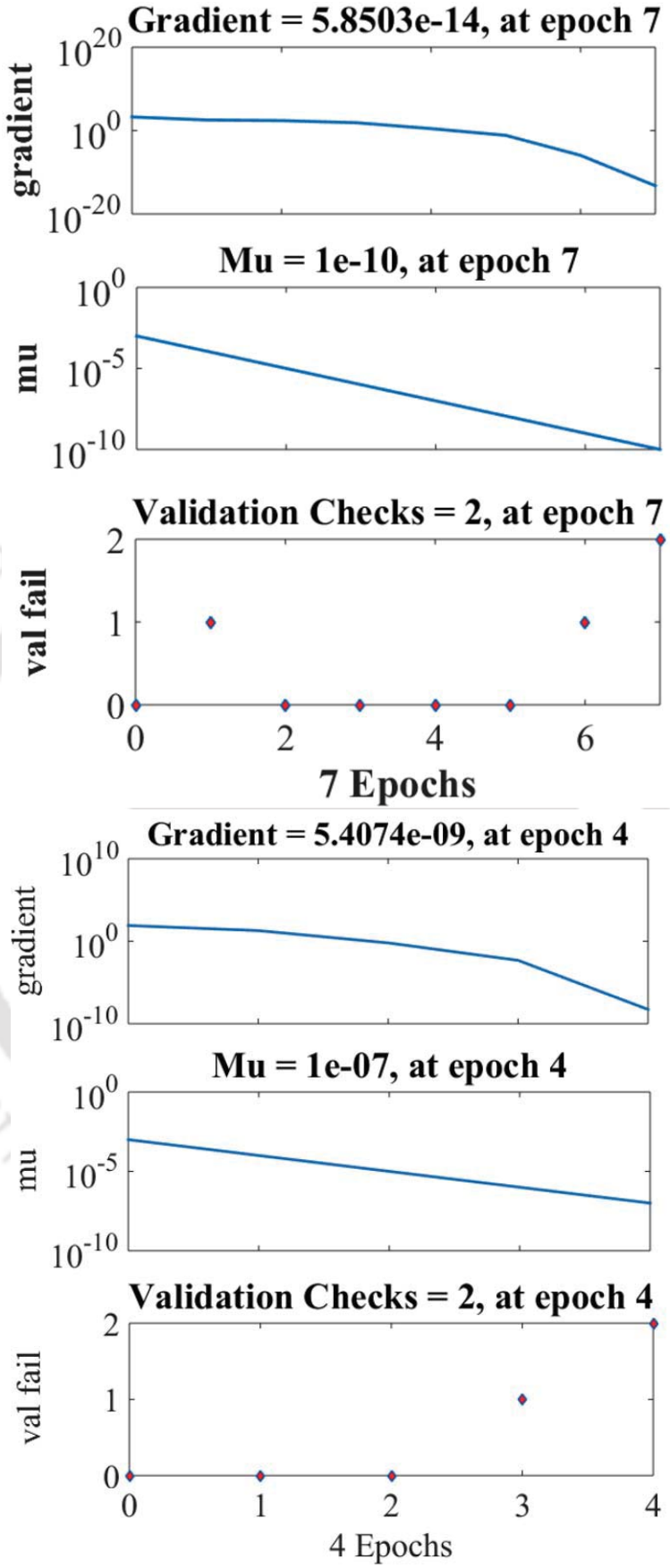

A.11 ANN validation check plot and gradient value for (left) CG12 and (right) GS12 (Chapter 7).

18 S rDNA sequencing of microalgae

>Chlorella CG12 (522 bp)
CCTTGGGCTC ACCCCCTGGG GCTGTCGTCG GCCAAAACCC CTGTATCCAA CCTTTTTTTA
ACACACCCCA AACCACAACC AACTCTGAAG CATCTTTGGT GGCCCGGCCC CGTGCCGTCC
ACTCCAAACC AAAGACAACT CTCAACAACG GATATCTTGG CTCCCGTATC GATGAAGAAC
GCAGCGAAAT GCGATACGTA GTGTGAATTG CAGAATTCCG TGAACCATCG AATCTTTGAA
CGCAAATTGC GCCCGAGGCT TCGGCCGAGG GCATGTCTGC CTCAGCGTCG GTTTACACCC
TCGCCCTCCC CCCCTGTGGG GGGCGGTGCG GACCTGGCCC TCCCGGCTCC GCTCTCTCCC
GAGCGTCCGG GTTGGCTGAA GCACAGAGGC TTGAGCATGG ACCCCGTTTG TAGGGCAATG
GCTTGGTAGG TAGGCACCCC CTACGCAGCC TGCCGTTGCC CGAGGGGACT TTGCTGGAGG
CCCAGCAGGA ATCCGGCCCT TCCCGGCCGG ACTACTCACT CA

>Desmodesmus GS12 (629 bp)
GGGGGCTGCG GAAGGATCAT TGAATATGCA AACCACAACA CGCACTCTTT TACTTGTGTA
CCGACGTTAG GTCGAACCCT CACCGGTTTG GCCTACTTAC ACACACACAC ACCATTGACC
AACCATTGAT TAAACCAAAC TCTGAAGTTT CGGCTGCTGT TAATCGGCAG TTTTAACGAA
AACAACTCTC AACAACGGAT ATCTTGGCTC TCGCAACGAT GAAGAACGCA GCGAAATGCG
ATACGTAGTG TGAATTGCAG AATTCCGTGA ACCATCGAAT CTTTGAACGC ATATTGCGCT
CGACTCCTCG GAGAAGAGCA TGTCTGCCTC AGCGTCGGTT AACACCCTCA CCCCTCTTCC
TCTTCGGAGG GAGCTTGTCG TGCTTGCTTA AGCCGGCATC AGGGGAGGAT CTGGCCCTCC
CAATCGGAGT CACATCTGGT TGGGTTGGCT GAAGCACAGA GGCTTAAACT GGGACCCGAT
TCGGGCTCAA CTGGATAGGT AGCAACACCC TTGTGGTGCC TACACGAAGT TGTGTCTGAG
GACCTGGTTA GGAGCCAAGC AGGAAACGTG CCTTTGGCAC GTATCTCTTT ATTCGACCTG
AGCTCAGGCA AGGCTACCCG CTGAACTTA

Research output

Publications

1. Garima Srivastava, Atanu Kumar Paul and Vaibhav V. Goud (2018). Optimization of non-catalytic transesterification of microalgae oil to biodiesel under supercritical methanol condition. Energy Conversion and Management, 156, 269-278. (Impact factor-5.589, Citations 1)
2. Garima Srivastava, Nischal and Vaibhav V. Goud (2017). Salinity induced lipid production in microalgae and cluster analysis. Bioresource Technology, 242, 244-252. (Impact factor-5.651, Citations 5)
3. Purabi Mazumdar, Swarooparani Dasari, Venubabu Borugadda, Garima Srivastava, Lingraj Sahoo, Vaibhav V. Goud (2013). Biodiesel production from high free fatty acids content Jatropha curcas L. oil using dual step process, Biomass conversion and Biorefinary, 3,361-369. (Citations-6)

Manuscript under review

1. Garima Srivastava, Atanu Kumar Paul and Vaibhav V. Goud (2018) Strategic Development of Culture Conditions for Qualitative Recovery of Oil from Freshwater Microalgae of North-East India (Bioresources and Bioprocessing).
2. Garima Srivastava, Vikas Kumar, Rahul Tiwari and Vaibhav V. Goud (2018) Anaerobic co-digestion of defatted microalgae residue and rice straw as an emerging trend for waste utilization and sustainable bio-refinery development (Algal research).

Manuscript under preparation

1. Garima Srivastava and V.V. Goud (2018). Microalgae: A promising solution to present problems.

Accessions

1. *Chlorella sorokiniana* strain CG12 internal transcribed spacer 1, partial sequence; 5.8S ribosomal RNA gene, complete sequence; and internal transcribed spacer 2, partial sequence (KR905186).
2. *Desmodesmus sp*. GS12 internal transcribed spacer 1, partial sequence; 5.8S ribosomal RNA gene, complete sequence; and internal transcribed spacer 2, partial sequence (KR905187).

Conference

1. Garima Srivastava, Vikas Kumar, Rahul Tiwari and Vaibhav V. Goud. Anaerobic Co-Digestion of Defatted Microalgae Residue and Rice Straw as an Emerging Trend for Waste Utilization and Sustainable Bio-Refinery Development. 8-10 October 2017, WBC-2017, NEERI Nagpur (**Best Poster Award**).
2. Garima Srivastava, Nishchal, and Vaibhav V. Goud. Salinity Induced Lipid Production in Microalgae and Cluster Analysis. 8-10 December 2016, ICCB-2016, VIT Vellore (poster presentation).
3. Garima Srivastava, Vikas Kumar, and Vaibhav V. Goud. Biomass-Based Energy Generation: Coupling of Biogas Production and Microalgae Biodiesel. 1-2 April 2016; RECYCLE 2016, IIT Guwahati (oral presentation).
4. Garima Srivastava, Atanu Kumar Paul, Pushpita Das and Vaibhav V. Goud. Biofuels from microorganisms. 16-18 March 2015, Research Conclave, Indian Institute of Technology Guwahati (3rd Best poster).
5. Garima Srivastava, Vaibhav V. Goud. Biodiesel production from microalgae. 27-30 Dec, 2015; CHEMCON-15, IIT Guwahati (oral presentation).

6. Garima Srivastava, Vaibhav V. Goud. Salinity induced lipid overproduction in microalgae. 21-22 March, 2015; Biotechnology and Human Welfare: New Vistas, Jaunpur University, Jaunpur, India (oral presentation).
7. Garima Srivastava, Vaibhav V. Goud. Effect of Salt concentration on growth and lipid accumulation properties of *Chlorella sp.* 27-30 Dec, 2014; CHEMCON-2014, Punjab University, Chandigarh, India (Poster presentation).
8. Garima Srivastava, Vaibhav V. Goud. Comparative growth studies of *Desmodesmus* species for biomass and lipid production under variable culture conditions. 29-31 January, 2014; International conference on harnessing Natural resources for Sustainable Development: Global Trends, Cotton College Guwahati, Assam, India (Poster presentation).

Workshop

1. Participated in Sensitization of Woman, NASI, Nov 4-5, 2017 organized by Department of Biosciences and Bioengineering, Indian Institute of Technology Guwahati.
2. Participated in Recent Trends in Fuel Cell Technology, Dec 2015 in Centre for Energy, Indian Institute of Technology Guwahati.
3. Participated in ADMAT 2015 organized by IEEE, Indian Institute of Technology Guwahati.
4. Participated in Research Conclave 2015, organized by Student Academic Board (SAB), Indian Institute of Technology, Guwahati.
5. Indo-Finish Workshop on green chemistry (2013) organized by Tezpur University and IIT Guwahati.
6. Participated in Indo-Japan DBT workshop (2012) organized by IIT Guwahati.